**Hidden sources and sinks of Fe(II) in the sedimentary biogeochemical iron cycle – The role of light**

**Dissertation**

der Mathematisch-Naturwissenschaftlichen Fakultät

der Eberhard Karls Universität Tübingen

zur Erlangung des Grades eines

Doktors der Naturwissenschaften

(Dr. rer. nat.)

vorgelegt von

M. Sc. Ulf Lüder

aus Heidenheim an der Brenz

Tübingen 2019

# Contents

# Summary

Iron (Fe) is an important and abundant redox active element in freshwater and marine sediments. Sediments are typically stratified by redox zones that are formed as a consequence of mineralization of organic matter following thermodynamic constraints. The redox cycle of Fe is coupled to many other sedimentary element cycles and speciation and appearance of Fe, i.e. dissolved or as Fe minerals, influence the fate and the (im)mobilization of many contaminants or nutrients. Therefore, it is crucial to better understand processes involved in the biogeochemical Fe cycle of sediments. The consequences of light and physical perturbation on the distribution of dissolved Fe(II) ($Fe^{2+}$) in sediments and on the substrate availability for the inhabiting Fe-metabolizing bacteria are so far only poorly understood and they might therefore represent hidden Fe(II) sources and sinks. In this PhD thesis project, freshwater sediments (Lake Constance, Germany) and marine sediments (Norsminde Fjord, Denmark) were incubated in the lab and high-resolution microsensor measurements were applied to decipher hidden sources and sinks of Fe(II) that impact sedimentary Fe biogeochemistry.

Although light can induce the reduction of organically complexed Fe(III) (photoreduction) in oxic water columns, it is unclear whether this process might provide Fe(II) to sunlit sediments. We could show that Fe(III) photoreduction produces $Fe^{2+}$ in micromolar concentrations in oxic, illuminated freshwater sediment layers depending on the concentration of dissolved organic carbon. The photochemically produced $Fe^{2+}$ is in the same order of magnitude of $Fe^{2+}$ produced in reduced sediment layers below. Similar amount of $Fe^{2+}$ was produced during incubation with 90 % lower light intensity indicating this process is not light-limited in sediments. Proving the existence of light-induced $Fe^{2+}$ release as well in marine sunlit sediments, we were able to validate the hypothesis that Fe(III) photoreduction represents a hidden $Fe^{2+}$ source in sediments.

Apart from light illumination, sediments are also frequently exposed to physical perturbation, such as storms or mixing by tidal movement. By that, prevalent geochemical conditions and redox zonation get disturbed with so far unknown consequences for the fate of $Fe^{2+}$. By simulating a storm event in 12h light-dark incubated marine sediment cores, we could show that hundreds of micromolar $Fe^{2+}$ (up to 300 µM) were repeatedly released into the sediment pore water during physical perturbation after $Fe^{2+}$ significantly decreased within days during undisturbed incubation. $Fe^{2+}$ concentrations were closely coupled to the formation and dissolution of metastable Fe-sulphide mineral phases, indicating not only the importance of sulphide but also physical perturbation as sinks and sources of Fe(II).

In many sediments filamentous cable bacteria electrically couple the oxidation of sulphide to oxygen reduction. However, we found that in light/dark incubated marine sediment cores cable bacteria responded towards illumination. Under illumination we found high cable bacteria abundance with concomitant low $Fe^{2+}$ concentrations after 7 days of incubation in visible light (400-700 nm) in reduced sediment layers, suggesting that the activity of cable bacteria might be related to sedimentary $Fe^{2+}$ depletion. Either cable bacteria can oxidize Fe(II) themselves or they serve Fe(II)-oxidizing bacteria as electron sink; another so far undiscovered process that impacts the sedimentary Fe(II) availability.

Overall, the findings of this PhD thesis deciphered a series of hidden Fe(II) sources and sinks that are closely related to illumination and perturbation of freshwater and marine sediments using high-resolution in-situ microsensor measurements. The implementation of these so far neglected Fe(II) sources to the "classical" Fe cycle that is characterized by opposing Fe(II) and Fe(III) gradients provides a novel vision of the sedimentary biogeochemical Fe redox cycle in which dynamic physico-chemical features control the availability of Fe(II) throughout the entire sediment column. This PhD thesis highlights the potential of overlooking versus deciphering biogeochemical processes simply by adapting the spatial and temporal resolution of in-situ and ex-situ measurements.

# Zusammenfassung

Eisen (Fe) ist ein wichtiges und häufig vorkommendes redox-aktives Element in Süß- und Salzwassersedimenten. Typischerweise sind Sedimente in Redoxzonen unterteilt. Diese bilden sich im Zuge der auf thermodynamischen Gesetzmäßigkeiten beruhenden Mineralisierung von organischem Material. Der Eisenkreislauf in Sedimenten ist eng verbunden mit vielen anderen Elementkreisläufen. Die Speziierung und Erscheinungsformen von Eisen, d.h. entweder in gelöster Form oder als Eisenminerale, kann die Eigenschaften und den Verbleib vieler Schadstoffe oder Nährstoffe beeinflussen. Deshalb ist von entscheidender Bedeutung, die Prozesse, die in den biogeochemischen Eisenkreislauf in Sedimenten involviert sind, besser zu begreifen. Die Auswirkungen von Licht und physischer Durchmischung sowohl auf die Verteilung von gelöstem Fe(II) ($Fe^{2+}$) in Sedimenten als auch auf die Substratverfügbarkeit für die im Sediment vorkommenden Eisen-verstoffwechselnden Bakterien werden bisher nur wenig verstanden; sie könnten deshalb verborgene Quellen und Senken von Fe(II) darstellen. In dieser Doktorarbeit wurden Süßwassersedimente (Bodensee, Deutschland) und Salzwassersedimente (Norsminde Fjord, Dänemark) im Labor inkubiert und hochauflösende Mikrosensor-Messungen vorgenommen, um verborgene Quellen und Senken von Fe(II) zu entschlüsseln, welche die Biogeochemie von Eisen in Sedimenten beeinflussen.

Obwohl Licht in der Lage ist, organisch komplexiertes Fe(III) in oxischen Wassersäulen zu reduzieren (Fe(III)-Photoreduktion), ist unklar, ob dieser Prozess auch in lichtdurchfluteten Sedimenten Fe(II) liefern kann. Wir konnten zeigen, dass Fe(III)-Photoreduktion in oxischen, lichtdurchfluteten Süßwassersedimenten $Fe^{2+}$ in mikromolarer Konzentration produziert. Diese Konzentration ist in der gleichen Größenordnung wie Fe(II), das in reduzierten Sedimentschichten darunter produziert wurde. Die Menge ist abhängig von der Konzentration an gelöstem organischen Kohlenstoff. Während der Inkubation mit 90% geringerer Lichtintensität wurden ähnliche Mengen an $Fe^{2+}$ freigesetzt, was darauf hindeutet, dass dieser Prozess in Sedimenten nicht Licht-limitiert ist. Da wir nachweisen konnten, dass eine Licht-induzierte Freisetzung von $Fe^{2+}$ auch in beleuchteten Salzwassersedimenten stattfindet, konnten wir die Hypothese, dass Fe(III)-Photoreduktion eine verborgene $Fe^{2+}$ Quelle in Sedimenten darstellt, validieren.

Neben der Beleuchtung mit Licht sind Sedimente auch häufig physischer Durchmischung ausgesetzt, beispielsweise bei Stürmen oder durch Gezeitenbewegung. Dadurch werden die vorherrschenden geochemischen Bedingungen und die Redoxzonierung gestört mit bisher

unbekannten Konsequenzen für $Fe^{2+}$. Das Nachstellen eines Sturmereignisses in 12 Stunden Licht-Dunkel inkubierten Salzwassersedimentkernen ergab, dass wiederholt Hunderte von mikromolar $Fe^{2+}$ (bis zu 300 µM) in das Sediment-Porenwasser bei physischer Durchmischung freigesetzt wurde, nachdem die $Fe^{2+}$ Konzentration während ungestörter Inkubation in den Tagen davor deutlich abgenommen hatte. Die $Fe^{2+}$ Konzentrationen waren eng mit der Bildung und Auflösung von metastabilen Fe-Sulfid Mineralphasen im Sediment gekoppelt, was nicht nur auf die Wichtigkeit von Sulfid, sondern auch auf die der physischen Durchmischung als Senken und Quellen von Fe(II) schließen lässt.

In vielen Sedimenten koppeln filamentös aufgebaute Kabelbakterien die Oxidation von Sulfid elektrisch an die Reduktion von Sauerstoff. Jedoch konnten wir in Licht/Dunkel inkubierten Salzwassersedimentkernen feststellen, dass Kabelbakterien auf Beleuchtung reagierten. Nach 7 Tagen Beleuchtung mit Licht im sichtbaren Bereich (400-700 nm) fanden wir Kabelbakterien in hoher Zahl, mit einhergehenden niedrigen $Fe^{2+}$ Konzentrationen in reduzierten Sedimentschichten, was darauf hinweist, dass die Aktivität von Kabelbakterien mit der Abnahme von $Fe^{2+}$ im Sediment zusammenhängt. Entweder können Kabelbakterien Fe(II) selbst oxidieren oder sie dienen Fe(II)-oxidierenden Bakterien als Elektronensenke; ein weiterer bisher unentdeckter Prozess, der die Fe(II)-Verfügbarkeit in Sedimenten zu beeinflussen scheint.

Insgesamt konnten die Ergebnisse dieser Doktorarbeit unter Zuhilfenahme von hochauflösenden in-situ Mikrosensormessungen eine Reihe verborgener Fe(II)-Quellen und -Senken aufdecken, die eng mit Licht und der physischen Durchmischung von Süß- oder Salzwassersedimenten zusammenhängen. Das Miteinbeziehen dieser bisher nicht betrachteten Fe(II) Quellen in den „klassischen" Eisenkreislauf, der durch gegenläufige Fe(II) und Fe(III) Gradienten charakterisiert ist, bietet eine neue Sicht auf den sedimentären biogeochemischen Eisenredoxkreislauf, bei der physikalisch-chemische Faktoren die Verfügbarkeit von Fe(II) durch die gesamte Sedimentsäule hindurch kontrollieren. Diese Doktorarbeit macht deutlich, dass biogeochemische Prozesse entweder nicht entdeckt oder aber entschlüsselt werden können, wenn man die räumliche und zeitliche Auflösung von in-situ und ex-situ Messungen anpasst.

# Chapter 1: Introduction and objectives of this study

Iron (Fe) is one of the most important redox-active elements on Earth and usually occurs in the environment as reduced ferrous (Fe(II)) or oxidized ferric (Fe(III)) iron. Fe is essential for almost all living organisms as it is integrated in many cellular compounds. It is either used as a nutrient or as energy source, electron donor or electron acceptor for Fe-metabolizing bacteria (Kappler & Straub, 2005). While in oxic water columns, such as the ocean, total Fe concentration generally is extremely low (pico- to nanomolar range) (Emmenegger et al., 2001; Boyd & Ellwood, 2010; King & Barbeau, 2011), the concentration in sediments usually is in the range of few to few hundreds micromolar (Thamdrup et al., 1994; Melton et al., 2014b; Schaedler et al., 2018). As Fe(III) is only poorly soluble at circumneutral pH (Cornell & Schwertmann, 2003), it typically occurs as solid Fe(III) (oxyhydr)oxides. However, organic complexation can increase the solubility of Fe(III) (Taillefert et al., 2000; Kraemer, 2004; Kappler & Straub, 2005). In contrast, Fe(II) is more soluble and therefore generally more bioavailable for organisms (Melton et al., 2014a). Many abiotic and biotic redox processes cycle Fe between its two main redox states (Melton et al., 2014a), thereby influencing properties such as solubility, bioavailability or sorption properties. These processes are determined by the presence and abundance of different Fe-metabolizing bacteria as well as geochemical parameters such as pH, light availability, organic carbon content, oxygen ($O_2$) or dissolved sulphide ($H_2S+HS^-+S^{2-}$) concentration or the redox potential of the surrounding environment.

## 1.1 Abiotic Fe redox reactions

At circumneutral pH, Fe(II) is readily abiotically oxidized by $O_2$ (Stumm & Lee, 1961; Millero et al., 1987) or reactive oxygen species (ROS) such as superoxide ($O_2^{-\bullet}$), hydrogen peroxide ($H_2O_2$) or hydroxyl radicals ($OH^\bullet$) (eq. 1.1-1.4) that are produced during the stepwise reduction of $O_2$ (Weiss, 1935).

$$Fe(II) + O_2 \rightarrow Fe(III) + O_2^{-\bullet} \qquad (1.1)$$

$$Fe(II) + O_2^{-\bullet} + 2H^+ \rightarrow Fe(III) + H_2O_2 \qquad (1.2)$$

$$Fe(II) + H_2O_2 \rightarrow Fe(III) + OH^\bullet + OH^- \qquad (1.3)$$

$$Fe(II) + OH^\bullet \rightarrow Fe(III) + OH^- \qquad (1.4)$$
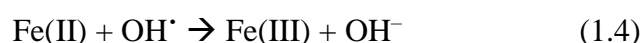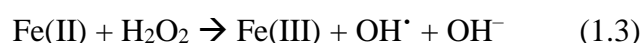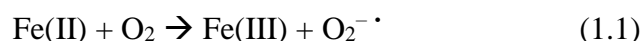
Kinetics of abiotic homogenous Fe(II) oxidation by $O_2$, i.e. the reaction of dissolved Fe(II) ($Fe^{2+}$) with dissolved $O_2$, is strongly dependent on pH (Stumm & Lee, 1961; Davison & Seed, 1983) and at circumneutral pH, the reaction is quite fast with half-life times of Fe(II) in fully oxygenated water being in the range of minutes (Millero et al., 1987; Stumm & Morgan, 1996). Due to its poor solubility at circumneutral pH (Cornell & Schwertmann, 2003), the formed Fe(III) will instantaneously precipitate as Fe(III) (oxyhydr)oxide thereby serving as surface catalyst for the faster heterogeneous Fe(II) oxidation (autocatalysis reaction) (Tamura et al., 1976; Rentz et al., 2007). Besides by $O_2$, Fe(II) can also abiotically be oxidized by manganese oxides and by reactive nitrogen species such as nitric oxide (NO) or nitrite ($NO_2^-$) (chemodenitrification) (Melton et al., 2014a).

On the other hand, Fe(III) can abiotically be reduced by reaction with reduced organic compounds such as humic substances (Sulzberger et al., 1989). Light is able to reduce Fe(III) to Fe(II), especially when Fe(III) is organically complexed, either directly by an electron transfer from the organic ligand to the complexed Fe(III) via ligand-to-metal charge transfer (LMCT) reaction, or by radicals like superoxide that are formed in secondary photochemical reactions (Barbeau, 2006). Abiotic reduction of Fe(III) by reduced sulphur species such as sulphide is of great importance especially in marine sediments (Canfield, 1989), where sulphide is produced by microbial sulphate reduction (Jørgensen, 1977). Formed Fe(II) will quickly react with sulphide and precipitate as Fe monosulphide (FeS) or even as pyrite ($FeS_2$) (Pyzik & Sommer, 1981; Canfield, 1989).

## 1.2 Microbially catalyzed Fe redox reactions

Besides abiotic Fe redox reactions, different microbes are able to use Fe for their metabolisms and contribute to a high extent to the cycling between the redox states of Fe (Weber et al., 2006). Even though the energy yield of Fe(II) oxidation is quite low and strongly depends on pH and organic complexation (Kappler & Straub, 2005; Emerson et al., 2010), Fe(II) can be used as electron donor for Fe(II)-oxidizing bacteria that couple the oxidation of Fe(II) to the reduction of either $O_2$ ("microaerophilic Fe(II)-oxidizers") (Emerson & Moyer, 1997), nitrate ("nitrate-reducing Fe(II)-oxidizers") (Straub et al., 1996) or, with light as energy source, the reduction, i.e. the fixation, of $CO_2$ ("anoxygenic phototrophic Fe(II)-oxidizers") (Widdel et al., 1993). While nitrate-reducing and phototrophic Fe(II)-oxidizers live in anoxic environments, microaerophilic Fe(II)-oxidizers need to compete with the kinetics of abiotic Fe(II) oxidation

at circumneutral pH. As abiotic Fe(II) oxidation typically dominates when $O_2$ concentration is too high (>50 µM) (Druschel et al., 2008), microaerophilic Fe(II)-oxidizers can be found in habitats with microoxic conditions, such as anoxic-oxic interfaces in sediments (Weber et al., 2006), where the half-life of Fe(II) is significantly longer (Roden et al., 2004). Microaerophilic Fe(II)-oxidizers can successfully compete with abiotic Fe(II) oxidation by $O_2$ and grow in $O_2$ concentrations of 5-40 µM (Lueder et al., 2018; Maisch et al., 2019).

Fe(III)-reducing bacteria live in anoxic environments and use Fe(III) as electron acceptor for the oxidation of organic carbon such as lactate or acetate (Lovley & Phillips, 1988; Lovley, 1991), as well as hydrogen (Lovley, 1991; Kashefi et al., 2002) or ammonium (Fe-ammox) (Clément et al., 2005; Sawayama, 2006; Yang et al., 2012). Due to low solubility, most of Fe(III) occurs in the form of solid Fe(III) (oxyhydr)oxides. Therefore, mechanisms for transferring electrons from the Fe(III) minerals to the bacteria are necessary. Besides direct cell-mineral contact, the use of environmental electron shuttles such as humic substances or potentially the connection via microbial nanowires, some bacteria produce Fe(III)-chelating ligands (e.g. siderophores) that bind to Fe(III) and bring it into solution (Lovley et al., 1996; Nevin & Lovley, 2002; Luu & Ramsay, 2003; Gorby et al., 2006). Microbial and abiotic Fe redox reactions are shown in Figure 1.1.
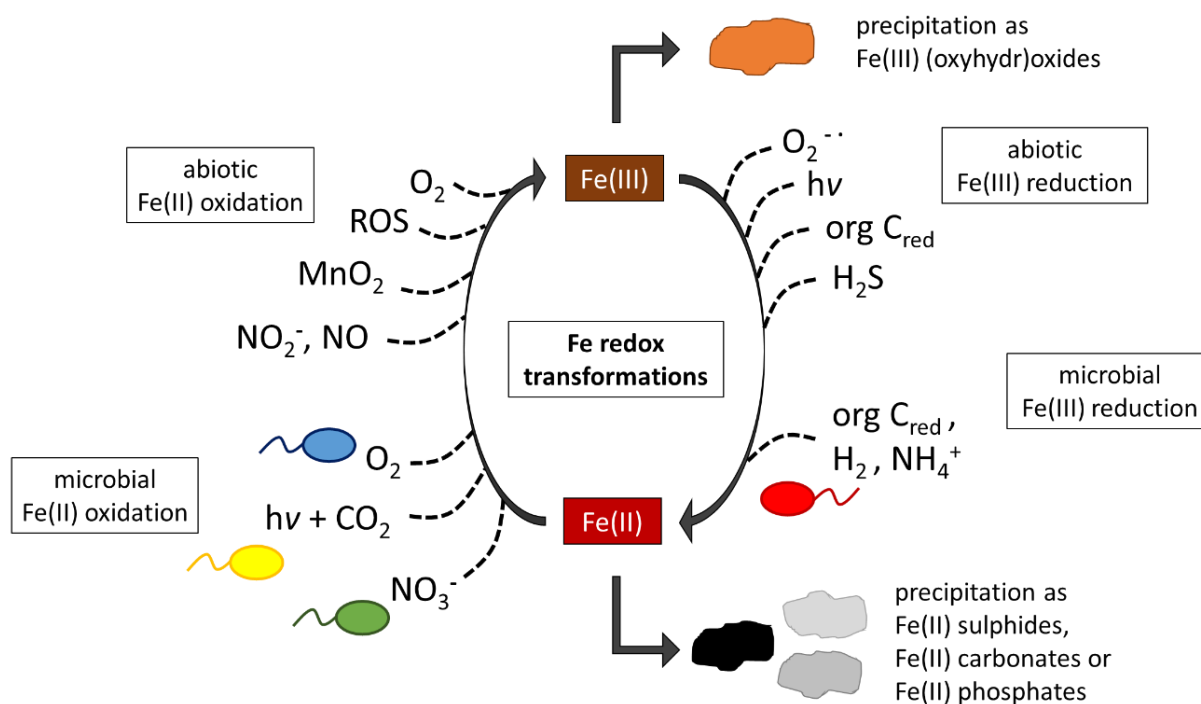
**Figure 1.1** Illustration of Fe redox transformations as well as possible Fe mineral precipitations. Fe(II) can microbially be oxidized by microaerophilic Fe(II)-oxidizers using oxygen ($O_2$) as electron acceptor (blue bacterium), by phototrophic Fe(II)-oxidizers using carbon dioxide ($CO_2$) as electron acceptor and light ($h\nu$) as energy source (yellow bacterium) as well as by nitrate-reducing Fe(II)-oxidizers using nitrate ($NO_3^-$) as electron acceptor (green bacterium). Fe(II) can abiotically be oxidized by $O_2$, reactive oxygen species (ROS), manganese oxides ($MnO_2$) and reactive nitrogen species such as nitrite ($NO_2^-$) or nitric oxide (NO). Fe(III) can microbially be reduced by Fe(III)-reducing bacteria (red bacterium) using reduced organic carbon ($C_{red}$), dihydrogen ($H_2$) or ammonium ($NH_4^+$). Fe(III) can abiotically be reduced by superoxide ($O_2^{-\cdot}$), light (usually when Fe(III) is organically complexed), reduced organic carbon and sulphide ($H_2S$).

## 1.3 Biogeochemical Fe cycling in freshwater and marine sediments

Both, abiotic and microbially catalyzed Fe redox reactions lead to the formation of Fe(II) and Fe(III) gradients in sediments (Burdige, 1993; Schmidt et al., 2010). In deeper, anoxic and reducing sediment layers, biotic and abiotic Fe(III) reduction is the dominant Fe redox process (Canfield & Thamdrup, 2009). The formed Fe(II) diffuses upwards along prevailing redox gradients until it gets either chemically or microbially oxidized (Burdige, 1993; Canfield & Thamdrup, 2009). This leads, generally expressed, to high Fe(II) concentrations in the lower, and high Fe(III) concentrations in the upper sediment layers. Not only via those abiotic and biotic Fe redox processes but also via Fe mineral dissolution or precipitation reactions, the

sedimentary biogeochemical Fe cycle is tightly coupled to other element cycles such as the carbon, nitrogen, sulphur or phosphorus cycle. By chemically reacting with other species present in the sediment, Fe might precipitate as Fe sulphides, carbonates, phosphates or (oxyhydr)oxides (Figure 1.1) (Berner, 1981; Burdige, 1993). The presence of Fe minerals also influences the mobility of contaminants such as heavy metals or organic pollutants (Borch et al., 2010).

The general biogeochemistry in sediments is characterized by gradients of different electron donors and acceptors that are mainly consumed or produced during the mineralization of organic matter (Canfield & Thamdrup, 2009). The availability of organic matter as well as the total concentrations of the respective electron acceptors or donors determine the exact spatial position and extent of the redox zones. However, the succession follows thermodynamic constraints depending on the energy yield of the microbially catalyzed reaction (Berner, 1981; Schmidt et al., 2010), even though these processes overlap in the environment (Figure 1.2) (Canfield & Thamdrup, 2009). These thermodynamically driven reactions would finally lead to steady state concentrations in the sediment. However, nature is not in equilibrium. Light availability (in sediments) changes during the day and sediment gets regularly disturbed by bioturbation, wave action or storms (Ward et al., 1984; Sanford, 1994; Kristensen & Mikkelsen, 2003; Na et al., 2008; Brand et al., 2010). This leads to fluctuating and frequently changing conditions in sediments with changing substrate fluxes across biogeochemical gradients. Microbes need to adapt to those fluctuations. All kind of Fe-metabolizing bacteria have been ubiquitously found in freshwater and marine sediments (Laufer et al., 2016b; Otte et al., 2018). They can co-exist in the same habitat competing for Fe and changing conditions in the sediment might even explain that their distribution is decoupled from prevailing geochemical gradients (Otte et al., 2018). As littoral sediments are a dynamic system that is subject to frequently changing conditions, it is unclear, how Fe gradients change and develop upon disturbing and mixing processes.
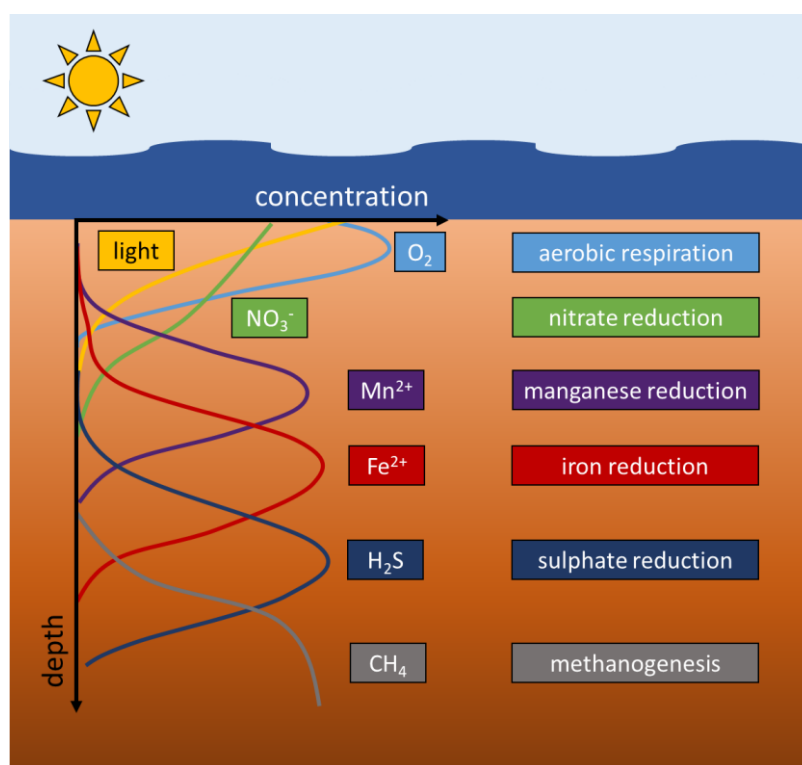
**Figure 1.2** Sketch of the theoretical depth distribution of different electron acceptors or donors or energy sources in sediments as well as respiration processes of the different redox zones following thermodynamic constraints.

Given the known sources and sinks of Fe(II) an Fe(III) in sediments in combination with the numerous connections to other elemental cycles, sedimentary Fe cycling is already very complex. However, hidden Fe(II) sources in freshwater or marine sediments could even complicate the classical sedimentary Fe cycling. With the discovery of several cryptic element cycles in the environment during the last years (Hansel et al., 2015; Kappler & Bryce, 2017), it became clear that even if certain processes or species are not visible, it does not mean that these processes do not take place or are not important – they might only have been overlooked so far. Light does not only provide energy for phototrophic Fe(II)-oxidizing bacteria (Widdel et al., 1993; Bryce et al., 2018) but also drives a series of processes in the environment such as oxygenic photosynthesis (van Grondelle et al., 1994), the degradation of organic molecules or the photochemical production of radical species (Moran & Zepp, 1997; Voelker et al., 2000; Mayer et al., 2006; Page et al., 2014). In open water bodies such as the ocean, light is able to induce photoreduction of organically complexed Fe(III), which represents an important source for nutritional $Fe^{2+}$ (Anderson & Morel, 1982; Johnson et al., 1994; Barbeau et al., 2001). In many littoral sediments, the prerequisites for this process (light and Fe(III)-organic complexes) are present as well (Kühl et al., 1994; Luther III et al., 1996; Taillefert et al., 2000), however, it was not proven yet, if it is a significant $Fe^{2+}$ source in sunlit sediments. If so, it is unclear how this additional source impacts Fe fluxes across the sedimentary redox zonation.

## 1.4 Field sites description

Two field sites were selected for this study (Figure 1.3).

Littoral freshwater sediment was collected from Lake Constance (47°41'42.63''N and 9°11'40.29''E), an oligotrophic freshwater lake with a surface area of 535 km$^2$ and a volume of 48.4 km$^3$. Lake Constance is located between Germany, Austria and Switzerland. The lake is mainly fed by the river Rhine, coming from the Alps. Coarse and fine-grained sediments transported by the Rhine accumulate in Lake Constance (Petri, 2006). Because of the glacial origin of the water, it generally only contains low amounts of minerals (Petri, 2006) and is used as drinking water. During the 1960s and 1970s, the concentration of phosphorus increased dramatically, leading to an eutrophication and changes in the biotic communities of Lake Constance (Petri, 2006). Implementations and improvements of sewage treatment plants and phosphorus reduction in detergents led to a recovery of the lake and today, Lake Constance has an oligotrophic state close to the tropic state at the beginning of the 20$^{th}$ century (Petri, 2006). Sediment from the sampling site at Lake Constance is fine to coarse grained and has a sandy texture.

Coastal marine sediment was collected from Norsminde Fjord (56°1.171'N and 10°15.390'E), a shallow estuary close to Aarhus Bay (Denmark). Norsminde Fjord has a surface area of 1.9 km$^2$ and the tidal influence is low (10-25 cm) (Jørgensen & Sørensen, 1985). The area around Norsminde Fjord is agriculturally used. The fjord is connected to the Baltic sea via a narrow opening but also receives freshwater from the river Odder (Jørgensen & Sørensen, 1985). Therefore, the salinity of the water locally varies. Sediment of Norsminde Fjord is quite muddy and fine grained and contains a lot of organic material (Laufer et al., 2016b).
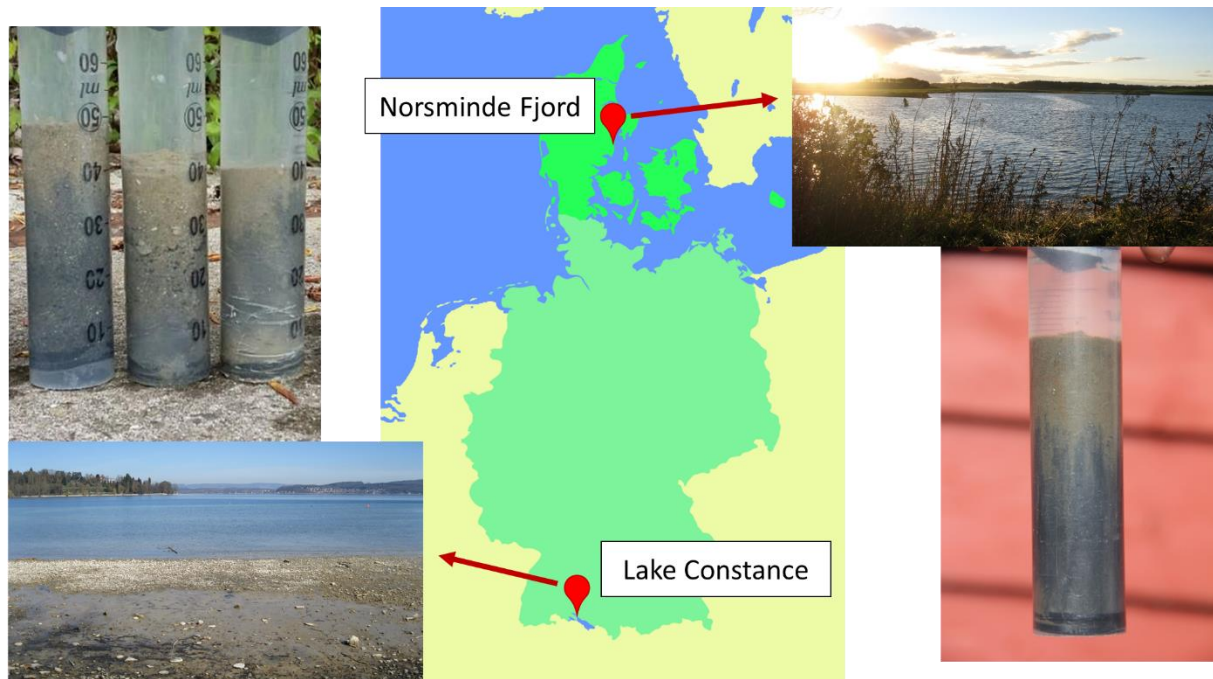
**Figure 1.3** Location, images and sediment cores of the field sites Lake Constance and Norsminde Fjord; Picture courtesy Dr. C. Schmidt and Prof. Dr. A. Kappler.

Both field sites were chosen as the geochemical parameters of the sediment and overlying water have extensively been characterized in earlier studies (Melton et al., 2012; Melton et al., 2014b; Laufer et al., 2016a; Laufer et al., 2016b; Otte et al., 2018; Schaedler et al., 2018; Otte et al., 2019). Also, all kind of Fe-metabolizing bacteria have been found to be present in the sediment of both field sites and their abundance and distribution were quantified (Laufer et al., 2016b; Otte et al., 2018). In general, the two sites represent contrasting environments in terms of salinity (freshwater vs. seawater), grain sizes (coarser, sandy vs. finer, muddy) or organic carbon content (oligotrophic vs. organic rich). Both sediments can be considered as representative sediments and therefore, comparable results obtained at sediments from both field sites can, taking into account the (bio)geochemistry, be generalized to a certain degree.

## 1.5 Objectives of this study

Although several biotic and abiotic reactions controlling Fe redox cycling are already known, the impact of light and physical perturbation has not extensively been studied towards Fe cycling in sediments yet. Therefore, in order to improve our understanding of controls of biogeochemical sedimentary Fe cycling and to reveal hidden sources and sinks of Fe(II) in sediments, the objectives of this study are:

- to first gather knowledge on Fe photochemistry in aquatic environments in order to give an overview about light availability in different habitats and to show the consequences of light driven reactions in different aquatic environments (**Chapter 2**).

- to demonstrate the impact of light on the distribution of $Fe^{2+}$ concentration gradients and $Fe^{2+}$ fluxes in sediments. Besides the use of light as energy source by phototrophic Fe(II)-oxidizing bacteria, other consequences of light as Fe(II) source or sink in sediments have not been determined yet (**Chapters 3 and 4**).

- to demonstrate that Fe(III) photoreduction does take place in freshwater sediments and to identify the dependence on light intensity and sedimentary organic carbon content. It needs to be proven if Fe(III) photoreduction is a cryptic $Fe^{2+}$ source, at which $Fe^{2+}$ is produced but immediately consumed without being able to quantify the extent of $Fe^{2+}$ production or if it is a significant $Fe^{2+}$ source leading to measurable concentrations of $Fe^{2+}$ (**Chapter 3**).

- to identify the impact of physical perturbation on the development of $Fe^{2+}$ gradients thereby serving as Fe(II) source or sink in coastal marine sediments. As upper sediment layers get frequently mixed by e.g. waves or storms, redox zones are also disturbed, including the classical Fe reduction zone. By the introduction of oxidants and the homogenization of different sediment layers, the prevailing conditions are strongly changed and the consequences for $Fe^{2+}$ concentrations and fluxes need to be deciphered (**Chapter 4**).

- to identify the impact of light on other sedimentary microorganisms (e.g. cable bacteria) besides phototrophic Fe(II)-oxidizing bacteria. Cable bacteria are known to electrically couple sulphide oxidation to the reduction of $O_2$ or nitrate over centimeter distances. If those bacteria could use light as energy source, light would have another tremendous impact on sedimentary element cycles. It was also not proven yet, if cable bacteria might be an Fe(II) sink in sediments by using Fe(II) as electron donors instead of sulphide (**Chapter 5**).

- to work out and estimate the importance of hidden Fe(II) sources and sinks in sediments with respect to Fe cycling and to add the discovered Fe(II) sources and sinks to the classical Fe cycle of opposed gradients of Fe(II) and Fe(III), as well as to summarize the role of light in sedimentary systems (**Chapter 6**).

## 1.6 References

Anderson, M. A. and Morel, F. M. M. (1982). The influence of aqueous iron chemistry on the uptake of iron by the coastal diatom *Thalassiosira weissflogii*. *Limnology and Oceanography*, **27**(5), 789-813.

Barbeau, K. (2006). Photochemistry of organic iron(III) complexing ligands in oceanic systems. *Photochemistry and Photobiology*, **82**(6), 1505-1516.

Barbeau, K., Rue, E. L., Bruland, K. W. and Butler, A. (2001). Photochemical cycling of iron in the surface ocean mediated by microbial iron(III)-binding ligands. *Nature*, **413**, 409.

Berner, R. A. (1981). A new geochemical classification of sedimentary environments. *Journal of Sedimentary Research*, **51**(2), 359-365.

Borch, T., Kretzschmar, R., Kappler, A., Cappellen, P. V., Ginder-Vogel, M., Voegelin, A. and Campbell, K. (2010). Biogeochemical redox processes and their impact on contaminant dynamics. *Environmental Science & Technology*, **44**(1), 15-23.

Boyd, P. W. and Ellwood, M. J. (2010). The biogeochemical cycle of iron in the ocean. *Nature Geoscience*, **3**, 675.

Brand, A., Lacy, J. R., Hsu, K., Hoover, D., Gladding, S. and Stacey, M. T. (2010). Wind-enhanced resuspension in the shallow waters of South San Francisco Bay: Mechanisms and potential implications for cohesive sediment transport. *Journal of Geophysical Research: Oceans*, **115**(C11).

Bryce, C., Blackwell, N., Schmidt, C., Otte, J., Huang, Y.-M., Kleindienst, S., Tomaszewski, E., Schad, M., Warter, V., Peng, C., Byrne, J. M. and Kappler, A. (2018). Microbial anaerobic Fe(II) oxidation – Ecology, mechanisms and environmental implications. *Environmental Microbiology*, **20**(10), 3462-3483.

Burdige, D. J. (1993). The biogeochemistry of manganese and iron reduction in marine sediments. *Earth-Science Reviews*, **35**(3), 249-284.

Canfield, D. E. (1989). Reactive iron in marine sediments. *Geochimica et Cosmochimica Acta*, **53**(3), 619-632.

Canfield, D. E. and Thamdrup, B. (2009). Towards a consistent classification scheme for geochemical environments, or, why we wish the term 'suboxic' would go away. *Geobiology*, **7**(4), 385-392.

Clément, J.-C., Shrestha, J., Ehrenfeld, J. G. and Jaffé, P. R. (2005). Ammonium oxidation coupled to dissimilatory reduction of iron under anaerobic conditions in wetland soils. *Soil Biology and Biochemistry*, **37**(12), 2323-2328.

Cornell, R. M. and Schwertmann, U. (2003). *The iron oxides: structure, properties, reactions, occurrences, and uses*. Weinheim, Wiley-VCH.

Davison, W. and Seed, G. (1983). The kinetics of the oxidation of ferrous iron in synthetic and natural waters. *Geochimica et Cosmochimica Acta*, **47**(1), 67-79.

Druschel, G. K., Emerson, D., Sutka, R., Suchecki, P. and Luther, G. W. (2008). Low-oxygen and chemical kinetic constraints on the geochemical niche of neutrophilic iron(II) oxidizing microorganisms. *Geochimica et Cosmochimica Acta*, **72**(14), 3358-3370.

Emerson, D., Fleming, E. J. and McBeth, J. M. (2010). Iron-Oxidizing Bacteria: An Environmental and Genomic Perspective. *Annual Review of Microbiology*, **64**(1), 561-583.

Emerson, D. and Moyer, C. (1997). Isolation and characterization of novel iron-oxidizing bacteria that grow at

circumneutral pH. *Applied and Environmental Microbiology*, **63**(12), 4784-4792.

Emmenegger, L., Schönenberger, R., Sigg, L. and Sulzberger, B. (2001). Light-induced redox cycling of iron in circumneutral lakes. *Limnology and Oceanography*, **46**(1), 49-61.

Gorby, Y. A., Yanina, S., McLean, J. S., Rosso, K. M., Moyles, D., Dohnalkova, A., Beveridge, T. J., Chang, I. S., Kim, B. H., Kim, K. S., Culley, D. E., Reed, S. B., Romine, M. F., Saffarini, D. A., Hill, E. A., Shi, L., Elias, D. A., Kennedy, D. W., Pinchuk, G., Watanabe, K., Ishii, S. i., Logan, B., Nealson, K. H. and Fredrickson, J. K. (2006). Electrically conductive bacterial nanowires produced by *Shewanella oneidensis* strain MR-1 and other microorganisms. *Proceedings of the National Academy of Sciences*, **103**(30), 11358-11363.

Hansel, C. M., Ferdelman, T. G. and Tebo, B. M. (2015). Cryptic cross-linkages among biogeochemical cycles: novel insights from reactive intermediates. *Elements*, **11**(6), 409-414.

Johnson, K. S., Coale, K. H., Elrod, V. A. and Tindale, N. W. (1994). Iron photochemistry in seawater from the equatorial Pacific. *Marine Chemistry*, **46**(4), 319-334.

Jørgensen, B. B. (1977). The sulfur cycle of a coastal marine sediment (Limfjorden, Denmark). *Limnology and Oceanography*, **22**(5), 814-832.

Jørgensen, B. B. and Sørensen, J. (1985). Seasonal cycles of $O_2$, $NO_3^-$ and $SO_4^{2-}$ reduction in estuarine sediments: the significance of an $NO_3^-$ reduction maximum in spring. *Marine Ecology Progress Series*, **24**(1/2), 65-74.

Kappler, A. and Bryce, C. (2017). Cryptic biogeochemical cycles: unravelling hidden redox reactions. *Environmental Microbiology*, **19**(3), 842-846.

Kappler, A. and Straub, K. L. (2005). Geomicrobiological cycling of iron. *Reviews in Mineralogy and Geochemistry*, **59**(1), 85-108.

Kashefi, K., Tor, J. M., Holmes, D. E., Gaw Van Praagh, C. V., Reysenbach, A.-L. and Lovley, D. R. (2002). Geoglobus ahangari gen. nov., sp. nov., a novel hyperthermophilic archaeon capable of oxidizing organic acids and growing autotrophically on hydrogen with Fe(III) serving as the sole electron acceptor. *International Journal of Systematic and Evolutionary Microbiology*, **52**(3), 719-728.

King, A. L. and Barbeau, K. A. (2011). Dissolved iron and macronutrient distributions in the southern California Current System. *Journal of Geophysical Research: Oceans*, **116**(C3).

Kraemer, S. M. (2004). Iron oxide dissolution and solubility in the presence of siderophores. *Aquatic Sciences*, **66**(1), 3-18.

Kristensen, E. and Mikkelsen, O. L. (2003). Impact of the burrow-dwelling polychaete Nereis diversicolor on the degradation of fresh and aged macroalgal detritus in a coastal marine sediment. *Marine Ecology Progress Series*, **265**, 141-153.

Kühl, M., Lassen, C. and Jørgensen, B. B. (1994). Light penetration and light intensity in sandy marine sediments measured with irradiance and scalar irradiance fiber-optic microprobes. *Marine Ecology Progress Series*, **105**(1/2), 139-148.

Laufer, K., Byrne, J. M., Glombitza, C., Schmidt, C., Jørgensen, B. B. and Kappler, A. (2016a). Anaerobic microbial Fe(II) oxidation and Fe(III) reduction in coastal marine sediments controlled by organic carbon content. *Environmental Microbiology*, **18**(9), 3159-3174.

Laufer, K., Nordhoff, M., Røy, H., Schmidt, C., Behrens, S., Jørgensen, B. B. and Kappler, A. (2016b). Coexistence of microaerophilic, nitrate-reducing, and phototrophic Fe(II)-oxidizers and Fe(III)-reducers in coastal marine sediment. *Applied and Environmental Microbiology*, **82**(5), 1433-1447.

Lovley, D. R. (1991). Dissimilatory Fe(III) and Mn(IV) reduction. *Microbiological Reviews*, **55**(2), 259-287.

Lovley, D. R., Coates, J. D., Blunt-Harris, E. L., Phillips, E. J. P. and Woodward, J. C. (1996). Humic substances as electron acceptors for microbial respiration. *Nature*, **382**(6590), 445-448.

Lovley, D. R. and Phillips, E. J. P. (1988). Novel mode of microbial energy metabolism: organic carbon oxidation coupled to dissimilatory reduction of iron or manganese. *Applied and Environmental Microbiology*, **54**(6), 1472-1480.

Lueder, U., Druschel, G., Emerson, D., Kappler, A. and Schmidt, C. (2018). Quantitative analysis of $O_2$ and $Fe^{2+}$ profiles in gradient tubes for cultivation of microaerophilic iron(II)-oxidizing bacteria. *FEMS Microbiology Ecology*, **94**(2).

Luther III, G. W., Shellenbarger, P. A. and Brendel, P. J. (1996). Dissolved organic Fe(III) and Fe(II) complexes in salt marsh porewaters. *Geochimica et Cosmochimica Acta*, **60**(6), 951-960.

Luu, Y.-S. and Ramsay, J. A. (2003). Review: microbial mechanisms of accessing insoluble Fe(III) as an energy source. *World Journal of Microbiology and Biotechnology*, **19**(2), 215-225.

Maisch, M., Lueder, U., Laufer, K., Scholze, C., Kappler, A. and Schmidt, C. (2019). Contribution of microaerophilic iron(II)-oxidizers to iron(III) mineral formation. *Environmental Science & Technology*, **53**(14), 8197-8204.

Mayer, L. M., Schick, L. L., Skorko, K. and Boss, E. (2006). Photodissolution of particulate organic matter from sediments. *Limnology and Oceanography*, **51**(2), 1064-1071.

Melton, E. D., Swanner, E. D., Behrens, S., Schmidt, C. and Kappler, A. (2014a). The interplay of microbially mediated and abiotic reactions in the biogeochemical Fe cycle. *Nat Rev Micro*, **12**(12), 797-808.

Melton, E. D., Schmidt, C. and Kappler, A. (2012). Microbial Iron(II) Oxidation in Littoral Freshwater Lake Sediment: The Potential for Competition between Phototrophic vs. Nitrate-Reducing Iron(II)-Oxidizers. *Frontiers in Microbiology*, **3**, 197.

Melton, E. D., Stief, P., Behrens, S., Kappler, A. and Schmidt, C. (2014b). High spatial resolution of distribution and interconnections between Fe- and N-redox processes in profundal lake sediments. *Environmental Microbiology*, **16**(10), 3287-3303.

Millero, F. J., Sotolongo, S. and Izaguirre, M. (1987). The oxidation kinetics of Fe(II) in seawater. *Geochimica et Cosmochimica Acta*, **51**(4), 793-801.

Moran, M. A. and Zepp, R. G. (1997). Role of photoreactions in the formation of biologically labile compounds from dissolved organic matter. *Limnology and Oceanography*, **42**(6), 1307-1316.

Na, T., Gribsholt, B., Galaktionov, O. S., Lee, T. and Meysman, F. J. R. (2008). Influence of advective bio-irrigation on carbon and nitrogen cycling in sandy sediments. *Journal of Marine Research*, **66**(5), 691-722.

Nevin, K. P. and Lovley, D. R. (2002). Mechanisms for Fe(III) oxide reduction in sedimentary environments. *Geomicrobiology Journal*, **19**(2), 141-159.

Otte, J. M., Blackwell, N., Ruser, R., Kappler, A., Kleindienst, S. and Schmidt, C. (2019). $N_2O$ formation by nitrite-induced (chemo)denitrification in coastal marine sediment. *Scientific Reports*, **9**(1), 10691-10691.

Otte, J. M., Harter, J., Laufer, K., Blackwell, N., Straub, D., Kappler, A. and Kleindienst, S. (2018). The distribution of active iron-cycling bacteria in marine and freshwater sediments is decoupled from geochemical gradients. *Environmental Microbiology*, **20**(7), 2483-2499.

Page, S. E., Logan, J. R., Cory, R. M. and McNeill, K. (2014). Evidence for dissolved organic matter as the primary source and sink of photochemically produced hydroxyl radical in arctic surface waters. *Environmental Science: Processes & Impacts*, **16**(4), 807-822.

Petri, M. (2006). Water Quality of Lake Constance. *The Rhine*. T. P. Knepper. Berlin, Heidelberg, Springer Berlin Heidelberg**:** 127-138.

Pyzik, A. J. and Sommer, S. E. (1981). Sedimentary iron monosulfides: Kinetics and mechanism of formation. *Geochimica et Cosmochimica Acta*, **45**(5), 687-698.

Rentz, J. A., Kraiya, C., Luther, G. W. and Emerson, D. (2007). Control of ferrous iron oxidation within circumneutral microbial iron mats by cellular activity and autocatalysis. *Environmental Science & Technology*, **41**(17), 6084-6089.

Roden, E., Sobolev, D., Glazer, B. and Luther, G. W. (2004). Potential for microscale bacterial Fe redox cycling at the aerobic-anaerobic interface. *Geomicrobiology Journal*, **21**(6), 379-391.

Sanford, L. P. (1994). Wave-forced resuspension of upper Chesapeake Bay muds. *Estuaries*, **17**(1), 148-165.

Sawayama, S. (2006). Possibility of anoxic ferric ammonium oxidation. *Journal of Bioscience and Bioengineering*, **101**(1), 70-72.

Schaedler, F., Lockwood, C., Lueder, U., Glombitza, C., Kappler, A. and Schmidt, C. (2018). Microbially mediated coupling of Fe and N cycles by nitrate-reducing Fe(II)-oxidizing bacteria in littoral freshwater sediments. *Applied and Environmental Microbiology*, **84**(2), e02013-02017.

Schmidt, C., Behrens, S. and Kappler, A. (2010). Ecosystem functioning from a geomicrobiological perspective a conceptual framework for biogeochemical iron cycling. *Environmental Chemistry*, **7**(5), 399-405.

Straub, K. L., Benz, M., Schink, B. and Widdel, F. (1996). Anaerobic, nitrate-dependent microbial oxidation of ferrous iron. *Applied and Environmental Microbiology*, **62**(4), 1458-1460.

Stumm, W. and Lee, G. F. (1961). Oxygenation of Ferrous Iron. *Industrial & Engineering Chemistry*, **53**(2), 143-146.

Stumm, W. and Morgan, J. J. (1996). *Aquatic chemistry: chemical equilibria and rates in natural waters*, Wiley.

Sulzberger, B., Suter, D., Siffert, C., Banwart, S. and Stumm, W. (1989). Dissolution of Fe(III)(hydr)oxides in natural waters; laboratory assessment on the kinetics controlled by surface coordination. *Marine Chemistry*, **28**(1), 127-144.

Taillefert, M., Bono, A. B. and Luther, G. W. (2000). Reactivity of freshly formed Fe(III) in synthetic solutions and (pore)waters: voltammetric evidence of an aging process. *Environmental Science & Technology*, **34**(11), 2169-2177.

Tamura, H., Goto, K. and Nagayama, M. (1976). The effect of ferric hydroxide on the oxygenation of ferrous ions in neutral

solutions. *Corrosion Science*, **16**(4), 197-207.

Thamdrup, B., Fossing, H. and Jørgensen, B. B. (1994). Manganese, iron and sulfur cycling in a coastal marine sediment, Aarhus bay, Denmark. *Geochimica et Cosmochimica Acta*, **58**(23), 5115-5129.

van Grondelle, R., Dekker, J. P., Gillbro, T. and Sundstrom, V. (1994). Energy transfer and trapping in photosynthesis. *Biochimica et Biophysica Acta (BBA) - Bioenergetics*, **1187**(1), 1-65.

Voelker, B. M., Sedlak, D. L. and Zafiriou, O. C. (2000). Chemistry of superoxide radical in seawater: reactions with organic Cu complexes. *Environmental Science & Technology*, **34**(6), 1036-1042.

Ward, L. G., Michael Kemp, W. and Boynton, W. R. (1984). The influence of waves and seagrass communities on suspended particulates in an estuarine embayment. *Marine Geology*, **59**(1), 85-103.

Weber, K. A., Achenbach, L. A. and Coates, J. D. (2006). Microorganisms pumping iron: anaerobic microbial iron oxidation and reduction. *Nat Rev Micro*, **4**(10), 752-764.

Weiss, J. (1935). Elektronenübergangsprozesse im Mechanismus von Oxydations- und Reduktionsreaktionen in Lösungen. *Naturwissenschaften*, **23**(4), 64-69.

Widdel, F., Schnell, S., Heising, S., Ehrenreich, A., Assmus, B. and Schink, B. (1993). Ferrous iron oxidation by anoxygenic phototrophic bacteria. *Nature*, **362**(6423), 834-836.

Yang, W. H., Weber, K. A. and Silver, W. L. (2012). Nitrogen loss from soil through anaerobic ammonium oxidation coupled to iron reduction. *Nature Geoscience*, **5**(8), 538-541.

## Chapter 2 – Personal contribution

Literature research was performed by myself. The manuscript was written by myself. Dr. Caroline Schmidt, Prof. Andreas Kappler and Prof. Bo Barker Jørgensen revised the manuscript.

# Chapter 2: Photochemistry of iron in aquatic environments

Ulf Lueder[1], Bo Barker Jørgensen[2], Andreas Kappler[1,2], Caroline Schmidt[1]

[1] Geomicrobiology, Center for Applied Geoscience (ZAG), University of Tuebingen, Germany

[2] Center for Geomicrobiology, Department of Bioscience, Aarhus University, Denmark

**Environmental significance statement**

Light drives a series of physico-chemical reactions in natural environments and it has a huge impact on the development of microbial life. Iron is required as trace element for almost any kind of living organisms and its provision in aquatic environments is controlled by iron(III) photoreduction. Here we summarize the current knowledge of the reaction network that connects light and aquatic environments via the redox cycling of iron and the consecutive formation of reactive oxygen species.

## 2.1 Abstract

Light energy is a driver for many biogeochemical element cycles in aquatic systems. The sunlight-induced photochemical reduction of ferric iron (Fe(III) photoreduction) to ferrous iron (Fe(II)) by either direct ligand-to-metal charge transfer or by photochemically produced radicals can be an important source of dissolved $Fe^{2+}_{aq}$ in aqueous and sedimentary environments. Reactive oxygen species (ROS) are formed by a variety of light-dependent reactions. Those ROS can oxidize Fe(II) or reduce Fe(III), and due to their high reactivity they are key oxidants in aquatic systems where they influence many other biogeochemical cycles. In oxic waters with circumneutral pH, the produced Fe(II) serves as a nutrient, whereas in acidic waters, freshwater and marine sediments, which are rich in $Fe^{2+}$, the photochemically formed Fe(II) can be used as additional electron donor for acidophilic aerobic, microaerophilic, phototrophic and, if nitrate is present, for nitrate-reducing Fe(II)-oxidizing bacteria. Therefore, Fe(III) photoreduction may not only control the primary productivity in the oceans but has a tremendous impact on Fe cycling in the littoral zone of freshwater and marine environments. In this review, we summarize photochemical reactions involving Fe, discuss the role of ROS in Fe cycling, and highlight the importance of photoreductive processes in the environment.

## 2.1 Light availability on Earth

The sun provides our planet with light and thereby with enormous amounts of energy (Dresselhaus & Thomas, 2001; Scholes et al., 2011). Light can be described as electromagnetic radiation, propagating as wave through space (Ball, 2007). It consists of a wide range of wavelengths (electromagnetic spectrum) ranging from the very short and energy-rich gamma rays (<0.01 nm) to the very long and energy-poor radio waves (>10 cm). The visible light (VIS) of the electromagnetic spectrum covers only a narrow band of wavelengths ranging from 400 nm (violet) to 700 nm (red) (Ball, 2007). Large parts of the electromagnetic spectrum coming from the sun are reflected or absorbed in the atmosphere, e.g. by ozone, aerosols or water vapor, before reaching the Earth's surface (Zepp & Cline, 1977; Horvath, 1993). Especially shorter wavelength radiation (<400 nm), which has the potential to photochemically damage cells (Karentz, 1994; Piazena et al., 2002), virtually does not pass the atmosphere or only to a small extent (Figure 2.1) (Zepp & Cline, 1977). On a cloudless day, typically 3-5% of the total surface irradiance is UVA (320 nm- 400 nm) and UVB (280 nm- 320 nm) light (Larson & Berenbaum, 1988; Nunez et al., 1994; Grant & Heisler, 2000), but the percentage depends on latitude, season, time of the day and absorbing substances in the atmosphere such as ozone (Larson & Berenbaum, 1988). Light can also be seen as particles of energy (photons) (Ball, 2006) and light intensity can be denoted as photon flux in $\mu$mol photons $m^{-2} s^{-1}$ (microeinstein) or as spectral irradiance in $W m^{-2} nm^{-1}$ giving the power of a particular wavelength of light (Scholes et al., 2011). The photon flux reaching the Earth's surface during the day is on average a few hundred (Scholes et al., 2011) to 2000 $\mu$mol photons $m^{-2} s^{-1}$ under full sunlight (Kiang et al., 2007; Masojídek & Torzillo, 2008). In lakes or in the ocean, the light intensity decreases exponentially with water depth by absorption and scattering (Zepp & Cline, 1977) and the light penetration depth into the water depends on concentration and composition of attenuating substances such as phytoplankton, particles or dissolved organic molecules in the water column as well as on wavelength (Figure 2.1) (Piazena et al., 2002). In the clearest natural waters, visible light reaches a depth of 170 m with 1% of the surface irradiance remaining, whereas in highly turbid waters, this threshold is already reached in a few meters depth (Smith & Baker, 1981; Piazena et al., 2002). The infrared wavelength region (IR, 700 nm to 100 $\mu$m) of the electromagnetic spectrum is absorbed most strongly in the water column, followed by UV light (1 nm to 400 nm) if the concentration of attenuating substances is low (Duntley, 1963; Johannessen et al., 2003). The greatest transparency of clear ocean water lies with 480 nm in the blue region of the VIS range (Duntley, 1963) and light attenuation in water generally increases with longer wavelengths (Smith & Baker, 1981). Reaching the sediment surface, e.g.

in littoral waters, light is penetrating into the sediment, depending on particle size and composition (Kühl et al., 1994). While UV light usually only penetrates some hundreds of micrometers into the sediment (Garcia-Pichel, 1995; Garcia-Pichel & Bebout, 1996). light in the VIS range can penetrate several millimeters whereby light penetration depth decreases with decreasing grain size (Kühl et al., 1994). Directly on the sediment surface, the scalar irradiance (i.e. the light coming from all directions at one point) (Kühl et al., 1994) can be up to 280% of the incident irradiance due to scattering effects of the sediment particles (Kühl et al., 1994). In contrast to the water column, light in the range of 450 to 500 nm (blue) is attenuated most strongly in sediments and attenuation decreases towards longer wavelengths, lowest in the IR region (Figure 2.1) (Kühl et al., 1994).
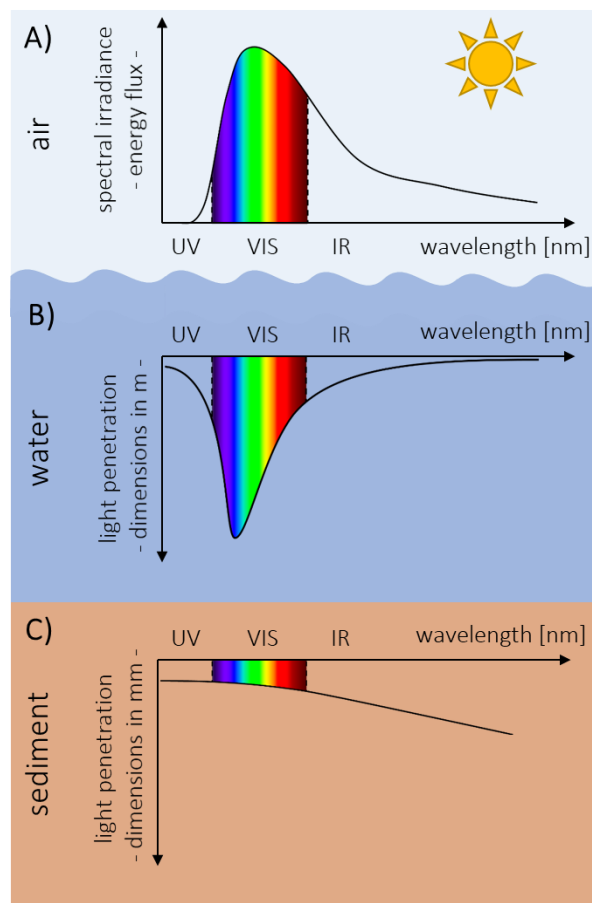


**Figure 2.1** A) Simplified daylight spectrum as energy flux reaching the Earth's surface; B) and C) Qualitative light penetration into water or sediment (here: pure sand) showing the relative depth, where 1% remains of the spectral energy flux at the water or sediment surface, respectively.

## 2.2 Impact of light in aquatic environments

The most important biochemical process in aquatic environments that is relying on light is oxygenic photosynthesis. During this process, plants or cyanobacteria absorb solar energy of specific wavelength regions in light-harvesting pigments by structures called chromophores (van Grondelle et al., 1994; Farjalla et al., 2009), convert light energy into chemical energy (ATP) and further by $CO_2$ fixation into biomass and release oxygen ($O_2$) as a by-product (Kiang et al., 2007). Additionally, also anoxygenic phototrophic microorganisms such as green sulphur, purple sulphur or purple non-sulphur bacteria, use light as energy source for their metabolisms. Instead of water, they use reduced inorganic or organic compounds as electron donor, e.g. sulphide, hydrogen or ferrous iron (Fe(II)) (anoxygenic photosynthesis) (Larsen, 1952; Widdel et al., 1993; Yurkov & Beatty, 1998; Bryce et al., 2018). However, light is not only the energy source of such biochemical reactions but also provides energy for purely photochemical processes in the environment. Larger molecules of dissolved organic matter (DOM) can photochemically be degraded by light, especially in the UV region (280-400 nm) (Moran & Zepp, 1997; Johannessen et al., 2003; Scully et al., 2003; Mayer et al., 2006). resulting in the production of a variety of organic molecules with reduced molecular weight (Geller, 1985; Miller & Moran, 1997; Moran & Zepp, 1997) or in the production of dissolved inorganic carbon (photochemical mineralization of DOM) (Miles & Brezonik, 1981; Miller & Zepp, 1995; Moran & Zepp, 1997). The photochemically formed products can have different chemical properties with increased or decreased bioavailability (Kieber et al., 1989; Miller & Moran, 1997; Moran & Zepp, 1997; Benner & Biddanda, 1998; Bertilsson & Stefan, 1998; Tranvik & Bertilsson, 2001; Scully et al., 2003). Light-induced dissolution of particulate organic matter from resuspended sediments releases significant amounts of dissolved organic carbon (DOC) into the water column, especially in coastal or estuarine regions that receive large sediment plumes (Kieber et al., 2006; Mayer et al., 2006; Riggsbee et al., 2008; Southwell et al., 2011). During photolysis of DOM, also reactive oxygen species (ROS) such as singlet oxygen ($^1O_2$), superoxide ($O_2^{-\bullet}$), hydroxyl radical ($OH^\bullet$) and hydrogen peroxide ($H_2O_2$) can form (Zepp et al., 1992; Scully et al., 1996; Sandvik et al., 2000; Barbeau, 2006; Farjalla et al., 2009; Garg et al., 2011; Page et al., 2014), which have tremendous implications on different biogeochemical processes due to their high reactivity (Voelker et al., 2000; Goldstone et al., 2002; Scully et al., 2003; Marshall et al., 2005; Garg et al., 2011). Photochemically produced superoxide or $H_2O_2$ are able to reduce for instance manganese oxides (Baral et al., 1985) and the photoreduction of manganese oxides by dissolved organic substances induced by sunlight

is an important reaction for maintaining dissolved Mn(II) concentrations in seawater for supply of manganese to phytoplankton (Sunda et al., 1983; Sunda & Huntsman, 1994).

Besides the importance of light in the cycling of carbon or manganese, light is also a driving force in the Fe redox cycle of aquatic environments and sediments as it is able to photochemically induce the reduction of Fe(III) to Fe(II) (Fe(III) photoreduction). Light induced reactions are shown in Figure 2.2. In this review, we summarize photochemical processes of Fe in aquatic ecosystems including the mechanisms responsible for light-induced reduction of Fe(III) and discuss the consequences of these photochemical reactions for biogeochemical Fe cycling.
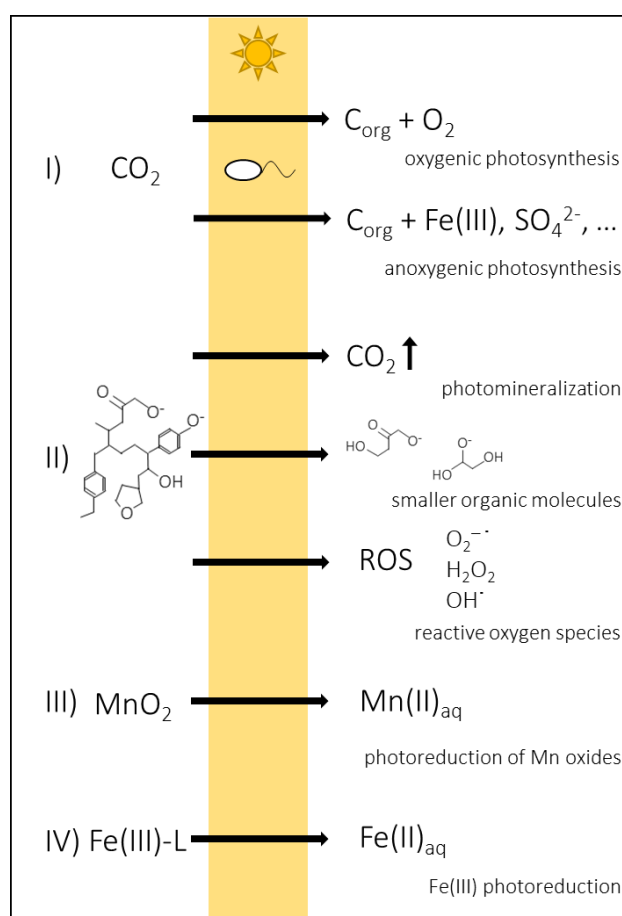


**Figure 2.2** Illustration of light induced reactions: I) Oxygenic and anoxygenic photosynthesis, II) Degradation of dissolved organic carbon (DOC) by light forming $CO_2$, smaller organic molecules and/or reactive oxygen species (ROS), III) Photoreduction of manganese oxides ($MnO_2$), IV) Photoreduction of organically complexed Fe(III) (Fe(III)-L).
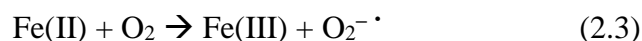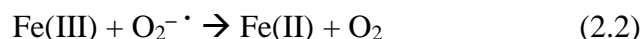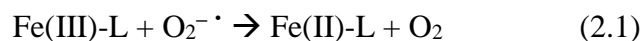
## 2.3 General mechanisms of Fe photochemistry

In aquatic systems and sediments with circumneutral pH, dissolved Fe(III) ($Fe^{3+}_{aq}$) occurs only complexed with organic molecules due to the poor solubility of Fe(III) and its tendency to precipitate as poorly soluble Fe(III) (oxyhydr)oxides (O'Sullivan et al., 1991; Kuma et al., 1995; Kuma et al., 1996; Sulzberger, 2015). Depending on the kind of organic ligand, organically complexed Fe(III) can undergo photochemical reactions i) by direct photon absorption and ligand-to-metal charge transfer (LMCT), at which an electron is transferred from the ligand to the Fe(III) (Kuma et al., 1995; Voelker et al., 1997; Barbeau, 2006), or ii) by indirect, secondary reactions with photochemically produced radicals such as superoxide (Miller et al., 1995; Voelker & Sedlak, 1995; Rose & Waite, 2005; Barbeau, 2006).

The type of organic ligand and its specific functional groups control the overall photochemical reactivity towards LMCT reactions of the dissolved complexes (Barbeau, 2006; Rijkenberg et al., 2006). For instance, the carboxylate group, which is a common functional group of dissolved organic compounds such as citrate or oxalate, is able to complex Fe(III) and to undergo photochemical reactions by photo-induced charge transfer (Faust & Hoigné, 1990; Zuo & Hoigne, 1992; Kuma et al., 1995; Feng & Nansheng, 2000). Organic ligands can also interact with Fe(III) (oxyhydr)oxide mineral or colloidal surfaces, where a photochemically mediated charge transfer from the ligand to the surface Fe(III) leads first to a reduction of Fe(III) to Fe(II), followed by either a re-oxidation of Fe(II) or by a dissociation of the formed Fe(II) from the surface leading to mineral dissolution (Waite & Morel, 1984; Sulzberger et al., 1989; Siffert & Sulzberger, 1991; Sulzberger & Laubscher, 1995; Barbeau, 2006; Borer et al., 2009a). Photoreductive dissolution rates of Fe(III) (oxyhydr)oxides and colloidal Fe particles generally decrease with increasing pH (Waite & Morel, 1984). For photoreductive mineral dissolution, organic complexation of Fe(III) is not a necessary prerequisite. However, the photochemically induced reduction of inorganic Fe(III)-hydroxo complexes on mineral surfaces by a charge transfer from the surface hydroxide ion to the Fe(III) proceeds less efficient and only at acidic pH (Waite & Morel, 1984; Sulzberger et al., 1989; Siffert & Sulzberger, 1991; King et al., 1993; Sherman, 2005; Borer et al., 2009a; Borer et al., 2009b). Therefore, photoreduction of inorganic Fe(III)-hydroxo complexes is not a significant source of Fe(II) in waters above pH 6.5 (King et al., 1995).
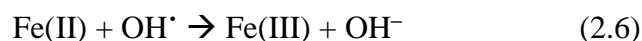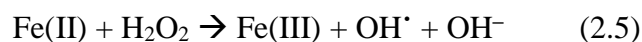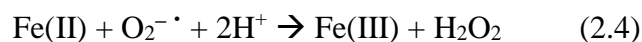
The rate of photochemical LMCT reactions depends, besides intrinsic properties of the Fe(III) complex, on temperature, pH and ionic strength of the surrounding environment, as well as on the intensity and wavelength of the absorbed light (David & David, 1976; Collienne, 1983;

Waite & Morel, 1984; King et al., 1993; Kuma et al., 1995; Sulzberger & Laubscher, 1995; Voelker et al., 1997; Emmenegger et al., 2001; McKnight et al., 2001). Higher light intensities and lower wavelengths lead to faster Fe(III) photoreduction rates (King et al., 1993; Sulzberger & Laubscher, 1995; Barbeau et al., 2001; Emmenegger et al., 2001; Borer et al., 2009b). Thus, light below certain wavelengths with sufficient energy is necessary to induce the photochemical LMCT reaction from a ligand to Fe(III), depending on the molecular structure of the complex. UV and lower wavelengths of the VIS region (<520 nm) of the solar spectrum are able to photochemically reduce Fe(III) complexes (Rich & Morel, 1990; Borer et al., 2009b).

Secondary photochemically induced reduction of Fe(III) in natural waters at circumneutral pH is most likely mediated by superoxide by either the reduction of a Fe(III)-ligand complex (Fe(III)-L) to a Fe(II)-ligand complex (Fe(II)-L) (eq. 2.1) or by the reduction of Fe(III) which dissociated from a ligand prior to reduction by superoxide (eq. 2.2) (Figure 2.3) (Miller et al., 1995; Voelker & Sedlak, 1995; Kustka et al., 2005; Rose & Waite, 2005). Superoxide forms in oxic waters by photochemical reaction of DOM with $O_2$ (Cooper et al., 1988; Garg et al., 2011), it can be produced by marine phytoplankton (Kim et al., 2000; Kustka et al., 2005; Rose et al., 2005) or during reaction of Fe(II) with $O_2$ (eq. 2.3) (Figure 2.3) (Meunier et al., 2005; Santana-Casiano et al., 2006).

$$Fe(III)\text{-}L + O_2^{-\bullet} \rightarrow Fe(II)\text{-}L + O_2 \qquad (2.1)$$

$$Fe(III) + O_2^{-\bullet} \rightarrow Fe(II) + O_2 \qquad (2.2)$$

$$Fe(II) + O_2 \rightarrow Fe(III) + O_2^{-\bullet} \qquad (2.3)$$

Superoxide can not only reduce Fe(III), but can also serve as oxidant of Fe(II) forming hydrogen peroxide (eq. 2.4), which in turn forms hydroxyl radicals after reaction with Fe(II) (Fenton reaction, eq. 2.5). Hydroxyl radicals can also oxidize Fe(II) forming hydroxide ions (eq. 2.6) (Figure 2.3) (Rose & Waite, 2002; Santana-Casiano et al., 2006).

$$Fe(II) + O_2^{-\bullet} + 2H^+ \rightarrow Fe(III) + H_2O_2 \qquad (2.4)$$

$$Fe(II) + H_2O_2 \rightarrow Fe(III) + OH^{\bullet} + OH^- \qquad (2.5)$$

$$Fe(II) + OH^{\bullet} \rightarrow Fe(III) + OH^- \qquad (2.6)$$
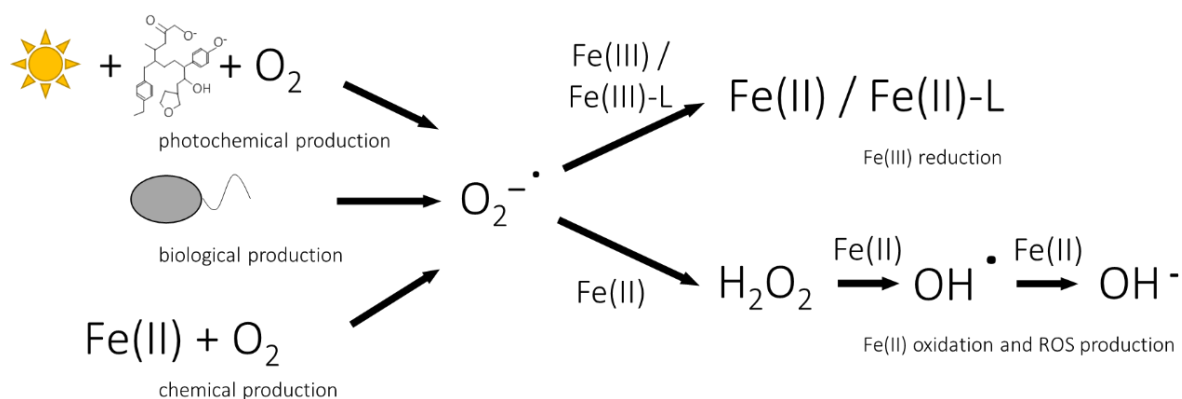
**Figure 2.3** Superoxide ($O_2^{-\cdot}$) production processes via photochemical reaction of DOM with $O_2$, biological production by marine phytoplankton or during the oxidation of Fe(II) by $O_2$ as well as superoxide consumption processes via Fe(III) reduction or Fe(II) oxidation.

Light energy is able to photo-oxidize dissolved Fe(II) to dissolved Fe(III) forming dihydrogen gas (eq. 2.7).

$$2Fe^{2+}_{aq}(II) + 2H^+ + h\nu \rightarrow 2Fe^{3+}_{aq}(III) + H_2 \quad (2.7)$$
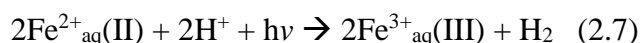
While at acidic pH the photo-oxidation of $Fe^{2+}_{aq}$ requires UV light with wavelengths in the range of 200-300 nm (Braterman et al., 1984; Borowska & Mauzerall, 1987; Konhauser et al., 2007), the reaction at circumneutral pH is induced also by UV light with higher wavelengths due to the formation of the complex $Fe(OH)^+$, which is sensitive to wavelengths >300 nm (Braterman et al., 1983; Braterman et al., 1984; François, 1986; Anbar & Holland, 1992). However, it was shown that this reaction does not produce significant amounts of Fe(III) at seawater conditions (Konhauser et al., 2007). Due to absorption in the atmosphere, e.g. by ozone (Horvath, 1993), only a low flux of UV is reaching the surface of the Earth and the oceans and due to only small concentrations of $Fe^{2+}_{aq}$ in oxic waters, the impact of photooxidation of Fe(II) in the water column and in sediments is presumably negligible.

## 2.4 Fe(III) photoreduction in oceans and the role of siderophores

Concentrations of dissolved Fe in oceans are extremely low (pico- to nanomolar range) (Boyd et al., 2000; Boyd & Ellwood, 2010; King & Barbeau, 2011; Schlosser et al., 2012) and Fe is a limiting nutrient for primary production in the open ocean (Martin & Fitzwater, 1988; Martin et al., 1994; Boyd et al., 2000; Barbeau, 2006). The thermodynamically stable form of Fe in oxic seawater, Fe(III), precipitates quickly as Fe(III) (oxyhydr)oxides at circumneutral pH and is therefore removed from the water column (Kuma et al., 1995; Barbeau, 2006). Especially in regions without continental or atmospheric input, Fe concentrations were shown to be only about 100 pM (Barbeau, 2006). More than 99.9% of the dissolved Fe in seawater is associated with biologically derived organic ligands of largely unknown identity (Gledhill & van den Berg, 1994; Rue & Bruland, 1995; Wu & Luther, 1995; Kuma et al., 1996; Barbeau, 2006; Rijkenberg et al., 2006; Boyd & Ellwood, 2010), which keep Fe in solution and control the photochemical reactivity of Fe (Kuma et al., 1996; Johnson et al., 1997; Barbeau et al., 2003; Barbeau, 2006; Muller, 2018). The organic compounds in seawater binding to iron are a mixture of different molecules including polysaccharides and humic substances (Gledhill & Buck, 2012; Bundy et al., 2015). Large parts of these Fe-binding ligands presumably are siderophores (Rue & Bruland, 1995; Barbeau et al., 2001; Barbeau et al., 2003; Boyd & Ellwood, 2010), that were produced and excreted by microorganisms for Fe acquisition under Fe-limiting conditions (Trick, 1989; Wilhelm & Trick, 1994). Siderophores strongly bind to Fe(III) and solubilize it from Fe minerals or colloids (Granger & Price, 1999; Amin et al., 2009). Depending on the functional groups binding to Fe(III), Fe(III)-siderophore complexes can undergo direct LMCT reactions leading to a reduction of Fe(III) to Fe(II) and an oxidation of the siderophore (Barbeau et al., 2003). While siderophores containing α-hydroxy carboxylate groups are susceptible to photooxidation when complexed with iron, complexes of catecholate and hydroxamate functional groups with iron are stable in light (Barbeau et al., 2003). Depending on the identity of the siderophore, the oxidized photolysis product can either maintain its Fe(III) chelating properties or be destroyed (Barbeau et al., 2001; Amin et al., 2009). The photoproduced Fe(II) can subsequently be complexed with an Fe(II) ligand present in seawater or taken up by microorganisms (Barbeau et al., 2001). The chemical and physical speciation of Fe determines its bioavailability (Rijkenberg et al., 2006; Sulzberger, 2015). Photochemically induced reduction of Fe(III) forms $Fe^{2+}_{aq}$ and more reactive Fe species, which are generally more bioavailable and are therefore an important nutrient source for phytoplankton in the oceans (Anderson & Morel, 1982; Wells & Mayer, 1991; Johnson et al., 1994; Sulzberger, 2015). Instead of being taken up by microorganisms, Fe(II) can also rapidly be re-oxidized, e.g. by $O_2$

or $H_2O_2$ (King et al., 1995; Miller et al., 1995; Barbeau et al., 2001; Rose & Waite, 2005; Santana-Casiano et al., 2006; Miller et al., 2012), which are the main oxidants of Fe(II) in seawater (González-Davila et al., 2005; Santana-Casiano et al., 2006). This re-oxidation of Fe(II) yields Fe(III) and the formation of ROS, which can further oxidize Fe(II) or reduce Fe(III) (eq. 2.1-2.6), leading to rapid, light induced cycling of Fe in the oceans (O'Sullivan et al., 1991; Miller et al., 1995; Barbeau et al., 2001; Sulzberger, 2015).

Besides direct LMCT reactions, Fe(III)-organic complexes can also undergo indirect photochemical reactions involving photochemically produced radical species such as superoxide, which is the most likely reductant of Fe(III) at seawater pH (Miller et al., 1995; Voelker & Sedlak, 1995; Pierre et al., 2002; Rose & Waite, 2005; Barbeau, 2006). As superoxide is formed by photochemical reactions of DOM with $O_2$ (Cooper et al., 1988; Garg et al., 2011), the contribution of the indirect photochemical reduction of Fe(III) via superoxide to the overall Fe(II) concentrations of the ocean is determined by the chemical composition of DOM present in seawater (Emmenegger et al., 2001; Barbeau, 2006; Sulzberger, 2015). In general, the interplay of both Fe(III) reduction pathways, direct LMCT reactions and indirect Fe(III) reduction involving superoxide, maintain the Fe(II) pool of the oceans (Voelker & Sedlak, 1995; Barbeau et al., 2003). The actual Fe(III) photoreduction rates in the ocean depend on the photosusceptibility of the different organic complexes as well as light intensity and wavelength of the incoming sunlight (King et al., 1993; Feng & Nansheng, 2000). Although UVB light is most efficient for Fe(III) photoreduction (Rijkenberg et al., 2004; Rijkenberg et al., 2005), the UVA and VIS regions are quantitatively more important for photochemical Fe(II) production in the ocean due to their lower atmospheric attenuation and their deeper penetration into the water column of the ocean compared to UVB light (Rijkenberg et al., 2004).

Despite fast oxidation of Fe(II) by $O_2$, $H_2O_2$ or other oxidants in the oceans, a steady state concentration of Fe(II) can build up if rates of light-induced Fe(III) reduction are high enough (O'Sullivan et al., 1991; Kuma et al., 1995; Barbeau et al., 2003; Rose & Waite, 2003). While Fe(III) photoreduction leads to significant Fe(II) concentrations in seawater following diurnal cycles (Kuma et al., 1992; Johnson et al., 1994; Rijkenberg et al., 2005) and elevated Fe(II) concentrations near the water surface (O'Sullivan et al., 1991; Emmenegger et al., 2001; Boyd & Ellwood, 2010), the combination of both, Fe(III) photoreduction and Fe(II) oxidation by $O_2$ and ROS, largely control the Fe(II) concentrations in irradiated seawater (Miller et al., 1995).

## 2.5 Fe(III) photoreduction in lakes and rivers

The photochemically induced reduction of Fe(III) does not only drive Fe cycling in the oceans, but also plays an important role for Fe(II) availability in freshwater systems (Sivan et al., 1998; Emmenegger et al., 2001; Meunier et al., 2005). Usually, Fe concentrations and DOM in coastal waters but also in freshwater lakes are higher than in the open ocean due to larger particulate inputs (Emmenegger et al., 1998; Emmenegger et al., 2001; Rose et al., 2005), with dissolved Fe almost entirely being present in organic complexes (Sivan et al., 1998; Meunier et al., 2005; Sulzberger, 2015). In circumneutral lakes, Fe(III) photoreduction leads to diel cycling of Fe(II) with maximum concentrations close to the water surface (Sivan et al., 1998; Emmenegger et al., 2001). Both, light-induced LMCT reactions and superoxide mediated reduction of Fe(III) are responsible for the photoproduced Fe(II) concentrations in the investigated circumneutral freshwater lakes (Emmenegger et al., 2001; Meunier et al., 2005). The molecular weight of DOM present influences the extent of Fe(III) photoreduction (Meunier et al., 2005; Sulzberger, 2015). As the rate of Fe(III) photoreduction generally increases with decreasing pH (King et al., 1993; Emmenegger et al., 2001), this light-driven process is an important Fe(II) source in acidic freshwater systems such as acidic rivers and lakes. The low pH of these waters often originates from contamination of acid mine drainage, leading typically to pH values between 2 to 4 (McKnight et al., 2001). Due to slower abiotic Fe(II) oxidation rates by $O_2$ at low pH (Singer & Stumm, 1970), higher dissolved Fe(II) concentrations can build up in these waters compared to waters with circumneutral pH, where abiotic Fe(II) oxidation to Fe(III) by $O_2$ and quick precipitation as Fe(III) (oxyhydr)oxides lead to a removal of Fe from the water column (Kuma et al., 1995; McKnight et al., 2001; Gammons et al., 2005a). Fe(II) concentrations in acidic rivers and lakes also follow diel cycles (Collienne, 1983; McKnight et al., 1988; Kimball et al., 1992; Sullivan et al., 1998) correlated with light intensity (Kimball et al., 1992; Gammons et al., 2008; Diez Ercilla et al., 2009) with maximum concentrations at midday and minimum concentrations at night. Waters influenced by acid mine drainage often have low concentrations of DOM (Sulzberger et al., 1990; Diez Ercilla et al., 2009), which lead to low photochemical production of superoxide and $H_2O_2$ (McKnight & Duren, 2004; Diez Ercilla et al., 2009). This would imply that direct LCMT reactions are the more important photochemical Fe(III) reduction pathway in acidic waters. Due to low pH and low DOM concentrations, photoreduction of dissolved inorganic Fe(III) species and photoreductive dissolution of particulate Fe(III) species or Fe(III) (oxyhydr)oxides play a relatively larger role in these environments (Waite & Morel, 1984; Sulzberger et al., 1990; McKnight et al., 2001) than in circumneutral waters. During mineral dissolution, formerly adsorbed phosphate or trace metals

such as Cu, Zn, As or Pb (Tate et al., 1995; Gammons et al., 2005a; Gammons et al., 2005b; Diez Ercilla et al., 2009) are released into the water and can impact the activity of aquatic biota (McKnight et al., 2001) on a relatively short time scale. With increasing pH, e.g. in rivers with a downstream pH gradient, dissolved $Fe^{2+}_{aq}$ is oxidized to Fe(III) and usually precipitates as Fe(III) (oxyhydr)oxides, resulting in the scavenging of trace metals due to sorption processes (Gammons et al., 2005a; Gammons et al., 2005b). At low pH, the dominant dissolved inorganic Fe(III) species is $Fe(III)OH_2^+$ (Collienne, 1983; McKnight & Duren, 2004) and a light-induced LMCT induced by UV-light generates Fe(II) and hydroxyl radicals (Faust & Hoigné, 1990; Sulzberger et al., 1990). The amounts of Fe(II) photochemically produced in acidic waters can be sufficient to serve as substrate for populations of Fe(II)-oxidizing bacteria (Gammons et al., 2008) as slow abiotic Fe(II) oxidation kinetics lead to longer residence times of Fe(II) in the water. If no other external sources of Fe(II) exist, e.g. supplied by inflow of anoxic groundwater or oxidation of pyrite (Fernández-Remolar et al., 2005; Gammons et al., 2008), Fe(III) photoreduction represents an important and also renewable Fe(II) source in acidic surface waters (Gammons et al., 2008). Dominant photochemical processes involving Fe(III) and the fate of produced $Fe^{2+}_{aq}$ in a river with a downstream pH gradient are illustrated in Figure 2.4.
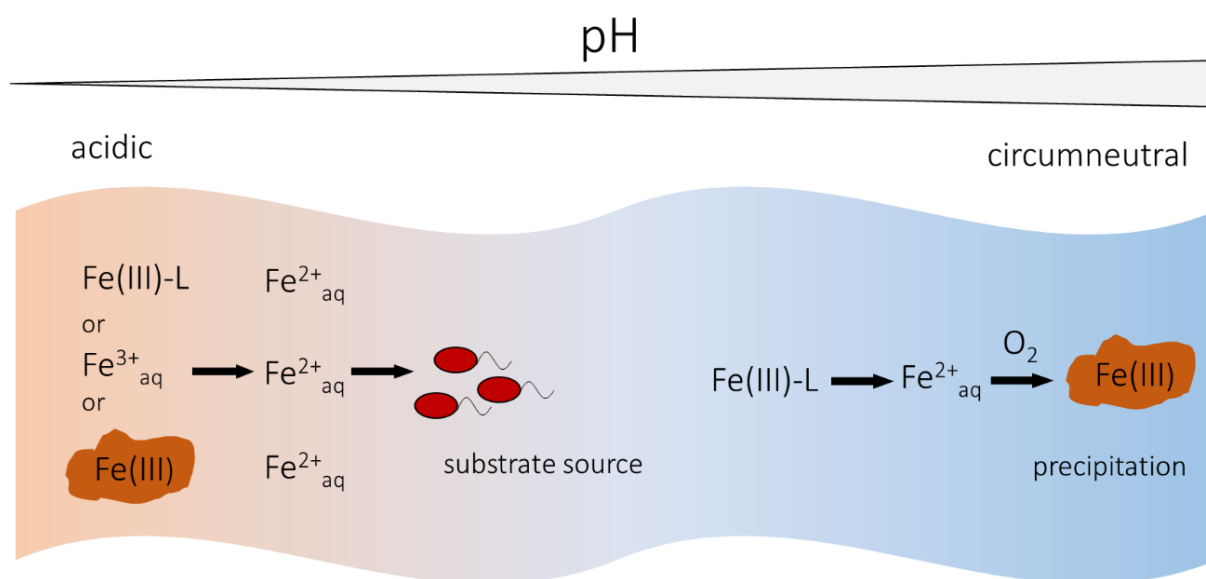


**Figure 2.4** River with downstream pH gradient showing dominant Fe processes in waters with acidic or circumneutral pH. At acidic pH, dissolved organically complexed (Fe(III)-L), dissolved inorganic Fe(III) species ($Fe^{3+}_{aq}$) or Fe(III) (oxyhydr)oxides can photochemically be reduced to $Fe^{2+}_{aq}$, which can, due to high concentrations, be used as substrate for Fe(II)-oxidizing bacteria. At circumneutral pH, dissolved Fe(III) occurs organically complexed and photoproduced $Fe^{2+}_{aq}$ is mostly re-oxidized, e.g. by $O_2$, and predominantly precipitates as Fe(III) (oxyhydr)oxides.

## 2.6 Sedimentary Fe(III) photoreduction

Only recently, Fe(III) photoreduction was found to form $Fe^{2+}_{aq}$ in the pore water of freshwater and marine sediments (Lueder et al., 2019a; Lueder et al., 2019b). In sediments, Fe concentrations usually are in the range of micromolar concentrations (Melton et al., 2014; Laufer et al., 2016; Schaedler et al., 2018) and therefore Fe is generally not considered to be a limiting nutrient. However, gradients of Fe(II) establish at a millimeter to centimeter scale with increasing concentrations downwards due to chemical redox processes and microbially catalyzed reactions, including Fe(III) reduction in deeper, anoxic as well as abiotic Fe(II) oxidation by $O_2$ in shallow, oxic sediment layers (Schaedler et al., 2018; Lueder et al., 2019a; Lueder et al., 2019b). Fe-metabolizing bacteria that use Fe for gaining electrons and energy, need Fe concentrations above the trace element level for growth. In the upper millimeters of light-influenced, oxic sediment layers, Fe(III) photoreduction produces substantial amounts (micromolar range) of $Fe^{2+}_{aq}$, where it is usually limited as substrate for growth (Lueder et al., 2019a). The produced $Fe^{2+}_{aq}$ persists even in the presence of $O_2$, probably due to stabilization by organic matter, which can slow down Fe(II) oxidation rates (Sulzberger et al., 1990; Croot et al., 2001; Meunier et al., 2005). By this, Fe(III) photoreduction has a strong impact on Fe(II) gradients in sediments and presumably has consequences for the inhabiting microbial community of Fe-metabolizing bacteria, which cannot only oxidize free, dissolved $Fe^{2+}_{aq}$ but also Fe(II)-organic complexes (Peng et al., 2018; Peng et al., 2019a; Peng et al., 2019b). Also in sediments, the extent of Fe(III) photoreduction is determined by the DOM concentration of the sediment pore water (Lueder et al., 2019a). So far, the relative contribution of direct LMCT and reduction of Fe(III) via photochemically produced superoxide to the overall photochemical Fe(II) production in sediments was not determined yet. However, photochemical production of superoxide and ROS in sediments can be expected by photolysis of dissolved DOM of the pore water, especially in organic rich sediments. Figure 2.5 summarizes sources and fate of Fe(II) in ocean and sediments.
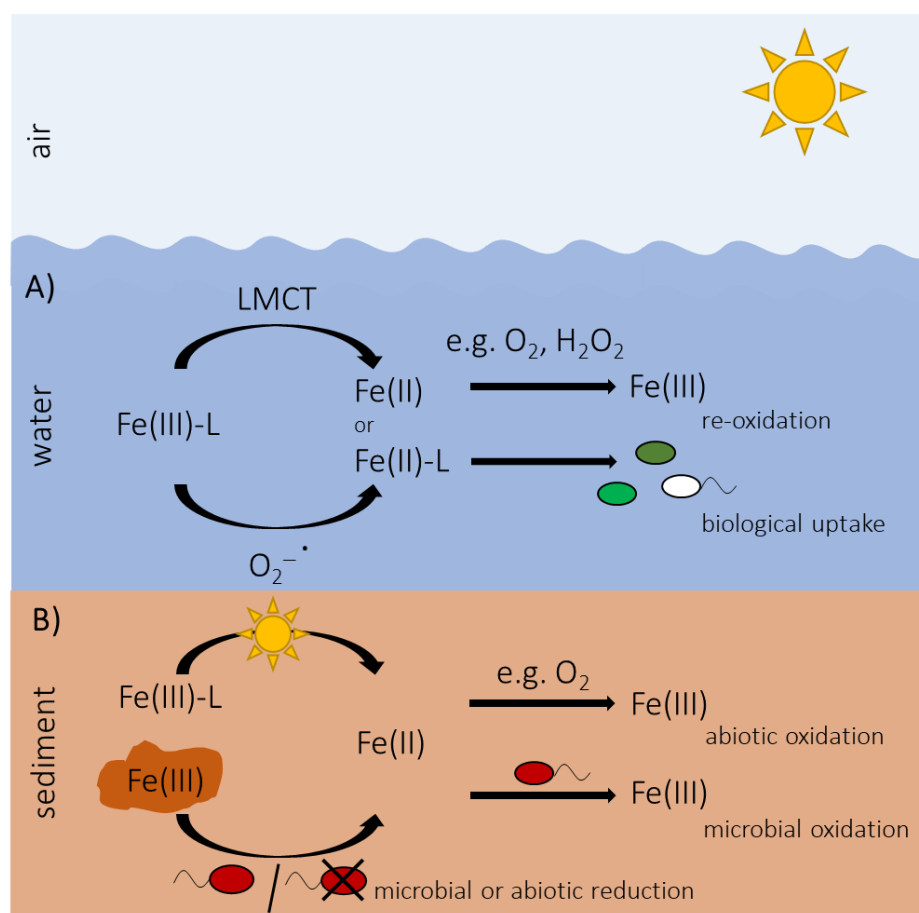
**Figure 2.5** A) Illustration of photoreduction in the water column of organically complexed Fe(III) (Fe(III)-L) via ligand-to-metal-charge transfer (LMCT) reaction or via superoxide ($O_2^{-\cdot}$) forming Fe(II), which either gets re-oxidized by e.g. $O_2$ or $H_2O_2$ to Fe(III) or is taken up by phytoplankton. B) Sketch of Fe(II) production in sediments by either Fe(III) photoreduction or by biotic or abiotic Fe(III) reduction. Fe(II) either gets abiotically re-oxidized, e.g. by $O_2$ or serves as substrate for microaerophilic, phototrophic or nitrate-reducing Fe(II)-oxidizing bacteria.

## 2.7 Light as driver of microbial Fe cycling

Besides the purely chemical process of Fe(III) photoreduction, light can also serve as energy source for the metabolism of anoxygenic phototrophic Fe(II)-oxidizing bacteria present in freshwater or marine sediments (Laufer et al., 2016; Otte et al., 2018) or in water columns (Walter et al., 2014; Llirós et al., 2015) which thereby couple the oxidation of Fe(II) to $CO_2$ fixation (Widdel et al., 1993). Anoxygenic photosynthesis was suggested to be an important metabolism in ancient environments of the Archean Ocean where $O_2$ was absent and reduced species such as Fe(II) dominated in the water column (Canfield et al., 2006; Poulton & Canfield, 2011). It probably accounted for most of the primary production in sunlit waters (Camacho et al., 2017). With the evolution of oxygenic photosynthesis, today's mostly oxic aquatic environments formed and anoxygenic photoferrotrophs were displaced to anoxic, sunlit niches.

However, they are still present as primary producers in many environments today and are part of the biogeochemical cycling of Fe (Bryce et al., 2018). The production of $O_2$ by oxygenic photosynthesis also has consequences for other Fe-metabolizing bacteria that either have anaerobic metabolisms or need to compete with the fast abiotic Fe(II) oxidation kinetics with $O_2$ at circumneutral pH. In contrast, the oxidation kinetics of Fe(II) by $O_2$ in acidic conditions is much slower (Singer & Stumm, 1970) and in acidic waters, Fe(III) photoreduction produces significant amounts of Fe(II) and can thus control the presence and distribution of Fe(II)-oxidizing acidophilic bacteria (Diez Ercilla et al., 2009) due to longer half-life times of Fe(II) at acidic pH (Singer & Stumm, 1970). The discovery of Fe(III) photoreduction in freshwater and marine sediments adds another Fe(II) source, besides biotic and abiotic Fe(III) reduction, to the sedimentary biogeochemical Fe cycle (Lueder et al., 2019a). By supplying light-influenced sediments with Fe(II) concentrations in the micromolar range, microaerophilic Fe(II)-oxidizing bacteria can grow in oxic sediment layers, in which rapid abiotic Fe(II) oxidation by $O_2$ would otherwise dominate due to the rapid oxidation kinetics at circumneutral pH (Millero et al., 1987). Light is therefore driving the biogeochemical cycling of Fe in modern aquatic environments and sediments by not only serving as energy source for phototrophic Fe(II)-oxidizers but also providing substantial amounts of Fe(II) for other Fe(II)-oxidizing bacteria.

## 2.8 ROS related processes in the dark

Sunlight is directly or indirectly driving many chemical and biological reactions in natural waters and sediments. However, most of our ecosystems on Earth are never reached by light and only exist in darkness – the deep biosphere (Edwards et al., 2012). However, even in the dark, there are parallel processes compared to photochemical mechanisms that involve, among others, the formation and consumption ROS species.

Due to their high temperatures, hydrothermal vents emit light into the dark of the ocean, mainly as thermal radiation in the IR wavelength region (>700 nm), but temporally also in small intensity in the VIS wavelength region (Van Dover et al., 1996; White et al., 2002). The energy of this radiation can potentially be used by photosynthetic bacteria such as green sulphur bacteria, which are potentially able to oxidize Fe(II), for the fixation of $CO_2$ to organic carbon (Figure 2.6) (Beatty et al., 2005). Apart from being used for photosynthesis, IR presumably does not deliver sufficient energy for the formation of ROS in the environment as photolysis of

DOM and concomitant ROS production usually occurs by absorption of UV and VIS light (Gao & Zepp, 1998; Johannessen et al., 2003; Scully et al., 2003).

The aeration of anoxic water containing Fe(II) leads to the formation of hydroxyl radicals by Fenton reactions (eq. 2.5) (Page et al., 2012; Minella et al., 2015), as the oxidation of Fe(II) by $O_2$ also proceeds in darkness producing $H_2O_2$ and further hydroxyl radicals (eq. 2.4 & 2.5). In general, biotic reductive processes (e.g. Fe(III)-reducing bacteria such as *Shewanella oneidensis*) or abiotic reductants (e.g. sulphide) that are able to reduce Fe(III) to Fe(II), enhance the formation of ROS, as was observed in natural waters or marsh sediments (Page et al., 2013; Murphy et al., 2014; Grossman & Kahan, 2016; Murphy et al., 2016). The formed Fe(II) further reacts as described in eq. 2.3-2.6 with $O_2$ forming ROS (Figure 2.6). These reactions involving $O_2$ are important e.g. at oxic-anoxic interfaces or anoxic soils or sediments that are flushed with oxygenated water (Trusiak et al., 2018). During abiotic or biotic Fe(III) reduction, the reducing equivalents are not photons, but they are produced in chemical and biological reactions, which have a similar impact on ROS production as photochemical sources (Murphy et al., 2014). Besides the Fenton-like reactions yielding ROS, the abiotic oxidation of reduced DOC or humic acids by $O_2$ forms ROS as well (Figure 2.6) (Page et al., 2012; Trusiak et al., 2018). Superoxide is also extracellularly produced by several microorganisms such as different heterotrophic bacteria or phytoplankton (Figure 2.6) (Kim et al., 2000; Kustka et al., 2005; Rose et al., 2005; Diaz et al., 2013). This light-independent biological production of superoxide in marine and freshwater systems is a significant source of ROS concentrations as measured in sunlit waters (Zhang et al., 2016). Those reactions also proceeding in darkness are similar important drivers of biogeochemical cycles as photochemically-induced processes.
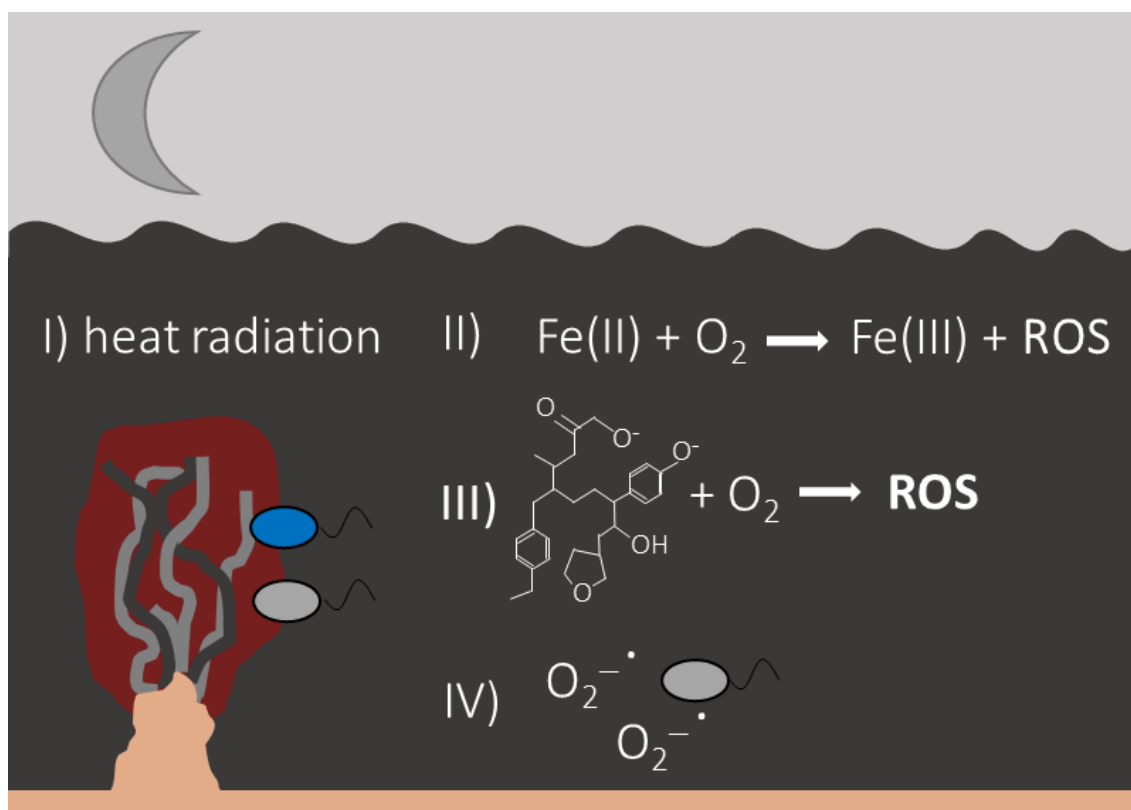
**Figure 2.6** Illustration of reactions proceeding in darkness I) IR light emission at hydrothermal vents, which may be used for anoxygenic photosynthesis, II) Fenton reaction forming ROS, III) ROS formation by oxidation of reduced organic molecules, IV) Extracellularly production of superoxide by bacteria or phytoplankton.

## 2.9 Conclusions

Photochemical reduction of Fe(III) by either direct LMCT reactions or by photochemically produced superoxide plays a major role in the Fe cycle of aquatic environments. It is the main source for the production of $Fe^{2+}_{aq}$, in water bodies such as the ocean and thus strongly influences the primary productivity of marine systems by supplying $Fe^{2+}_{aq}$. Besides biological uptake, rapid chemical oxidation of photochemically formed Fe(II), mainly by $O_2$ or $H_2O_2$ (González-Davila et al., 2005; Santana-Casiano et al., 2006), closes this photochemically driven diel Fe cycle in the oceans (O'Sullivan et al., 1991; Johnson et al., 1994; Waite et al., 1995). Fe(III) photoreduction also is a major source of ROS (eq. 2.1-2.6), which are key oxidants in natural waters (King et al., 1993; Croot et al., 2005) playing an important role in the biogeochemical cycling of trace metals and carbon (Hansel et al., 2015; Schneider et al., 2016). In acidic waters or sediments, Fe(III) photoreduction can even provide micromolar concentrations of $Fe^{2+}_{aq}$ and influence the presence and abundance of different Fe(II)-oxidizing bacteria. Photochemical effects generally decrease with water or sediment depth as light is

attenuated depending on the wavelength (Voelker et al., 1997). Especially light in the UV region, which is not only very efficient for Fe(III) photoreduction but also for the photochemical production of radicals (Barbeau, 2006; Garg et al., 2011), is strongly attenuated in both, water and sediments. Photochemical processes thus strongly impact and control the biological life and biotic processes in natural waters of different pH and in sediments, mainly by supplying bioavailable Fe(II) as nutrient or substrate for growth to the inhabiting organisms. Without those light-induced chemical processes, other element cycles such as the carbon cycle would lack an important driver.

**Acknowledgements**

## 2.10 References

Amin, S. A., Green, D. H., Küpper, F. C. and Carrano, C. J. (2009). Vibrioferrin, an unusual marine siderophore: iron binding, photochemistry, and biological implications. *Inorganic Chemistry*, **48**(23), 11451-11458.

Anbar, A. D. and Holland, H. D. (1992). The photochemistry of manganese and the origin of banded iron formations. *Geochimica et Cosmochimica Acta*, **56**(7), 2595-2603.

Anderson, M. A. and Morel, F. M. M. (1982). The influence of aqueous iron chemistry on the uptake of iron by the coastal diatom *Thalassiosira weissflogii*. *Limnology and Oceanography*, **27**(5), 789-813.

Ball, D. W. (2006). Light: particle or wave? *Spectroscopy*, **21**(6).

Ball, D. W. (2007). The electromagnetic spectrum: a history. *Spectroscopy*, **22**(3), 14-17.

Baral, S., Lume-Pereira, C., Janata, E. and Henglein, A. (1985). Chemistry of colloidal manganese dioxide. 2. Reaction with superoxide anion ($O_2^-$) and hydrogen peroxide (pulse radiolysis and stop flow studies). *The Journal of Physical Chemistry*, **89**(26), 5779-5783.

Barbeau, K. (2006). Photochemistry of organic iron(III) complexing ligands in oceanic systems. *Photochemistry and Photobiology*, **82**(6), 1505-1516.

Barbeau, K., Rue, E. L., Bruland, K. W. and Butler, A. (2001). Photochemical cycling of iron in the surface ocean mediated by microbial iron(III)-binding ligands. *Nature*, **413**(6854), 409-413.

Barbeau, K., Rue, E. L., Trick, C. G., Bruland, K. W. and Butler, A. (2003). Photochemical reactivity of siderophores produced by marine heterotrophic bacteria and cyanobacteria based on characteristic Fe(III) binding groups. *Limnology and Oceanography*, **48**(3), 1069-1078.

Beatty, J. T., Overmann, J., Lince, M. T., Manske, A. K., Lang, A. S., Blankenship, R. E., Van Dover, C. L., Martinson, T. A. and Plumley, F. G. (2005). An obligately photosynthetic bacterial anaerobe from a deep-sea hydrothermal vent. *Proceedings of the National Academy of Sciences of the United States of America*, **102**(26), 9306-9310.

Benner, R. and Biddanda, B. (1998). Photochemical transformations of surface and deep marine dissolved organic matter: Effects on bacterial growth. *Limnology and Oceanography*, **43**(6), 1373-1378.

Bertilsson, S. and Stefan, L. J. (1998). Photochemically produced carboxylic acids as substrates for freshwater bacterioplankton. *Limnology and Oceanography*, **43**(5), 885-895.

Borer, P., Sulzberger, B., Hug, S. J., Kraemer, S. M. and Kretzschmar, R. (2009a). Photoreductive dissolution of iron(III) (hydr)oxides in the absence and presence of organic ligands: experimental studies and kinetic modeling. *Environmental Science & Technology*, **43**(6), 1864-1870.

Borer, P., Sulzberger, B., Hug, S. J., Kraemer, S. M. and Kretzschmar, R. (2009b). Wavelength-dependence of photoreductive dissolution of lepidocrocite (γ-FeOOH) in the absence and presence of the siderophore DFOB. *Environmental Science & Technology*, **43**(6), 1871-1876.

Borowska, Z. K. and Mauzerall, D. C. (1987). Efficient near ultraviolet light

induced formation of hydrogen by ferrous hydroxide. *Origins of life and evolution of the biosphere*, **17**(3), 251-259.

Boyd, P. W. and Ellwood, M. J. (2010). The biogeochemical cycle of iron in the ocean. *Nature Geoscience*, **3**, 675.

Boyd, P. W., Watson, A. J., Law, C. S., Abraham, E. R., Trull, T., Murdoch, R., Bakker, D. C. E., Bowie, A. R., Buesseler, K. O., Chang, H., Charette, M., Croot, P., Downing, K., Frew, R., Gall, M., Hadfield, M., Hall, J., Harvey, M., Jameson, G., LaRoche, J., Liddicoat, M., Ling, R., Maldonado, M. T., McKay, R. M., Nodder, S., Pickmere, S., Pridmore, R., Rintoul, S., Safi, K., Sutton, P., Strzepek, R., Tanneberger, K., Turner, S., Waite, A. and Zeldis, J. (2000). A mesoscale phytoplankton bloom in the polar Southern Ocean stimulated by iron fertilization. *Nature*, **407**(6805), 695-702.

Braterman, P. S., Cairns-Smith, A. G. and Sloper, R. W. (1983). Photo-oxidation of hydrated $Fe^{2+}$ - significance for banded iron formations. *Nature*, **303**(5913), 163-164.

Braterman, P. S., Cairns-Smith, A. G., Sloper, R. W., Truscott, T. G. and Craw, M. (1984). Photo-oxidation of iron(II) in water between pH 7.5 and 4.0. *Journal of the Chemical Society, Dalton Transactions*(7), 1441-1445.

Bryce, C., Blackwell, N., Schmidt, C., Otte, J., Huang, Y.-M., Kleindienst, S., Tomaszewski, E., Schad, M., Warter, V., Peng, C., Byrne, J. M. and Kappler, A. (2018). Microbial anaerobic Fe(II) oxidation – Ecology, mechanisms and environmental implications. *Environmental Microbiology*, **20**(10), 3462-3483.

Bundy, R. M., Abdulla, H. A. N., Hatcher, P. G., Biller, D. V., Buck, K. N. and Barbeau, K. A. (2015). Iron-binding ligands and humic substances in the San Francisco Bay estuary and estuarine-influenced shelf regions of coastal California. *Marine Chemistry*, **173**, 183-194.

Camacho, A., Walter, X. A., Picazo, A. and Zopfi, J. (2017). Photoferrotrophy: Remains of an ancient photosynthesis in modern environments. *Frontiers in Microbiology*, **8**(323).

Canfield, D. E., Rosing, M. T. and Bjerrum, C. (2006). Early anaerobic metabolisms. *Philosophical Transactions of the Royal Society B: Biological Sciences*, **361**(1474), 1819-1836.

Collienne, R. H. (1983). Photoreduction of iron in the epilimnion of acidic lakes. *Limnology and Oceanography*, **28**(1), 83-100.

Cooper, W. J., Zika, R. G., Petasne, R. G. and Fischer, A. M. (1988). Sunlight-induced photochemistry of humic substances in natural waters: major reactive species. *Aquatic humic substances*, American Chemical Society. **219:** 333-362.

Croot, P. L., Bowie, A. R., Frew, R. D., Maldonado, M. T., Hall, J. A., Safi, K. A., La Roche, J., Boyd, P. W. and Law, C. S. (2001). Retention of dissolved iron and Fe(II) in an iron induced Southern Ocean phytoplankton bloom. *Geophysical Research Letters*, **28**(18), 3425-3428.

Croot, P. L., Laan, P., Nishioka, J., Strass, V., Cisewski, B., Boye, M., Timmermans, K. R., Bellerby, R. G., Goldson, L., Nightingale, P. and de Baar, H. J. W. (2005). Spatial and temporal distribution of Fe(II) and $H_2O_2$ during EisenEx, an open ocean mescoscale iron enrichment. *Marine Chemistry*, **95**(1), 65-88.

David, F. and David, P. G. (1976). Photoredox chemistry of iron(III) chloride and iron(III) perchlorate in aqueous media. A comparative study. *The Journal of Physical Chemistry*, **80**(6), 579-583.

Diaz, J. M., Hansel, C. M., Voelker, B. M., Mendes, C. M., Andeer, P. F. and Zhang, T. (2013). Widespread production of extracellular superoxide by heterotrophic bacteria. *Science*, **340**(6137), 1223-1226.

Diez Ercilla, M., López Pamo, E. and Sánchez España, J. (2009). Photoreduction of Fe(III) in the acidic mine pit lake of San Telmo (Iberian Pyrite Belt): field and experimental work. *Aquatic Geochemistry*, **15**(3), 391-419.

Dresselhaus, M. S. and Thomas, I. L. (2001). Alternative energy technologies. *Nature*, **414**(6861), 332-337.

Duntley, S. Q. (1963). Light in the sea. *Journal of the Optical Society of America*, **53**(2), 214-233.

Edwards, K. J., Becker, K. and Colwell, F. (2012). The deep, dark energy biosphere: Intraterrestrial life on earth. *Annual Review of Earth and Planetary Sciences*, **40**(1), 551-568.

Emmenegger, L., King, D. W., Sigg, L. and Sulzberger, B. (1998). Oxidation kinetics of Fe(II) in a eutrophic swiss lake. *Environmental Science & Technology*, **32**(19), 2990-2996.

Emmenegger, L., Schönenberger, R., Sigg, L. and Sulzberger, B. (2001). Light-induced redox cycling of iron in circumneutral lakes. *Limnology and Oceanography*, **46**(1), 49-61.

Farjalla, V. F., Amado, A. M., Suhett, A. L. and Meirelles-Pereira, F. (2009). DOC removal paradigms in highly humic aquatic ecosystems. *Environmental Science and Pollution Research*, **16**(5), 531-538.

Faust, B. C. and Hoigné, J. (1990). Photolysis of Fe (III)-hydroxy complexes as sources of OH radicals in clouds, fog and rain. *Atmospheric Environment. Part A. General Topics*, **24**(1), 79-89.

Feng, W. and Nansheng, D. (2000). Photochemistry of hydrolytic iron (III) species and photoinduced degradation of organic compounds. A minireview. *Chemosphere*, **41**(8), 1137-1147.

Fernández-Remolar, D. C., Morris, R. V., Gruener, J. E., Amils, R. and Knoll, A. H. (2005). The Río Tinto Basin, Spain: Mineralogy, sedimentary geobiology, and implications for interpretation of outcrop rocks at Meridiani Planum, Mars. *Earth and Planetary Science Letters*, **240**(1), 149-167.

François, L. M. (1986). Extensive deposition of banded iron formations was possible without photosynthesis. *Nature*, **320**(6060), 352-354.

Gammons, C. H., Nimick, D. A., Parker, S. R., Cleasby, T. E. and McCleskey, R. B. (2005a). Diel behavior of iron and other heavy metals in a mountain stream with acidic to neutral pH: Fisher Creek, Montana, USA. *Geochimica et Cosmochimica Acta*, **69**(10), 2505-2516.

Gammons, C. H., Nimick, D. A., Parker, S. R., Snyder, D. M., McCleskey, R. B., Amils, R. and Poulson, S. R. (2008). Photoreduction fuels biogeochemical cycling of iron in Spain's acid rivers. *Chemical Geology*, **252**(3), 202-213.

Gammons, C. H., Wood, S. A. and Nimick, D. A. (2005b). Diel behavior of rare earth elements in a mountain stream with acidic to neutral pH. *Geochimica et Cosmochimica Acta*, **69**(15), 3747-3758.

Gao, H. and Zepp, R. G. (1998). Factors influencing photoreactions of dissolved organic matter in a coastal river of the Southeastern United States. *Environmental Science & Technology*, **32**(19), 2940-2946.

Garcia-Pichel, F. (1995). A scalar irradiance fiber-optic microprobe for the measurement of ultraviolet radiation at high spatial resolution. *Photochemistry and Photobiology*, **61**(3), 248-254.

Garcia-Pichel, F. and Bebout, B. M. (1996). Penetration of ultraviolet radiation into shallow water sediments: high exposure for photosynthetic communities. *Marine Ecology Progress Series*, **131**, 257-262.

Garg, S., Rose, A. L. and Waite, T. D. (2011). Photochemical production of superoxide and hydrogen peroxide from natural organic matter. *Geochimica et Cosmochimica Acta*, **75**(15), 4310-4320.

Geller, A. (1985). Light-induced conversion of refractory, high molecular weight lake water constituents. *Swiss journal of hydrology*, **47**(1), 21-26.

Gledhill, M. and Buck, K. (2012). The organic complexation of iron in the marine environment: A review. *Frontiers in Microbiology*, **3**(69).

Gledhill, M. and van den Berg, C. M. G. (1994). Determination of complexation of iron(III) with natural organic complexing ligands in seawater using cathodic stripping voltammetry. *Marine Chemistry*, **47**(1), 41-54.

Goldstone, J. V., Pullin, M. J., Bertilsson, S. and Voelker, B. M. (2002). Reactions of hydroxyl radical with humic substances: bleaching, mineralization, and production of bioavailable carbon substrates. *Environmental Science & Technology*, **36**(3), 364-372.

González-Davila, M., Santana-Casiano, J. M. and Millero, F. J. (2005). Oxidation of iron (II) nanomolar with $H_2O_2$ in seawater. *Geochimica et Cosmochimica Acta*, **69**(1), 83-93.

Granger, J. and Price, N. M. (1999). The importance of siderophores in iron nutrition of heterotrophic marine bacteria. *Limnology and Oceanography*, **44**(3), 541-555.

Grant, R. H. and Heisler, G. M. (2000). Estimation of ultraviolet-B irradiance under variable cloud conditions. *Journal of Applied Meteorology*, **39**(6), 904-916.

Grossman, J. N. and Kahan, T. F. (2016). Hydroxyl radical formation from bacteria-assisted Fenton chemistry at neutral pH under environmentally relevant conditions. *Environmental Chemistry*, **13**(4), 757-766.

Hansel, C. M., Ferdelman, T. G. and Tebo, B. M. (2015). Cryptic cross-linkages among biogeochemical cycles: novel insights from reactive intermediates. *Elements*, **11**(6), 409-414.

Horvath, H. (1993). Atmospheric light absorption—A review. *Atmospheric Environment. Part A. General Topics*, **27**(3), 293-317.

Johannessen, S. C., Miller, W. L. and Cullen, J. J. (2003). Calculation of UV attenuation and colored dissolved organic matter absorption spectra from measurements of ocean color. *Journal of Geophysical Research: Oceans*, **108**(C9).

Johnson, K. S., Coale, K. H., Elrod, V. A. and Tindale, N. W. (1994). Iron photochemistry in seawater from the equatorial Pacific. *Marine Chemistry*, **46**(4), 319-334.

Johnson, K. S., Gordon, R. M. and Coale, K. H. (1997). What controls dissolved

iron concentrations in the world ocean? *Marine Chemistry*, **57**(3), 137-161.

Karentz, D. (1994). Impact of UV-B radiation on pelagic freshwater ecosystems: Report of working group on bacteria and phytoplankton. *Advances in limnology*, **43**, 31-69.

Kiang, N. Y., Siefert, J., Govindjee and Blankenship, R. E. (2007). Spectral signatures of photosynthesis I: Review of earth organisms. *Astrobiology*, **7**(1), 222-251.

Kieber, D. J., McDaniel, J. and Mopper, K. (1989). Photochemical source of biological substrates in sea water: implications for carbon cycling. *Nature*, **341**(6243), 637-639.

Kieber, R. J., Whitehead, R. F. and Skrabal, S. A. (2006). Photochemical production of dissolved organic carbon from resuspended sediments. *Limnology and Oceanography*, **51**(5), 2187-2195.

Kim, D., Nakamura, A., Okamoto, T., Komatsu, N., Oda, T., Iida, T., Ishimatsu, A. and Muramatsu, T. (2000). Mechanism of superoxide anion generation in the toxic red tide phytoplankton Chattonella marina: possible involvement of NAD(P)H oxidase. *Biochimica et Biophysica Acta (BBA) - General Subjects*, **1524**(2), 220-227.

Kimball, B. A., McKnight, D. M., Wetherbee, G. A. and Harnish, R. A. (1992). Mechanisms of iron photoreduction in a metal-rich, acidic stream (St. Kevin Gulch, Colorado, U.S.A.). *Chemical Geology*, **96**(1), 227-239.

King, A. L. and Barbeau, K. A. (2011). Dissolved iron and macronutrient distributions in the southern California Current System. *Journal of Geophysical Research: Oceans*, **116**(C3).

King, D. W., Lounsbury, H. A. and Millero, F. J. (1995). Rates and mechanism of Fe(II) oxidation at nanomolar total iron concentrations. *Environmental Science & Technology*, **29**(3), 818-824.

King, W. D., Aldrich, R. A. and Charnecki, S. E. (1993). Photochemical redox cycling of iron in NaCl solutions. *Marine Chemistry*, **44**(2), 105-120.

Konhauser, K. O., Amskold, L., Lalonde, S. V., Posth, N. R., Kappler, A. and Anbar, A. (2007). Decoupling photochemical Fe(II) oxidation from shallow-water BIF deposition. *Earth and Planetary Science Letters*, **258**(1), 87-100.

Kühl, M., Lassen, C. and Jørgensen, B. B. (1994). Light penetration and light intensity in sandy marine sediments measured with irradiance and scalar irradiance fiber-optic microprobes. *Marine Ecology Progress Series*, **105**(1/2), 139-148.

Kuma, K., Nakabayashi, S. and Matsunaga, K. (1995). Photoreduction of Fe(III) by hydroxycarboxylic acids in seawater. *Water Research*, **29**(6), 1559-1569.

Kuma, K., Nakabayashi, S., Suzuki, Y., Kudo, I. and Matsunaga, K. (1992). Photo-reduction of Fe(III) by dissolved organic substances and existence of Fe(II) in seawater during spring blooms. *Marine Chemistry*, **37**(1), 15-27.

Kuma, K., Nishioka, J. and Matsunaga, K. (1996). Controls on iron(III) hydroxide solubility in seawater: The influence of pH and natural organic chelators. *Limnology and Oceanography*, **41**(3), 396-407.

Kustka, A. B., Shaked, Y., Milligan, A. J., King, D. W. and Morel, F. M. M. (2005). Extracellular production of superoxide by marine diatoms: Contrasting effects on iron redox chemistry and bioavailability.

*Limnology and Oceanography*, **50**(4), 1172-1180.

Larsen, H. (1952). On the culture and general physiology of the green sulfur bacteria. *Journal of Bacteriology*, **64**(2), 187-196.

Larson, R. A. and Berenbaum, M. R. (1988). Environmental phototoxicity. *Environmental Science & Technology*, **22**(4), 354-360.

Laufer, K., Nordhoff, M., Røy, H., Schmidt, C., Behrens, S., Jørgensen, B. B. and Kappler, A. (2016). Coexistence of microaerophilic, nitrate-reducing, and phototrophic Fe(II) oxidizers and Fe(III) reducers in coastal marine sediment. *Applied and Environmental Microbiology*, **82**(5), 1433-1447.

Llirós, M., García–Armisen, T., Darchambeau, F., Morana, C., Triadó–Margarit, X., Inceoğlu, Ö., Borrego, C. M., Bouillon, S., Servais, P., Borges, A. V., Descy, J. P., Canfield, D. E. and Crowe, S. A. (2015). Pelagic photoferrotrophy and iron cycling in a modern ferruginous basin. *Scientific Reports*, **5**, 13803.

Lueder, U., Jørgensen, B. B., Kappler, A. and Schmidt, C. (2019a). Fe(III) photoreduction producing $Fe^{2+}_{aq}$ in oxic freshwater sediment. *submitted*.

Lueder, U., Maisch, M., Laufer, K., Jørgensen, B. B., Kappler, A. and Schmidt, C. (2019b). Influence of physical perturbation on Fe(II) supply in coastal marine sediments. *submitted*.

Marshall, J.-A., Ross, T., Pyecroft, S. and Hallegraeff, G. (2005). Superoxide production by marine microalgae. *Marine Biology*, **147**(2), 541-549.

Martin, J. H., Coale, K. H., Johnson, K. S., Fitzwater, S. E., Gordon, R. M., Tanner, S. J., Hunter, C. N., Elrod, V. A.,

Nowicki, J. L., Coley, T. L., Barber, R. T., Lindley, S., Watson, A. J., Van Scoy, K., Law, C. S., Liddicoat, M. I., Ling, R., Stanton, T., Stockel, J., Collins, C., Anderson, A., Bidigare, R., Ondrusek, M., Latasa, M., Millero, F. J., Lee, K., Yao, W., Zhang, J. Z., Friederich, G., Sakamoto, C., Chavez, F., Buck, K., Kolber, Z., Greene, R., Falkowski, P., Chisholm, S. W., Hoge, F., Swift, R., Yungel, J., Turner, S., Nightingale, P., Hatton, A., Liss, P. and Tindale, N. W. (1994). Testing the iron hypothesis in ecosystems of the equatorial Pacific Ocean. *Nature*, **371**(6493), 123-129.

Martin, J. H. and Fitzwater, S. E. (1988). Iron deficiency limits phytoplankton growth in the north-east Pacific subarctic. *Nature*, **331**(6154), 341-343.

Masojídek, J. and Torzillo, G. (2008). Mass cultivation of freshwater microalgae. *Encyclopedia of Ecology*. S. E. Jørgensen and B. D. Fath. Oxford, Academic Press**:** 2226-2235.

Mayer, L. M., Schick, L. L., Skorko, K. and Boss, E. (2006). Photodissolution of particulate organic matter from sediments. *Limnology and Oceanography*, **51**(2), 1064-1071.

McKnight, D. M. and Duren, S. M. (2004). Biogeochemical processes controlling midday ferrous iron maxima in stream waters affected by acid rock drainage. *Applied Geochemistry*, **19**(7), 1075-1084.

McKnight, D. M., Kimball, B. A. and Bencala, K. E. (1988). Iron photoreduction and oxidation in an acidic mountain stream. *Science*, **240**(4852), 637-640.

McKnight, D. M., Kimball, B. A. and Runkel, R. L. (2001). pH dependence of iron photoreduction in a rocky mountain stream affected by acid mine drainage. *Hydrological Processes*, **15**(10), 1979-1992.

Melton, E. D., Stief, P., Behrens, S., Kappler, A. and Schmidt, C. (2014). High spatial resolution of distribution and interconnections between Fe- and N-redox processes in profundal lake sediments. *Environmental Microbiology*, **16**(10), 3287-3303.

Meunier, L., Laubscher, H., Hug, S. J. and Sulzberger, B. (2005). Effects of size and origin of natural dissolved organic matter compounds on the redox cycling of iron in sunlit surface waters. *Aquatic Sciences*, **67**(3), 292-307.

Miles, C. J. and Brezonik, P. L. (1981). Oxygen consumption in humic-colored waters by a photochemical ferrous-ferric catalytic cycle. *Environmental Science & Technology*, **15**(9), 1089-1095.

Miller, C. J., Vincent Lee, S. M., Rose, A. L. and Waite, T. D. (2012). Impact of natural organic matter on $H_2O_2$-mediated oxidation of Fe(II) in coastal seawaters. *Environmental Science & Technology*, **46**(20), 11078-11085.

Miller, W. L., King, D. W., Lin, J. and Kester, D. R. (1995). Photochemical redox cycling of iron in coastal seawater. *Marine Chemistry*, **50**(1), 63-77.

Miller, W. L. and Moran, M. A. (1997). Interaction of photochemical and microbial processes in the degradation of refractory dissolved organic matter from a coastal marine environment. *Limnology and Oceanography*, **42**(6), 1317-1324.

Miller, W. L. and Zepp, R. G. (1995). Photochemical production of dissolved inorganic carbon from terrestrial organic matter: Significance to the oceanic organic carbon cycle. *Geophysical Research Letters*, **22**(4), 417-420.

Millero, F. J., Sotolongo, S. and Izaguirre, M. (1987). The oxidation kinetics of Fe(II) in seawater. *Geochimica et Cosmochimica Acta*, **51**(4), 793-801.

Minella, M., De Laurentiis, E., Maurino, V., Minero, C. and Vione, D. (2015). Dark production of hydroxyl radicals by aeration of anoxic lake water. *Science of the Total Environment*, **527-528**, 322-327.

Moran, M. A. and Zepp, R. G. (1997). Role of photoreactions in the formation of biologically labile compounds from dissolved organic matter. *Limnology and Oceanography*, **42**(6), 1307-1316.

Muller, F. L. L. (2018). Exploring the potential role of terrestrially derived humic substances in the marine biogeochemistry of iron. *Frontiers in Earth Science*, **6**(159).

Murphy, S. A., Meng, S., Solomon, B. M., Dias, D. M. C., Shaw, T. J. and Ferry, J. L. (2016). Hydrous ferric oxides in sediment catalyze formation of reactive oxygen species during sulfide oxidation. *Frontiers in Marine Science*, **3**(227).

Murphy, S. A., Solomon, B. M., Meng, S., Copeland, J. M., Shaw, T. J. and Ferry, J. L. (2014). Geochemical production of reactive oxygen species from biogeochemically reduced Fe. *Environmental Science & Technology*, **48**(7), 3815-3821.

Nunez, M., Forgan, B. and Roy, C. (1994). Estimating ultraviolet radiation at the earth's surface. *International Journal of Biometeorology*, **38**(1), 5-17.

O'Sullivan, D. W., Hanson, A. K., Miller, W. L. and Kester, D. R. (1991). Measurement of Fe(II) in surface water of the equatorial Pacific. *Limnology and Oceanography*, **36**(8), 1727-1741.

Otte, J. M., Harter, J., Laufer, K., Blackwell, N., Straub, D., Kappler, A. and Kleindienst, S. (2018). The

distribution of active iron-cycling bacteria in marine and freshwater sediments is decoupled from geochemical gradients. *Environmental Microbiology*, **20**(7), 2483-2499.

Page, S. E., Kling, G. W., Sander, M., Harrold, K. H., Logan, J. R., McNeill, K. and Cory, R. M. (2013). Dark formation of hydroxyl radical in arctic soil and surface waters. *Environmental Science & Technology*, **47**(22), 12860-12867.

Page, S. E., Logan, J. R., Cory, R. M. and McNeill, K. (2014). Evidence for dissolved organic matter as the primary source and sink of photochemically produced hydroxyl radical in arctic surface waters. *Environmental Science: Processes & Impacts*, **16**(4), 807-822.

Page, S. E., Sander, M., Arnold, W. A. and McNeill, K. (2012). Hydroxyl radical formation upon oxidation of reduced humic acids by oxygen in the dark. *Environmental Science & Technology*, **46**(3), 1590-1597.

Peng, C., Bryce, C., Sundman, A., Borch, T. and Kappler, A. (2019a). Organic matter complexation promotes Fe(II) oxidation by the photoautotrophic Fe(II)-oxidizer Rhodopseudomonas palustris TIE-1. *ACS Earth and Space Chemistry*, **3**(4), 531-536.

Peng, C., Bryce, C., Sundman, A. and Kappler, A. (2019b). Cryptic cycling of complexes containing Fe(III) and organic matter by phototrophic Fe(II)-oxidizing bacteria. *Applied and Environmental Microbiology*, **85**(8), e02826-02818.

Peng, C., Sundman, A., Bryce, C., Catrouillet, C., Borch, T. and Kappler, A. (2018). Oxidation of Fe(II)–organic matter complexes in the presence of the mixotrophic nitrate-reducing Fe(II)-oxidizing bacterium Acidovorax sp. BoFeN1. *Environmental Science & Technology*, **52**(10), 5753-5763.

Piazena, H., Perez-Rodrigues, E., Häder, D. P. and Lopez-Figueroa, F. (2002). Penetration of solar radiation into the water column of the central subtropical Atlantic Ocean—optical properties and possible biological consequences. *Deep Sea Research Part II: Topical Studies in Oceanography*, **49**(17), 3513-3528.

Pierre, J. L., Fontecave, M. and Crichton, R. R. (2002). Chemistry for an essential biological process: the reduction of ferric iron. *BioMetals*, **15**(4), 341-346.

Poulton, S. W. and Canfield, D. E. (2011). Ferruginous conditions: A dominant feature of the ocean through Earth's history. *Elements*, **7**(2), 107-112.

Rich, H. W. and Morel, F. M. M. (1990). Availability of well-defined iron colloids to the marine diatom Thalassiosira weissflogii. *Limnology and Oceanography*, **35**(3), 652-662.

Riggsbee, J. A., Orr, C. H., Leech, D. M., Doyle, M. W. and Wetzel, R. G. (2008). Suspended sediments in river ecosystems: Photochemical sources of dissolved organic carbon, dissolved organic nitrogen, and adsorptive removal of dissolved iron. *Journal of Geophysical Research: Biogeosciences*, **113**(G3).

Rijkenberg, M. J. A., Fischer, A. C., Kroon, J. J., Gerringa, L. J. A., Timmermans, K. R., Wolterbeek, H. T. and de Baar, H. J. W. (2005). The influence of UV irradiation on the photoreduction of iron in the Southern Ocean. *Marine Chemistry*, **93**(2), 119-129.

Rijkenberg, M. J. A., Gerringa, L. J. A., Carolus, V. E., Velzeboer, I. and de Baar, H. J. W. (2006). Enhancement and inhibition of iron photoreduction by individual ligands in open ocean seawater. *Geochimica et Cosmochimica Acta*, **70**(11), 2790-2805.

Rijkenberg, M. J. A., Gerringa, L. J. A., Neale, P. J., Timmermans, K. R., Buma, A. G. J. and de Baar, H. J. W. (2004). UVA variability overrules UVB ozone depletion effects on the photoreduction of iron in the Southern Ocean. *Geophysical Research Letters*, **31**(24).

Rose, A. L., Salmon, T. P., Lukondeh, T., Neilan, B. A. and Waite, T. D. (2005). Use of superoxide as an electron shuttle for iron acquisition by the marine cyanobacterium lyngbya majuscula. *Environmental Science & Technology*, **39**(10), 3708-3715.

Rose, A. L. and Waite, T. D. (2002). Kinetic model for Fe(II) oxidation in seawater in the absence and presence of natural organic matter. *Environmental Science & Technology*, **36**(3), 433-444.

Rose, A. L. and Waite, T. D. (2003). Predicting iron speciation in coastal waters from the kinetics of sunlight-mediated iron redox cycling. *Aquatic Sciences*, **65**(4), 375-383.

Rose, A. L. and Waite, T. D. (2005). Reduction of organically complexed ferric iron by superoxide in a simulated natural water. *Environmental Science & Technology*, **39**(8), 2645-2650.

Rue, E. L. and Bruland, K. W. (1995). Complexation of iron(III) by natural organic ligands in the Central North Pacific as determined by a new competitive ligand equilibration/adsorptive cathodic stripping voltammetric method. *Marine Chemistry*, **50**(1), 117-138.

Sandvik, S. L. H., Bilski, P., Pakulski, J. D., Chignell, C. F. and Coffin, R. B. (2000). Photogeneration of singlet oxygen and free radicals in dissolved organic matter isolated from the Mississippi and Atchafalaya River plumes. *Marine Chemistry*, **69**(1), 139-152.

Santana-Casiano, J. M., González-Dávila, M. and Millero, F. J. (2006). The role of Fe(II) species on the oxidation of Fe(II) in natural waters in the presence of $O_2$ and $H_2O_2$. *Marine Chemistry*, **99**(1), 70-82.

Schaedler, F., Lockwood, C., Lueder, U., Glombitza, C., Kappler, A. and Schmidt, C. (2018). Microbially mediated coupling of Fe and N cycles by nitrate-reducing Fe(II)-oxidizing bacteria in littoral freshwater sediments. *Applied and Environmental Microbiology*, **84**(2), e02013-02017.

Schlosser, C., De La Rocha, C. L., Streu, P. and Croot, P. L. (2012). Solubility of iron in the Southern Ocean. *Limnology and Oceanography*, **57**(3), 684-697.

Schneider, R. J., Roe, K. L., Hansel, C. M. and Voelker, B. M. (2016). Species-level variability in extracellular production rates of reactive oxygen species by diatoms. *Frontiers in Chemistry*, **4**(5).

Scholes, G. D., Fleming, G. R., Olaya-Castro, A. and van Grondelle, R. (2011). Lessons from nature about solar light harvesting. *Nature Chemistry*, **3**, 763.

Scully, N. M., Cooper, W. J. and Tranvik, L. J. (2003). Photochemical effects on microbial activity in natural waters: the interaction of reactive oxygen species and dissolved organic matter. *FEMS Microbiology Ecology*, **46**(3), 353-357.

Scully, N. M., McQueen, D. J. and Lean, D. R. S. (1996). Hydrogen peroxide formation: The interaction of ultraviolet radiation and dissolved organic carbon in lake waters along a 43–75°N gradient. *Limnology and Oceanography*, **41**(3), 540-548.

Sherman, D. M. (2005). Electronic structures of iron(III) and manganese(IV) (hydr)oxide minerals: Thermodynamics of photochemical reductive dissolution in

aquatic environments. *Geochimica et Cosmochimica Acta*, **69**(13), 3249-3255.

Siffert, C. and Sulzberger, B. (1991). Light-induced dissolution of hematite in the presence of oxalate. A case study. *Langmuir*, **7**(8), 1627-1634.

Singer, P. C. and Stumm, W. (1970). Acidic mine drainage: the rate-determining step. *Science*, **167**(3921), 1121-1123.

Sivan, O., Erel, Y., Mandler, D. and Nishri, A. (1998). The dynamic redox chemistry of iron in the epilimnion of Lake Kinneret (Sea of Galilee). *Geochimica et Cosmochimica Acta*, **62**(4), 565-576.

Smith, R. C. and Baker, K. S. (1981). Optical properties of the clearest natural waters (200–800 nm). *Applied Optics*, **20**(2), 177-184.

Southwell, M. W., Mead, R. N., Luquire, C. M., Barbera, A., Avery, G. B., Kieber, R. J. and Skrabal, S. A. (2011). Influence of organic matter source and diagenetic state on photochemical release of dissolved organic matter and nutrients from resuspendable estuarine sediments. *Marine Chemistry*, **126**(1), 114-119.

Sullivan, A. B., Drever, J. I. and McKnight, D. M. (1998). Diel variation in element concentrations, Peru Creek, Summit County, Colorado. *Journal of Geochemical Exploration*, **64**(1), 141-145.

Sulzberger, B. (2015). Light-induced redox cycling of iron: Roles for $CO_2$ uptake and release by aquatic ecosystems. *Aquatic Geochemistry*, **21**(2), 65-80.

Sulzberger, B. and Laubscher, H. (1995). Reactivity of various types of iron(III) (hydr)oxides towards light-induced dissolution. *Marine Chemistry*, **50**(1), 103-115.

Sulzberger, B., Schnoor, J. L., Giovanoli, R., Hering, J. G. and Zobrist, J. (1990). Biogeochemistry of iron in an acidic lake. *Aquatic Sciences*, **52**(1), 56-74.

Sulzberger, B., Suter, D., Siffert, C., Banwart, S. and Stumm, W. (1989). Dissolution of Fe(III)(hydr)oxides in natural waters; laboratory assessment on the kinetics controlled by surface coordination. *Marine Chemistry*, **28**(1), 127-144.

Sunda, W. G. and Huntsman, S. A. (1994). Photoreduction of manganese oxides in seawater. *Marine Chemistry*, **46**(1), 133-152.

Sunda, W. G., Huntsman, S. A. and Harvey, G. R. (1983). Photoreduction of manganese oxides in seawater and its geochemical and biological implications. *Nature*, **301**(5897), 234-236.

Tate, C. M., Broshears, R. E. and McKnight, D. M. (1995). Phosphate dynamics in an acidic mountain stream: Interactions involving algal uptake, sorption by iron oxide, and photoreduction. *Limnology and Oceanography*, **40**(5), 938-946.

Tranvik, L. J. and Bertilsson, S. (2001). Contrasting effects of solar UV radiation on dissolved organic sources for bacterial growth. *Ecology Letters*, **4**(5), 458-463.

Trick, C. G. (1989). Hydroxamate-siderophore production and utilization by marine eubacteria. *Current Microbiology*, **18**(6), 375-378.

Trusiak, A., Treibergs, L. A., Kling, G. W. and Cory, R. M. (2018). The role of iron and reactive oxygen species in the production of $CO_2$ in arctic soil waters. *Geochimica et Cosmochimica Acta*, **224**, 80-95.

Van Dover, C. L., Reynolds, G. T., Chave, A. D. and Tyson, J. A. (1996). Light at

deep-sea hydrothermal vents. *Geophysical Research Letters*, **23**(16), 2049-2052.

van Grondelle, R., Dekker, J. P., Gillbro, T. and Sundstrom, V. (1994). Energy transfer and trapping in photosynthesis. *Biochimica et Biophysica Acta (BBA) - Bioenergetics*, **1187**(1), 1-65.

Voelker, B. M., Morel, F. M. M. and Sulzberger, B. (1997). Iron redox cycling in surface waters: effects of humic substances and light. *Environmental Science & Technology*, **31**(4), 1004-1011.

Voelker, B. M. and Sedlak, D. L. (1995). Iron reduction by photoproduced superoxide in seawater. *Marine Chemistry*, **50**(1), 93-102.

Voelker, B. M., Sedlak, D. L. and Zafiriou, O. C. (2000). Chemistry of superoxide radical in seawater: reactions with organic Cu complexes. *Environmental Science & Technology*, **34**(6), 1036-1042.

Waite, T. D. and Morel, F. M. M. (1984a). Photoreductive dissolution of colloidal iron oxide: Effect of citrate. *Journal of Colloid and Interface Science*, **102**(1), 121-137.

Waite, T. D. and Morel, F. M. M. (1984b). Photoreductive dissolution of colloidal iron oxides in natural waters. *Environmental Science & Technology*, **18**(11), 860-868.

Waite, T. D., Szymczak, R., Espey, Q. I. and Furnas, M. J. (1995). Diel variations in iron speciation in northern Australian shelf waters. *Marine Chemistry*, **50**(1), 79-91.

Walter, X. A., Picazo, A., Miracle, M. R., Vicente, E., Camacho, A., Aragno, M. and Zopfi, J. (2014). Phototrophic Fe(II)-oxidation in the chemocline of a ferruginous meromictic lake. *Frontiers in Microbiology*, **5**(713).

Wells, M. L. and Mayer, L. M. (1991). The photoconversion of colloidal iron oxyhydroxides in seawater. *Deep Sea Research Part A. Oceanographic Research Papers*, **38**(11), 1379-1395.

White, S. N., Chave, A. D. and Reynolds, G. T. (2002). Investigations of ambient light emission at deep-sea hydrothermal vents. *Journal of Geophysical Research: Solid Earth*, **107**(B1), EPM 1-1-EPM 1-13.

Widdel, F., Schnell, S., Heising, S., Ehrenreich, A., Assmus, B. and Schink, B. (1993). Ferrous iron oxidation by anoxygenic phototrophic bacteria. *Nature*, **362**(6423), 834-836.

Wilhelm, S. W. and Trick, C. G. (1994). Iron-limited growth of cyanobacteria: Multiple siderophore production is a common response. *Limnology and Oceanography*, **39**(8), 1979-1984.

Wu, J. and Luther, G. W. (1995). Complexation of Fe(III) by natural organic ligands in the Northwest Atlantic Ocean by a competitive ligand equilibration method and a kinetic approach. *Marine Chemistry*, **50**(1), 159-177.

Yurkov, V. V. and Beatty, J. T. (1998). Aerobic anoxygenic phototrophic bacteria. *Microbiology and Molecular Biology Reviews*, **62**(3), 695-724.

Zepp, R. G. and Cline, D. M. (1977). Rates of direct photolysis in aquatic environment. *Environmental Science & Technology*, **11**(4), 359-366.

Zepp, R. G., Faust, B. C. and Hoigne, J. (1992). Hydroxyl radical formation in aqueous reactions (pH 3-8) of iron(II) with hydrogen peroxide: the photo-

Fenton reaction. *Environmental Science & Technology*, **26**(2), 313-319.

Zhang, T., Hansel, C. M., Voelker, B. M. and Lamborg, C. H. (2016). Extensive dark biological production of reactive oxygen species in brackish and freshwater ponds. *Environmental Science & Technology*, **50**(6), 2983-2993.

Zuo, Y. and Hoigne, J. (1992). Formation of hydrogen peroxide and depletion of oxalic acid in atmospheric water by photolysis of iron(III)-oxalato complexes. *Environmental Science & Technology*, **26**(5), 1014-1022.

## Chapter 3 – Personal contribution

Experiments were conceptualized by myself and Dr. Caroline Schmidt. Sediment sampling was done by myself and Dr. C. Schmidt. The experiments and data collection were carried out by myself. The discussion and analysis of the obtained results were done by myself and Dr. C. Schmidt, Prof. Dr. Andreas Kappler and Prof. Dr. Bo Barker Jørgensen. The manuscript was written by myself. Dr. C. Schmidt, Prof. A. Kappler and Prof. B.B. Jørgensen revised the manuscript.

# Chapter 3: Fe(III) photoreduction producing Fe$^{2+}_{aq}$ in oxic freshwater sediment

Ulf Lueder[1], Bo Barker Jørgensen[2], Andreas Kappler[1,2], Caroline Schmidt[1]

[1] Geomicrobiology, Center for Applied Geoscience (ZAG), University of Tuebingen, Germany

[2] Center for Geomicrobiology, Department of Bioscience, Aarhus University, Denmark

## 3.1 Abstract

Iron(III) (Fe(III)) photoreduction plays an important role in Fe cycling and Fe(II) bioavailability in the upper ocean. Although well described for water columns, it is currently unknown to what extent light impacts the production of dissolved Fe(II) ($Fe^{2+}$) in aquatic sediments. We performed high-resolution voltammetric microsensor measurements and demonstrated light-induced $Fe^{2+}$ release in freshwater sediments from Lake Constance. $Fe^{2+}$ concentrations increased up to 40 µM in the top 3 mm of the sediment during illumination in the visible range of light (400-700 nm), even in the presence of oxygen (100-280 µM). The $Fe^{2+}$ release was strongly dependent on the organic matter content of the sediment. A lack of photo-reduced $Fe^{2+}$ was measured in sediments with concentrations of organic carbon <6 mg $L^{-1}$. The simultaneous presence of sedimentary Fe(III) photoreduction besides microbial and abiotic $Fe^{2+}$ oxidation by oxygen suggests active Fe redox cycling in the oxic and photic zone of aquatic sediments. Here, we provide evidence for a relevant contribution of Fe(III) photoreduction to the biogeochemical Fe redox cycle in aquatic freshwater sediments.

**Graphical Abstract**
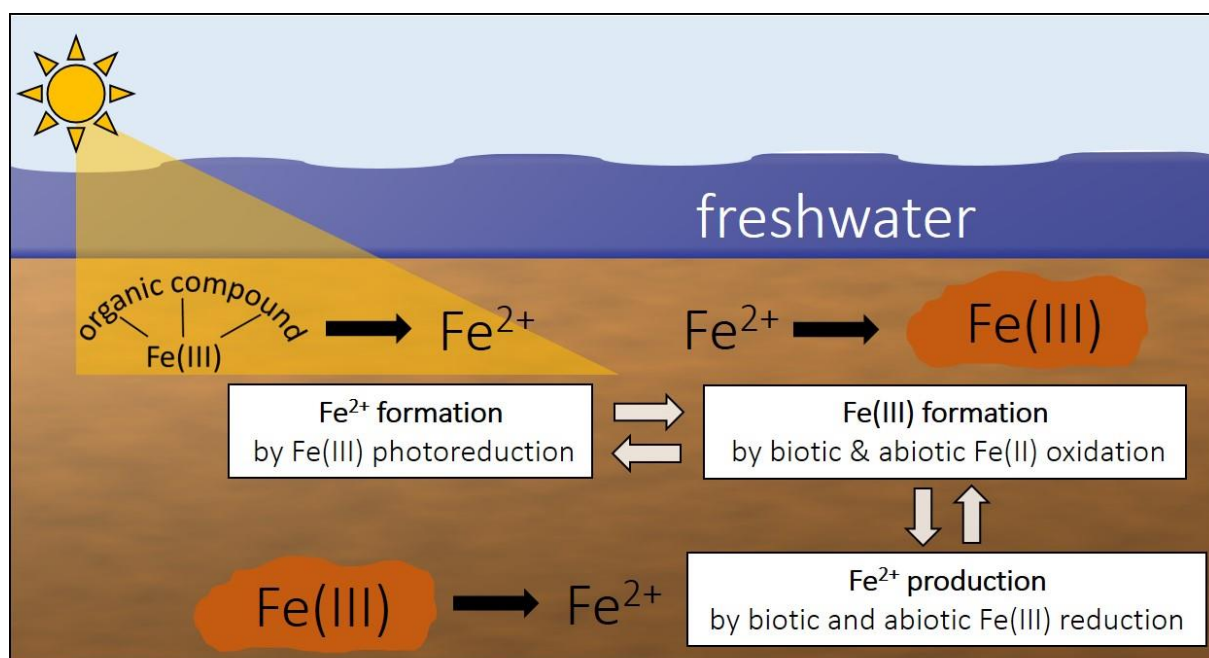
## 3.2 Introduction

The iron (Fe) cycle in freshwater and marine sediments involves diffusion of dissolved ferrous iron ($Fe^{2+}$) from the anoxic subsurface ferric iron (Fe(III)) reduction zone to the top of the sediment along prevailing redox gradients. The $Fe^{2+}$ is produced by Fe(III)-reducing microorganisms (Lovley & Phillips, 1988) or by abiotic Fe(III) reduction with sulphide or natural organic matter (NOM) (Canfield, 1989; Sulzberger et al., 1989). When $Fe^{2+}$ reaches the oxidized surface sediment it may serve as substrate for nitrate-reducing, phototrophic or microaerophilic Fe(II)-oxidizing bacteria, all of which are ubiquitously found in marine and freshwater sediments (Laufer et al., 2016; Otte et al., 2018b). Besides microbial oxidation, $Fe^{2+}$ is also re-oxidized abiotically by oxygen ($O_2$) (Millero et al., 1987), which functions as a barrier against $Fe^{2+}$ release into the water column and causes precipitation of Fe(III) minerals in the top layers of littoral sediments. Although Fe(III) is typically present in the form of poorly soluble Fe(III) (oxyhydr)oxides in oxic sediment layers, laboratory studies have shown that organic material can interact with solid phase Fe and enhance light induced mineral dissolution via Fe complexation (Sulzberger et al., 1989).

The photochemically induced reduction of organically complexed Fe(III) to $Fe^{2+}$ is an important source of nutritional Fe in the water column of Fe depleted oceans, lakes or rivers (Miles & Brezonik, 1981; Collienne, 1983; O'Sullivan et al., 1991; Kuma et al., 1992; Kuma et al., 1995; Miller et al., 1995) and plays a major role in the aquatic Fe redox cycle. Photoreduction depends on the chemical structure of the Fe-binding functional groups (Barbeau et al., 2003). The reduction of organically complexed Fe(III) is either directly induced by light absorption and ligand-to-metal charge transfer (LMCT), or by reactions with photochemically produced radicals such as superoxide (Sulzberger et al., 1989; Kuma et al., 1995; Barbeau, 2006). In the ocean, where more than 99% of the dissolved Fe is complexed by organic ligands (Gledhill & van den Berg, 1994; van den Berg, 1995) such as photo-susceptible siderophores (Barbeau et al., 2001), Fe(III) photoreduction is the most important process delivering bioavailable $Fe^{2+}$ (Sulzberger, 2015). Although Fe(III) photoreduction was demonstrated to be an important process in the water column, it is unknown to what extent light induces $Fe^{2+}$ release in freshwater sediments. Thus, the ubiquitous presence of Fe(III)- and Fe(II)-organic complexes in sediments (Luther III et al., 1996; Taillefert et al., 2000; Carey & Taillefert, 2005) has not yet been related to the natural production of $Fe^{2+}$ via Fe(III) photoreduction in littoral systems. However, as light penetrates several mm into sediments (Kühl et al., 1994), the prerequisites for Fe(III) photoreduction, i.e. organically complexed Fe(III) and light, may also be present in

many littoral sediments. Many shallow lakes have extensive littoral zones in which Fe(III) photoreduction could be a significant $Fe^{2+}$ source.

Therefore, the objectives of this study were i) to quantify the photochemically produced $Fe^{2+}$ in the upper sediment layer, ii) to relate the extent of Fe(III) photoreduction to the DOC content of the sediment and iii) to evaluate the impact of this potential $Fe^{2+}$ source for the sedimentary Fe cycle.

## 3.3 Materials & Methods

### Sediment core incubations

Freshwater sediment and water were collected from two locations with different sedimentary organic carbon (C) content close to the island of Mainau (September, November 2017) in the littoral zone of Lake Constance, Germany, and kept in the dark at 4°C until further processing. For core incubations, gravel and shells were removed from the sediment to enable undisturbed microsensor application. Homogenized sediment was filled to a height of 6 cm into cut 50 ml syringes and overlaid with 4 cm Lake Constance water. Pictures of the field site and the experimental setup are shown in the Supporting Information (Figure S3.1). Homogenization of the sampled sediment was done to ensure homogeneous and reproducible starting conditions of the sediment cores. The homogenized cores resemble natural sediment, which is often exposed to mixing of the upper millimeters, e.g. caused by wave action. A similar setup has been used in previous studies in order to study biotic and abiotic processes at high spatial resolution (Nielsen et al., 2010; Pfeffer et al., 2012). The sediment cores were incubated in the light or in the dark at 20°C for 3 days with continuous aeration. One set of sediment cores was incubated under anoxic conditions ($N_2$-flushed glovebox) in the light. The cores were re-filled regularly with Lake Constance water to compensate for evaporation. The light intensity during incubations was adjusted to either 400-500 or 40 µmol photons $m^{-2}$ $s^{-1}$, calibrated by a spherical light meter (ULM-500 and US-SQS/L sensor, Walz, Germany). 400-500 µmol photons $m^{-2}$ $s^{-1}$ corresponds to a natural light intensity that may reach the sediment at 5-6 m water depth after attenuation in oligotrophic Lake Constance water at full daylight (Tilzer, 1988), which is approx. 2000 µmol photons $m^{-2}$ $s^{-1}$ (Demmig-Adams & Adams III, 2000). The light-incubated sediment cores were continuously illuminated with two LED lamps (Samsung SI-P8V151DB1US, 14 W, 3000 K, and SMD 2835, 15 W, 6000 K) in order to mimic the visible spectrum of sunlight (400-700 nm). In order to prevent light penetration from the sides, the sediment cores were wrapped in aluminum foil from the sediment-water interface downwards.

The dependence of Fe(III) photoreduction on the organic C content was determined by incubation of sediments sampled at two different locations that are approx. 1 km apart and that differ naturally in organic C content. High-organic C sediment had $1.55\pm0.05\%$ (n=4) TOC and a dissolved organic carbon (DOC) concentration of $15.8\pm3.5$ mg C L$^{-1}$ (n=3) in the pore water. Low-organic C sediment had $0.051\pm0.002\%$ (n=4) TOC and $3.3 \pm 0.6$ mg C L$^{-1}$ DOC. More information on the different sediments is given in the Supporting Information (Table S3.1).

Natural dissolved organic matter that was used to test the dependence of Fe(III) photoreduction on organic complexing agents, was extracted from low-organic C sediment. This procedure allowed to increase the concentration of dissolved organic matter with exactly the same composition in the $C_{org}$ depleted sediments. For this, 100 g sediment was mixed with 400 ml deionized water (Milli-Q Integral System, Merck, Millipore) and stored on a rolling shaker for 24 hours at 20°C in dark. The supernatant of the extraction slurry was subsequently flushed with nitrogen gas ($N_2$), filter-sterilized (0.22 µm) and mixed with the sediment prior to filling it into cut 50 ml syringes. To show whether the observed light-dependent production of $Fe^{2+}$ was purely abiotic, high-organic C sediment was filled into plastic bags and was gamma-sterilized at a cobalt 60 radiation field with a dose of 62 kGy, (Synergy Health Allershausen GmbH, Germany). The gamma-sterilized sediment was incubated in the light prior to high-resolution $O_2$, $Fe^{2+}$ and light gradient measurements.

## Biogeochemical measurements

$Fe^{2+}$ concentration profiles were measured by voltammetry with a three-electrode system using a DLK-70 web-potentiostat (Analytical Instrument Systems, Flemington, NJ). The working electrode was a lab-constructed glass-encased 100 µm gold amalgam (Au/Hg) electrode (Brendel & Luther III, 1995). An Ag wire coated with AgCl and a Pt wire were used as reference and counter electrode, respectively. Calibration for $Fe^{2+}$ was performed applying the pilot ion method (Brendel & Luther III, 1995; Slowey & Marvin-DiPasquale, 2012) with $Mn^{2+}$. Cyclic voltammograms for $Fe^{2+}$ and $Mn^{2+}$ were recorded by conditioning the electrode at -0.05 V for 2 s and subsequently scanning from -0.05 V to -2 V and back with a scan rate of 1000 mV s$^{-1}$. Before each scan, a potential of -0.9 V was applied for 5 s to clean the electrode surface. Ten scans were run at every measurement depth and the final three voltammograms were analyzed using the VOLTINT program for Matlab® (Bristow & Taillefert, 2008). $Fe^{2+}$ concentrations were recorded 1 mm above and directly at the sediment surface, as well as in 0.5, 1, 1.5, 2, 3,

4, 6, 10, 15 and 30 mm depth. Error bars show the standard deviation of triplicate voltammograms.

Dissolved $O_2$ was measured with a 100 μm tip diameter Clark-type $O_2$ microelectrode (Unisense, Denmark) as described by Revsbech (1989). A two-point calibration was done in fully air-saturated and in anoxic water. Vertical $O_2$ concentration profiles were recorded in triplicate with a spatial resolution of 200 μm using a manual micromanipulator with the software Sensor Trace Suite (Unisense, Denmark). Calculated error bars show the standard deviation of triplicate measurements.

Profiles of scalar irradiance as a measure of light intensity were recorded with lab-constructed light sensors (Kühl & Jørgensen, 1992) connected to a spectrometer (USB4000-XR1-ES, Ocean Optics, Germany) with the software SpectraSuite (Ocean Optics, Germany). For light measurement, sediment cores were illuminated vertically from above with a halogen cold light source (Euromex Illuminator EK-1, Netherlands). The spatial resolution of the scalar irradiance profile was 200 μm. Data were normalized as percentage of the scalar irradiance at the sediment surface.

For quantification of the TOC content, the sediment was dried at 60°C until constant weight. The dry sediment was ground in a planetary mill and acidified with 16% HCl to remove the inorganic carbon. After washing with deionized water and subsequent drying, the TOC content was measured with a total carbon analyzer (Vario EL, Elementar, Germany). The DOC concentration of the sediment pore water and the sediment extract was measured with a dissolved carbon analyzer (Multi N/C 2100s, Analytik Jena, Germany).

Half-life times of $Fe^{2+}$ $(t_{\frac{1}{2}}(Fe^{2+}))$ in the sediment were calculated by

$$t_{\frac{1}{2}}(Fe^{2+}) = \frac{\ln(2)}{k_0 \cdot [O_2] \cdot [OH^-]^2} \tag{3.1}$$

with the universal rate constant for homogeneous $Fe^{2+}$ oxidation by $O_2$, $k_0$, being $2.3 \cdot 10^{14}$ mol$^3$ L$^{-3}$ s$^{-1}$ at 25°C (Tamura et al., 1976) as well as in situ concentrations of $[O_2]$ and $[OH^-]$.

## 3.4 Results & Discussion

**Dissolved Fe(II) concentrations in freshwater sediments**

Light penetrated approx. 2.5 mm into the incubated sediment (Figure 3.1a). A pronounced $Fe^{2+}$ concentration peak of 40 µM occurred in the top millimeter of the sediment (Figure 3.1a) after incubation in light for two days. As the cores were freshly prepared from homogenized sediment, geochemical and photochemical gradients first needed to develop before the pronounced peak of photo-produced $Fe^{2+}$ established. The maximum $Fe^{2+}$ concentration in the light-influenced surface layer of the high-organic C sediment reached 60% of the $Fe^{2+}$ concentration measured in a depth of 30 mm, where the major zone of microbial Fe(III) reduction and $Fe^{2+}$ production is expected (Schmidt et al., 2010). Sediment cores incubated in the dark did not show the $Fe^{2+}$ peak in the top millimeters but only a gradual increase with depth from <10 µM at the surface to 50 µM at 30 mm (Figure 3.1b). Thus, $Fe^{2+}$ concentrations were five-fold higher in the top mm of the sediment in the illuminated cores compared to the dark incubated cores. Below 6 mm, $Fe^{2+}$ concentrations increased to a similar range, in both light and dark incubated cores (Figure 3.1b). In both light and dark incubations, $O_2$ co-occurred (100-280 µM) with elevated $Fe^{2+}$ concentrations and penetrated down to approx. 3 mm (Figure 3.1a). As Lake Constance is an oligotrophic lake, photosynthetic activity in the incubated sediment cores was quite low and did not lead to significantly increased $O_2$ concentrations in the light incubated cores (Figure S3.2). The laboratory cores thereby resembled $O_2$ profiles recorded in natural intact sediment cores of similar sediment composition (Schaedler et al., 2018). Under these conditions (pH 7.8), fast abiotic $Fe^{2+}$ oxidation by $O_2$ is predicted with a half-life of $Fe^{2+}$ in the range of 0.5-1.5 minutes, yet, $Fe^{2+}$ persisted in the presence of $O_2$. The $Fe^{2+}$ concentrations reached by light-induced $Fe^{2+}$ release are in the same order as concentrations generated in the main Fe(III) reduction zone below (Melton et al., 2014). This highlights the efficiency of Fe(III) photoreduction as a $Fe^{2+}$ source in the sediment.

In order to exclude that the $Fe^{2+}$ was produced by microbial Fe(III) reduction in the light-incubated sediment cores, sterilized sediment was also incubated in the light. This revealed a $Fe^{2+}$ concentration peak in the upper 3 mm (Figure S3.3), even more pronounced than in non-sterilized sediment. This pronounced peak was partly caused by the gamma-sterilization, which releases Fe from the sediment and increases the DOC concentrations of the pore water significantly (Otte et al., 2018a) (to approx. 850 mg C $L^{-1}$). Higher DOC concentrations potentially also increase the effect of Fe(III) photoreduction.
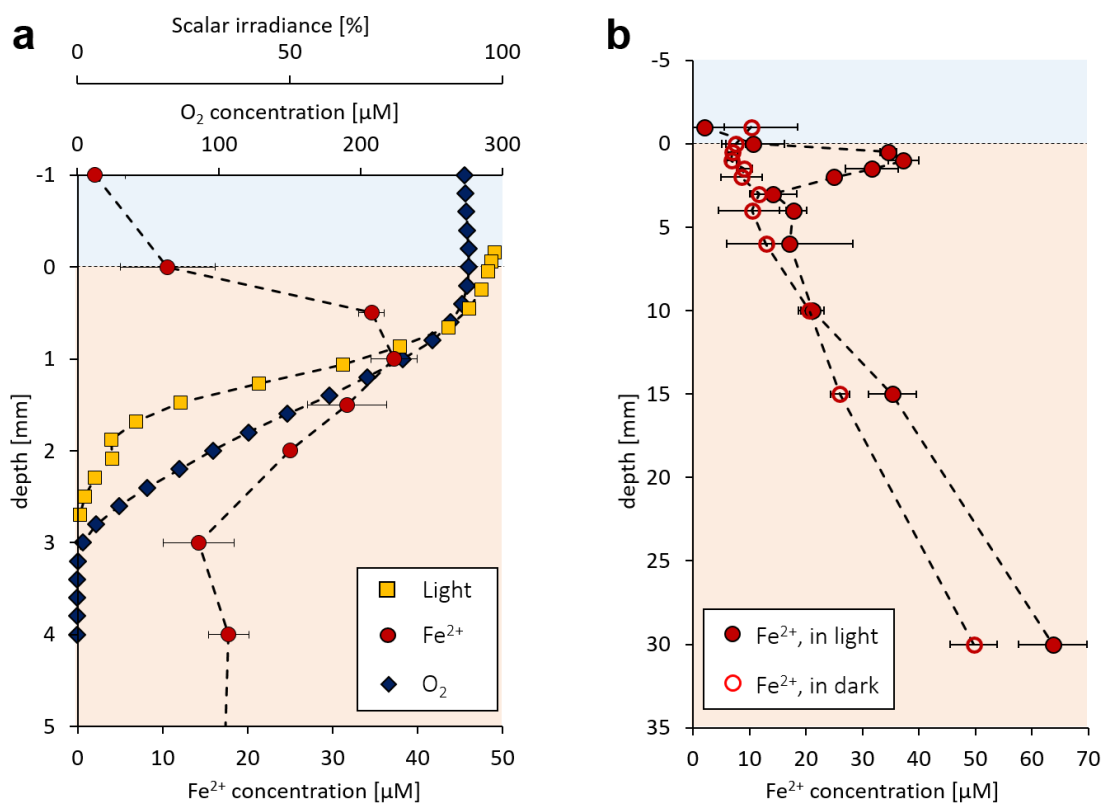
**Figure 3.1** Concentration profiles in laboratory-incubated Lake Constance sediment cores. (a) Light intensity (expressed as % of surface scalar irradiance), $Fe^{2+}$ and $O_2$ in the top 5 mm. (b) Comparison of $Fe^{2+}$ in light and dark in the upper 30 mm. Error bars show standard deviations of triplicate voltammograms recorded in one sediment core.

## Dependence of Fe(III) photoreduction on organic carbon concentration

In order to determine the relationship between the sedimentary organic C content and Fe(III) photoreduction, low-organic C sediment was similarly incubated in light and dark at 20°C. Similar $Fe^{2+}$ concentrations were measured in both light and dark incubations of the low-organic C sediment (Figure S3.4). Only a minor $Fe^{2+}$ peak of 5 μM was produced at 3 mm depth (Figure 3.2). The amendment with dissolved organic carbon (DOC 2.8 mg C $L^{-1}$) (extracted from bulk low-organic C sediment prior to the experiment) to the sediment pore water, triggered the formation of a distinct $Fe^{2+}$ peak in the upper millimeters reaching concentrations of up to 30 μM after two days of light incubation (Figure 3.2). The doubling of DOC concentration induced more than 2.5 fold higher $Fe^{2+}$ concentrations in 1 mm depth compared to $Fe^{2+}$ concentrations in the non-amended low-organic C sediment (Figure 3.2). In dark-incubated control cores of low-organic C sediment with amended DOC, no increase in $Fe^{2+}$ concentration was observed in the top millimeters (Figure S3.5).

We have shown that light-induced $Fe^{2+}$ release in sediments strongly depends on the availability of organic molecules that could function as Fe-complexing agents. A measurable peak of photo-produced $Fe^{2+}$ was only detected when the concentration of dissolved organic carbon was > approx. 6 mg C $L^{-1}$. In many sediments, Fe(III)-complexing organic ligands such as NOM, plant or bacterial exudates are present (Luther III et al., 1992; Laglera et al., 2007; Gledhill & Buck, 2012). We have shown that Fe(III) photoreduction can be stimulated in sediment with naturally low organic carbon content when organic material is added. Fe(III) photoreduction may therefore be an important $Fe^{2+}$ source, also for sediments characterized by fluctuations in organic carbon content (e.g. via seasonal surface runoff, rainfall or deposition of plankton detritus from the water column). Another important photochemical process has been shown for resuspended sediments, where DOC gets produced by photo-dissolution of particulate organic matter (Mayer et al., 2006; Southwell et al., 2011), which is an important source of DOC in estuarine and coastal ecosystems (Kieber et al., 2006). Thus, photo-produced DOC might also enhance the effect of Fe(III) photoreduction by delivering additional DOC to the sediment column. Organic matter can also stabilize $Fe^{2+}$ against oxidation by complexation (Kurimura et al., 1968; Suzuki et al., 1992), thereby slowing down $Fe^{2+}$ oxidation kinetics and leading to a longer $Fe^{2+}$ half-life times. This phenomenon might explain the observed build-up and persistence of elevated $Fe^{2+}$ concentrations in oxic sediment layers in the presence of $O_2$ in light incubated sediment cores and might also explain the presence of some $Fe^{2+}$ in the surface of dark incubated sediment cores.
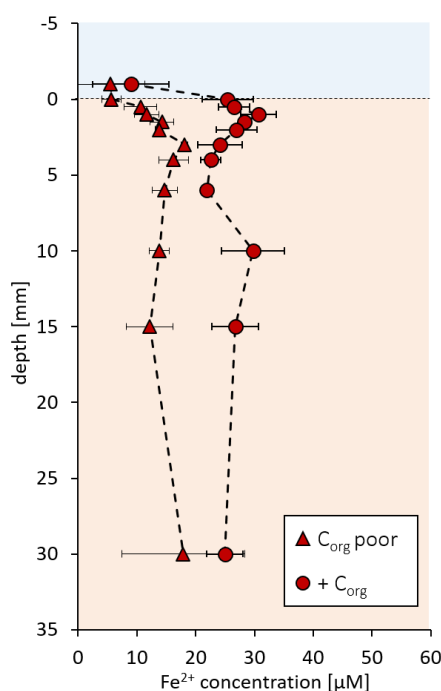
**Figure 3.2** $Fe^{2+}$ concentration profiles in low-organic C sediment in the light without carbon amendment ($C_{org}$ poor, triangles) and with the amendment with sediment-extracted dissolved organic matter (+ $C_{org}$, circles). Error bars show the standard deviation of triplicate voltammograms recorded in one sediment core.

## Effects of light intensity and absence of $O_2$ on photochemical production of $Fe^{2+}$

As the process of Fe(III) photoreduction depends on the light energy (Kimball et al., 1992; Waite et al., 1995), high-organic C sediment was also incubated with 10% of the initially chosen light intensity. Even at this low light intensity, a $Fe^{2+}$ peak of approx. 40 µM was measured in the top millimeter of the sediment, similar to the full light energy incubation (Figure 3.3). Considering a light intensity of 2000 µmol photons $m^{-2}$ $s^{-1}$ on a sunny day and a light attenuation coefficient for Lake Constance water of 0.27 $m^{-1}$, light which reaches water depths of up to 14.5 m is still sufficient to induce Fe(III) photoreduction (40 µmol photons $m^{-2}$ $s^{-1}$). The shallow water zone of Lake Constance is defined by a depth of 10 m and its surface measures 75 $km^2$, which represents almost 17% of the lake surface. If DOC is > 6 mg $L^{-1}$ in that zone, the upper millimeters of the sediment in this area will be influenced by Fe(III) photoreduction.

Wavelengths below 520 nm photoreduce Fe(III) (Rich & Morel, 1990), as the shorter wavelengths have sufficient energy to excite and transfer electrons from the organic ligand to the Fe(III). Although UVA (315-400 nm) and UVB (280-315 nm) light is strongly absorbed by attenuating substances in water, some still reaches the sediment surface and penetrates several

hundred micrometers into the sediment (Garcia-Pichel & Bebout, 1996). It presumably contributes to the overall light-induced release of $Fe^{2+}$ and, therefore, the photo-produced $Fe^{2+}$ concentrations measured in this study might even be underestimated relative to in situ sunlit conditions in Lake Constance.

In order to quantify the maximum capacity of Fe(III) photoreduction, we incubated sediment cores under anoxic and full light conditions. Anoxic conditions prevent fast re-oxidation of the photochemically produced $Fe^{2+}$ by $O_2$ and represent also the $Fe^{2+}$ that might be engaged in fast Fe redox cycling (Figure 3.3). Anoxic incubations increase anoxic sediment layers and thus enlarge the niche for anoxygenic phototrophic Fe(II)-oxidizers (present in these sediments) (Otte et al., 2018b) and leading to more $Fe^{2+}$ consumption in comparison to the oxic sediment. Only recently was it shown that even organically complexed $Fe^{2+}$ can be metabolized by phototrophic Fe(II)-oxidizers (Peng et al., 2019). Another explanation is ii) that $Fe^{2+}$ in illuminated sediments is not only produced by LMCT reactions but also in secondary reactions with photochemically produced reactive oxygen species (ROS) such as superoxide (Voelker & Sedlak, 1995; Öztürk et al., 2004; Rose & Waite, 2005; Barbeau, 2006). Superoxide is simultaneously forming from photochemical reactions of $O_2$ with dissolved organic matter (Rose & Waite, 2005; Rose, 2012) and during abiotic Fe(II) oxidation by $O_2$ (King et al., 1995) and is a potential reductant of Fe(III) species (Rose & Waite, 2005; Barbeau, 2006; Rose, 2012). Organic material that is present in sediments can also inhibit abiotic re-oxidation of photochemically produced $Fe^{2+}$ in oxic sediment layers due to scavenging of other ROS such as $H_2O_2$ that could otherwise oxidize $Fe^{2+}$ (McKnight et al., 1988; Öztürk et al., 2004). In oxic sediments, therefore, not only $Fe^{2+}$ oxidation by $O_2$ occurs but also $Fe^{2+}$ production by e.g. superoxide leading to similar $Fe^{2+}$ concentrations as in anoxic illuminated sediment layers, where less ROS should form photochemically due to the lack of $O_2$.
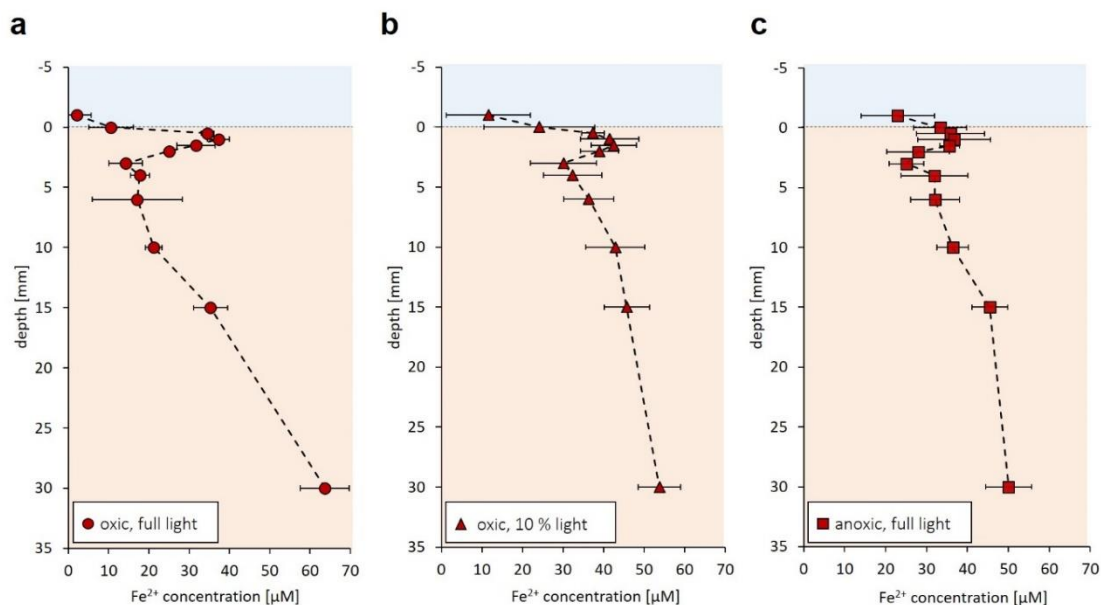
**Figure 3.3** $Fe^{2+}$ concentration profiles in Lake Constance sediment cores. (a) Incubated under full light and oxic conditions. (b) Incubated with 10% light intensity and oxic conditions. (c) Incubated with full light and anoxic conditions Error bars show standard deviations of triplicate voltammograms recorded in one sediment core.

## Environmental consequences of Fe(III) photoreduction in sediments

In the ocean, Fe(III) photoreduction produces $Fe^{2+}$ in the range of nanomolar per hour (Miller et al., 1995) and thereby produces an essential micro-nutrient or trace metal for diverse organisms in seawater (Voelker & Sedlak, 1995; Roy et al., 2008). In sediments, $Fe^{2+}$ concentrations reach micromolar range and $Fe^{2+}$ is therefore not a limiting nutrient. However, sedimentary nitrate-reducing, phototrophic and microaerophilic microorganisms, which conserve energy and reducing equivalents for $CO_2$ fixation from the enzymatic oxidation of $Fe^{2+}$, all require $Fe^{2+}$ in excess of the trace element level. In natural sediments, the main source of $Fe^{2+}$ has been expected to be biotic or abiotic Fe(III) reduction (Lovley & Phillips, 1988; Canfield, 1989; Sulzberger et al., 1989) in the anoxic layers. From these layers, $Fe^{2+}$ diffuses upwards into sediment layers where it gets recycled by microbial and chemical oxidation processes. As soon as $Fe^{2+}$ reaches oxygenated sediment layers, it is rapidly oxidized chemically by $O_2$ (Millero et al., 1987), which limits its availability for microaerophilic Fe(II)-oxidizing bacteria. It is exactly in this narrow zone that Fe(III) photoreduction may produce substantial amounts of $Fe^{2+}$. This process might, thereby, represent an important $Fe^{2+}$ source for Fe(II)-oxidizing bacteria, enabling growth of these bacteria in sediment layers in which, based on $Fe^{2+}$ oxidation kinetics and measured $O_2$ and $Fe^{2+}$ profiles, abiotic $Fe^{2+}$ oxidation would otherwise dominate.

## Implications on the sedimentary Fe cycle

The discovery of Fe(III) photoreduction in freshwater sediments adds a new feature to our current understanding of the biogeochemical Fe cycling. So far, light-induced $Fe^{2+}$ release has been an overlooked $Fe^{2+}$ source in such sediments, probably because high-resolution in-situ measurements of $Fe^{2+}$ combined with appropriate experiments are necessary for its detection. Classical solid-phase acid extractions do not detect the process (Figure S3.6). Continuous $Fe^{2+}$ production via photoreduction and simultaneous $Fe^{2+}$ removal through fast oxidation by $O_2$ prevent the precipitation of Fe(II) mineral phases and do not leave a measurable net signal behind in the solid mineral phase.

We have thus shown that Fe(III) photoreduction represents a so far overlooked $Fe^{2+}$ source in the upper, light-influenced sediment layers, even in the presence of $O_2$. Fe(III) photoreduction produces sufficient $Fe^{2+}$, even at low light intensities, to maintain it in tens of μM concentrations in oxic freshwater sediment layers. Until now, $Fe^{2+}$ was described to originate from reducing, anoxic sediment layers where biotic or abiotic Fe(III) reduction produce $Fe^{2+}$ and drive the upwards diffusion of $Fe^{2+}$ towards surface sediment layers (Figure 3.4). With a peak of $Fe^{2+}$ at concentrations similar to those found in deeper sediment layers, light-induced $Fe^{2+}$ release delivers $Fe^{2+}$ as a substrate for Fe(II)-oxidizing microorganisms in sediment layers far above the main Fe(III) reduction zone, thereby enhancing microbial Fe(II) oxidation and establishing a downward diffusion gradient of $Fe^{2+}$. This complicates the classical Fe(II) vs. Fe(III) concentration gradients and overlays small-scale redox conversions of Fe in the sediment (Figure 3.4). The findings show that Fe(III) photoreduction might represent a powerful process in freshwater sediments and adds new perspectives to our understanding of Fe redox cycling.
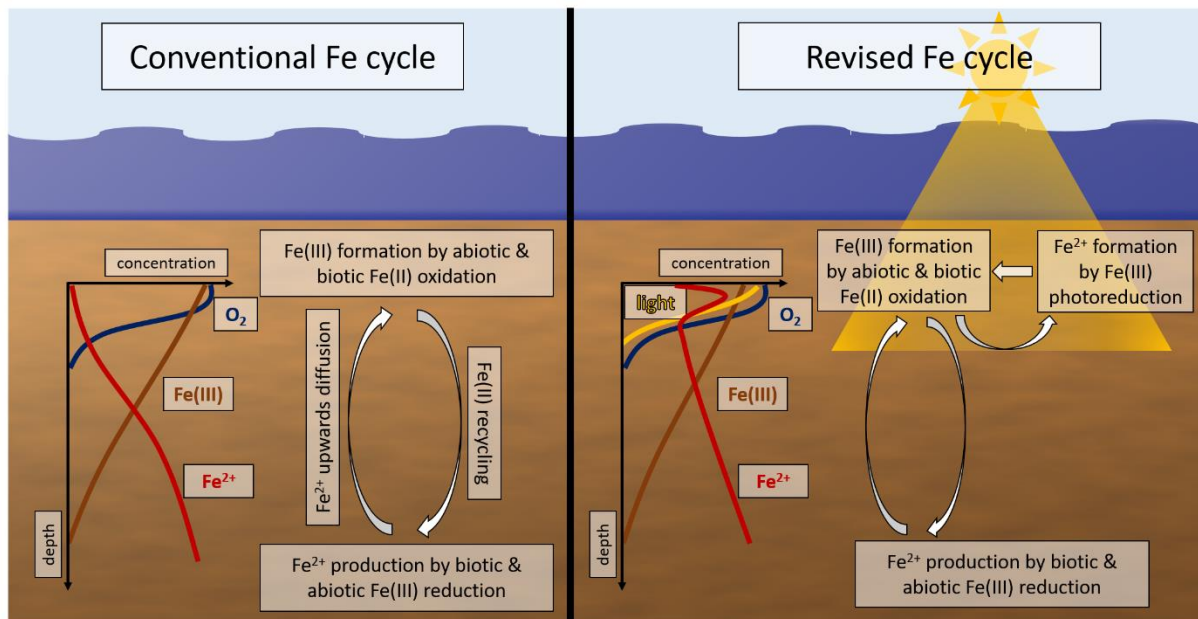
**Figure 3.4** Schematic overview of the conventional Fe cycling in freshwater sediments (left) and the revised view under consideration of Fe(III) photoreduction as a substantial $Fe^{2+}$ source in upper, oxic, light-penetrated freshwater sediments (right).

## Acknowledgements

## 3.5 References

Barbeau, K. (2006). Photochemistry of organic iron(III) complexing ligands in oceanic systems. *Photochemistry and Photobiology*, **82**(6), 1505-1516.

Barbeau, K., Rue, E. L., Bruland, K. W. and Butler, A. (2001). Photochemical cycling of iron in the surface ocean mediated by microbial iron(III)-binding ligands. *Nature*, **413**, 409.

Barbeau, K., Rue, E. L., Trick, C. G., Bruland, K. W. and Butler, A. (2003). Photochemical reactivity of siderophores produced by marine heterotrophic bacteria and cyanobacteria based on characteristic Fe(III) binding groups. *Limnology and Oceanography*, **48**(3), 1069-1078.

Brendel, P. J. and Luther III, G. W. (1995). Development of a gold amalgam voltammetric microelectrode for the determination of dissolved Fe, Mn, $O_2$, and S(-II) in porewaters of marine and freshwater sediments. *Environmental Science & Technology*, **29**(3), 751-761.

Bristow, G. and Taillefert, M. (2008). VOLTINT: A Matlab®-based program for semi-automated processing of geochemical data acquired by voltammetry. *Computers & Geosciences*, **34**(2), 153-162.

Canfield, D. E. (1989). Reactive iron in marine sediments. *Geochimica et Cosmochimica Acta*, **53**(3), 619-632.

Carey, E. and Taillefert, M. (2005). The role of soluble Fe(III) in the cycling of iron and sulfur in coastal marine sediments. *Limnology and Oceanography*, **50**(4), 1129-1141.

Collienne, R. H. (1983). Photoreduction of iron in the epilimnion of acidic lakes. *Limnology and Oceanography*, **28**(1), 83-100.

Demmig-Adams, B. and Adams III, W. W. (2000). Harvesting sunlight safely. *Nature*, **403**, 371.

Garcia-Pichel, F. and Bebout, B. M. (1996). Penetration of ultraviolet radiation into shallow water sediments: high exposure for photosynthetic communities. *Marine Ecology Progress Series*, **131**, 257-262.

Gledhill, M. and Buck, K. (2012). The organic complexation of iron in the marine environment: a review. *Frontiers in Microbiology*, **3**(69).

Gledhill, M. and van den Berg, C. M. G. (1994). Determination of complexation of iron(III) with natural organic complexing ligands in seawater using cathodic stripping voltammetry. *Marine Chemistry*, **47**(1), 41-54.

Kieber, R. J., Whitehead, R. F. and Skrabal, S. A. (2006). Photochemical production of dissolved organic carbon from resuspended sediments. *Limnology and Oceanography*, **51**(5), 2187-2195.

Kimball, B. A., McKnight, D. M., Wetherbee, G. A. and Harnish, R. A. (1992). Mechanisms of iron photoreduction in a metal-rich, acidic stream (St. Kevin Gulch, Colorado, U.S.A.). *Chemical Geology*, **96**(1), 227-239.

King, D. W., Lounsbury, H. A. and Millero, F. J. (1995). Rates and mechanism of Fe(II) oxidation at nanomolar total iron concentrations. *Environmental Science & Technology*, **29**(3), 818-824.

Kühl, M. and Jørgensen, B. B. (1992). Spectral light measurements in microbenthic phototrophic communities

with a fiber-optic microprobe coupled to a sensitive diode array detector. *Limnology and Oceanography*, **37**(8), 1813-1823.

Kühl, M., Lassen, C. and Jørgensen, B. B. (1994). Light penetration and light intensity in sandy marine sediments measured with irradiance and scalar irradiance fiber-optic microprobes. *Marine Ecology Progress Series*, **105**(1/2), 139-148.

Kuma, K., Nakabayashi, S. and Matsunaga, K. (1995). Photoreduction of Fe(III) by hydroxycarboxylic acids in seawater. *Water Research*, **29**(6), 1559-1569.

Kuma, K., Nakabayashi, S., Suzuki, Y., Kudo, I. and Matsunaga, K. (1992). Photo-reduction of Fe(III) by dissolved organic substances and existence of Fe(II) in seawater during spring blooms. *Marine Chemistry*, **37**(1), 15-27.

Kurimura, Y., Ochiai, R. and Matsuura, N. (1968). Oxygen oxidation of ferrous ions induced by chelation. *Bulletin of the Chemical Society of Japan*, **41**(10), 2234-2239.

Laglera, L. M., Battaglia, G. and van den Berg, C. M. G. (2007). Determination of humic substances in natural waters by cathodic stripping voltammetry of their complexes with iron. *Analytica Chimica Acta*, **599**(1), 58-66.

Laufer, K., Nordhoff, M., Røy, H., Schmidt, C., Behrens, S., Jørgensen, B. B. and Kappler, A. (2016). Coexistence of microaerophilic, nitrate-reducing, and phototrophic Fe(II)-oxidizers and Fe(III)-reducers in coastal marine sediment. *Applied and Environmental Microbiology*, **82**(5), 1433-1447.

Lovley, D. R. and Phillips, E. J. P. (1988). Novel mode of microbial energy metabolism: organic carbon oxidation coupled to dissimilatory reduction of iron or manganese. *Applied and Environmental Microbiology*, **54**(6), 1472-1480.

Luther III, G. W., Kostka, J. E., Church, T. M., Sulzberger, B. and Stumm, W. (1992). Seasonal iron cycling in the salt-marsh sedimentary environment: the importance of ligand complexes with Fe(II) and Fe(III) in the dissolution of Fe(III) minerals and pyrite, respectively. *Marine Chemistry*, **40**(1), 81-103.

Luther III, G. W., Shellenbarger, P. A. and Brendel, P. J. (1996). Dissolved organic Fe(III) and Fe(II) complexes in salt marsh porewaters. *Geochimica et Cosmochimica Acta*, **60**(6), 951-960.

Mayer, L. M., Schick, L. L., Skorko, K. and Boss, E. (2006). Photodissolution of particulate organic matter from sediments. *Limnology and Oceanography*, **51**(2), 1064-1071.

McKnight, D. M., Kimball, B. A. and Bencala, K. E. (1988). Iron photoreduction and oxidation in an acidic mountain stream. *Science*, **240**(4852), 637-640.

Melton, E. D., Stief, P., Behrens, S., Kappler, A. and Schmidt, C. (2014). High spatial resolution of distribution and interconnections between Fe- and N-redox processes in profundal lake sediments. *Environmental Microbiology*, **16**(10), 3287-3303.

Miles, C. J. and Brezonik, P. L. (1981). Oxygen consumption in humic-colored waters by a photochemical ferrous-ferric catalytic cycle. *Environmental Science & Technology*, **15**(9), 1089-1095.

Miller, W. L., King, D. W., Lin, J. and Kester, D. R. (1995). Photochemical redox cycling of iron in coastal seawater. *Marine Chemistry*, **50**(1), 63-77.

Millero, F. J., Sotolongo, S. and Izaguirre, M. (1987). The oxidation kinetics of Fe(II) in seawater. *Geochimica et Cosmochimica Acta*, **51**(4), 793-801.

Nielsen, L. P., Risgaard-Petersen, N., Fossing, H., Christensen, P. B. and Sayama, M. (2010). Electric currents couple spatially separated biogeochemical processes in marine sediment. *Nature*, **463**, 1071.

O'Sullivan, D. W., Hanson, A. K., Miller, W. L. and Kester, D. R. (1991). Measurement of Fe(II) in surface water of the equatorial Pacific. *Limnology and Oceanography*, **36**(8), 1727-1741.

Otte, J. M., Blackwell, N., Soos, V., Rughöft, S., Maisch, M., Kappler, A., Kleindienst, S. and Schmidt, C. (2018a). Sterilization impacts on marine sediment---Are we able to inactivate microorganisms in environmental samples? *FEMS Microbiology Ecology*, **94**(12), fiy189-fiy189.

Otte, J. M., Harter, J., Laufer, K., Blackwell, N., Straub, D., Kappler, A. and Kleindienst, S. (2018b). The distribution of active iron-cycling bacteria in marine and freshwater sediments is decoupled from geochemical gradients. *Environmental Microbiology*, **20**(7), 2483-2499.

Öztürk, M., Croot, P. L., Bertilsson, S., Abrahamsson, K., Karlson, B., David, R., Fransson, A. and Sakshaug, E. (2004). Iron enrichment and photoreduction of iron under UV and PAR in the presence of hydroxycarboxylic acid: implications for phytoplankton growth in the Southern Ocean. *Deep Sea Research Part II: Topical Studies in Oceanography*, **51**(22), 2841-2856.

Peng, C., Bryce, C., Sundman, A. and Kappler, A. (2019). Cryptic cycling of complexes containing Fe(III) and organic matter by phototrophic Fe(II)-oxidizing bacteria. *Applied and Environmental Microbiology*, **85**(8), e02826-02818.

Pfeffer, C., Larsen, S., Song, J., Dong, M., Besenbacher, F., Meyer, R. L., Kjeldsen, K. U., Schreiber, L., Gorby, Y. A., El-Naggar, M. Y., Leung, K. M., Schramm, A., Risgaard-Petersen, N. and Nielsen, L. P. (2012). Filamentous bacteria transport electrons over centimetre distances. *Nature*, **491**, 218.

Revsbech, N. P. (1989). An oxygen microsensor with a guard cathode. *Limnology and Oceanography*, **34**(2), 474-478.

Rich, H. W. and Morel, F. M. M. (1990). Availability of well-defined iron colloids to the marine diatom Thalassiosira weissflogii. *Limnology and Oceanography*, **35**(3), 652-662.

Rose, A. (2012). The influence of extracellular superoxide on iron redox chemistry and bioavailability to aquatic microorganisms. *Frontiers in Microbiology*, **3**(124).

Rose, A. L. and Waite, T. D. (2005). Reduction of organically complexed ferrici ron by superoxide in a simulated natural water. *Environmental Science & Technology*, **39**(8), 2645-2650.

Roy, E. G., Wells, M. L. and King, D. W. (2008). Persistence of iron(II) in surface waters of the western subarctic Pacific. *Limnology and Oceanography*, **53**(1), 89-98.

Schaedler, F., Lockwood, C., Lueder, U., Glombitza, C., Kappler, A. and Schmidt, C. (2018). Microbially mediated coupling of Fe and N cycles by nitrate-reducing Fe(II)-oxidizing bacteria in littoral freshwater sediments. *Applied and Environmental Microbiology*, **84**(2), e02013-02017.

Schmidt, C., Behrens, S. and Kappler, A. (2010). Ecosystem functioning from a geomicrobiological perspective a conceptual framework for biogeochemical iron cycling. *Environmental Chemistry*, **7**(5), 399-405.

Slowey, A. and Marvin-DiPasquale, M. (2012). How to overcome inter-electrode variability and instability to quantify dissolved oxygen, Fe(II), Mn(II), and S(II) in undisturbed soils and sediments using voltammetry. *Geochemical Transactions*, **13**(1), 6.

Southwell, M. W., Mead, R. N., Luquire, C. M., Barbera, A., Avery, G. B., Kieber, R. J. and Skrabal, S. A. (2011). Influence of organic matter source and diagenetic state on photochemical release of dissolved organic matter and nutrients from resuspendable estuarine sediments. *Marine Chemistry*, **126**(1), 114-119.

Sulzberger, B. (2015). Light-induced redox cycling of iron: Roles for $CO_2$ uptake and release by aquatic ecosystems. *Aquatic Geochemistry*, **21**(2), 65-80.

Sulzberger, B., Suter, D., Siffert, C., Banwart, S. and Stumm, W. (1989). Dissolution of Fe(III)(hydr)oxides in natural waters; laboratory assessment on the kinetics controlled by surface coordination. *Marine Chemistry*, **28**(1), 127-144.

Suzuki, Y., Kuma, K., Kudo, I., Hasebe, K. and Matsunaga, K. (1992). Existence of stable Fe(II) complex in oxic river water and its determination. *Water Research*, **26**(11), 1421-1424.

Taillefert, M., Bono, A. B. and Luther III, G. W. (2000). Reactivity of freshly formed Fe(III) in synthetic solutions and (pore)waters: voltammetric evidence of an aging process. *Environmental Science & Technology*, **34**(11), 2169-2177.

Tamura, H., Goto, K. and Nagayama, M. (1976). The effect of ferric hydroxide on the oxygenation of ferrous ions in neutral solutions. *Corrosion Science*, **16**(4), 197-207.

Tilzer, M. M. (1988). Secchi disk — chlorophyll relationships in a lake with highly variable phytoplankton biomass. *Hydrobiologia*, **162**(2), 163-171.

van den Berg, C. M. G. (1995). Evidence for organic complexation of iron in seawater. *Marine Chemistry*, **50**(1), 139-157.

Voelker, B. M. and Sedlak, D. L. (1995). Iron reduction by photoproduced superoxide in seawater. *Marine Chemistry*, **50**(1), 93-102.

Waite, T. D., Szymczak, R., Espey, Q. I. and Furnas, M. J. (1995). Diel variations in iron speciation in northern Australian shelf waters. *Marine Chemistry*, **50**(1), 79-91.

## 3.6 Supporting Information

The oligotrophic Lake Constance is the third largest freshwater lake in central Europe with a 273 km long coastline and light penetration through the water column deeper than 30 m (1% of surface light intensity). The sediment mainly consists of coarse sand and contains fine-grained material and has an organic carbon content of about 1%.

Light attenuation in the water column can be calculated using the following equation:

$$I_D = I_0 \cdot e^{-kz} \qquad\qquad (3.2)$$

with $I_D$ as the light intensity at depth $z$, $I_0$ as the light intensity at the water surface and $k$ as the light attenuation coefficient.
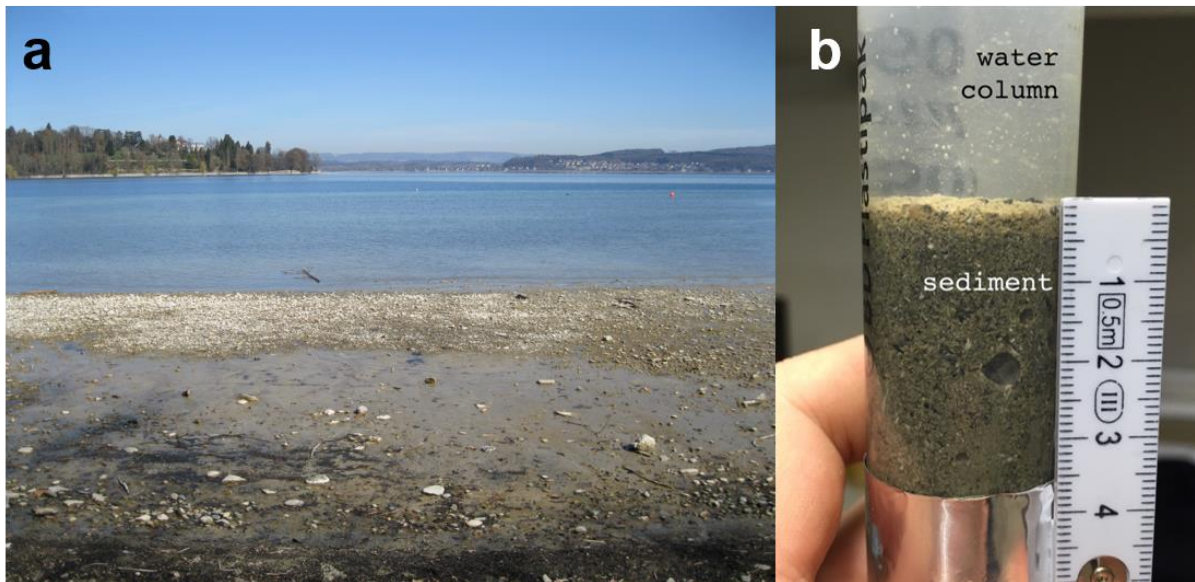


**Figure S3.1** (a) Photograph of littoral sediment from Lake Constance. The lake is characterized by a shallow littoral zone containing gravel and biological remains in the sandy matrix. (b) Photograph of a lab-incubated sediment core as used in this study.
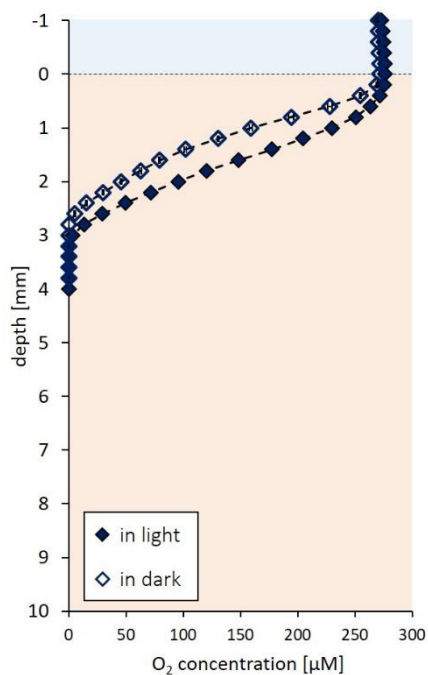
**Figure S3.2** $O_2$ concentration profiles in Lake Constance sediment cores incubated in the laboratory either in the light (closed diamonds) or in the dark (open diamonds). Error bars show the standard deviation of triplicate measurements recorded in one sediment core.
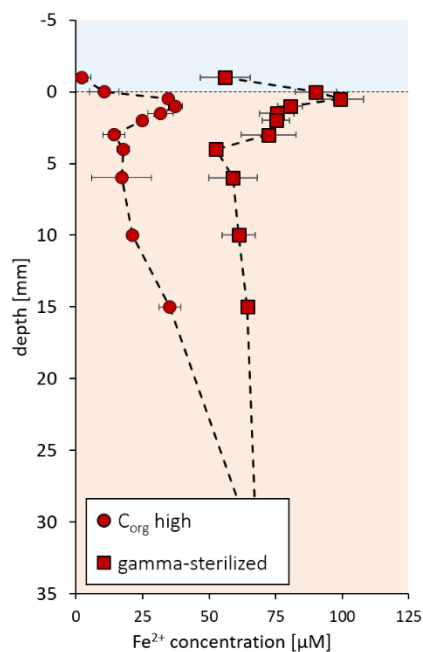


**Figure S3.3** $Fe^{2+}$ concentration profiles in non-sterilized high-organic C ($C_{org}$ high, circles) and gamma-sterilized (squares) high organic C Lake Constance sediment determined in-situ using voltammetric microelectrodes. Error bars show the standard deviation of triplicate voltammograms recorded in one sediment core.
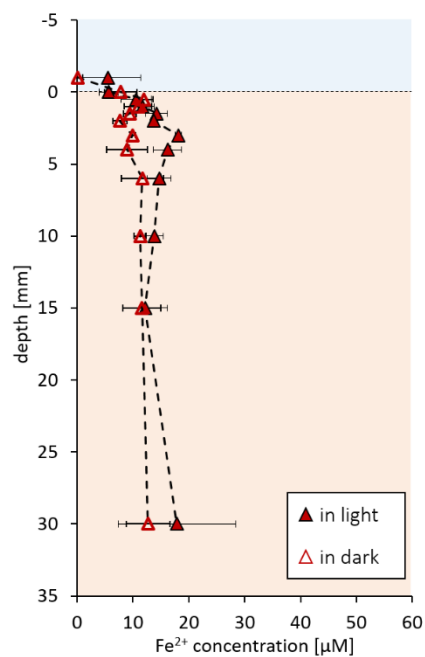
**Figure S3.4** Fe$^{2+}$ concentration profiles in low-organic sediment in light (closed triangles) and dark (open triangles) incubation determined in-situ using voltammetric microelectrodes. Error bars show the standard deviations of triplicate voltammograms recorded in one sediment core.
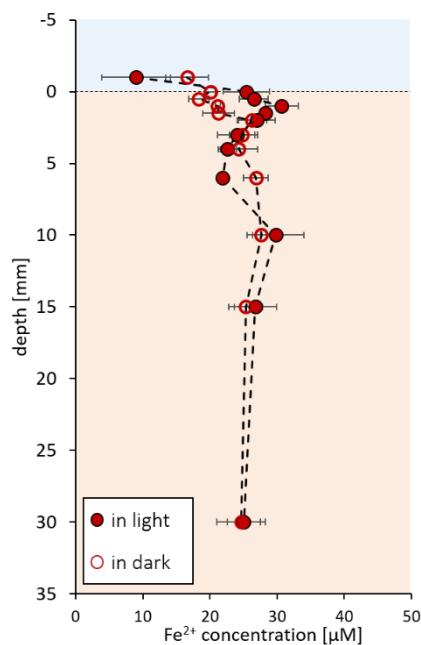


**Figure S3.5** Fe$^{2+}$ concentration profiles in low-organic sediment after amendment with sediment-extracted dissolved organic matter in light (closed circles) and dark (open circles) incubation determined in-situ using voltammetric microelectrodes. Error bars show the standard deviations of triplicate voltammograms recorded in one sediment core.
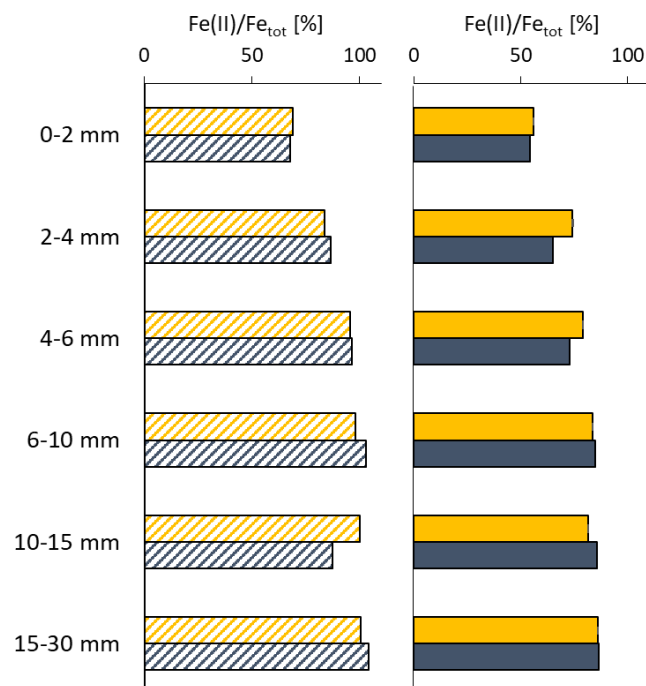
**Figure S3.6** Ratio of Fe(II) to total Fe in % of high-organic sediment either in the light (yellow bars) or dark (blue bars) incubations determined by Fe extractions using 0.5 M HCl (dashed bars) for dissolution of poorly crystalline Fe minerals and 6 M HCl (closed bars) for dissolution of highly crystalline Fe minerals at different depths.

**Table S3.1** General characterization of sediments with high and low organic carbon (C) that were used in the present study.

| | High-organic C sediment | Low-organic C sediment |
|---|---|---|
| TOC[a] content [%] | 1.55±0.05 | 0.05±0.00 |
| DOC[b] pore water concentration [mg C L$^{-1}$] | 15.8±3.5 | 3.3±0.6 |
| Sedimentary matrix | fine | coarse, sandy |
| Total Fe content[c] [mg Fe g$^{-1}$ dry sediment] | 3.75 | 3.12 |
| O$_2$ penetration depth [mm] | 2-3 | 5-6 |
| Light penetration depth[d] [mm] | 2.5 | 2.5 |

**(a) total organic carbon; (b) dissolved organic carbon; (c) determined by 6 M HCl extraction of bulk sediment; (d) determined by lab-constructed microsensors measured as scalar irradiance**

## Chapter 4 – Personal contribution

Experiments were conceptualized by myself and Dr. Caroline Schmidt. Sediment sampling was done by myself. The experiments and data collection were carried out by myself. Markus Maisch performed Mössbauer spectroscopy and XRD analysis and evaluated the data. The discussion and analysis of the obtained results were done by myself and Dr. C. Schmidt, Prof. Dr. A. Kappler and Prof. Dr. B.B. Jørgensen, Dr. Katja Laufer and M. Maisch. The manuscript was written by myself. Dr. C. Schmidt, Prof. A. Kappler, Prof. B.B. Jørgensen, Dr. K. Laufer and M. Maisch revised the manuscript.

# Chapter 4: Influence of physical perturbation on Fe(II) supply in coastal marine sediments

Ulf Lueder[1], Markus Maisch[1], Katja Laufer[2,3], Bo B. Jørgensen[2], Andreas Kappler[1,2], Caroline Schmidt[1]

[1] Geomicrobiology, Center for Applied Geoscience (ZAG), University of Tuebingen, Germany

[2] Center for Geomicrobiology, Department of Bioscience, Aarhus University, Denmark

[3] GEOMAR Helmholtz Center for Ocean Research Kiel, Germany

## 4.1 Abstract

Iron (Fe) biogeochemistry in marine sediments is driven by redox transformations, mediated by both biotic and abiotic processes, leading to Fe(II) and Fe(III) concentration gradients. As sediments are often physically mixed by wave action or bioturbation, Fe gradients re-establish regularly. In order to identify the response of dissolved Fe(II) ($Fe^{2+}$) and Fe mineral phases towards such mixing processes, we performed voltammetric high-resolution microsensor measurements, sequential Fe extractions, and Mössbauer spectroscopic analyses of 12 h light-dark-cycle incubated marine coastal sediment. When we homogenized sediment and filled it into cores, we found a decrease of $Fe^{2+}$ during the following 7 days of undisturbed incubation with $Fe^{2+}$ maxima changing from approx. 400 to 60 µM. In the first 2-4 days of incubation, $Fe^{2+}$ concentrations of up to 100 µM were measured in the top 2 mm due to Fe(III) photoreduction. After physical perturbation at day 7, $Fe^{2+}$ was re-mobilized reaching concentrations of 320 µM in 30 mm depth, which decreased to below detection limit within 2 days of subsequent undisturbed incubation. Mössbauer spectroscopy showed that the relative abundance of metastable iron-sulphur mineral phases ($FeS_x$) increased during the initial incubation and decreased after the perturbation. Our results show that $Fe^{2+}$ mobilization in marine sediments is stimulated by physical disturbances, and that the Fe redox distribution is influenced by physical mixing. In summary, our study suggests that in addition to abiotic Fe(III) reduction, microbial Fe(III) reduction and Fe(III) photoreduction, physical mixing processes also provide sediments and the inhabiting microbial community with $Fe^{2+}$.

**Graphical Abstract**
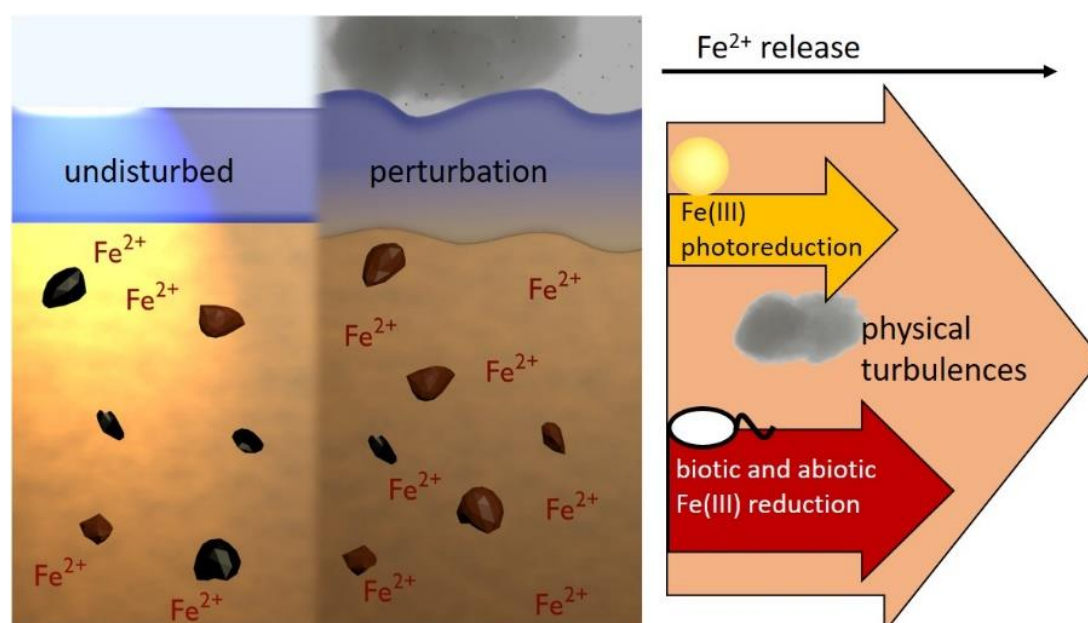
## 4.2 Introduction

Iron (Fe) is an important redox-active element in coastal marine sediments. It is an essential element for many living organisms and can be used as substrate, i.e. as electron donor, energy source or electron acceptor, for growth by Fe-metabolizing bacteria (Kappler & Straub, 2005). In the environment, Fe is cycled between its two main redox states, ferrous (Fe(II)) and ferric iron (Fe(III)), by many biotic and abiotic reactions (Melton et al., 2014). Microbial Fe(II) oxidation can be catalyzed by microaerophilic, nitrate-reducing or anoxygenic phototrophic microorganisms, that are ubiquitously present in coastal marine sediments (Laufer et al., 2016b; Laufer et al., 2017; Otte et al., 2018; McAllister et al., 2019). Fe(II) can also be abiotically oxidized by oxygen ($O_2$), reactive nitrogen species or manganese(IV) minerals (Melton et al., 2014). Additionally, Fe(II) can be produced in sunlit sediments by Fe(III) photoreduction (Lueder et al., 2019). In anoxic sediments, Fe(III) is reduced to Fe(II) by heterotrophic or autotrophic Fe(III)-reducing microorganisms coupled to the oxidation of organic compounds or hydrogen (Lovley & Phillips, 1988; Lovley, 1991; Kashefi et al., 2002), or by abiotic Fe(III) reduction by redox-active natural organic matter or dissolved sulphide ($H_2S+HS^-+S^{2-}$) (Pyzik & Sommer, 1981; Canfield, 1989; Sulzberger et al., 1989). Upward diffusion of dissolved Fe(II) ($Fe^{2+}$) along prevailing redox gradients and re-oxidation by e.g. $O_2$ (Millero et al., 1987), as well as mineral precipitation or dissolution lead to decreasing $Fe^{2+}$ concentrations in the sedimentary pore water towards the sediment-water interface (Davison et al., 1991; Burdige, 1993; Schmidt et al., 2010).

Fe redox changes have important consequences for the biogeochemical cycling of other elements, e.g. via precipitation of mineral phases such as Fe (oxyhydr)oxides, carbonates, phosphates or sulphides (Burdige, 1993; Canfield et al., 1993; Haese et al., 1998) or sorption of heavy metals or nutrients to Fe minerals (Su & Suarez, 2000; Giammar & Hering, 2001; Dixit & Hering, 2003; Khare et al., 2005). Fe(III) (oxyhydr)oxides that are able to rapidly react with sulphide ("reactive iron") (Berner, 1984; Canfield, 1989; Rickard, 1989; Canfield et al., 1992) control the distribution of dissolved sulphide in the pore water, which is produced by bacterial sulphate reduction in marine sediments (Jørgensen, 1977; Jørgensen, 1982; Berner, 1984). During the reaction of Fe(III) (oxyhydr)oxides with sulphide, $Fe^{2+}$ is formed, which further reacts with sulphide to form various iron-sulphide minerals (Canfield, 1989). The resulting Fe-S phases precipitate as metastable Fe(II) monosulphide (FeS) or as pyrite ($FeS_2$), which is the most stable form of Fe sulphides under environmental conditions (Howarth, 1979; Pyzik & Sommer, 1981; Luther et al., 1982; Boesen & Postma, 1988; Canfield, 1989). Those

formed minerals as well as dissolved and particulate Fe species are mainly transported by sedimentation and diffusion processes in stagnant coastal sediments without physical perturbation (Burdige, 1993). In contrast, in bioturbated or wave influenced sediments, advection is an important transport process and iron- or FeS-containing minerals can be actively transported towards the sediment surface or be buried deeper into the sediment where they undergo oxidation or reduction accomplishing rapid recycling processes (Aller et al., 1990; Canfield et al., 1993; Thamdrup et al., 1994). In shallow bays and estuaries, interactions between currents and waves lead to extensive sediment resuspension and transport (Brand et al., 2010), with wind-induced wave motion reaching the seabed down to 12 m water depth in some estuaries (Ward et al., 1984; Sanford, 1994; You, 2005). More extensive disturbances of the sediment, e.g. caused by a storm or rigorous tidal movement, can completely rearrange the sediment layers. This leads to shifts in sediment pore water geochemical gradients. $O_2$ profiles establish rapidly in sediments and respond quickly to temperature and light intensity changes (Epping & Kühl, 2000; Gerhardt et al., 2005). However, it is not known how fast $Fe^{2+}$ profiles react upon changing geochemical conditions, especially considering the occurrence of sulphur compounds in marine sediments with complex interactions between $Fe^{2+}$, Fe colloids, Fe(III) (oxyhydr)oxides and sulphide and the formation of highly reactive metastable Fe-S-phases.

Here we quantified $Fe^{2+}$ concentrations and determined mineralogical changes of solid-phase iron during incubation of marine sediment and after a simulated storm event. The objectives of this study were i) to understand the consequences of heavy perturbations caused during a storm event on the $Fe^{2+}$ concentration gradient and Fe redox stability in the sediment and ii) to decipher mechanisms for fluctuations of sedimentary $Fe^{2+}$ gradients.

## 4.3 Material & Methods

**Sediment core incubations and experimental approach**

Marine bulk sediment (from 0.5 m depth) and seawater were collected from a brackish shallow estuary, Norsminde Fjord, Denmark (Laufer et al., 2016b) (March 2017), near its narrow entrance to the Baltic Sea and kept in dark at 4°C until further processing. In the lab, stones and macrofauna were removed from the sediment in order to enable microsensor application and 5 cm of homogenized sediment were filled into cut 50 ml syringes, overlaid with 4 cm Norsminde Fjord water (artificial sediment cores). Homogenization of the sampled sediment was done to ensure homogeneous and reproducible starting conditions of the experiment. The artificial sediment cores were continuously aerated and re-filled with Norsminde Fjord water to

compensate evaporation. The sediment cores were incubated in a 12-hour light-dark cycle with a combination of two LED lamps (Samsung SI-P8V151DB1US, 14 W, 3000 K and SMD 2835, 15 W, 6000 K) and an adjusted light intensity of 250-300 μmol photons $m^{-2} s^{-1}$ using a spherical light meter (ULM-500 and US-SQS/L sensor, Walz, Germany). In order to prevent light penetration from the sides, the cores were wrapped in aluminum foil from the sediment-water interface downwards. After 7 days of incubation, the sediment cores were completely mixed using a spatula and consecutively bubbled with ambient air through a silicon tubing with an attached needle using a fish tank pump. The bubbling lasted for 1 hour and was strong enough to continuously mix the sediment and keep it in suspension simulating a storm event. The cores were incubated for 3 more days before the sediment was again rigorously mixed and aerated for 1 hour. Sediment cores that were prepared for incubation are shown in Figure S4.1.

In order to compare concentration changes of solid phase and dissolved Fe, 17 artificial sediment cores were prepared at the beginning of the experiment. Microsensor measurements of $Fe^{2+}$ and $O_2$ were related to results obtained from sequential solid-phase Fe extractions and [57]Fe Mössbauer spectroscopy. 13 of the artificial sediment cores that were prepared at the beginning of the experiment were used to monitor the development of $Fe^{2+}$ and $O_2$ gradients with microsensors. Each day, another sediment core was used (sacrificial setup). At days 0, 2 and 7 of undisturbed sediment core incubation as well as after the simulated storm event, samples for Mössbauer spectroscopy were taken from these artificial sediment cores after the microsensor measurements. For sequential Fe extractions, three artificial sediment cores were prepared, of which one replicate was used for extraction after 0 and 7 days of undisturbed incubation, and directly after the simulated storm. In order to test how sensitive the $Fe^{2+}$ release from the sediment is towards physical perturbation, we tested the impact of physical sediment movement and aeration on the $Fe^{2+}$ mobilization. For that, another artificial sediment core was prepared and cyclic voltammetric scans for $Fe^{2+}$ detection were run in (i) the sediment core that was incubated for 7 days, (ii) a homogenized layer of sediment after slicing the core, and (iii) the supernatant after centrifuging (oxic conditions, maximal disturbance) the homogenized sediment layer for 5 min at 12,045 g. A detailed scheme of the experimental approach is shown in Figure S4.2.

The DOC concentration of the sediment pore water was quantified with a carbon analyzer (Multi N/C 2100s, Analytik Jena, Germany).

## Microsensor measurements

Microsensor measurements were performed daily after 6 hours of light exposure as well as approximately 30 minutes after the simulated storm event. $Fe^{2+}$ concentration profiles were recorded by voltammetry using a DLK-70 web-potentiostat (Analytical Instrument Systems, Flemington, NJ) and a standard three electrode system with a lab-constructed glass-encased 100 µm gold amalgam (Au/Hg) working electrode (Brendel & Luther III, 1995), a solid state Ag wire coated with Ag/AgCl reference electrode, and a Pt wire counter electrode. Cyclic voltammograms were collected by scanning from -0.05 V to -1.8 V and back with at a scan rate of 2000 mV s$^{-1}$ and with an initial potential of -0.05 V held for 2 s for conditioning the electrode. Before each scan, a potential of -0.9 V was applied for 5 s to clean the electrode surface electrochemically. Calibration for $Fe^{2+}$ was done by applying the pilot ion method with $Mn^{2+}$ (Brendel & Luther III, 1995; Slowey & Marvin-DiPasquale, 2012). 10 scans were run at every measurement depth and the last 3 voltammograms were analyzed using VOLTINT program for Matlab® (Bristow & Taillefert, 2008). $Fe^{2+}$ concentrations were recorded 1 mm above and directly at the sediment surface, as well as in 0.5, 1, 1.5, 2, 3, 4, 6, 10, 15 and 30 mm depth. Additionally, cyclic voltammetry was performed during a simulated storm event in approx. 30 mm depth.

Dissolved $O_2$ was measured with a 100 µm tip diameter Clark-type $O_2$ microelectrode (Unisense, Denmark) as described by Revsbech (Revsbech, 1989). A two-point calibration was performed in fully air-saturated or anoxic Norsminde Fjord water. $O_2$ concentration profiles were recorded with the software Sensor Trace Suite (Unisense, Denmark) in triplicates with a spatial resolution of 200 µm. Error bars show the standard deviation of triplicate measurements. Light penetration depth was determined by measuring the scalar irradiance with lab-constructed light sensors (Kühl & Jørgensen, 1992) connected to a spectrometer (USB4000-XR1-ES, Ocean Optics, Germany) with the software SpectraSuite (Ocean Optics, Germany). High-resolution profiles of $H_2S$ and pH were additionally measured using glass microelectrodes (Unisense, Denmark) at the end of the incubation period. $O_2$ and redox potential profiles were measured with glass microelectrodes (Unisense, Denmark) in in-situ sediment cores in the field shortly before and 2 days after a strong storm event at the sampling field site in October 2013.

## Sequential Fe extractions

Sequential Fe extractions were used to follow changes in solid-phase Fe redox transformation over time. Anoxic Na-acetate (pH 5), 0.5 M HCl and 6 M HCl were used to consecutively dissolve different Fe phases with increasing crystallinity. Na-acetate was chosen for extracting adsorbed Fe(II) (Tessier et al., 1979; Roden & Zachara, 1996) and Fe in Fe sulphides (Shannon & White, 1991), 0.5 M HCl for extracting poorly crystalline, amorphous Fe (oxyhydr)oxides and (remaining) reduced Fe(II) species such as $FeCO_3$ or FeS (Heron et al., 1994), and 6 M HCl for extracting the higher crystalline, remaining reactive Fe fractions of the sediment. Artificial sediment cores were sliced under anoxic conditions (100% $N_2$, remaining $O_2$ <100 ppm) at 0-2, 2-4, 9-11 and 29-31 mm depth and approx. 0.5 g homogenized sediment of each sliced depth were added into Eppendorf tubes. Pore water was removed after centrifugation (5 min, 12,045 g), 1 ml of anoxic Na-acetate solution (pH 5) was added to the pellet, mixed and incubated (dark, 24 h). After centrifugation (5 min, 12,045 g), 100 µl of the supernatant was stabilized with 900 µl anoxic 1 M HCl and the residual Na-acetate was discarded. 1 ml of anoxic 0.5 M HCl was added to the pellet, mixed and incubated in the dark for 2 hours. After centrifugation, stabilization of 100 µl supernatant in 900 µl anoxic 1 M HCl and removal of the residual supernatant, 1 ml of anoxic 6 M HCl was added to the pellet, mixed and incubated for 24 hours in the dark as last extraction step. The extractants were subsequently analyzed in technical triplicates by the spectrophotometric Ferrozine assay (Stookey, 1970).

## Fe mineral analysis

Sediment for [57]Fe Mössbauer spectroscopy was collected under anoxic conditions (100 % $N_2$) from the sediment cores in a depth of approx. 30 mm at the beginning (day 0) and after 2 and 7 days of incubation, as well as shortly after the first simulated storm event. The sediment was loaded into a plexi-glass holder and was stored anoxically at -80°C until measurement. Mössbauer spectroscopy was performed in transmission mode and absorption spectra were collected at 77 K and 5 K respectively. Sample analysis was carried out using the Voigt Based Fitting (VBF) routine (Rancourt & Ping, 1991) with an $\alpha$[57]Fe foil (7 µm thick, room temperature) for center shift calibration. Sediment for X-ray diffraction (XRD) analysis was anoxically collected in a depth of approx. 30 mm after 7 days of incubation and analyzed twice as i) native anoxic wet sediment and ii) dried under oxic conditions. Detailed XRD parameters are shown in the Supporting Information.

## 4.4 Results & Discussion

### Development of $Fe^{2+}$ gradients during undisturbed incubation after preparation of artificial sediment cores

One hour after preparation of the artificial sediment cores from homogenized marine sediment, highest $Fe^{2+}$ concentrations of approx. 400 µM were measured in 30 mm depth with decreasing $Fe^{2+}$ concentrations upwards (Figure 4.1). $Fe^{2+}$ concentrations continuously decreased over time in the undisturbed sediment cores throughout the complete depth gradient during the following 7 days of incubation to approx. 60 µM in 30 mm depth (Figure 4.1). This decrease in $Fe^{2+}$ can be attributed to the fact that geochemical gradients first need to establish in the freshly prepared sediment cores, leading to a change of the sedimentary Fe speciation and the resulting gradients by ongoing Fe redox reactions (e.g. $Fe^{2+}$ oxidation), $Fe^{2+}$ adsorption to minerals and Fe phase transitions between the dissolved, adsorbed, colloidal and mineral fractions. After the preparation of the artificial sediment cores, $O_2$ concentrations were quite low (50 µM in the water column, 1 mm penetration into the sediment; Figure 4.1) indicating high $O_2$ consuming processes and a reduced state of the sediment. However, oxygenic photosynthesis in the sediment led to $O_2$ supersaturation (Jørgensen et al., 1979; Lassen et al., 1992) within 2 days of undisturbed incubation (Figure 4.1 and Figure S4.3), thus enhancing abiotic $Fe^{2+}$ oxidation in oxic sediment layers. Due to higher salinity, abiotic $Fe^{2+}$ oxidation kinetics by $O_2$ in seawater is slower compared to freshwater (Millero et al., 1987). In deeper and anoxic sediment layers, $Fe^{2+}$ is produced by abiotic and biotic Fe(III) reduction, diffuses upwards and is oxidized by different processes, e.g. by abiotic oxidation by $O_2$ (Millero et al., 1987) or by microbial $Fe^{2+}$ oxidation (Melton et al., 2014). Therefore, increasing $Fe^{2+}$ concentrations with depth can be expected (Davison et al., 1991; Burdige, 1993; Schmidt et al., 2010). $Fe^{2+}$ concentrations of up to 100 µM in the top 2 mm of the sediment were quantified during the first 2-4 days of incubation (Figure 4.1). $Fe^{2+}$ production in light-penetrated, oxic sediment layers has very recently been demonstrated to be caused by Fe(III) photoreduction (Lueder et al., 2019). The $Fe^{2+}$ concentration measured in the top sediment layers after 2 days of undisturbed light-dark incubation was 60% of the concentration in 30 mm depth (approx. 170 µM), which is in the same range as previously observed in laboratory light-incubated freshwater sediments (Lueder et al., 2019). In the incubated marine sediment, light penetrates 2.2 mm (Figure S4.4). Besides the presence of light, there are some necessary geochemical prerequisites for Fe(III) photoreduction, such as the complexation of Fe(III) by organic carbon (Peng et al., 2019). In fact, the sediment used for this study is characterized by high dissolved organic carbon

concentrations in the pore water ($84.5\pm14.4$ mg $L^{-1}$), which allows for the formation of such Fe(III)-organic complexes, as confirmed by voltammetry (Taillefert et al., 2000).
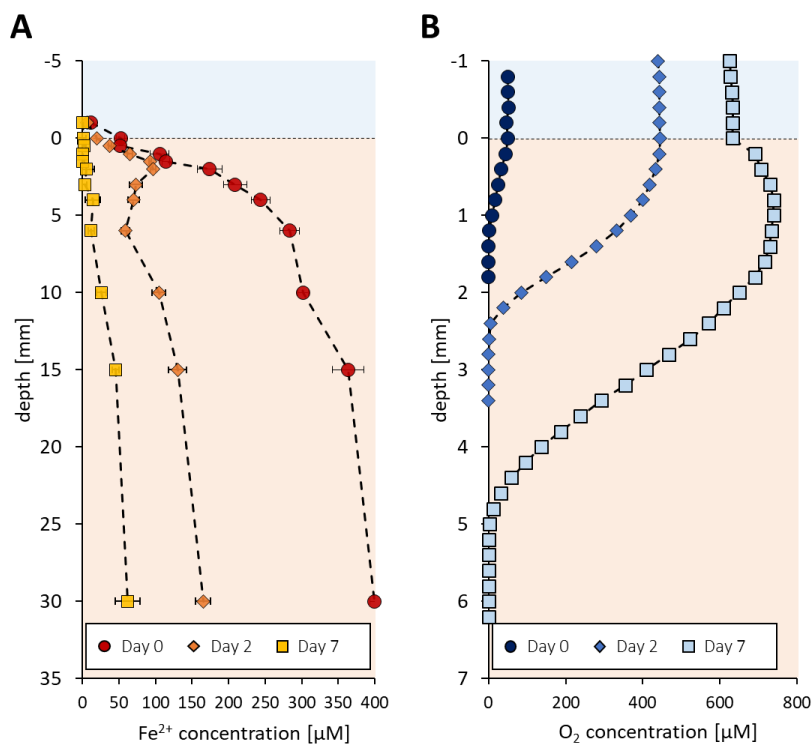


**Figure 4.1** Concentration profiles after 6 hours of light exposure in 12 h light-dark lab-incubated artificial marine sediment cores at the start (day 0) and after 2 and 7 days of undisturbed incubation. A) $Fe^{2+}$ concentration profiles; Error bars show standard deviation of triplicate voltammograms. B) $O_2$ concentration profiles.

## Impact of physical perturbation on $Fe^{2+}$ gradients

Extensive physical mixing after 7 days of undisturbed sediment core incubation simulated a storm event and introduced $O_2$ into the sediment. This led to extensive re-mobilization and release of $Fe^{2+}$ of up to 320 µM (in 30 mm depth) 30 minutes after the storm event (Figure 4.2). Despite the aeration of the sediment for one hour, the sediment pore water was clearly undersaturated with respect to $O_2$ (Figure 4.2). Reduced or mobilized sedimentary compounds that got in contact with $O_2$ during the simulated storm event or afterwards during sediment settling removed large parts of the introduced $O_2$ via oxidation. Thus, directly during the storm event $Fe^{2+}$ gets released and is temporarily measurable at very high concentrations (Figure S4.5), before getting oxidized by $O_2$ during settlement of the sediment particles leading to lower $Fe^{2+}$ concentrations measured in the sediment core (Figure 4.2). The undersaturated $O_2$ conditions might also increase the persistence of $Fe^{2+}$ in the sediment pore water after the storm

event. After physical perturbation, the sediment re-fractionates by particle size during settling, which presumably leads to different geochemical conditions at different sediment depths. Therefore, pore space or the amount of Fe minerals might differ with sediment depth potentially influencing diffusion, dissolution or sorption of $Fe^{2+}$. Voltammetric $Fe^{2+}$ measurements performed during the simulated storm event showed the immediate release of $Fe^{2+}$ (Figure S4.5). The $Fe^{2+}$ profile after the storm represents the result of $Fe^{2+}$ production (during the storm event) and consumption, including $Fe^{2+}$ oxidation by $O_2$ in the top millimeters or microbial depletion processes. Due to the rate at which $Fe^{2+}$ was mobilized (a few hundred µM within minutes), microbial or abiotic Fe(III) reduction as sole source of $Fe^{2+}$ is unlikely. For comparison, Laufer et al. (2016a) determined maximum Fe(III) reduction rates in Norsminde Fjord sediment to be in the range of 180-590 µM day$^{-1}$ suggesting that abiotic and microbial Fe(III) reduction is too slow to account for the sole mechanism for all the observed $Fe^{2+}$ mobilization during the simulated storm event. The mobilized $Fe^{2+}$ decreased to below detection limit throughout the sediment column already within 2 days of subsequent undisturbed incubation (Figure 4.2). After additional 3 days of undisturbed light-dark incubation, simulation of a further storm event led to an immediate but lower re-mobilization of $Fe^{2+}$ (~ 110 µM) into the pore water (Figure 4.2). This indicates that the incubated artificial sediment cores are depletive towards $Fe^{2+}$ mobilization probably due lacking renewability of the sedimentary system compared to in-situ conditions. The mobilization of $Fe^{2+}$ by the simulated storm event also led to micromolar concentrations (30-40 µM) in the water column (Figure 4.2), caused by the mixing of the water column with the sediment. The $Fe^{2+}$ might be taken up by aquatic organisms before it gets oxidized, e.g. by $O_2$. In marine waters, concentrations of dissolved Fe naturally are only in the pico- to nanomolar range (Boyd et al., 2000; Boyd & Ellwood, 2010; King & Barbeau, 2011). Compared to other Fe(II) sources to the water column, such as diffusional Fe flux from sediments (µmolar range Fe m$^{-2}$ d$^{-1}$) (Elrod et al., 2004), aquatic Fe(III) photoreduction (production of nanomolar concentrations) (O'Sullivan et al., 1991; Kuma et al., 1992) or Fe input from rivers, where Fe is primarily present in the form of ferric oxides (Krachler et al., 2010), the occasional $Fe^{2+}$ input into the water column induced by storm events might therefore represent a significant $Fe^{2+}$ source also to the marine water column.
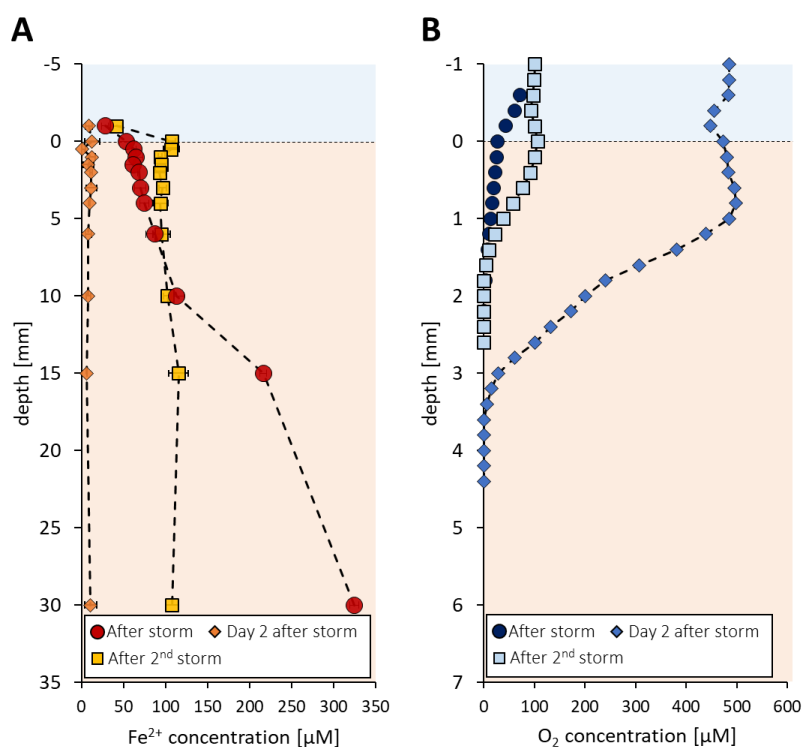
**Figure 4.2** Concentration profiles measured in 12 h light-dark lab-incubated artificial marine sediment cores approximately 30 minutes after a simulated storm event (labeled "After storm"), after 2 days of undisturbed incubation after 6 hours of light exposure ("Day 2 after storm") as well as approximately 30 minutes after a second simulated storm event ("After 2nd storm"). A) $Fe^{2+}$ concentration profiles. Error bars show standard deviation of triplicate voltammograms. B) $O_2$ concentration profiles.

The extreme sensitivity of $Fe^{2+}$ mobilization from the sediments to physical disturbance and introduction of oxidants was demonstrated in a separate experiment. $Fe^{2+}$ measurements with voltammetric microsensors were performed in a homogenized sediment core (incubated for 7 days without physical disturbance) and compared to measurements in homogenized slices of sediment from 3 depths (0-2, 9-11 and 29-31 mm), as well as in the pore water of sliced, centrifuged sediment layers. While only 15 µM $Fe^{2+}$ were measured in 10 mm depth in the intact sediment core, the $Fe^{2+}$ concentration in the corresponding sliced and homogenized, and therefore disturbed, sediment layer was 240 µM, i.e. 16 times higher than $Fe^{2+}$ concentrations in the undisturbed sediment cores (Figure S4.6). In 30 mm depth in the intact sediment core, $Fe^{2+}$ (90 µM) was still about 2.5 times lower compared to the gently prepared homogenized sediment slice (230 µM) (Figure S4.6). These experiments highlight that physically disturbing processes are able to mobilize $Fe^{2+}$ from the sediment, despite the simultaneous introduction of oxidants, and potentially increase its bioavailability as nutrient or substrate for various microorganisms. Wave and tidal movement, as well as bioturbation represent perturbation

87

processes that constantly proceed in natural sediments leading to particle shearing and sediment reworking (Hines et al., 1982; Aller, 1994). In shallow coastal waters, bottom shear stress generated by tidal currents and wave movements is responsible for sediment resuspension into the water column, sediment mixing and transport processes (Jing & Ridd, 1996; Brand et al., 2010). The critical shear stress needed for sediment movement may vary widely and depends on the type of sediment and its degree of compaction (Ward et al., 1984; Scheffer et al., 2003). Wind-induced waves have been observed to resuspend sediment in water depths up to 2-12 m in many estuaries (Ward et al., 1984; Sanford, 1994). Storms are even recognized to be the dominant physical force to suspend sediment on continental shelfs (Sanford, 1994). Based on our data, movement of sediment would have a strong impact on the release of $Fe^{2+}$ into the pore water and overlying seawater.

The in-situ effects of storms to produce disturbed sediment and re-adjustment of geochemical gradients were also demonstrated by comparing $O_2$ and redox potential profiles of in-situ measurements in sediment cores taken before and 2 days after a strong natural storm at the sampling field site (Supporting Information). Even 2 days after the storm, the redox potential measured in the sediment was still more positive even in a sediment depth of 14 mm compared to the redox potential measured before the storm (Figure S4.7), showing the relevance of storms for disturbing the sediment in the environment. The more positive redox potential in the upper 14 mm of the sediment measured after the storm (Figure S4.7) illustrates the more oxidized conditions of the sediment and that the geochemical gradients of the sediment are still in the process of re-adjusting to reach the same state as measured before the storm. The shape of the recorded $O_2$ concentration profiles (Figure S4.7) differed before and 2 days after the storm indicating higher consumption of $O_2$ in the sediment after the storm. Due to mixing processes, reduced compounds can get oxidized and fresh organic matter enters the sediment leading to higher aerobic microbial respiration. Due to the time point of the storm (October 2013), low photosynthetic activity did not lead to $O_2$ supersaturation in the sediment. Besides heavy sediment perturbation caused by storms, already minor sediment mixing processes such as bioturbation affect the sediment geochemistry. Thamdrup et al. (1994) pointed out the importance of bioturbation in sedimentary Fe cycling by transporting redox-active substrates across the oxic-anoxic interface, i.e. Fe(III) to anoxic layers, where microbial Fe(III) reduction occurs, and reversely, Fe(II) towards the oxic sediment surface where it gets oxidized by microbial and chemical reactions (Canfield et al., 1993).

**Impact of physical perturbation on $O_2$ and sulphide geochemistry**

Photosynthetic organisms are also mixed during physical perturbation. However, in comparison to $Fe^{2+}$ gradients, the $O_2$ gradients re-establish faster in sediment cores [9, 11, 12], as oxygenic photosynthesis responds immediately to incoming light. Steady-state $O_2$ concentrations are reached rapidly and $O_2$ concentrations change dynamically depending on changes in light intensity (Colijn & van Buurt, 1975; Whitney & Darley, 1983). Oxygenic photosynthesis leads to supersaturation of $O_2$ in sediment pore water during illumination (Jørgensen et al., 1979; Lassen et al., 1992; MacIntyre et al., 1996). $O_2$ concentrations dramatically decreased in the sediment after the simulated storm event (Figure 4.2), presumably by reactions of $O_2$ with reduced sediment constituents. However, already 2 days after undisturbed light-dark incubation, $O_2$ supersaturation was reached in the incubated artificial sediment cores (Figure S4.3), whereas $Fe^{2+}$ in the sediment pore water still was decreasing across the complete redox gradient, thereby influencing the whole sedimentary redox system. $O_2$ supersaturation of up to 600 µM re-established within a day after the simulated storm (Figure S4.3).

Apart from the influence by $O_2$, the Fe geochemistry in marine sediments is strongly influenced by sulphur species, which are involved in various chemical or microbially mediated redox reactions (Jørgensen, 1977). However, we did not detect dissolved sulphide by microsensor measurements in the incubated sediment cores shortly before or after the simulated storm event (data not shown). This lack of sulphide indicates that there is enough reactive iron present in this marine sediment to readily react with dissolved sulphide, potentially strongly controlling its pore water concentrations and (bio)availability (Berner, 1984; Canfield, 1989; Canfield et al., 1992). Dissolved sulphide is likely produced constantly by bacterial sulphate reduction in the sediment (Jørgensen, 1982), but is instantaneously removed by chemical reactions (e.g. by the formation of metastable FeS phases or even by reaction with FeS minerals to produce $FeS_2$ (Thiel et al., 2018) leading to non-detectable (<1 µM) concentrations of dissolved sulphide in the pore water. In support of the formation of such Fe-S species, we recorded a voltammetric signal that resembles dissolved FeS clusters (Theberge & Luther III, 1997; Davison et al., 1998; Rickard et al., 1999) directly after the initial preparation of the homogenized sediment cores throughout the entire core, as well as in smaller amounts directly after the simulated storm event. Also, dissolved FeS clusters could be detected during the simulated storm event simultaneously to the detection of $Fe^{2+}$. Dissolved FeS clusters can form without immediate precipitation of solid FeS (Luther et al., 1996) but are indicative of solid amorphous FeS to be present in the sediment as well (Rickard et al., 1999). Dissolved FeS clusters were measurable only for a short time after the simulated storm and then disappeared within a day, highlighting

the high reactivity of these species towards precipitation as FeS mineral phases and the importance of sulphur for the Fe redox system in the sediment.

## Fe solid phase crystallinity changes

Sequential dissolution of different iron pools by different extractants allows insights into Fe crystallinity changes (Poulton & Canfield, 2005). One hour after preparation of the artificial sediment cores, the adsorbed Fe fraction (on Fe(III) (oxyhydr)oxides and poorly crystalline carbonates) and Fe from FeS (Shannon & White, 1991); extracted by 1 M Na acetate, pH 5) as well as the poorly crystalline Fe mineral fraction (extracted by 0.5 M HCl) was all in the reduced state of Fe(II). Only the fraction of highest Fe crystallinity (extracted by 6 M HCl) contained Fe(III) (19-32 %) (Figure 4.3). After 7 days of incubation, a shift from adsorbed/amorphous Fe phases (decrease from 1.17 mg Fe $g^{-1}$ sediment averaged over depth; 25.49% of total Fe) after preparation of the sediment cores to 0.50 mg Fe $g^{-1}$ sediment (10.12% of total Fe after 7 days of undisturbed incubation) towards higher crystalline Fe phases. There was an increase of poorly and highly crystalline Fe phases averaged over depth from 3.14 mg Fe $g^{-1}$ sediment (74.51% of total Fe) to 4.40 mg Fe $g^{-1}$ sediment (89.88% of total Fe) during incubation, with an increasing relative amount of Fe(III) observed (Figure 4.3), potentially caused by oxidation of adsorbed Fe(II) or Fe(II) minerals and mineral restructuring by Ostwald ripening processes (Morse & Casey, 1988). This change in crystallinity during undisturbed incubation of the sediment was most pronounced in the top 4 mm. In contrast, after the simulated storm event, amorphous Fe mineral phases increased again to concentrations close to the initial state (1.38 mg Fe $g^{-1}$ sediment averaged over depth) (Figure 4.3). The total amount of solid phase Fe slightly increased during the 7 days of undisturbed incubation from 4.59 to 4.89 mg Fe $g^{-1}$ sediment and to 4.94 mg Fe $g^{-1}$ sediment averaged for all sediment depths after the simulated storm event. The data suggest that during undisturbed incubation, Fe mineralogy is mostly driven by an increase in crystallinity, potentially due to Ostwald ripening or continuous Fe(II) catalyzed dissolution and re-precipitation. However, physical perturbation and concomitant sediment reworking seem to dissolve and re-precipitate parts of the poorly and highly crystalline Fe minerals, leading to a regeneration of the sediment back to more amorphous Fe phases. This likely has consequences for the Fe bioavailability to microorganisms that use Fe(II) as substrate or nutrient. The crystallinity of Fe minerals determines the rate and extent of microbial Fe(III) reduction (Hansel et al., 2004; Cutting et al., 2009). By providing more less crystalline Fe phases to the sediment, microbially catalyzed Fe redox reactions are presumably

enhanced. We suggest that constant mixing of sediment, e.g. by waves, prevents mineral ripening and increases the amount of dissolved or colloidal and more reactive Fe phases, thereby driving a dynamic and very reactive redox environment.
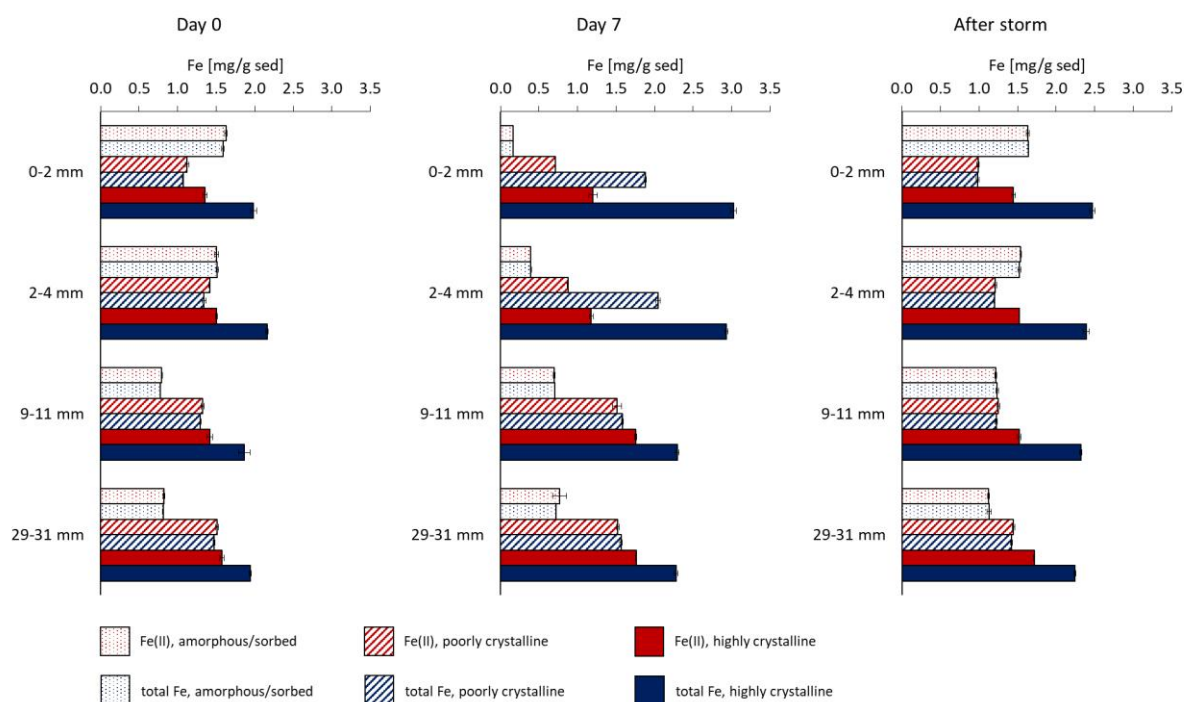


**Figure 4.3** Sequential Fe extractions of different sliced sediment layers from sediment cores at the beginning (Day 0) and after 7 days (Day 7) of undisturbed incubation as well as shortly after a simulated storm event (After storm). Error bars show standard deviation of technical triplicates.

## Transformation of Fe mineral phases after physical perturbation

The Fe mineralogy in the solid phase during incubation and after the storm event was identified by Mössbauer spectroscopy and XRD. Mössbauer spectra collected at 77 K showed similar properties for all measured samples collected from 30 mm depth at different time points (Figure S4.8). Additional measurements at 5 K revealed a poorly defined sextet in the recorded Mössbauer spectra (Figure S4.9), potentially resembling a metastable Fe-sulphur mineral phase that is present in the measured sediment samples of all time points (detailed Mössbauer spectroscopy data are shown in the Supporting Information (Figures S4.8 & S4.9 and Table S4.1). In accordance with Wan et al. (2017) and Thiel et al. (2018), this phase was denoted as metastable $FeS_x$, representing a yet unknown Fe mineral phase undergoing magnetic ordering at 5 K. Besides the metastable $FeS_x$, vivianite ($Fe_3(PO_4)_2 \cdot 8H_2O$) and $FeS_2$ were detected as

Fe(II) phases. Applying the VBF fit-model of the 5 K spectra (Rancourt & Ping, 1991), the relative abundances of the three iron phases ($FeS_2$, $Fe_3(PO_4)_2x8H_2O$ and the metastable $FeS_x$) varied slightly during incubation (Figure 4.4). An increase of the relative abundance of $FeS_x$ from initial $19.3\pm2.9$ to $24.7\pm2.1\%$ after 7 days of undisturbed incubation, and the decrease back to $18.2\pm2.2\%$ after the stimulated storm event suggests that during undisturbed incubation $Fe^{2+}$ reacts rapidly with sulphide or another intermediate sulphur species to form metastable and highly reactive $FeS_x$ phases (Pyzik & Sommer, 1981; Schoonen & Barnes, 1991; Wan et al., 2017). Physical perturbation led to a partial removal of $FeS_x$, e.g. due to oxidation by $O_2$ entering the sediment during mixing or presumably as a result of breaking of very amorphous $FeS_x$ minerals by shearing forces. The accumulation of $FeS_x$ during incubation and the subsequent partial removal after sediment perturbation, deciphers one of the mechanisms responsible for the fluctuations of $Fe^{2+}$ in the sediment pore water. Besides the metastable $FeS_x$, $FeS_2$ is present as another Fe sulphide mineral in the sediment cores and represents the quantitatively dominant Fe(II) phase ($45\pm0.2\%$ after 7 days of incubation) before the simulated storm event. Its relative abundance dropped together with the $FeS_x$ phases after the simulated storm event to $35.6\pm0.3\%$ (Figure 4.4), although $FeS_2$ is thermodynamically more stable than Fe monosulphides (Giblin & Howarth, 1984). The presence of $FeS_2$ was confirmed by XRD. Detailed XRD results are shown in the Supporting Information and in Figure S4.10. In marine sediments, $FeS_2$ usually is the most abundant Fe sulphide mineral (Cornwell & Morse, 1987) and its rapid formation has been shown (Howarth, 1979; Howarth & Jørgensen, 1984). Physical perturbations transport $FeS_2$ to oxic sediment layers, where it is chemically oxidized by $O_2$ (Thamdrup et al., 1994; Schippers & Jørgensen, 2002) especially when the $FeS_2$ particles are small.
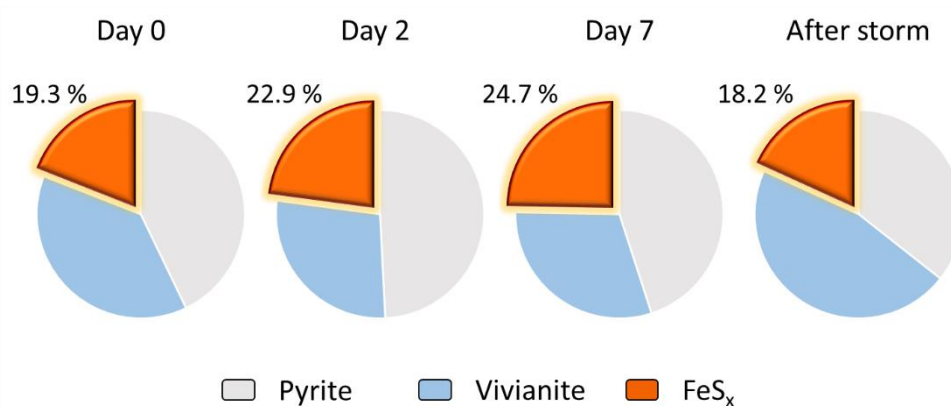


**Figure 4.4** Relative abundances of pyrite, vivianite and metastable $FeS_x$ mineral phases in the sediment cores in a depth of 30 mm over the course of undisturbed 12 h light-dark incubation (Day 0, 2 and 7) and shortly after a simulated storm event (After storm) determined by Mössbauer spectroscopy.

## Environmental implications

In the present study we showed that physical perturbation, induced e.g. by storms, bioturbation or wave/tidal movement, is able to strongly impact the Fe geochemistry in marine sediments by shifting the predominant Fe phases from highly crystalline Fe minerals into more poorly or amorphous Fe phases and by partly oxidizing metastable $FeS_x$, thereby potentially releasing $Fe^{2+}$ into the pore water. So far, only abiotic and biotic Fe(III) reduction were considered to be sources of $Fe^{2+}$ in marine sediments (Lovley & Phillips, 1988; Sulzberger et al., 1989; Lovley, 1991; Burdige, 1993; Canfield et al., 1993). On the other hand, Fe(II) oxidation processes, e.g. fast $Fe^{2+}$ oxidation by $O_2$, are limiting $Fe^{2+}$ availability (Millero et al., 1987). However, considering Fe(III) photoreduction and $Fe^{2+}$ mobilization from metastable $FeS_x$ as important $Fe^{2+}$ sources in marine sediments, the additionally produced $Fe^{2+}$ is expected to be used as nutrient or as substrate by Fe(II)-oxidizing bacteria. The mineral transformations might also lead to desorption of adsorbed Fe(II), of other nutrients or of pollutants (e.g. heavy metals) (Su & Suarez, 2000; Giammar & Hering, 2001; Dixit & Hering, 2003; Khare et al., 2005) and lead to a regeneration of the sediment by providing fresh Fe mineral reaction sites. The high reactivity of metastable $FeS_x$ might drive a fast turnover of Fe(II) in the sediment. Although the concentration profiles were recorded in single sediment cores, the starting conditions of all incubated sediment cores were the same due to homogenization of the sediment and we therefore obtained consistent temporal and spatial data that show that the $Fe^{2+}$ distribution in sediments is highly sensitive and dynamic and changes drastically towards less crystalline Fe solid-phases and the release of high amounts of $Fe^{2+}$ caused by physical disturbances and/or the introduction of oxidants. The fast re-adjustment of $O_2$ gradients in the sediment (Epping & Kühl, 2000; Gerhardt et al., 2005) may give the impression that pre-storm redox conditions are quickly re-established after storm events. However, based on the interactions between dissolved and metastable Fe phases, we showed that the Fe geochemistry in sediments is highly variable with highly reactive intermediates playing a key role in sedimentary Fe cycling and bioavailability. This study demonstrated that the fast $Fe^{2+}$ mobilization as a result of physical perturbation is an overlooked Fe(II) source, which likely makes an important contribution to Fe as well as other biogeochemical cycles in sediments.

## Acknowledgements

## 4.5 References

Aller, R. C. (1994). Bioturbation and remineralization of sedimentary organic matter: effects of redox oscillation. *Chemical Geology*, **114**(3), 331-345.

Aller, R. C., Charnock, H., Edmond, J. M., McCave, I. N., Rice, A. L. and Wilson, T. R. S. (1990). Bioturbation and manganese cycling in hemipelagic sediments. *Philosophical Transactions of the Royal Society of London. Series A, Mathematical and Physical Sciences*, **331**(1616), 51-68.

Berner, R. A. (1984). Sedimentary pyrite formation: An update. *Geochimica et Cosmochimica Acta*, **48**(4), 605-615.

Boesen, C. and Postma, D. (1988). Pyrite formation in anoxic environments of the Baltic. *American Journal of Science*, **288**(6), 575-603.

Boyd, P. W. and Ellwood, M. J. (2010). The biogeochemical cycle of iron in the ocean. *Nature Geoscience*, **3**, 675.

Boyd, P. W., Watson, A. J., Law, C. S., Abraham, E. R., Trull, T., Murdoch, R., Bakker, D. C. E., Bowie, A. R., Buesseler, K. O., Chang, H., Charette, M., Croot, P., Downing, K., Frew, R., Gall, M., Hadfield, M., Hall, J., Harvey, M., Jameson, G., LaRoche, J., Liddicoat, M., Ling, R., Maldonado, M. T., McKay, R. M., Nodder, S., Pickmere, S., Pridmore, R., Rintoul, S., Safi, K., Sutton, P., Strzepek, R., Tanneberger, K., Turner, S., Waite, A. and Zeldis, J. (2000). A mesoscale phytoplankton bloom in the polar Southern Ocean stimulated by iron fertilization. *Nature*, **407**(6805), 695-702.

Brand, A., Lacy, J. R., Hsu, K., Hoover, D., Gladding, S. and Stacey, M. T. (2010). Wind-enhanced resuspension in the shallow waters of South San Francisco Bay: Mechanisms and potential implications for cohesive sediment transport. *Journal of Geophysical Research: Oceans*, **115**(C11).

Brendel, P. J. and Luther III, G. W. (1995). Development of a gold amalgam voltammetric microelectrode for the determination of dissolved Fe, Mn, $O_2$, and S(-II) in porewaters of marine and freshwater sediments. *Environmental Science & Technology*, **29**(3), 751-761.

Bristow, G. and Taillefert, M. (2008). VOLTINT: A Matlab®-based program for semi-automated processing of geochemical data acquired by voltammetry. *Computers & Geosciences*, **34**(2), 153-162.

Burdige, D. J. (1993). The biogeochemistry of manganese and iron reduction in marine sediments. *Earth-Science Reviews*, **35**(3), 249-284.

Canfield, D. E. (1989). Reactive iron in marine sediments. *Geochimica et Cosmochimica Acta*, **53**(3), 619-632.

Canfield, D. E., Raiswell, R. and Bottrell, S. H. (1992). The reactivity of sedimentary iron minerals toward sulfide. *American Journal of Science*, **292**(9), 659-683.

Canfield, D. E., Thamdrup, B. and Hansen, J. W. (1993). The anaerobic degradation of organic matter in Danish coastal sediments: Iron reduction, manganese reduction, and sulfate reduction. *Geochimica et Cosmochimica Acta*, **57**(16), 3867-3883.

Colijn, F. and van Buurt, G. (1975). Influence of light and temperature on the photosynthetic rate of marine benthic diatoms. *Marine Biology*, **31**(3), 209-214.

Cornwell, J. C. and Morse, J. W. (1987). The characterization of iron sulfide

minerals in anoxic marine sediments. *Marine Chemistry*, **22**(2), 193-206.

Cutting, R. S., Coker, V. S., Fellowes, J. W., Lloyd, J. R. and Vaughan, D. J. (2009). Mineralogical and morphological constraints on the reduction of Fe(III) minerals by Geobacter sulfurreducens. *Geochimica et Cosmochimica Acta*, **73**(14), 4004-4022.

Davison, W., Buffle, J. and DeVitre, R. (1998). Voltammetric characterization of a dissolved iron sulphide species by laboratory and field studies. *Analytica Chimica Acta*, **377**(2), 193-203.

Davison, W., Grime, G. W., Morgan, J. A. W. and Clarke, K. (1991). Distribution of dissolved iron in sediment pore waters at submillimetre resolution. *Nature*, **352**(6333), 323-325.

Dixit, S. and Hering, J. G. (2003). Comparison of arsenic(V) and arsenic(III) sorption onto iron oxide minerals: Implications for arsenic mobility. *Environmental Science & Technology*, **37**(18), 4182-4189.

Elrod, V. A., Berelson, W. M., Coale, K. H. and Johnson, K. S. (2004). The flux of iron from continental shelf sediments: A missing source for global budgets. *Geophysical Research Letters*, **31**(12).

Epping, E. and Kühl, M. (2000). The responses of photosynthesis and oxygen consumption to short-term changes in temperature and irradiance in a cyanobacterial mat (Ebro Delta, Spain). *Environmental Microbiology*, **2**(4), 465-474.

Gerhardt, S., Brune, A. and Schink, B. (2005). Dynamics of redox changes of iron caused by light–dark variations in littoral sediment of a freshwater lake. *Biogeochemistry*, **74**(3), 323-339.

Giammar, D. E. and Hering, J. G. (2001). Time scales for sorption−desorption and surface precipitation of uranyl on goethite. *Environmental Science & Technology*, **35**(16), 3332-3337.

Giblin, A. E. and Howarth, R. W. (1984). Porewater evidence for a dynamic sedimentary iron cycle in salt marshes1. *Limnology and Oceanography*, **29**(1), 47-63.

Haese, R. R., Petermann, H., Dittert, L. and Schulz, H. D. (1998). The early diagenesis of iron in pelagic sediments: a multidisciplinary approach. *Earth and Planetary Science Letters*, **157**(3), 233-248.

Hansel, C. M., Benner, S. G., Nico, P. and Fendorf, S. (2004). Structural constraints of ferric (hydr)oxides on dissimilatory iron reduction and the fate of Fe(II). *Geochimica et Cosmochimica Acta*, **68**(15), 3217-3229.

Heron, G., Crouzet, C., Bourg, A. C. M. and Christensen, T. H. (1994). Speciation of Fe(II) and Fe(III) in contaminated aquifer sediments using chemical extraction techniques. *Environmental Science and Technology*, **28**(9), 1698-1705.

Hines, M. E., Orem, W. H., Lyons, W. B. and Jones, G. E. (1982). Microbial activity and bioturbation-induced oscillations in pore water chemistry of estuarine sediments in spring. *Nature*, **299**(5882), 433-435.

Howarth, R. W. (1979). Pyrite: Its rapid formation in a salt marsh and its importance in ecosystem metabolism. *Science*, **203**(4375), 49-51.

Howarth, R. W. and Jørgensen, B. B. (1984). Formation of ^{35}S-labelled elemental sulfur and pyrite in coastal marine sediments (Limfjorden and Kysing Fjord, Denmark) during short-term [35]$SO_4^{2-}$ reduction measurements.

*Geochimica et Cosmochimica Acta*, **48**(9), 1807-1818.

Jing, L. and Ridd, P. V. (1996). Wave-current bottom shear stresses and sediment resuspension in Cleveland Bay, Australia. *Coastal Engineering*, **29**(1), 169-186.

Jørgensen, B. B. (1977). The sulfur cycle of a coastal marine sediment (Limfjorden, Denmark). *Limnology and Oceanography*, **22**(5), 814-832.

Jørgensen, B. B. (1982). Mineralization of organic matter in the sea bed—the role of sulphate reduction. *Nature*, **296**(5858), 643-645.

Jørgensen, B. B., Revsbech, N. P., Blackburn, T. H. and Cohen, Y. (1979). Diurnal cycle of oxygen and sulfide microgradients and microbial photosynthesis in a cyanobacterial mat sediment. *Applied and Environmental Microbiology*, **38**(1), 46-58.

Kappler, A. and Straub, K. L. (2005). Geomicrobiological cycling of iron. *Reviews in Mineralogy and Geochemistry*, **59**(1), 85-108.

Kashefi, K., Tor, J. M., Holmes, D. E., Gaw Van Praagh, C. V., Reysenbach, A.-L. and Lovley, D. R. (2002). Geoglobus ahangari gen. nov., sp. nov., a novel hyperthermophilic archaeon capable of oxidizing organic acids and growing autotrophically on hydrogen with Fe(III) serving as the sole electron acceptor. *International Journal of Systematic and Evolutionary Microbiology*, **52**(3), 719-728.

Khare, N., Hesterberg, D. and Martin, J. D. (2005). XANES investigation of phosphate sorption in single and binary systems of iron and aluminum oxide minerals. *Environmental Science & Technology*, **39**(7), 2152-2160.

King, A. L. and Barbeau, K. A. (2011). Dissolved iron and macronutrient distributions in the southern California Current System. *Journal of Geophysical Research: Oceans*, **116**(C3).

Krachler, R., Krachler, R. F., von der Kammer, F., Süphandag, A., Jirsa, F., Ayromlou, S., Hofmann, T. and Keppler, B. K. (2010). Relevance of peat-draining rivers for the riverine input of dissolved iron into the ocean. *Science of the Total Environment*, **408**(11), 2402-2408.

Kühl, M. and Jørgensen, B. B. (1992). Spectral light measurements in microbenthic phototrophic communities with a fiber-optic microprobe coupled to a sensitive diode array detector. *Limnology and Oceanography*, **37**(8), 1813-1823.

Kuma, K., Nakabayashi, S., Suzuki, Y., Kudo, I. and Matsunaga, K. (1992). Photo-reduction of Fe(III) by dissolved organic substances and existence of Fe(II) in seawater during spring blooms. *Marine Chemistry*, **37**(1), 15-27.

Lassen, C., Ploug, H. and Jorgensen, B. B. (1992). Microalgal photosynthesis and spectral scalar irradiance in coastal marine sediments of Limfjorden, Denmark. *Limnology and Oceanography*, **37**(4), 760-772.

Laufer, K., Byrne, J. M., Glombitza, C., Schmidt, C., Jørgensen, B. B. and Kappler, A. (2016a). Anaerobic microbial Fe(II) oxidation and Fe(III) reduction in coastal marine sediments controlled by organic carbon content. *Environmental Microbiology*, **18**(9), 3159-3174.

Laufer, K., Nordhoff, M., Halama, M., Martinez, R. E., Obst, M., Nowak, M., Stryhanyuk, H., Richnow, H. H. and Kappler, A. (2017). Microaerophilic Fe(II)-oxidizing Zetaproteobacteria isolated from low-Fe marine coastal

sediments: physiology and composition of their twisted stalks. *Applied and Environmental Microbiology*, **83**(8), e03118-03116.

Laufer, K., Nordhoff, M., Røy, H., Schmidt, C., Behrens, S., Jørgensen, B. B. and Kappler, A. (2016b). Coexistence of microaerophilic, nitrate-reducing, and phototrophic Fe(II)-oxidizers and Fe(III)-reducers in coastal marine sediment. *Applied and Environmental Microbiology*, **82**(5), 1433-1447.

Lovley, D. R. (1991). Dissimilatory Fe(III) and Mn(IV) reduction. *Microbiological Reviews*, **55**(2), 259-287.

Lovley, D. R. and Phillips, E. J. P. (1988). Novel mode of microbial energy metabolism: organic carbon oxidation coupled to dissimilatory reduction of iron or manganese. *Applied and Environmental Microbiology*, **54**(6), 1472-1480.

Lueder, U., Jørgensen, B. B., Kappler, A. and Schmidt, C. (2019). Fe(III) photoreduction producing $Fe^{2+}_{aq}$ in oxic freshwater sediment. *submitted*.

Luther, G. W., Giblin, A., Howarth, R. W. and Ryans, R. A. (1982). Pyrite and oxidized iron mineral phases formed from pyrite oxidation in salt marsh and estuarine sediments. *Geochimica et Cosmochimica Acta*, **46**(12), 2665-2669.

Luther, G. W., Rickard, D. T., Theberge, S. and Olroyd, A. (1996). Determination of metal (bi)sulfide stability constants of $Mn^{2+}$, $Fe^{2+}$, $Co^{2+}$, $Ni^{2+}$, $Cu^{2+}$, and $Zn^{2+}$ by voltammetric methods. *Environmental Science & Technology*, **30**(2), 671-679.

MacIntyre, H. L., Geider, R. J. and Miller, D. C. (1996). Microphytobenthos: The ecological role of the "secret garden" of unvegetated, shallow-water marine habitats. I. Distribution, abundance and primary production. *Estuaries*, **19**(2), 186-201.

McAllister, S. M., Moore, R. M., Gartman, A., Luther, G. W., III, Emerson, D. and Chan, C. S. (2019). The Fe(II)-oxidizing Zetaproteobacteria: Historical, ecological, and genomic perspectives. *FEMS Microbiology Ecology*.

Melton, E. D., Swanner, E. D., Behrens, S., Schmidt, C. and Kappler, A. (2014). The interplay of microbially mediated and abiotic reactions in the biogeochemical Fe cycle. *Nat Rev Micro*, **12**(12), 797-808.

Millero, F. J., Sotolongo, S. and Izaguirre, M. (1987). The oxidation kinetics of Fe(II) in seawater. *Geochimica et Cosmochimica Acta*, **51**(4), 793-801.

Morse, J. W. and Casey, W. H. (1988). Ostwald processes and mineral paragenesis in sediments. *American Journal of Science*, **288**(6), 537-560.

O'Sullivan, D. W., Hanson, A. K., Miller, W. L. and Kester, D. R. (1991). Measurement of Fe(II) in surface water of the equatorial Pacific. *Limnology and Oceanography*, **36**(8), 1727-1741.

Otte, J. M., Harter, J., Laufer, K., Blackwell, N., Straub, D., Kappler, A. and Kleindienst, S. (2018). The distribution of active iron-cycling bacteria in marine and freshwater sediments is decoupled from geochemical gradients. *Environmental Microbiology*, **20**(7), 2483-2499.

Peng, C., Bryce, C., Sundman, A. and Kappler, A. (2019). Cryptic cycling of complexes containing Fe(III) and organic matter by phototrophic Fe(II)-oxidizing bacteria. *Applied and Environmental Microbiology*, **85**(8), e02826-02818.

Poulton, S. W. and Canfield, D. E. (2005). Development of a sequential extraction

procedure for iron: implications for iron partitioning in continentally derived particulates. *Chemical Geology*, **214**(3), 209-221.

Pyzik, A. J. and Sommer, S. E. (1981). Sedimentary iron monosulfides: Kinetics and mechanism of formation. *Geochimica et Cosmochimica Acta*, **45**(5), 687-698.

Rancourt, D. G. and Ping, J. Y. (1991). Voigt-based methods for arbitrary-shape static hyperfine parameter distributions in Mössbauer spectroscopy. *Nuclear Instruments and Methods in Physics Research Section B: Beam Interactions with Materials and Atoms*, **58**(1), 85-97.

Revsbech, N. P. (1989). An oxygen microsensor with a guard cathode. *Limnology and Oceanography*, **34**(2), 474-478.

Rickard, D. (1989). Experimental concentration-time curves for the iron(II) sulphide precipitation process in aqueous solutions and their interpretation. *Chemical Geology*, **78**(3), 315-324.

Rickard, D., Oldroyd, A. and Cramp, A. (1999). Voltammetric evidence for soluble FeS complexes in anoxic estuarine muds. *Estuaries*, **22**(3), 693-701.

Roden, E. E. and Zachara, J. M. (1996). Microbial reduction of crystalline iron(III) oxides: Influence of oxide surface area and potential for cell growth. *Environmental Science & Technology*, **30**(5), 1618-1628.

Sanford, L. P. (1994). Wave-forced resuspension of upper Chesapeake Bay muds. *Estuaries*, **17**(1), 148-165.

Scheffer, M., Portielje, R. and Zambrano, L. (2003). Fish facilitate wave resuspension of sediment. *Limnology and Oceanography*, **48**(5), 1920-1926.

Schippers, A. and Jørgensen, B. B. (2002). Biogeochemistry of pyrite and iron sulfide oxidation in marine sediments. *Geochimica et Cosmochimica Acta*, **66**(1), 85-92.

Schmidt, C., Behrens, S. and Kappler, A. (2010). Ecosystem functioning from a geomicrobiological perspective a conceptual framework for biogeochemical iron cycling. *Environmental Chemistry*, **7**(5), 399-405.

Schoonen, M. A. A. and Barnes, H. L. (1991). Reactions forming pyrite and marcasite from solution: II. Via FeS precursors below 100°C. *Geochimica et Cosmochimica Acta*, **55**(6), 1505-1514.

Shannon, R. D. and White, J. R. (1991). The selectivity of a sequential extraction procedure for the determination of iron oxyhydroxides andiron sulfides in lake sediments. *Biogeochemistry*, **14**(3), 193-208.

Slowey, A. and Marvin-DiPasquale, M. (2012). How to overcome inter-electrode variability and instability to quantify dissolved oxygen, Fe(II), Mn(II), and S(II) in undisturbed soils and sediments using voltammetry. *Geochemical Transactions*, **13**(1), 6.

Stookey, L. L. (1970). Ferrozine - a new spectrophotometric reagent for iron. *Analytical Chemistry*, **42**(7), 779-781.

Su, C. and Suarez, D. L. (2000). Selenate and selenite sorption on iron oxides: An infrared and electrophoretic study 1 *Soil Science Society of America Journal*, **64**(1), 101-111.

Sulzberger, B., Suter, D., Siffert, C., Banwart, S. and Stumm, W. (1989). Dissolution of Fe(III)(hydr)oxides in natural waters; laboratory assessment on the kinetics controlled by surface

coordination. *Marine Chemistry*, **28**(1), 127-144.

Taillefert, M., Bono, A. B. and Luther III, G. W. (2000). Reactivity of freshly formed Fe(III) in synthetic solutions and (pore)waters: voltammetric evidence of an aging process. *Environmental Science & Technology*, **34**(11), 2169-2177.

Tessier, A., Campbell, P. G. C. and Bisson, M. (1979). Sequential extraction procedure for the speciation of particulate trace metals. *Analytical Chemistry*, **51**(7), 844-851.

Thamdrup, B., Fossing, H. and Jørgensen, B. B. (1994). Manganese, iron and sulfur cycling in a coastal marine sediment, Aarhus bay, Denmark. *Geochimica et Cosmochimica Acta*, **58**(23), 5115-5129.

Theberge, S. M. and Luther III, G. W. (1997). Determination of the electrochemical properties of a soluble aqueous FeS species present in sulfidic solutions. *Aquatic Geochemistry*, **3**(3), 191-211.

Thiel, J., Byrne, J., Kappler, A., Schink, B. and Pester, M. (2018). Pyrite formation from FeS and $H_2S$ is mediated by a novel type of microbial energy metabolism. *bioRxiv*, 396978.

Wan, M., Schröder, C. and Peiffer, S. (2017). Fe(III):S(-II) concentration ratio controls the pathway and the kinetics of pyrite formation during sulfidation of ferric hydroxides. *Geochimica et Cosmochimica Acta*, **217**, 334-348.

Ward, L. G., Michael Kemp, W. and Boynton, W. R. (1984). The influence of waves and seagrass communities on suspended particulates in an estuarine embayment. *Marine Geology*, **59**(1), 85-103.

Whitney, D. E. and Darley, W. M. (1983). Effect of light intensity upon salt marsh benthic microalgal photosynthesis. *Marine Biology*, **75**(2), 249-252.

You, Z.-J. (2005). Fine sediment resuspension dynamics in a large semi-enclosed bay. *Ocean Engineering*, **32**(16), 1982-1993.

## 4.6 Supporting Information
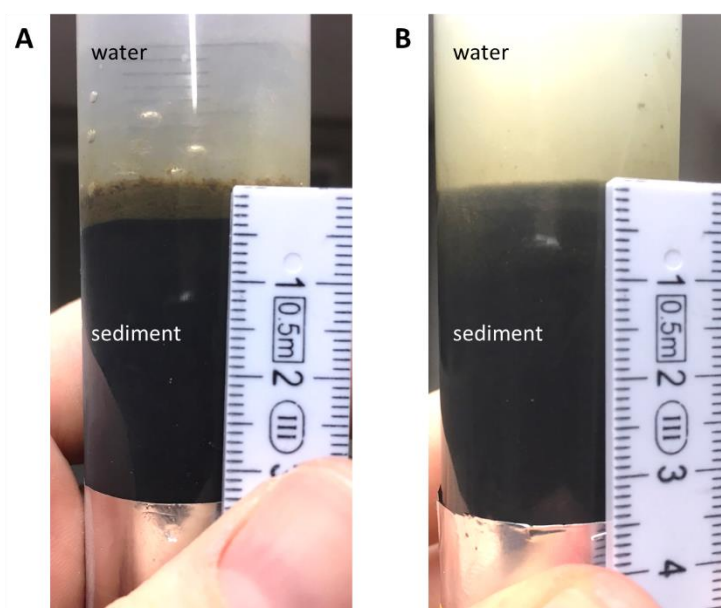


**Figure S4.1** One of the 17 sediment cores prepared for this study from homogenized sediment in order to enable reproducible starting conditions of the sediment cores, (A) after 7 days of undisturbed 12 h light-dark incubation, (B) shortly after the simulated storm event. Please note the difference in turbidity due to suspended sediment after the storm event.
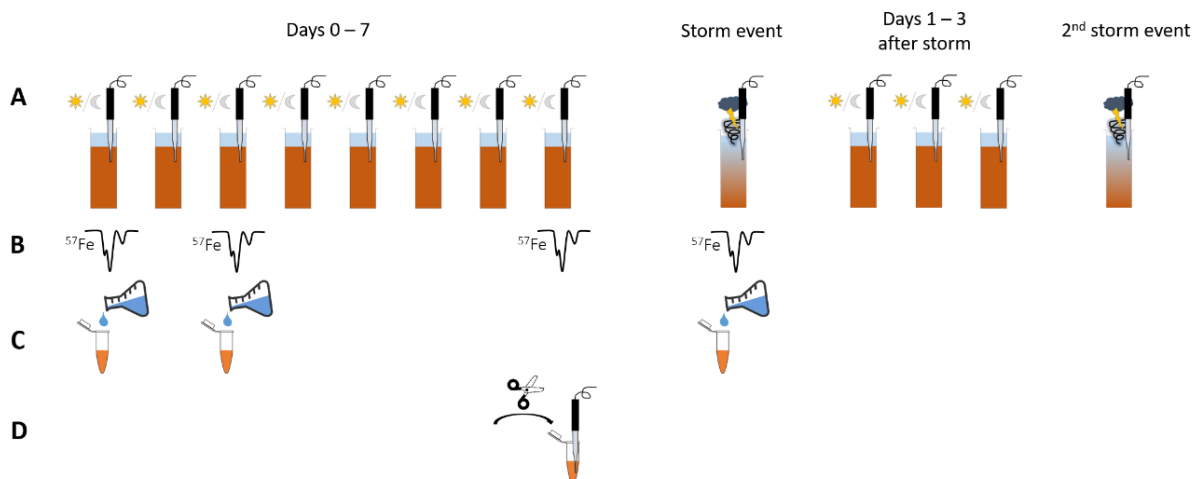


**Figure S4.2** Scheme of the experimental approach, (A) daily microsensor measurements during undisturbed 12 h light-dark incubation and shortly after storm events, (B) selected time points for Mössbauer spectroscopy analysis, (C) selected time points for sequential Fe extractions and (D) test of the impact of physical perturbation simply due to slicing the sediment core and voltammetric measurements in the sediment slurry and centrifuged supernatant.
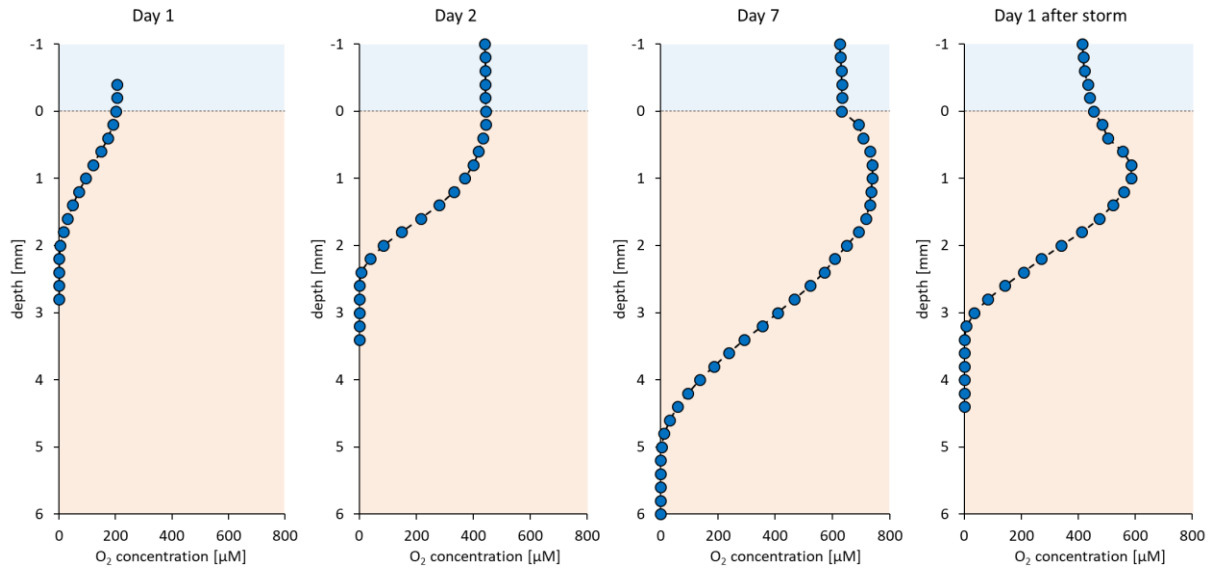
**Figure S4.3** $O_2$ concentration profiles after 1, 2 and 7 days of undisturbed 12h light-dark incubation and 1 day after the simulated storm event.
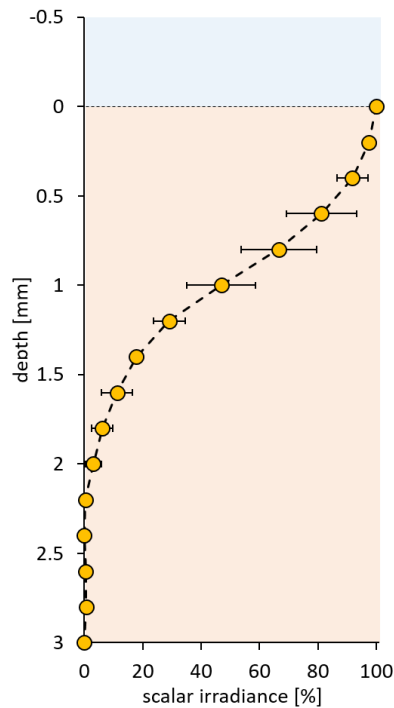


**Figure S4.4** Light intensity (expressed as scalar irradiance) in the sediment, normalized to the light intensity reaching the sediment surface. Error bars show the standard deviation of five recorded scalar irradiance profiles.
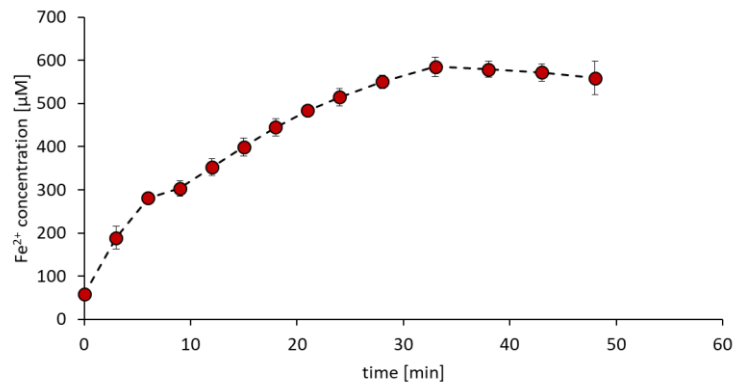
**Figure S4.5** $Fe^{2+}$ development during a simulated storm event in the sediment core determined by voltammetric measurements. The high $Fe^{2+}$ concentrations reaching >500 μM can be attributed to release of $Fe^{2+}$, e.g. from metastable $FeS_x$ mineral phases into the sedimentary pore water during the physical perturbation without subsequent equilibration of the sediment. Error bars show standard deviation of triplicate voltammograms.
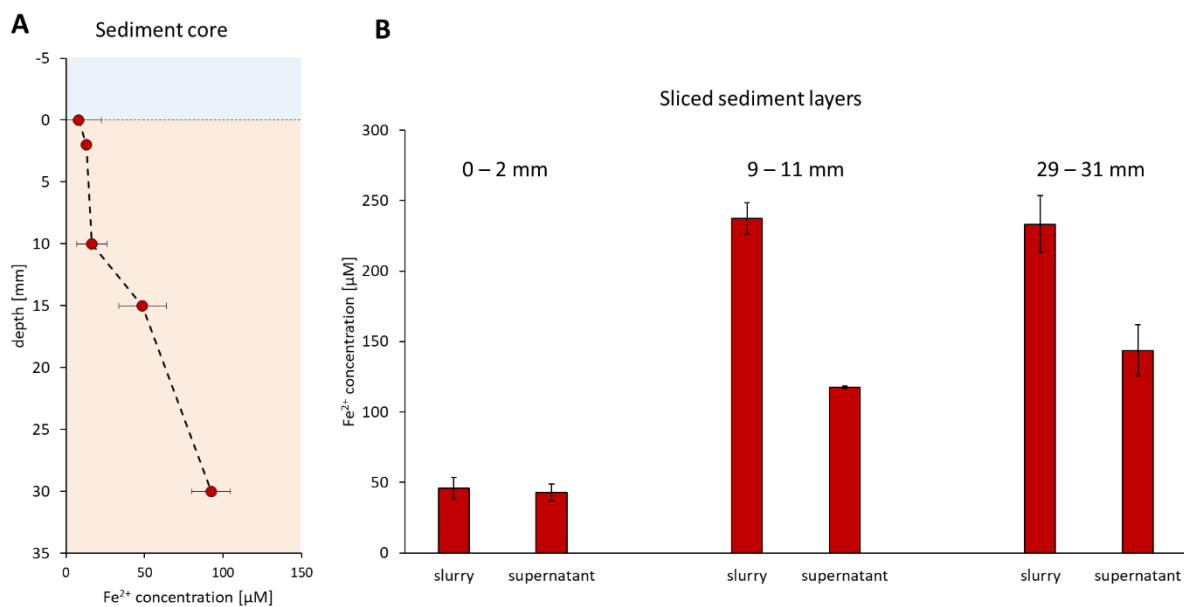


**Figure S4.6** Impact of physical movement (slicing and homogenization) of sediment on $Fe^{2+}$ mobilization, (A) $Fe^{2+}$ concentrations in an undisturbed sediment core determined by voltammetry, (B) $Fe^{2+}$ concentrations in sliced and homogenized sediment layers (0-2 mm, 9-11 mm and 29-31 mm depth) determined in the homogenized sediment slurry and in the supernatant of centrifuged sediment. Error bars show standard deviation of triplicate voltammograms.

Cyclone Christian with wind speeds of up to 190 km h^{-1} did hit western Europe in October 2013. During this storm, the water and sediment of the sampling site Norsminde Fjord (Denmark) were completely mixed and resuspended. Microsensor profiles of $O_2$ and redox potential were recorded in in-situ sediment cores before and 2 days after this storm event (Figure S4.7).
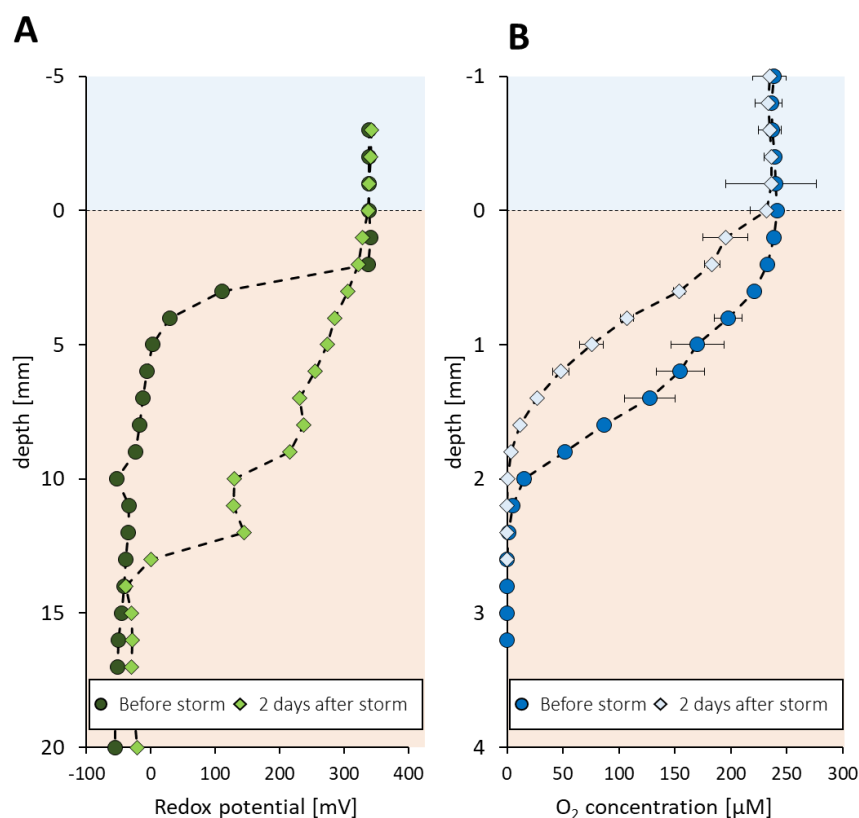


**Figure S4.7** Profiles in in-situ sediment cores before and 2 days after a storm at the sampling field site, (A) redox potential profiles, (B) $O_2$ concentration profiles. Error bars show the standard deviation of triplicate measurements. Note the different scales of the y-axes.

## Mössbauer & XRD data

Mössbauer spectroscopy parameters are listed in Table S4.1. The spectra collected at 77 K show two clear and well pronounced doublet features (Db), with one broad doublet (Db1) and a narrow doublet (Db2) which are overlapping at the isomer center (Figure S4.8). The hyperfine parameters of these two doublets have very similar properties for all four samples at 77 K with a center shift (CS) of CS = 1.23 – 1.25 mm s^{-1} for Db1 and CS = 0.42 mm s^{-1} for Db2. The relatively high quadrupole splitting ($\Delta E_Q$) of $\Delta E_Q$ = 2.9 mm s^{-1} for Db1 is suggesting the

presence of a high spin Fe(II) mineral phase with a relative abundance of around $40.5 \pm 1.5\%$ in all samples. The low quadrupole splitting parameters of Db2 with $\Delta E_Q = 0.57 \pm 0.1$ mm s$^{-1}$ could be interpreted as high-spin Fe(III) phase or low-spin Fe(II). In order to resolve this uncertainty, the sample was additionally analyzed at 5 K. The narrow splitting which resulted at the low temperature confirmed the absence of an internal field and a magnetic ordering and implies the presence of a second Fe(II) phase – a low-spin Fe(II) mineral. Spectra that were collected at 5 K show a high similarity to spectra collected at 77 K. The wide Db1 and narrow Db2 are the predominant features in all samples. Their hyperfine characteristics change slightly with a decrease in their center shift to $CS = 1.13 \pm 0.05$ mm s$^{-1}$ for Db1 and $CS = 0.41 \pm 0.01$ mm s$^{-1}$ for Db2. The increase in their quadrupole splitting to $\Delta E_Q = 2.9 \pm 0.2$ mm s$^{-1}$ for Db1 and $\Delta E_Q = 0.67 \pm 0.3$ mm s$^{-1}$ for Db2 is consistent with their interpretation as a high-spin Fe(II) phase represented by Db1 and an additional low-spin Fe(II) phase being detected in Db2. In addition to the doublet features, also the presence of a magnetically-ordered iron phase can be interpreted by the residual peaks in the background. In order to achieve a satisfactory fit, an additional poorly defined hyperfine field distribution site (HFD-site) was required. The best-fit model for all spectra collected at 5 K (Figure S4.9) suggests a narrow sextet (S1) with relatively consistent hyperfine field parameters, CS at around $CS = 0.8 - 0.9$ mm s$^{-1}$ and a hyperfine field ($B_{hf}$) of $B_{hf} = 25 - 27$ T. According to Wan et al. (2017), this poorly defined sextet could potentially resemble a metastable iron-sulphur mineral phase (FeS$_x$) undergoing magnetic ordering at 5 K and is present in all samples. The magnetic resonance splitting of this metastable mineral phase was potentially hidden behind the well pronounced doublet features of Db1 and Db2 at the higher temperature of 77 K but only became detectable at 5 K. The hyperfine field parameters of the other two doublets suggest that vivianite (Fe$_3$(PO$_4$)$_2$x8H$_2$O) is a likely candidate as a high-spin Fe(II) phase being represented by the wide doublet Db1 in all samples, while the hyperfine field parameters of the narrow doublet Db2 are very similar to pyrite (FeS$_2$) as a low-spin Fe(II) phase. As stated above, the relative abundance of these two mineral phases is relatively consistent among the 77 K spectra (Table S4.1) with FeS$_2$ being the more dominant phase over potential Fe$_3$(PO$_4$)$_2$x8H$_2$O. However, considering the fit-model of the 5 K spectra, the relative abundances of all three iron phases vary slightly.

**Table S4.1** Hyperfine parameters: Sample name, temperature sample was analyzed at, CS – Center shift, $\Delta E_Q$ – Quadrupole splitting, $\varepsilon$ – Quadrupole shift, $B_{hf}$ – Hyperfine field, Pop. – relative abundance, $\chi^2$ – goodness of fit, matched candidate phase with Viv/Sid = vivianite/siderite.

| Sample | Temp. | Phase | CS | $\Delta E_Q$ | $\varepsilon$ | $B_{hf}$ | Pop | $\pm$ | $\chi^2$ | Mineral phase |
|---|---|---|---|---|---|---|---|---|---|---|
| | [K] | | [mm s$^{-1}$] | [mm s$^{-1}$] | [mm s$^{-1}$] | [T] | [%] | | | |
| Day 0 | 77 | Db1 | 1.25 | 2.91 | | | 41.8 | 0.3 | 0.57 | Viv/Sid |
| | | Db2 | 0.44 | 0.56 | | | 58.2 | 0.2 | | Pyrite |
| | 5 | Db1 | 1.18 | 2.92 | | | 38.0 | 1.0 | 0.75 | Viv/Sid |
| | | Db2 | 0.39 | 0.69 | | | 42.7 | 0.3 | | Pyrite |
| | | S1 | 0.89 | | 0.19 | 24.7 | 19.3 | 2.9 | | FeS$_x$ |
| Day 2 | 77 | Db1 | 1.25 | 2.93 | | | 41.6 | 0.2 | 0.62 | Viv/Sid |
| | | Db2 | 0.44 | 0.57 | | | 58.4 | 0.2 | | Pyrite |
| | 5 | Db1 | 1.18 | 3.03 | | | 27.9 | 0.3 | 0.93 | Viv/Sid |
| | | Db2 | 0.42 | 0.65 | | | 49.2 | 0.3 | | Pyrite |
| | | S1 | 0.80 | | -0.03 | 26.5 | 22.9 | 2.46 | | FeS$_x$ |
| Day 7 | 77 | Db1 | 1.24 | 2.92 | | | 40.5 | 0.3 | 0.68 | Sid/Viv |
| | | Db2 | 0.44 | 0.60 | | | 59.5 | | | Pyrite |
| | 5 | Db1 | 1.16 | 3.11 | | | 30.3 | 0.6 | 0.8 | Sid/Viv |
| | | Db2 | 0.41 | 0.70 | | | 45.0 | 0.2 | | Pyrite |
| | | S1 | 0.97 | | -0.04 | 27.1 | 24.7 | 2.1 | | FeS$_x$ |
| After storm | 77 | Db1 | 1.23 | 2.94 | | | 38.7 | 0.3 | 0.79 | Sid/Viv |
| | | Db2 | 0.42 | 0.58 | | | 61.3 | 0.2 | | Pyrite |
| | 5 | Db1 | 1.08 | 2.89 | | | 46.2 | 1.4 | 0.93 | Sid/Viv |
| | | Db2 | 0.39 | 0.64 | | | 35.6 | 0.3 | | Pyrite |
| | | S1 | 0.55 | | 0.14 | 27.1 | 18.2 | 2.2 | | FeS$_x$ |
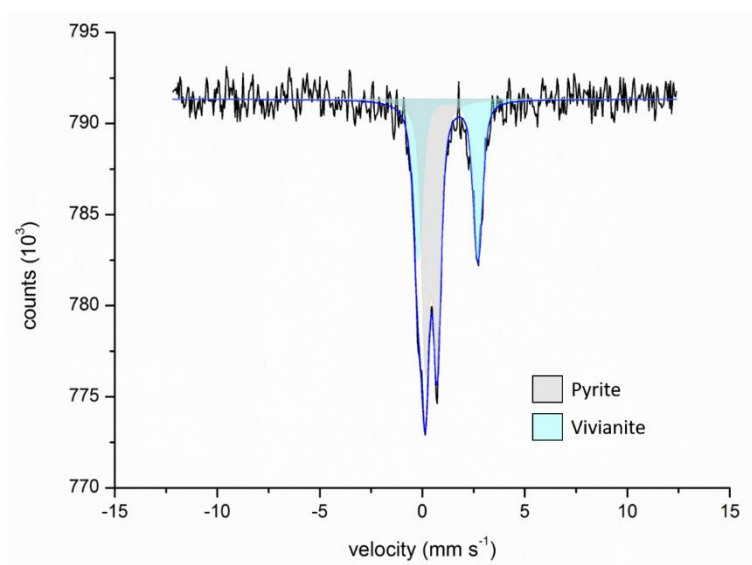
**Figure S4.8** Representative Mössbauer model fit (blue line) of spectra collected at 77 K (black line), characterized by two dominant doublets, likely representing vivianite (light blue) and pyrite (grey).
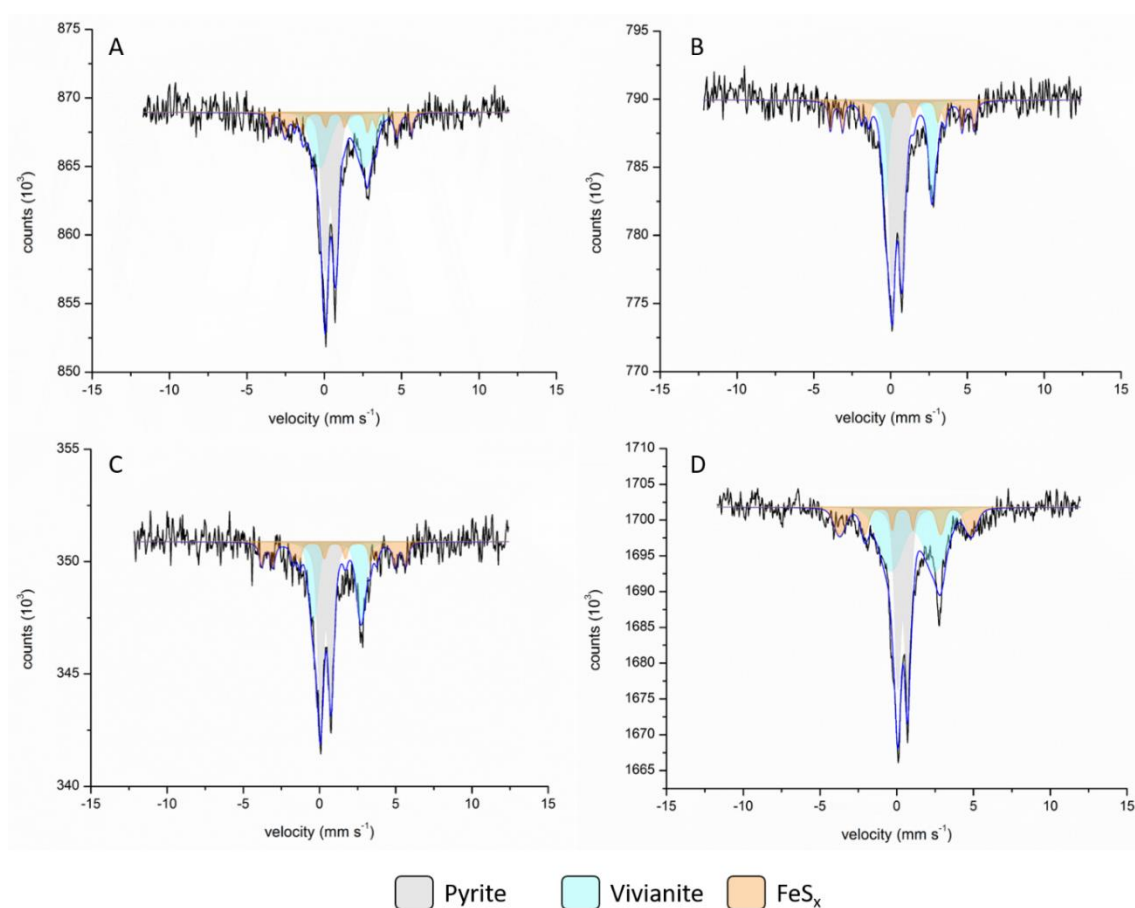


**Figure S4.9** Mössbauer spectroscopy – Model fit (blue line) of spectra collected at 5 K (black line) for samples of (A) day 0, (B) day 2 and (C) day 7 of undisturbed light-dark incubation as well as (D) after the simulated storm event. All samples show two dominant doublet features that can likely be attributed to the presence of vivianite (light blue), pyrite (grey) and a poorly developed sextet potentially representing a metastable Fe-S-phase ($FeS_X$, orange).

The sediment sample for XRD was collected and dried under anoxic conditions, loaded onto a silica wafer (sample size ø 2mm) and kept constantly anoxic until analysis. The analysis was carried out on a 2D-Microdiffractometer (Bruker D8 Discover with GADDS, µ-XRD[2], Bruker AXS GmbH, Karlsruhe, Germany), using a cobalt anode tube as x-ray source with a Co-Kα wavelength of 1.79030 Å and a 2D detector with 40° angle cover (Bruker Våntec 500 Bruker AXS GmbH, Karlsruhe, Germany). The sample was not rotated and reflection patterns were collected for 120 seconds per angle setting. Reflection pattern analysis and mineral identification was carried out using Match! program for phase identification from powder diffraction (Match!, Crystal Impact, Bonn, Germany). XRD diffraction pattern of both samples, wet and dried sediment, showed a clear signal for quartz being the most dominant and crystalline mineral phase in the sediment matrix (Figure S4.10). In the wet sample, small reflections were detected that could be indicative for $FeS_2$ being present as Fe(II) mineral. However, the reflections were not significant enough to clearly confirm its presence, potentially due to scattering interferences with the wet sample matrix. As $FeS_2$ is thermodynamically more stable than Fe monosulphides (Giblin & Howarth, 1984) and the oxidation kinetics of $FeS_2$ by $O_2$ is significantly slower after the formation and accumulation of a ferric (oxyhydr)oxide layer on the sulphide surface (Nicholson et al., 1990), the sample was dried in air for some minutes in order to remove the water from the sediment matrix. The XRD pattern of the dried sample showed the two major reflections for $FeS_2$ and clearly approved its presence as Fe(II) phase. Due to the drying process, also halite (NaCl) crystallized and precipitated as an evaporation product (Figure S4.10).
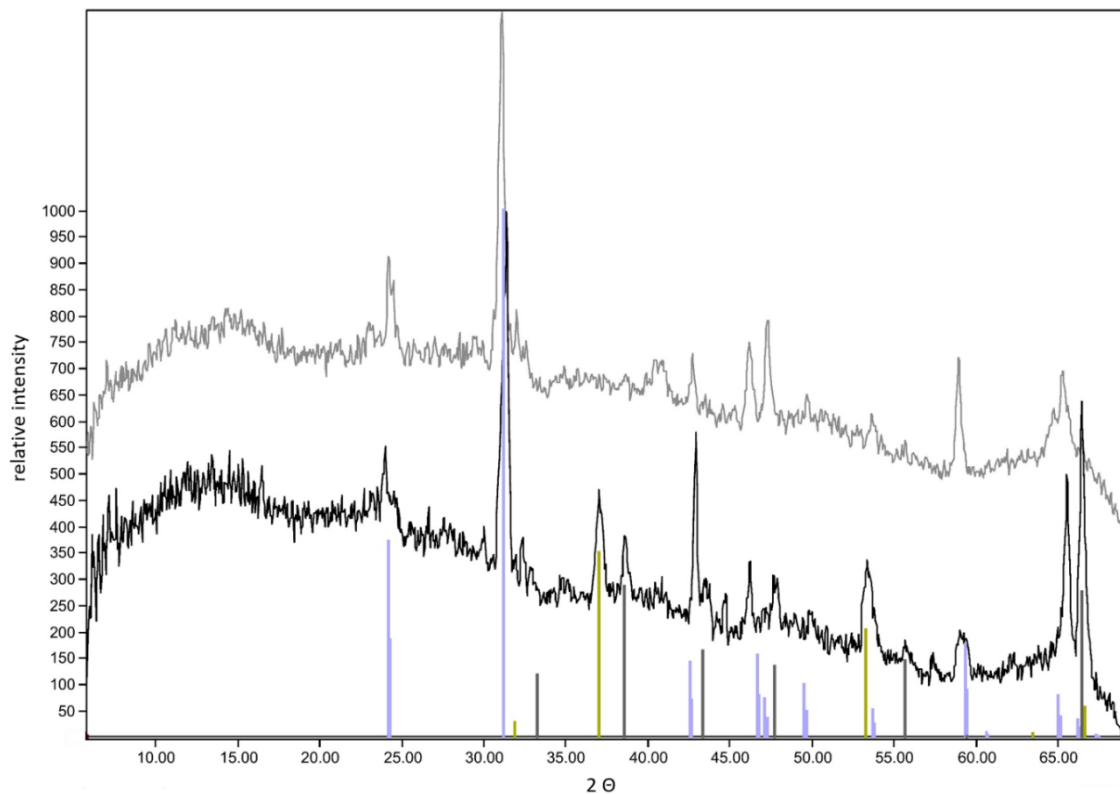
**Figure S4.10** X-ray diffraction pattern collected from the native sample material (anoxic, wet – upper, grey line) and the dried sediment material (air-dried – lower, black line). Both patterns show a clear signal for quartz (light blue reference). $FeS_2$ (grey reference) was clearly detectable in the air-dried sample material only, while also halite (NaCl – olive reference) precipitated in the air-dried sediment due to evaporation

## References

Giblin, A. E. and Howarth, R. W. (1984). Porewater evidence for a dynamic sedimentary iron cycle in salt marshes1. *Limnology and Oceanography*, **29**(1), 47-63.

Nicholson, R. V., Gillham, R. W. and Reardon, E. J. (1990). Pyrite oxidation in carbonate-buffered solution: 2. Rate control by oxide coatings. *Geochimica et Cosmochimica Acta*, **54**(2), 395-402.

Wan, M., Schröder, C. and Peiffer, S. (2017). Fe(III):S(-II) concentration ratio controls the pathway and the kinetics of pyrite formation during sulfidation of ferric hydroxides. *Geochimica et Cosmochimica Acta*, **217**, 334-348.

## Chapter 5 – Personal contribution

Experiments were conceptualized by myself and Dr. Caroline Schmidt. Sediment sampling was done by myself. The experiments and data collection were carried out by myself. Markus Maisch helped with sampling during the experiment. The discussion and analysis of the obtained results were done by myself and Dr. C. Schmidt, Prof. Dr. Andreas Kappler and Prof. Dr. Bo Barker Jørgensen and M. Maisch. The manuscript was written by myself. Dr. C. Schmidt, Prof. A. Kappler, Prof. B.B. Jørgensen, and M. Maisch revised the manuscript.

# Chapter 5: The impact of light on the development of cable bacteria in marine coastal sediments

Ulf Lueder[1], Markus Maisch[1], Bo B. Jørgensen[2], Andreas Kappler[1,2], Caroline Schmidt[1]

[1] Geomicrobiology, Center for Applied Geoscience (ZAG), University of Tuebingen, Germany

[2] Center for Geomicrobiology, Department of Bioscience, Aarhus University, Denmark

Unpublished manuscript

## 5.1 Abstract

Cable bacteria are filamentous bacteria that electrically couple the oxidation of sulphide to the reduction of oxygen ($O_2$) in sediments over centimeter distances. Recent studies also suggested a connection of cable bacteria to the iron (Fe) redox cycle. However, it is currently unknown how cable bacteria alter the distribution of Fe-redox species in sediments. Moreover, the impact of light on cable bacteria activity has not been investigated so far. Here, we performed high-resolution microsensor measurements of light and dark incubated marine coastal sediment cores. We found decreasing concentrations of dissolved Fe(II) ($Fe^{2+}$) in light incubated sediment cores from 470 µM to 10 µM in 30 mm depth, compared to 150 µM in dark incubated sediment cores. The formation of an orange layer in the sediment as well as a pH peak in the upper sediment layers after 7 days strongly hint towards cable bacteria activity. Cable bacteria were present in high abundance (manually picked) in the light incubated setup compared to dark conditions. DCMU-addition for suppressing oxygenic photosynthesis and concomitant $O_2$ supersaturation lead to similar $Fe^{2+}$ concentration profiles in both, light and dark incubated sediment cores, and cable bacteria could not be found in either setup. Our data suggest that light stimulates growth of cable bacteria and that their activity significantly alters the availability of $Fe^{2+}$ in reduced sediment layers. High abundance of cable bacteria and concomitant $Fe^{2+}$ removal in the light setup could either be explained by the direct use of $Fe^{2+}$ as electron donor by cable bacteria or by interaction with Fe(II)-oxidizing bacteria that might transfer electrons via e.g. nanowires to the cable bacteria and use them as electron sink. Our data provides new insights on a potential link between cable bacteria and light, thereby impacting the Fe(II) availability in sediments.

## 5.2 Introduction

Iron (Fe) is cycled in marine sediments by many biotic and abiotic processes (Melton et al., 2014). Fe(II) is produced in anoxic sediments by Fe(III)-reducing bacteria that reduce Fe(III) by coupling it to the oxidation of organic compounds or hydrogen (Lovley & Phillips, 1988; Lovley, 1991; Kashefi et al., 2002). It can also be produced by abiotic Fe(III) reduction by dissolved sulphide ($H_2S+HS^-+S^{2-}$) or natural organic matter (Pyzik & Sommer, 1981; Canfield, 1989; Sulzberger et al., 1989). In upper, light illuminated sediment layers that contain dissolved Fe(III)-organic complexes, Fe(II) can be produced by Fe(III) photoreduction, even under oxic conditions (Lueder et al., 2019a; Lueder et al., 2019b). Dissolved Fe(II) ($Fe^{2+}$) diffuses through the sediment pore water and gets oxidized by microaerophilic, nitrate-reducing or phototrophic Fe(II)-oxidizing bacteria, that are ubiquitously present in marine sediments (Laufer et al., 2016; Otte et al., 2018b; McAllister et al., 2019) or abiotically by e.g. $O_2$ (Millero et al., 1987). Diffusion of atmospheric $O_2$ and oxygenic photosynthesis lead to aeration of sediment layers, while respiratory processes or chemical reactions involving the depletion of $O_2$ eventually lead to anoxic conditions in the sediment (Revsbech et al., 1980; Jørgensen & Revsbech, 1985). Another important chemical component in marine sediments is dissolved sulphide. It is formed by bacterial sulphate reduction and can react with Fe(II) to form various iron-sulphide minerals (Jørgensen, 1977; Jørgensen, 1982; Canfield, 1989).

Few years ago, filamentous, multicellular bacteria were discovered in marine sediments that electrically couple the oxidation of sulphide to the reduction of $O_2$ or nitrate (Marzocchi et al., 2014) over centimeter distances (Pfeffer et al., 2012). Those cable bacteria belong to the *Desulfobulbaceae* family and are able to conduct electrons (Meysman et al., 2019) produced by sulphide oxidation in deeper sediment layers to $O_2$ near the sediment-water interface (Nielsen et al., 2010; Pfeffer et al., 2012; Trojan et al., 2016). The electrons are conducted in continuous periplasmic fibers that run along the entire filament length (Pfeffer et al., 2012; Meysman et al., 2019). This spatially separated redox reaction leads to the formation of a suboxic zone spanning over several centimeters with non-detectable levels of $H_2S$ and $O_2$ (Nielsen et al., 2010; Risgaard-Petersen et al., 2012; Schauer et al., 2014; Meysman et al., 2015). Proton consumption during $O_2$ reduction (eq.5.1) by cable bacteria lead to the formation of a characteristic pH peak in the oxic zone (Nielsen et al., 2010; Pfeffer et al., 2012; Meysman et al., 2015).

$$O_2 + 4H^+ + 4e^- \rightarrow 2H_2O \qquad (5.1)$$

In contrast, pore water of deeper sediment layers gets acidified due to proton production during oxidation of sulphate (eq. 5.2) and leads to dissolution of carbonates or Fe sulphides (Risgaard-Petersen et al., 2012; Seitaj et al., 2015; Rao et al., 2016).

$$\frac{1}{2} H_2S + 2H_2O \rightarrow \frac{1}{2} SO_4^{2-} + 5H^+ + 4e^- \qquad (5.2)$$
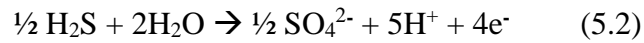
Mobilized $Fe^{2+}$ diffuses upwards into the oxic zone, gets oxidized and precipitates as Fe (oxyhydr)oxides forming an orange layer in the sediment (Risgaard-Petersen et al., 2012; Rao et al., 2016). This Fe (oxyhydr)oxide layer reacts chemically with dissolved sulphide, which is toxic to higher organisms (Seitaj et al., 2015; Nielsen, 2016). By this 'firewall' (Seitaj et al., 2015), the release of sulphide into the water column is avoided or retarded during seasonal $O_2$ depletion of some regions, e.g. in the Baltic Sea (Seitaj et al., 2015; Hermans et al., 2019). The microbially mediated electron transport also lead to the generation of an electric potential gradient in the sediment (Risgaard-Petersen et al., 2012; Damgaard et al., 2014; Risgaard-Petersen et al., 2014). Since their discovery, cable bacteria have been found in many environments, including marine sediments, salt marshes, freshwater streams, aquifers, mangroves or the rhizosphere of aquatic plants (Larsen et al., 2015; Malkin & Meysman, 2015; Risgaard-Petersen et al., 2015; Burdorf et al., 2016; Müller et al., 2016; Burdorf et al., 2017; Scholz et al., 2019). So far, the only proven electron donor for cable bacteria is dissolved sulphide. However, it is unclear, whether these bacteria are able to perform alternative metabolic modes and potentially use solid or dissolved Fe(II) as electron donor.

Although many heterotrophic and autotrophic processes in sediments rely on chemical energy acquisition, light represents an important energy source for many microorganisms. Cyanobacteria use light for oxygenic photosynthesis (Blankenship & Hartman, 1998), whereas anoxygenic phototrophic bacteria use it for coupling the fixation of $CO_2$ to the oxidation of e.g. sulphide, sulphur or Fe(II) (Larsen, 1952; Widdel et al., 1993; Bryce et al., 2018). So far, it is unclear how light impacts the activity and metabolic mode of cable bacteria. Although it was shown that oxygenic photosynthesis at sediment surfaces had an immediate effect on the sulphide concentration on deeper sediment layers (Malkin & Meysman, 2015), it is unclear whether this effect was only related to increasing $O_2$ concentrations due to enhanced oxygenic photosynthesis, or to the use of light energy by cable bacteria as metabolic energy source. The goals of this study were to determine if i) light has a direct impact on the development and abundance of cable bacteria and ii) cable bacteria have a connection to the sedimentary biogeochemical iron cycle. For this, we incubated marine coastal sediment cores in light and in dark and linked $Fe^{2+}$, $O_2$ concentrations and pH to the presence and abundance of cable bacteria.

## 5.3 Materials & Methods

**Sediment core incubations**

Bulk sediment and seawater were sampled from a shallow estuary near its narrow entrance to the Baltic Sea in March 2017 (Norsminde Fjord, Denmark). The water depth was 0.5 m and light still reached the sediment surface. Samples were kept in the dark at 4°C until further processing. Stones and macrofauna were removed in the lab in order to enable microsensor application. The sediment was homogenized, filled into cut 50 ml syringes (approx. 5cm) and overlaid with 4 cm Norsminde Fjord water. The artificial sediment cores were continuously aerated and re-filled with Norsminde Fjord water to compensate evaporation. The sediment cores were incubated in light or dark at 20°C for 7 days with continuous aeration in order to maintain oxic conditions and to prevent stratification of the water column. The sediment cores were continuously illuminated. Light intensity during incubations was adjusted to 400-500 µmol photons $m^{-2}$ $s^{-1}$ using a spherical light meter (ULM-500 and US-SQS/L sensor, Walz, Germany) with a combination of two LED lamps (Samsung SI-P8V151DB1US, 14 W, 3000 K and SMD 2835, 15 W, 6000 K). The cores were wrapped in aluminum foil from the sediment-water interface downwards in order to prevent light penetration of the sediment from the sides.

In order to determine the microbial impact on $Fe^{2+}$ production/consumption in the sediment, Norsminde Fjord sediment was gamma-sterilized (dose 62kGy) and incubated in light and dark prior to geochemical measurements. In an additional experimental setup, DCMU (3-(3,4-dichlorophenyl)-1,1-dimethylurea; 300µl 1mM DCMU, dissolved in DMSO) was added to the water column and mixed into the first millimeters of the freshly prepared sediment cores in order to suppress oxygenic photosynthesis (Hoch et al., 1963) and to determine the influence of $O_2$ supersaturation caused by oxygenic photosynthesis on the growth of cable bacteria.

**Microsensor measurements**

$Fe^{2+}$ concentration profiles were determined by cyclic voltammetry using a standard three-electrode system with a DLK-70 web-potentiostat (Analytical Instrument Systems, Flemington, NJ). The working electrode was a lab-constructed glass-encased 100µm gold amalgam (Au/Hg) electrode (Brendel & Luther III, 1995). A solid state Pt wire and a Ag wire coated with AgCl were used as counter and reference electrode, respectively. Voltammograms were obtained by scanning from -0.05V to -1.8V and back with a scan rate of 2000 mV $s^{-1}$. For conditioning of the electrode, an initial potential of -0.05V was held for 2s and before each scan, a potential of

-0.9V was held for 5s for electrochemical cleaning of the electrode surface. For calibration of $Fe^{2+}$, the pilot ion method using $Mn^{2+}$ was applied (Brendel & Luther III, 1995; Slowey & Marvin-DiPasquale, 2012). $Fe^{2+}$ concentration profiles were measured 1 mm above and directly at the sediment surface as well as in in 0.5, 1, 1.5, 2, 3, 4, 6, 10, 15 and 30 mm depth. Ten scans were run at each measurement point and the final 3 voltammograms were analyzed using VOLTINT program for Matlab® (Bristow & Taillefert, 2008). The analytical error was calculated as standard deviations of analyzed triplicate voltammograms.

High resolution profiles of dissolved $O_2$ and sulphide ($H_2S+HS^-+S^{2-}$) as well as pH were measured with glass microelectrodes with 100 μm tip diameter (Unisense, Denmark). The profiles were recorded with the Software Sensor Trace Suite (Unisense, Denmark) using a manual micromanipulator. For dissolved $O_2$, a two-point calibration was performed in fully air-saturated and anoxic Norsminde Fjord water and triplicate measurements were performed in the sediment cores with a spatial resolution of 200 μm. Vertical profiles of dissolved sulphide and pH were recorded with a spatial resolution of 500 μm. The analytical error was calculated as standard deviation of triplicate measurements in a single core.

Microsensor measurements for $Fe^{2+}$, $O_2$ and $H_2S$ were performed directly after the preparation of the artificial sediment cores, as well as after 3 and 7 days of incubation. pH profiles were collected only after 7 days of incubation. DCMU amended sediment cores were additionally measured after 17 days.

Profiles of scalar irradiance were recorded with lab-constructed light sensors (Kühl & Jørgensen, 1992) connected to a spectrometer (USB4000-XR1-ES, Ocean Optics, Germany) with the software SpectraSuite (Ocean Optics, Germany) with a spatial resolution of 200 μm. For the measurements, the sediment cores were illuminated with a halogen cold-light source (Euromex EK-1, Netherlands). The recorded scalar irradiance was normalized to the irradiance measured at the sediment surface.

## Visual detection of cable bacteria

In order to detect the presence of cable bacteria, sediment was removed from the sediment cores after 7 days of incubation and diluted with MilliQ water on a glass slide. With the help of a small glass hook, cable bacteria were pulled out of the sediment and could visually be seen as shiny string under a binocular microscope. Additionally, an elevated pH in oxic sediment layers as well as an orange layer of potentially Fe (oxyhydr)oxides in some millimeters depth were

used as proxies for the presence of cable bacteria as those indicators usually form as a consequence of cable bacterial activity. Photos of the light and dark incubated sediment cores were taken after 7 days of incubation and linked to the geochemical data and the presence or absence of cable bacteria.

## 5.4 Results and Discussion

**Impact of light on sedimentary geochemistry**

After incubation of the artificial sediment cores for 3 days, $Fe^{2+}$ concentration in 30 mm depth decreased from 470 µM directly one hour after preparation to 140 µM and 90 µM in the dark and light incubated sediment core respectively (Figures 5.1A & 5.1B). Within the upper 2 mm of the illuminated sediment core, $Fe^{2+}$ concentrations were below 10 µM, which is in strong contrast to $Fe^{2+}$ concentrations measured in the dark incubated sediment core in these depths (80 – 110 µM). This can partly be explained by $O_2$ supersaturation measured in the water column and sediment pore water of the illuminated setup, presumably produced by oxygenic photosynthesis, of up to 640 µM $O_2$ in 2 mm depth (Figure 5.1B) and consequently fast $Fe^{2+}$ oxidation rates (Millero et al., 1987). In comparison, the water column of the dark incubated sediment core was slightly undersaturated with respect to $O_2$ despite continuous aeration indicating high $O_2$ consuming processes in the water column and therefore, $O_2$ penetrated only 2 mm into the sediment (Figure 5.1B). After 7 days of incubation, no $Fe^{2+}$ concentrations higher than 30 µM could be measured in the light incubated core over the whole measurement depth whereas $Fe^{2+}$ concentrations in the dark setup were between 100 µM directly at the sediment surface and 150 µM in 30 mm depth (Figure 5.1C). The low $Fe^{2+}$ concentrations of the light incubated sediment core cannot solely be explained by oxidation by $O_2$ as the $O_2$ penetration depth was only 6 mm (Figure 5.1C). Also, processes induced directly by light cannot be immediately responsible for the observed overall decrease of $Fe^{2+}$ in the illuminated setup as light penetration into the sediment was only approx. 2.2 mm (Figure 5.2). pH measurements in the sediment cores after 7 days of incubation revealed a peak of up to pH 10 in the upper millimeters of the light incubated sediment core, which was not observed in the dark setup (Figure 5.1D). This pH peak can be an indication for the presence and activity of cable bacteria as the reduction of $O_2$ resulting from the electron transfer from deeper sediment layers leads to a consumption of protons (eq. 5.1) (Nielsen et al., 2010; Pfeffer et al., 2012; Meysman et al., 2015). However, also other proton producing or consuming processes such as photosynthesis or respiratory processes can cause changes in pH (Revsbech et al., 1983). Anoxygenic and

oxygenic photosynthesis lead to higher pH values due to $CO_2$ fixation and concomitant removal from the sediment pore water (Kühl et al., 1995). The observed pH peak might thus represent a cumulative result of high photosynthetic and cable bacteria activity.



**Figure 5.1** Concentration profiles in lab-incubated sediment cores. A) $Fe^{2+}$ 1 hour after preparation of the sediment core; B) $Fe^{2+}$ and $O_2$ after 3 days in light and dark incubation; C) $Fe^{2+}$ and $O_2$ after 7 days in light and dark incubation; D) pH after 7 days in light and dark incubation. Error bars show the standard deviation of the voltammograms ($Fe^{2+}$) or triplicate measurements ($O_2$, pH) recorded in one sediment core.
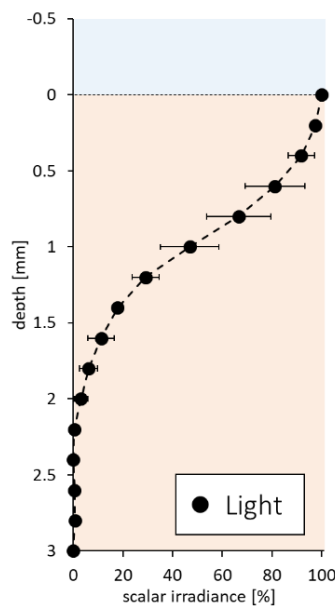


**Figure 5.2** Profile of light intensity expressed as scalar irradiance, normalized to the light intensity reaching the sediment surface. Error bars show the standard deviation of 5 scalar irradiance profiles.

In order to test the response of $Fe^{2+}$ concentrations in the sediment pore water upon changing illumination conditions, another set of sediment cores were placed for 7 days in the light, followed by 3 days of incubation in dark and one day. After 3 days of illumination, generally decreasing $Fe^{2+}$ concentrations were measured. However, also a peak of 80 µM $Fe^{2+}$ in the upper 2-3 mm of the sediment were observed (Figures 5.3A & 5.3B). $Fe^{2+}$ in those light illuminated sediment layers presumably was produced by Fe(III) photoreduction (Lueder et al., 2019a; Lueder et al., 2019b). The presence of Fe(III)-organic complexes, which are a pre-requisite for Fe(III) photoreduction was voltammetrically confirmed. After 7 days in light, $Fe^{2+}$ was below detection limit at all depths (Figure 5.3C). Back in darkness for 3 days, $Fe^{2+}$ built up from 100 µM at the sediment surface to 400 µM in 30 mm depth (Figure 5.3D). After the sediment core was placed back in light, $Fe^{2+}$ was removed from the sediment pore water after one day (Figure 5.3E). Light is triggering rapid $O_2$ production via oxygenic photosynthesis. Therefore, $O_2$ concentrations in the overlying water column changed from supersaturation after 7 days of light incubation (Figure 5.3C) to undersaturation after the 3 days of incubation in dark (Figure 5.3D) and back to slight supersaturation after one day of illumination (Figure 5.3E) with concomitant changes in the sediment $O_2$ penetration depth. Faster $Fe^{2+}$ oxidation rates can explain the decrease of $Fe^{2+}$ in the upper millimeters of the sediment, however, $O_2$ was not penetrating deeper than 4 mm and therefore, the increased $O_2$ concentrations cannot solely explain the overall $Fe^{2+}$ concentration decrease in up to 30 mm depth.
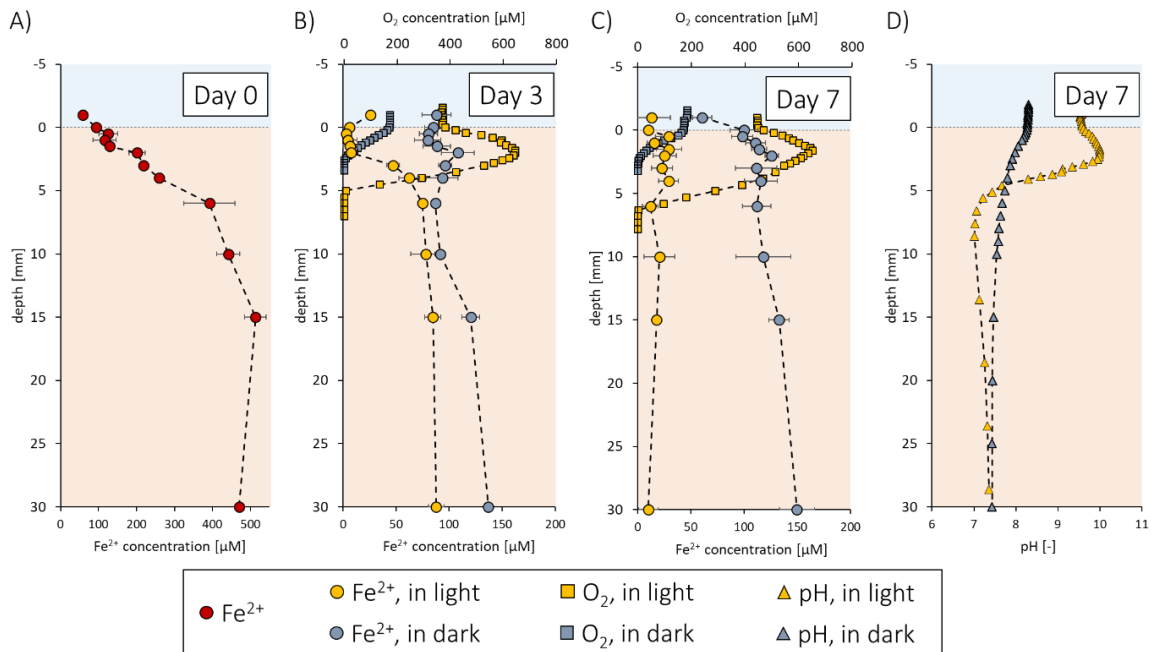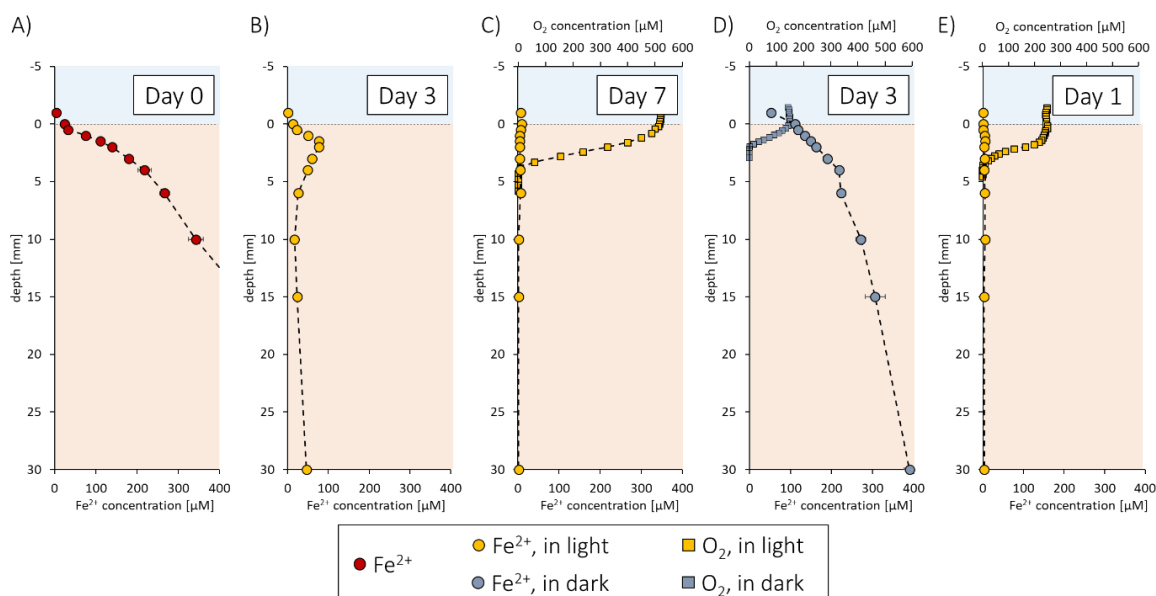


**Figure 5.3** Concentration profiles in lab-incubated sediment cores. A) $Fe^{2+}$ 1 hour after preparation of the sediment core; B) $Fe^{2+}$ after 3 days in light incubation; C) $Fe^{2+}$ and $O_2$ after 7 days in light incubation; D) $Fe^{2+}$ and $O_2$ after 3 days in subsequent dark incubation; E) $Fe^{2+}$ and $O_2$ after 1 day back in light incubation. Error bars show the standard deviation of the voltammograms ($Fe^{2+}$) or triplicate measurements ($O_2$) recorded in one sediment core.

Light seems to control the $Fe^{2+}$ distribution in the incubated sediment cores. One possibility is that light is responsible for the observed $Fe^{2+}$ decrease in up to 30 mm depth. For that, light conducting processes or structures like optical fibers in the sediment would be necessary to bring the light photons into deeper sediment layers, where they could be used for metabolic or chemical processes. Optical fibers consist of two parts. The inner core has a higher refraction index than the surrounding layer. If the incidence angle of the light ray exceeds the critical angle, total internal reflection of the light photons occurs at the interface of the materials and by that, the photons are conducted along the optical fiber. So far, such light conducting structures are not known in sediments. If such light-conducting structures exist, light energy could be used e.g. by phototrophic Fe(II)-oxidizers in sediment depths, where light would usually not occur. The metabolic activity of those bacteria in deeper sediment layers could explain the $Fe^{2+}$ removal over the whole measurement depth and also why phototrophic Fe(II)-oxidizers were found homogenously distributed in marine sediments and decoupled from geochemical gradients (Otte et al., 2018b).

**Potential impact of light on cable bacteria population**

Apart from the impact of light on the sedimentary geochemistry, a potential link between light illumination and growth of cable bacteria was speculated. Besides the measured pH peak in the light incubated sediment cores after 7 days (Figure 5.1D), the formation of an orange layer in the upper part of the sediment could be observed, which did not form in the dark setup (Figures 5.4A & 5.4B). Additionally, cable bacteria could be pulled out manually from the light, but not from the dark incubated sediment and visually be seen under the binocular microscope (Figures 5.4C & 5.4D).
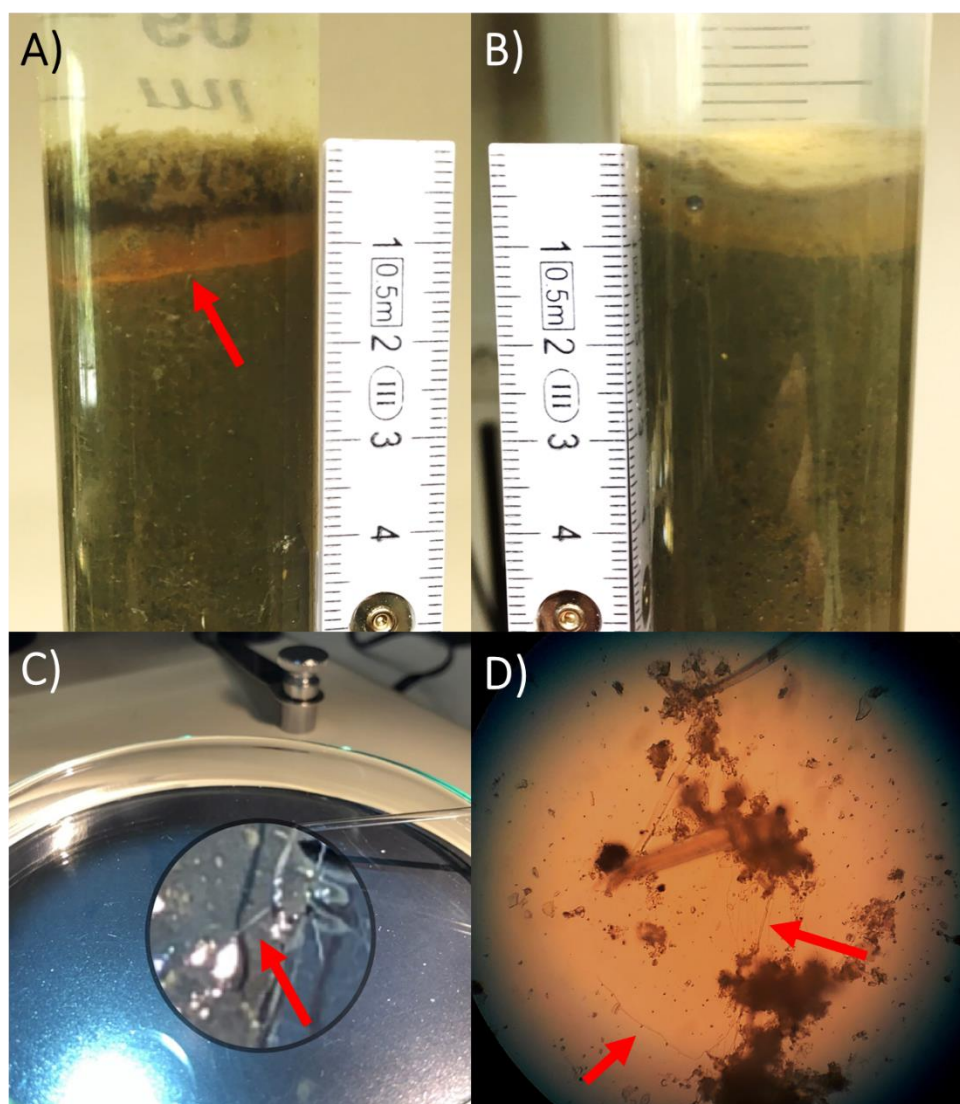
**Figure 5.4** A), B) Images of a sediment core after 7 days in light (A) and dark (B) incubation. The red arrow highlights an orange layer (presumably Fe (oxyhydr)oxides) indicative for cable bacteria activity; C) Image of manual picking of cable bacteria from a light incubated sediment core after 7 days. The red arrow highlights a single cable bacteria fiber; D) Cable bacteria under a binocular microscope; the red arrows highlight cable bacteria fibers.

The obvious presence and growth of cable bacteria in the light setup could be triggered by the supersaturation of $O_2$ caused by oxygenic photosynthesis. As cable bacteria need $O_2$ (or nitrate) as electron acceptor (Pfeffer et al., 2012; Marzocchi et al., 2014), the excess of $O_2$ in the light setup could enable faster growth of cable bacteria. Malkin and Meysman (2015) found rapid decreasing concentrations of pore water sulphide upon irradiation as a result of stimulated photosynthesis and in the time scale of days, the suboxic zone expanded and got more acidic. This was linked to the fact that greater $O_2$ supply enables cable bacteria to harvest more

electrons from the sediment. In order to exclude $O_2$ supersaturation as reason for the fast growth of cable bacteria in light, DCMU was added to the overlying water column and upper sediment layers to suppress oxygenic photosynthesis (Hoch et al., 1963). In both, light and dark setup, no $O_2$ supersaturation of the water column was observed and $O_2$ penetration was approx. 2 mm into the sediment during the incubation (data not shown). No major differences in $Fe^{2+}$ concentrations were measured neither after 3, 7 or even 17 days (Figure 5.5). Also, no pH peak was measured after 7 days of incubation (Figure 5.5B), no indicative orange Fe (oxyhydr)oxide layer was observed and no cable bacteria could visually be found in the sediment cores. These results suggest that either DCMU is toxic for cable bacteria and or prevent them to grow. It cannot be excluded that the high abundance of cable bacteria in light incubated sediment cores is only due to supersaturation of $O_2$.



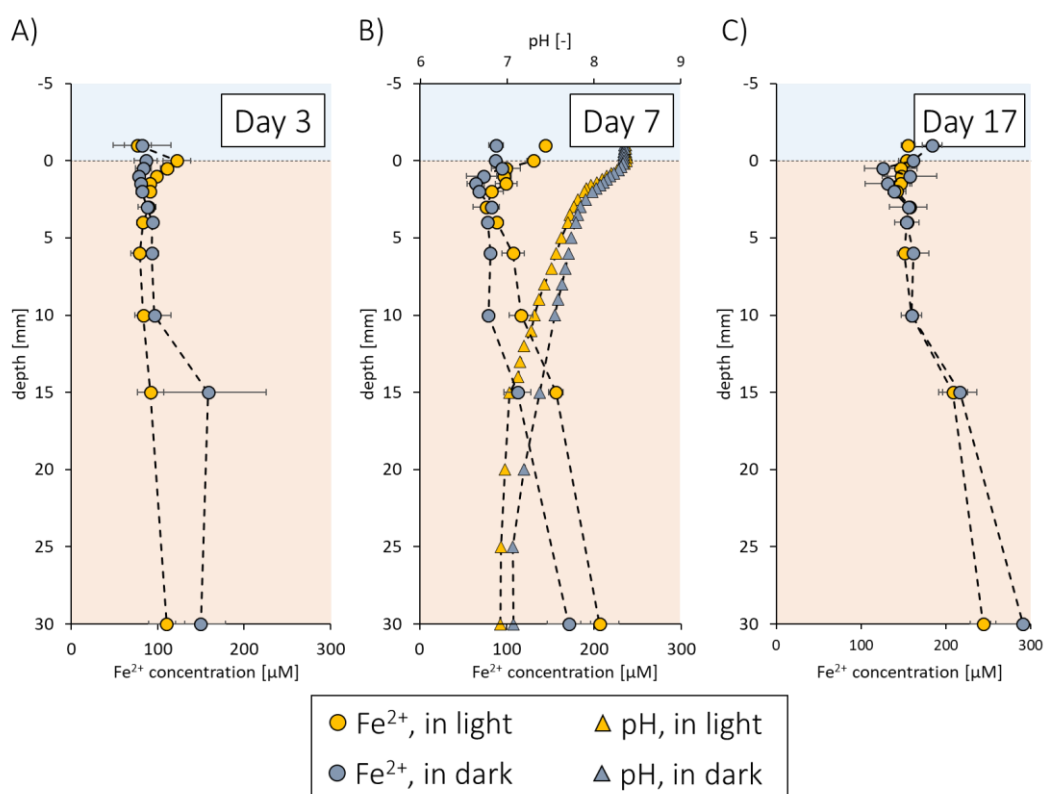**Figure 5.5** Concentration profiles in lab-incubated, DCMU-amended sediment cores. A) $Fe^{2+}$ after 3 days in light and dark incubation; B) $Fe^{2+}$ and pH profiles after 7 days of light and dark incubation; C) $Fe^{2+}$ profiles after 17 days in light and dark incubation. Error bars show the standard deviation of the voltammograms ($Fe^{2+}$) or triplicate measurements (pH) recorded in one sediment core.

$Fe^{2+}$ and $O_2$ concentration as well as pH profiles in gamma-sterilized sediment cores did not show clear differences between light and dark setups (Figure 5.6). Therefore, the observed $Fe^{2+}$ depletion in natural sediment cores can be caused by microbial processes. However, it must be kept in mind that gamma radiation also changes geochemical parameters such as dissolved organic carbon concentrations (Otte et al., 2018a).
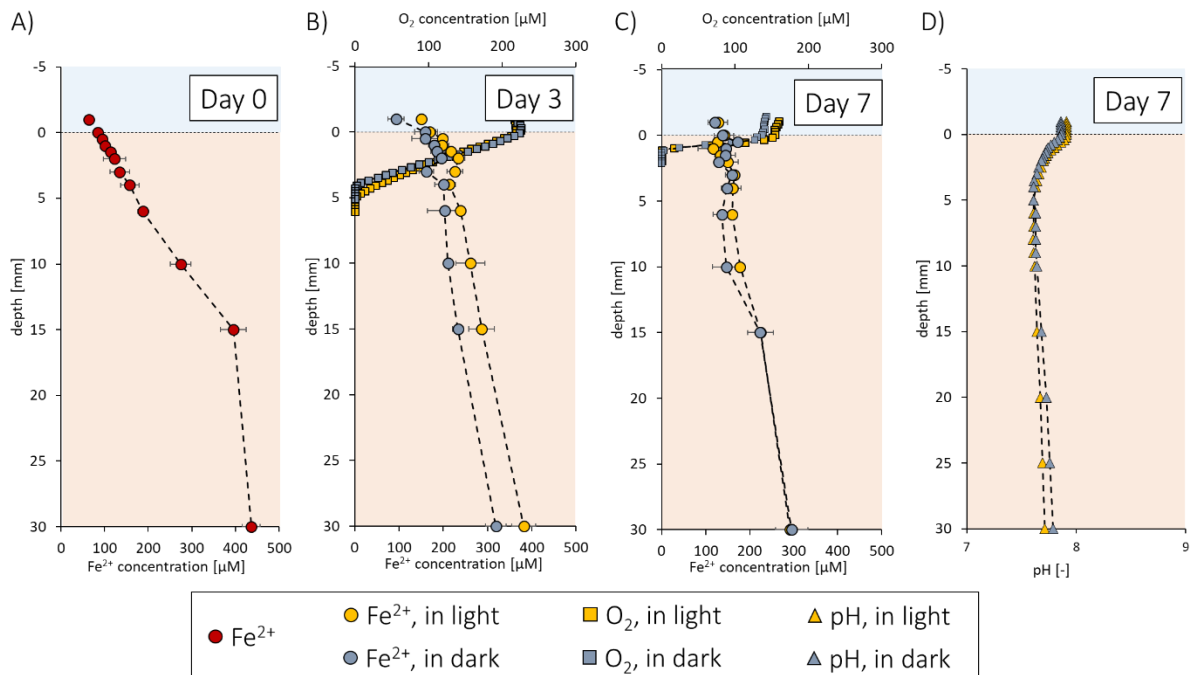


**Figure 5.6** Concentration profiles in lab-incubated, gamma-sterilized sediment cores. A) $Fe^{2+}$ one hour after preparation of the sediment core; B) $Fe^{2+}$ and $O_2$ after 3 days in light and dark incubation; C) $Fe^{2+}$ and $O_2$ after 7 days in light and dark incubation; D) pH after 7 days in light and dark incubation. Error bars show the standard deviation of the voltammograms ($Fe^{2+}$) or triplicate measurements ($O_2$, pH) recorded in one sediment core.

It is possible that cable bacteria are directly responsible for the $Fe^{2+}$ decrease by using $Fe^{2+}$ instead of dissolved sulphide as electron donor. From an energetic point of view, more metabolic energy can be obtained by sulphide oxidation than from Fe(II) oxidation coupled to $O_2$. Therefore, cable bacteria would potentially use first available dissolved sulphide before using $Fe^{2+}$. During incubation of the sediment, no dissolved sulphide was detected. It is therefore possible that $Fe^{2+}$ might be used as an alternative electron donor.

Cable bacteria might also not necessarily oxidize $Fe^{2+}$ themselves but interact with Fe(II)-oxidizing bacteria. Fe(II)-oxidizing bacteria could donate electrons, e.g. via nanowires, to cable bacteria that conduct them to electron acceptors such as $O_2$. By that, Fe(II)-oxidizing bacteria would only need the electron donor $Fe^{2+}$ in their close proximity but not the electron

acceptor and could therefore oxidize Fe(II) in these depths. Reguera (2018) found that cable bacteria are often surrounded by swarming bacteria, whose identity and function are not known so far, so it is possible that some of those bacteria are Fe(II)-oxidizing bacteria interacting with the cable bacteria as hypothesized by Otte et al. (2018b). Vasquez-Cardenas et al. (2015) suggested a tight coupling between chemolithoautotrophic sulphur-oxidizing bacteria and cable bacteria in the suboxic and anoxic zone of sediments. They indicated that the chemolithoautotrophs might transfer electrons via nanowires or nanotubes to the cable bacteria and use them as electron sink.

So far, it could not be shown that cable bacteria are capable to grow phototrophically but get their energy from redox reactions (i.e. sulphide oxidation coupled to $O_2$ or nitrate reduction). However, the high abundance of cable bacteria in light incubated sediment cores raise the question if cable bacteria can additionally use light energy for their metabolism.

## Implications and suggestions for further experiments

Assuming cable bacteria are able to not only oxidize sulphide but also being able to switch and use ferrous iron as electron donor instead, this would have tremendous implications on the $Fe^{2+}$ distribution in sediments. Due to the higher energy yield of the oxidation by $O_2$, dissolved sulphide would presumably be used first by cable bacteria but when freely dissolved sulphide is depleted or trapped as Fe-S-minerals such as pyrite, $Fe^{2+}$ could be the alternative electron donor. By oxidizing $Fe^{2+}$, competition to other Fe(II)-oxidizing bacteria occurring in the sediment would increase. In deeper, anoxic sediment layers, where Fe(III) reduction usually dominates (Schmidt et al., 2010), an additional Fe(II)-oxidizing process besides so far known biotic and abiotic processes would be added to the sedimentary Fe cycling.

If Fe-metabolizing bacteria could use cable bacteria as conducting cables for electron transport, as hypothesized by Otte et al. (2018b), those bacteria would not be restricted to areas where both, electron acceptor and donor occur simultaneously but could also live in places, where only one of them is present and decouple the presence of those bacteria from geochemical gradients in sediments (Otte et al., 2018b). Assuming that light energy can directly be used by cable bacteria as energy source, illumination would tremendously enhance their growth, what would support the observations made in this study. By that, the suboxic zone formed by cable bacteria would form faster.

In order to decipher, if cable bacteria can i) oxidize $Fe^{2+}$ and/or ii) use directly light energy for their growth, further experiments are necessary. By frequently cutting (e.g. daily) the sediment cores with a wire or string at the right position, cable bacteria are divided and the conduction of electrons is interrupted (Pfeffer et al., 2012). By that, potential $Fe^{2+}$ oxidation by cable bacteria should be stopped and $Fe^{2+}$ would not further be depleted in the sediment pore water. By running sediment core incubations with different light intensities coupled to $Fe^{2+}$ microelectrode measurements and determination of the abundance of cable bacteria using FISH-analysis (Schauer et al., 2014; Sulu-Gambari et al., 2016), abundance of cable bacteria could be linked to light intensity and potentially $Fe^{2+}$ oxidation rates. However, different light intensities would also imply different rates of oxygenic photosynthesis and consequently different $O_2$ concentrations and penetration depths. Therefore, oxygenic photosynthesis must be suppressed by different substances than DCMU as no growth of cable bacteria was observed in DCMU amended sediment cores.

## 5.5 References

Blankenship, R. E. and Hartman, H. (1998). The origin and evolution of oxygenic photosynthesis. *Trends in Biochemical Sciences*, **23**(3), 94-97.

Brendel, P. J. and Luther III, G. W. (1995). Development of a gold amalgam voltammetric microelectrode for the determination of dissolved Fe, Mn, $O_2$, and S(-II) in porewaters of marine and freshwater sediments. *Environmental Science & Technology*, **29**(3), 751-761.

Bristow, G. and Taillefert, M. (2008). VOLTINT: A Matlab®-based program for semi-automated processing of geochemical data acquired by voltammetry. *Computers & Geosciences*, **34**(2), 153-162.

Bryce, C., Blackwell, N., Schmidt, C., Otte, J., Huang, Y.-M., Kleindienst, S., Tomaszewski, E., Schad, M., Warter, V., Peng, C., Byrne, J. M. and Kappler, A. (2018). Microbial anaerobic Fe(II) oxidation – Ecology, mechanisms and environmental implications. *Environmental Microbiology*, **20**(10), 3462-3483.

Burdorf, L. D. W., Hidalgo-Martinez, S., Cook, P. L. M. and Meysman, F. J. R. (2016). Long-distance electron transport by cable bacteria in mangrove sediments. *Marine Ecology Progress Series*, **545**, 1-8.

Burdorf, L. D. W., Tramper, A., Seitaj, D., Meire, L., Hidalgo-Martinez, S., Zetsche, E. M., Boschker, H. T. S. and Meysman, F. J. R. (2017). Long-distance electron transport occurs globally in marine sediments. *Biogeosciences*, **14**(3), 683-701.

Canfield, D. E. (1989). Reactive iron in marine sediments. *Geochimica et Cosmochimica Acta*, **53**(3), 619-632.

Damgaard, L. R., Risgaard-Petersen, N. and Nielsen, L. P. (2014). Electric potential microelectrode for studies of electrobiogeophysics. *Journal of Geophysical Research: Biogeosciences*, **119**(9), 1906-1917.

Hermans, M., Lenstra, W. K., Hidalgo-Martinez, S., van Helmond, N. A. G. M., Witbaard, R., Meysman, F. J. R., Gonzalez, S. and Slomp, C. P. (2019). Abundance and biogeochemical impact of cable bacteria in Baltic Sea sediments. *Environmental Science & Technology*, **53**(13), 7494-7503.

Hoch, G., Owens, O. v. H. and Kok, B. (1963). Photosynthesis and respiration. *Archives of Biochemistry and Biophysics*, **101**(1), 171-180.

Jørgensen, B. B. (1977). The sulfur cycle of a coastal marine sediment (Limfjorden, Denmark). *Limnology and Oceanography*, **22**(5), 814-832.

Jørgensen, B. B. (1982). Mineralization of organic matter in the sea bed—the role of sulphate reduction. *Nature*, **296**(5858), 643-645.

Jørgensen, B. B. and Revsbech, N. P. (1985). Diffusive boundary layers and the oxygen uptake of sediments and detritus. *Limnology and Oceanography*, **30**(1), 111-122.

Kashefi, K., Tor, J. M., Holmes, D. E., Gaw Van Praagh, C. V., Reysenbach, A.-L. and Lovley, D. R. (2002). Geoglobus ahangari gen. nov., sp. nov., a novel hyperthermophilic archaeon capable of oxidizing organic acids and growing autotrophically on hydrogen with Fe(III) serving as the sole electron acceptor. *International Journal of Systematic and Evolutionary Microbiology*, **52**(3), 719-728.

Kühl, M., Cohen, Y., Dalsgaard, T., Jørgensen, B. B. and Revsbech, N. P. (1995). Microenvironment and photosynthesis of zooxanthellae in scleractinian corals studied with microsensors for $O_2$, pH and light. *Marine Ecology Progress Series*, **117**(1/3), 159-172.

Kühl, M. and Jørgensen, B. B. (1992). Spectral light measurements in microbenthic phototrophic communities with a fiber-optic microprobe coupled to a sensitive diode array detector. *Limnology and Oceanography*, **37**(8), 1813-1823.

Larsen, H. (1952). On the culture and general physiology of the green sulfur bacteria. *Journal of Bacteriology*, **64**(2), 187-196.

Larsen, S., Nielsen, L. P. and Schramm, A. (2015). Cable bacteria associated with long-distance electron transport in New England salt marsh sediment. *Environmental Microbiology Reports*, **7**(2), 175-179.

Laufer, K., Nordhoff, M., Røy, H., Schmidt, C., Behrens, S., Jørgensen, B. B. and Kappler, A. (2016). Coexistence of microaerophilic, nitrate-reducing, and phototrophic Fe(II) oxidizers and Fe(III) reducers in coastal marine sediment. *Applied and Environmental Microbiology*, **82**(5), 1433-1447.

Lovley, D. R. (1991). Dissimilatory Fe(III) and Mn(IV) reduction. *Microbiological Reviews*, **55**(2), 259-287.

Lovley, D. R. and Phillips, E. J. P. (1988). Novel mode of microbial energy metabolism: organic carbon oxidation coupled to dissimilatory reduction of iron or manganese. *Applied and Environmental Microbiology*, **54**(6), 1472-1480.

Lueder, U., Jørgensen, B. B., Kappler, A. and Schmidt, C. (2019a). Fe(III) photoreduction producing $Fe^{2+}_{aq}$ in oxic freshwater sediment. *submitted*.

Lueder, U., Maisch, M., Laufer, K., Jørgensen, B. B., Kappler, A. and Schmidt, C. (2019b). Influence of physical perturbation on Fe(II) supply in coastal marine sediments. *submitted*.

Malkin, S. Y. and Meysman, F. J. R. (2015). Rapid redox signal transmission by "Cable Bacteria" beneath a photosynthetic biofilm. *Applied and Environmental Microbiology*, **81**(3), 948-956.

Marzocchi, U., Trojan, D., Larsen, S., Louise Meyer, R., Peter Revsbech, N., Schramm, A., Peter Nielsen, L. and Risgaard-Petersen, N. (2014). Electric coupling between distant nitrate reduction and sulfide oxidation in marine sediment. *The Isme Journal*, **8**, 1682.

McAllister, S. M., Moore, R. M., Gartman, A., Luther, G. W., III, Emerson, D. and Chan, C. S. (2019). The Fe(II)-oxidizing Zetaproteobacteria: Historical, ecological, and genomic perspectives. *FEMS Microbiology Ecology*.

Melton, E. D., Swanner, E. D., Behrens, S., Schmidt, C. and Kappler, A. (2014). The interplay of microbially mediated and abiotic reactions in the biogeochemical Fe cycle. *Nat Rev Micro*, **12**(12), 797-808.

Meysman, F. J. R., Cornelissen, R., Trashin, S., Bonné, R., Martinez, S. H., van der Veen, J., Blom, C. J., Karman, C., Hou, J.-L., Eachambadi, R. T., Geelhoed, J. S., Wael, K. D., Beaumont, H. J. E., Cleuren, B., Valcke, R., van der Zant, H. S. J., Boschker, H. T. S. and Manca, J. V. (2019). A highly conductive fibre network enables centimetre-scale electron transport in multicellular cable

bacteria. *Nature Communications*, **10**(1), 4120.

Meysman, F. J. R., Risgaard-Petersen, N., Malkin, S. Y. and Nielsen, L. P. (2015). The geochemical fingerprint of microbial long-distance electron transport in the seafloor. *Geochimica et Cosmochimica Acta*, **152**, 122-142.

Millero, F. J., Sotolongo, S. and Izaguirre, M. (1987). The oxidation kinetics of Fe(II) in seawater. *Geochimica et Cosmochimica Acta*, **51**(4), 793-801.

Müller, H., Bosch, J., Griebler, C., Damgaard, L. R., Nielsen, L. P., Lueders, T. and Meckenstock, R. U. (2016). Long-distance electron transfer by cable bacteria in aquifer sediments. *The Isme Journal*, **10**, 2010.

Nielsen, Lars P. (2016). Ecology: Electrical cable bacteria save marine life. *Current Biology*, **26**(1), R32-R33.

Nielsen, L. P., Risgaard-Petersen, N., Fossing, H., Christensen, P. B. and Sayama, M. (2010). Electric currents couple spatially separated biogeochemical processes in marine sediment. *Nature*, **463**, 1071.

Otte, J. M., Blackwell, N., Soos, V., Rughöft, S., Maisch, M., Kappler, A., Kleindienst, S. and Schmidt, C. (2018a). Sterilization impacts on marine sediment---Are we able to inactivate microorganisms in environmental samples? *FEMS Microbiology Ecology*, **94**(12), fiy189-fiy189.

Otte, J. M., Harter, J., Laufer, K., Blackwell, N., Straub, D., Kappler, A. and Kleindienst, S. (2018b). The distribution of active iron-cycling bacteria in marine and freshwater sediments is decoupled from geochemical gradients. *Environmental Microbiology*, **20**(7), 2483-2499.

Pfeffer, C., Larsen, S., Song, J., Dong, M., Besenbacher, F., Meyer, R. L., Kjeldsen, K. U., Schreiber, L., Gorby, Y. A., El-Naggar, M. Y., Leung, K. M., Schramm, A., Risgaard-Petersen, N. and Nielsen, L. P. (2012). Filamentous bacteria transport electrons over centimetre distances. *Nature*, **491**, 218.

Pyzik, A. J. and Sommer, S. E. (1981). Sedimentary iron monosulfides: Kinetics and mechanism of formation. *Geochimica et Cosmochimica Acta*, **45**(5), 687-698.

Rao, A. M. F., Malkin, S. Y., Hidalgo-Martinez, S. and Meysman, F. J. R. (2016). The impact of electrogenic sulfide oxidation on elemental cycling and solute fluxes in coastal sediment. *Geochimica et Cosmochimica Acta*, **172**, 265-286.

Reguera, G. (2018). Biological electron transport goes the extra mile. *Proceedings of the National Academy of Sciences*, **115**(22), 5632-5634.

Revsbech, N. P., Jørgensen, B. B., Blackburn, T. H. and Cohen, Y. (1983). Microelectrode studies of the photosynthesis and $O_2$, $H_2S$, and pH profiles of a microbial mat. *Limnology and Oceanography*, **28**(6), 1062-1074.

Revsbech, N. P., Sorensen, J., Blackburn, T. H. and Lomholt, J. P. (1980). Distribution of oxygen in marine sediments measured with microelectrodes1. *Limnology and Oceanography*, **25**(3), 403-411.

Risgaard-Petersen, N., Damgaard, L. R., Revil, A. and Nielsen, L. P. (2014). Mapping electron sources and sinks in a marine biogeobattery. *Journal of Geophysical Research: Biogeosciences*, **119**(8), 1475-1486.

Risgaard-Petersen, N., Kristiansen, M., Frederiksen, R. B., Dittmer, A. L., Bjerg, J. T., Trojan, D., Schreiber, L.,

Damgaard, L. R., Schramm, A. and Nielsen, L. P. (2015). Cable bacteria in freshwater sediments. *Applied and Environmental Microbiology*, **81**(17), 6003-6011.

Risgaard-Petersen, N., Revil, A., Meister, P. and Nielsen, L. P. (2012). Sulfur, iron-, and calcium cycling associated with natural electric currents running through marine sediment. *Geochimica et Cosmochimica Acta*, **92**, 1-13.

Schauer, R., Risgaard-Petersen, N., Kjeldsen, K. U., Tataru Bjerg, J. J., B Jørgensen, B., Schramm, A. and Nielsen, L. P. (2014). Succession of cable bacteria and electric currents in marine sediment. *The Isme Journal*, **8**, 1314.

Schmidt, C., Behrens, S. and Kappler, A. (2010). Ecosystem functioning from a geomicrobiological perspective a conceptual framework for biogeochemical iron cycling. *Environmental Chemistry*, **7**(5), 399-405.

Scholz, V. V., Müller, H., Koren, K., Nielsen, L. P. and Meckenstock, R. U. (2019). The rhizosphere of aquatic plants is a habitat for cable bacteria. *FEMS Microbiology Ecology*, **95**(6).

Seitaj, D., Schauer, R., Sulu-Gambari, F., Hidalgo-Martinez, S., Malkin, S. Y., Burdorf, L. D. W., Slomp, C. P. and Meysman, F. J. R. (2015). Cable bacteria generate a firewall against euxinia in seasonally hypoxic basins. *Proceedings of the National Academy of Sciences*, **112**(43), 13278-13283.

Slowey, A. and Marvin-DiPasquale, M. (2012). How to overcome inter-electrode variability and instability to quantify dissolved oxygen, Fe(II), Mn(II), and S(II) in undisturbed soils and sediments using voltammetry. *Geochemical Transactions*, **13**(1), 6.

Sulu-Gambari, F., Seitaj, D., Meysman, F. J. R., Schauer, R., Polerecky, L. and Slomp, C. P. (2016). Cable bacteria control iron–phosphorus dynamics in sediments of a coastal hypoxic basin. *Environmental Science & Technology*, **50**(3), 1227-1233.

Sulzberger, B., Suter, D., Siffert, C., Banwart, S. and Stumm, W. (1989). Dissolution of Fe(III)(hydr)oxides in natural waters; laboratory assessment on the kinetics controlled by surface coordination. *Marine Chemistry*, **28**(1), 127-144.

Trojan, D., Schreiber, L., Bjerg, J. T., Bøggild, A., Yang, T., Kjeldsen, K. U. and Schramm, A. (2016). A taxonomic framework for cable bacteria and proposal of the candidate genera Electrothrix and Electronema. *Systematic and Applied Microbiology*, **39**(5), 297-306.

Vasquez-Cardenas, D., van de Vossenberg, J., Polerecky, L., Malkin, S. Y., Schauer, R., Hidalgo-Martinez, S., Confurius, V., Middelburg, J. J., Meysman, F. J. R. and Boschker, H. T. S. (2015). Microbial carbon metabolism associated with electrogenic sulphur oxidation in coastal sediments. *The Isme Journal*, **9**, 1966.

Widdel, F., Schnell, S., Heising, S., Ehrenreich, A., Assmus, B. and Schink, B. (1993). Ferrous iron oxidation by anoxygenic phototrophic bacteria. *Nature*, **362**(6423), 834-836.

# Chapter 6: General conclusions and outlook

Light plays an important role in the environment. By providing energy, it drives many biogeochemical processes, such as oxygenic photosynthesis (van Grondelle et al., 1994) or degradation of organic carbon (Farjalla et al., 2009), especially in terrestrial and aquatic habitats. However, although being partly attenuated in atmosphere and water columns (Horvath, 1993; Piazena et al., 2002), light has also directly or indirectly tremendous consequences for processes, element cycles and microorganisms in sediments. For instance, light is the energy source for anoxygenic photosynthesis (Larsen, 1952; Widdel et al., 1993; Yurkov & Beatty, 1998; Bryce et al., 2018), that was not only suggested to be an important metabolism on ancient Earth (Canfield et al., 2006), but anoxygenic phototrophic microorganisms are still present today in many (anoxic) environments such as sediments (Laufer et al., 2016). Here, they are part of biogeochemical element cycles of iron and sulphur. Light also impacts particulate organic matter (POM; $0.053mm < POM < 2mm$), which can be converted to lower molecular weight compounds and dissolved in the water body upon light absorption of specific wavelengths (Mayer et al., 2006; Riggsbee et al., 2008). By this, dissolved organic carbon (DOC) and other nutrients such as nitrate or phosphate are concomitantly released and provided to the sediment pore water (Southwell et al., 2011). This has tremendous consequences for the bioavailability of nutrients for the inhabiting organisms. During the photochemical degradation of DOC, reactive oxygen species (ROS) are formed that themselves are key oxidants in many environmental habitats and due to their high reactivity, they impact many element cycles (Voelker et al., 2000; Garg et al., 2011; Page et al., 2014; Hansel et al., 2015). Via Fe(III) photoreduction, light also provides Fe(II) as nutrient for e.g. phytoplankton in the ocean (Barbeau et al., 2001) or potentially as substrate for growth for Fe(II)-oxidizing bacteria.

The goal of this PhD was to identify how light and physical perturbation influence the $Fe^{2+}$ availability in sediments by acting as hidden Fe(II) sources and sinks. Both parameters, i.e. light and physical perturbation, are important in sediments, as they constantly change the prevalent physico-chemical conditions. In order to achieve the objectives of this PhD, the consequences of sedimentary Fe(III) photoreduction as Fe(II) source were demonstrated. Moreover, the impact of light on the growth of cable bacteria including their potential use of $Fe^{2+}$ as alternative electron donor, thereby acting as Fe(II) sink were determined. Finally, the mechanisms of $Fe^{2+}$ mobilization upon physical perturbation and Fe(II) mineral formation in sediments were identified in order to determine the role of physical perturbation as Fe(II) source and sink.

A better understanding towards the controls of Fe(II) in sediments including so far overlooked processes is crucial in order to fully understand sedimentary Fe cycling comprising the complex interactions with other element cycles. By identifying and quantifying hidden sources and sinks of Fe(II), they can be implemented in the Fe cycle of freshwater and marine sediments and motivate to think about a revised view on the classical sedimentary Fe cycling of opposed gradients of Fe(II) and Fe(III).

## 6.1 The role of light in the sedimentary Fe cycling

Light is an important contributor of sedimentary Fe cycling – either directly by providing energy for phototrophic Fe(II)-oxidizing bacteria and by Fe(III) photoreduction or indirectly by photochemically producing species such as $O_2$ or ROS, that are able to oxidize or reduce Fe.

By providing energy for phototrophic Fe(II)-oxidizing bacteria, microbial Fe(II) oxidation in sediments is stimulated. Their habitat in sediments is theoretically restricted to sunlit but anoxic layers (Schmidt et al., 2010). At both selected field sites, phototrophic Fe(II)-oxidizing bacteria were found to be present at the lowest abundance amongst all Fe(II)-oxidizing bacteria (Otte et al., 2018). Nevertheless, they contribute to the overall Fe(II) oxidation in sediments. Light is also driving oxygenic photosynthesis in sediments which can lead to $O_2$ supersaturation in sediment pore water (Jørgensen et al., 1979). During oxygenic photosynthesis, $CO_2$ is fixed and removed from the pore water, which increases the pH (Kühl et al., 1995). As the rate of abiotic Fe(II) oxidation by $O_2$ is dependent on both, $O_2$ concentration and pH (eq. 6.1), oxygenic photosynthesis increases the rate of abiotic Fe(II) oxidation and leads by that to an accelerated removal of $Fe^{2+}$ in sediments.

$$- \frac{d[Fe^{2+}]}{dt} = k_0 \cdot [Fe^{2+}] \cdot [O_2] \cdot [OH^-]^2 \qquad (6.1)$$

with $k_0$ being the universal rate constant for homogeneous $Fe^{2+}$ oxidation, as well as the respective concentrations of $Fe^{2+}$, $O_2$ and $OH^-$, which can be calculated by $[OH^-] = 10^{-(14-pH)}$.

On the other hand, the process of Fe(III) photoreduction, which is induced by light energy, is a powerful $Fe^{2+}$ source in sunlit sediment layers, even at oxic conditions and leads to a peak in $Fe^{2+}$ concentration in the upper millimeters of sunlit sediment (Chapters **3** & **4**). By providing $Fe^{2+}$ concentrations that are in the same order of magnitude as $Fe^{2+}$ concentrations measured in the "classical" Fe(III) reduction zone, this additional and so far overlooked $Fe^{2+}$ source lead to changes in $Fe^{2+}$ concentration gradients in the sediment pore water. Besides an upward diffusion

from the Fe(III) reduction zone, photochemically produced $Fe^{2+}$ in the upper sediment layers potentially also diffuses downwards. The additional $Fe^{2+}$ can be used by Fe(II)-oxidizing bacteria. As Fe(III) photoreduction spatially produces $Fe^{2+}$ in sediment layers close to the sediment-water interface, $O_2$ is usually present as well. Therefore, the additional $Fe^{2+}$ might mainly be used as electron donor by microaerophilic Fe(II)-oxidizers that metabolically do not need to live in anoxic habitats. Despite completely different geochemical conditions, elevated $Fe^{2+}$ concentrations produced by Fe(III) photoreduction could be found in both, freshwater and marine sediment (Chapters **3** & **4**). The discovery of sedimentary Fe(III) photoreduction is however only a starting point for more open questions. Control factors of Fe(III) photoreduction in sediments still exactly need to be determined. Although the rate and extent of photoproduced $Fe^{2+}$ in water columns is directly related to the incident light intensity (Waite et al., 1995), similar amounts of $Fe^{2+}$ were produced in sediments at both, low (40 µmol photons $m^{-2}$ $s^{-1}$) and high light intensities (400-500 µmol photons $m^{-2}$ $s^{-1}$). Therefore, Fe(III) photoreduction does not seem to be a light limited process in sediments, however, the actual dependence of sedimentary Fe(III) photoreduction on light is still poorly understood. Photolysis of DOC leads to production of ROS (Scully et al., 2003), which can oxidize Fe(II) (eq. 1.1-1.4). However, superoxide is also able to reduce Fe(III) (Rose, 2012). Depending on the kind of ROS produced and/or the ratio of other ROS to superoxide, Fe(II) oxidation or Fe(III) reduction may be the dominating process. The exact contribution of superoxide to the overall photochemically produced $Fe^{2+}$ in sediments is not known. Although superoxide can be expected to be produced during photolysis of DOC in sediment pore water, it cannot be quantified in situ in sediments so far. In general, the ratio of ligand-to-metal charge transfer (LMCT) reactions to superoxide mediated Fe(III) photoreduction depends on the chemical composition of the present DOC (Barbeau, 2006). The availability and concentration of organic carbon, i.e. more precisely the organic carbon that can complex Fe(III) and that is susceptible to light, should directly control the extent of photochemically produced $Fe^{2+}$. If not sufficient DOC is present in sediments, no measurable $Fe^{2+}$ peak will appear in the upper sediment layers (Chapter **3**), presumably as the low amount of photochemically produced $Fe^{2+}$ is immediately re-oxidized, e.g. by $O_2$ or $H_2O_2$, which are the main oxidants of Fe(II) in seawater (Santana-Casiano et al., 2006). Theoretically, organic complexation is not a necessary prerequisite for Fe(III) photoreduction, however, photoreduction of inorganic Fe(III) or light-induced dissolution of Fe(III) minerals only occurs at acidic pH (Borer et al., 2009). As light is able to degrade POM to smaller weight compounds (Mayer et al., 2006; Riggsbee et al., 2008), DOC concentrations in the sediment pore water will increase upon illumination and, depending on the structure of the organic molecules, would

also increase the concentration of Fe(III)-organic complexes. This could enhance the extent of Fe(III) photoreduction. Finally, in order to predict concentrations of photochemically produced $Fe^{2+}$ in sedimentary pore waters, a better understanding of the control parameters, i.e. the exact dependence of Fe(III) photoreduction on light, DOC concentration, the kind of organic molecules present, inhabiting microbial community as well as geochemical parameters such as pH and $O_2$ concentration, need to be deciphered. However, we were able to show that Fe(III) photoreduction is an important and environmentally relevant $Fe^{2+}$ source that naturally takes place in sunlit freshwater and marine sediments if sufficient DOC is present, influencing Fe(II) substrate availability and fluxes. Light-driven processes influencing Fe(II) availability in sediments are summarized in Figure 6.1.
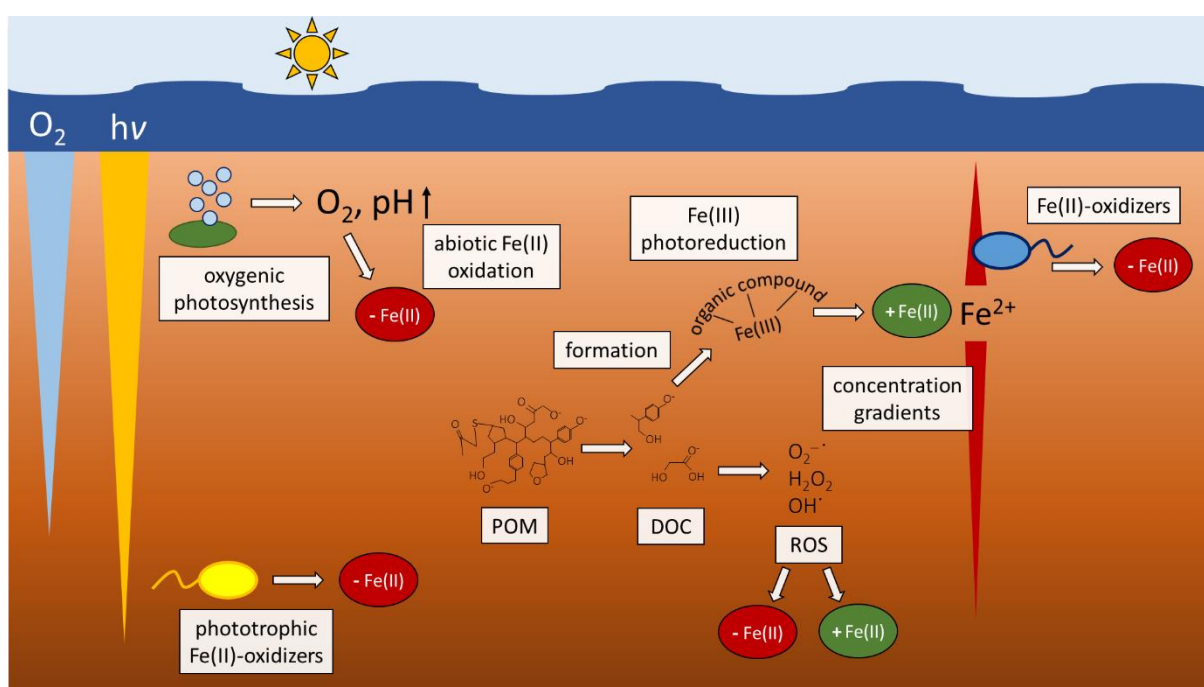


**Figure 6.1** Overview of light-driven processes in sediments including their consequences for Fe(II) availability. Oxygen ($O_2$) and light ($h\nu$) penetrate in different gradients into the sediment. Oxygenic photosynthesis releases $O_2$ into the pore water and increases the pH, which both lead to accelerated abiotic Fe(II) oxidation by $O_2$. Phototrophic Fe(II)-oxidizers use Fe(II) as electron donor. Fe(III) photoreduction produces dissolved Fe(II) ($Fe^{2+}$), which diffuses up- and downwards forming $Fe^{2+}$ concentration gradients. Formed $Fe^{2+}$ can be used as electron donors for Fe(II)-oxidizing bacteria. Particulate organic matter (POM) is photodegraded to smaller parts that form dissolved organic carbon (DOC), which might enhance Fe(III) photoreduction by the formation of Fe(III)-organic complexes. Reactive oxygen species (ROS; superoxide ($O_2^-$ ·), hydrogen peroxide ($H_2O_2$), hydroxyl radicals (OH·)) produced by photochemical reaction of DOC can either oxidize Fe(II) or reduce Fe(III).

It is possible that light might has influences on other microorganisms in the sediment besides anoxygenic phototrophic bacteria. For instance, if light conducting structures such as optical fibers would exist in sediments, light photons might reach deeper sediment layers than they normally would, and could there be used by phototrophic microorganisms. We were able to show that the abundance of cable bacteria was higher in light illuminated sediment cores than in sediment cores incubated in the dark (Chapter **5**). Therefore, we suggested that cable bacteria are able to use light directly as energy source for their metabolisms. Another explanation is that light creates suitable growth conditions for cable bacteria by triggering oxygenic photosynthesis in sediments leading to both, elevated $O_2$ concentrations and deeper $O_2$ penetration depth (Jørgensen et al., 1979). As $O_2$ is used as electron acceptor by cable bacteria (Pfeffer et al., 2012), the high $O_2$ concentrations could be responsible for the observed abundance of cable bacteria in light illuminated sediment. Concomitant to the high abundance of cable bacteria, a strong decrease of $Fe^{2+}$ concentrations in the sediment pore water was observed, which can indicate that $Fe^{2+}$ may be used as electron acceptor instead of sulphide by the cable bacteria. Although sulphide oxidation coupled to $O_2$ reduction is thermodynamically more favorable, cable bacteria could switch to $Fe^{2+}$ oxidation instead if dissolved sulphide is depleted. Also, cable bacteria are often surrounded by swarming bacteria (Reguera, 2018). Their identity and function is not deciphered yet, however, it was hypothesized that those bacteria might partially be Fe(II)-oxidizing bacteria that may transfer electrons to cable bacteria and use them as electron sink (Otte et al., 2018). By that, they would locally be decoupled from their electron acceptors such as $O_2$ and only need the proximity of their electron donors. An increased abundance of cable bacteria in light illuminated sediments could thereby also lead to increased Fe(II) oxidation rates. Therefore, cable bacteria might either directly or indirectly be connected to the microbial Fe cycle in sediments. Potential explanations for the observed high abundance of cable bacteria and concomitant low $Fe^{2+}$ concentrations in light illuminated sediment are illustrated in Figure 6.2.
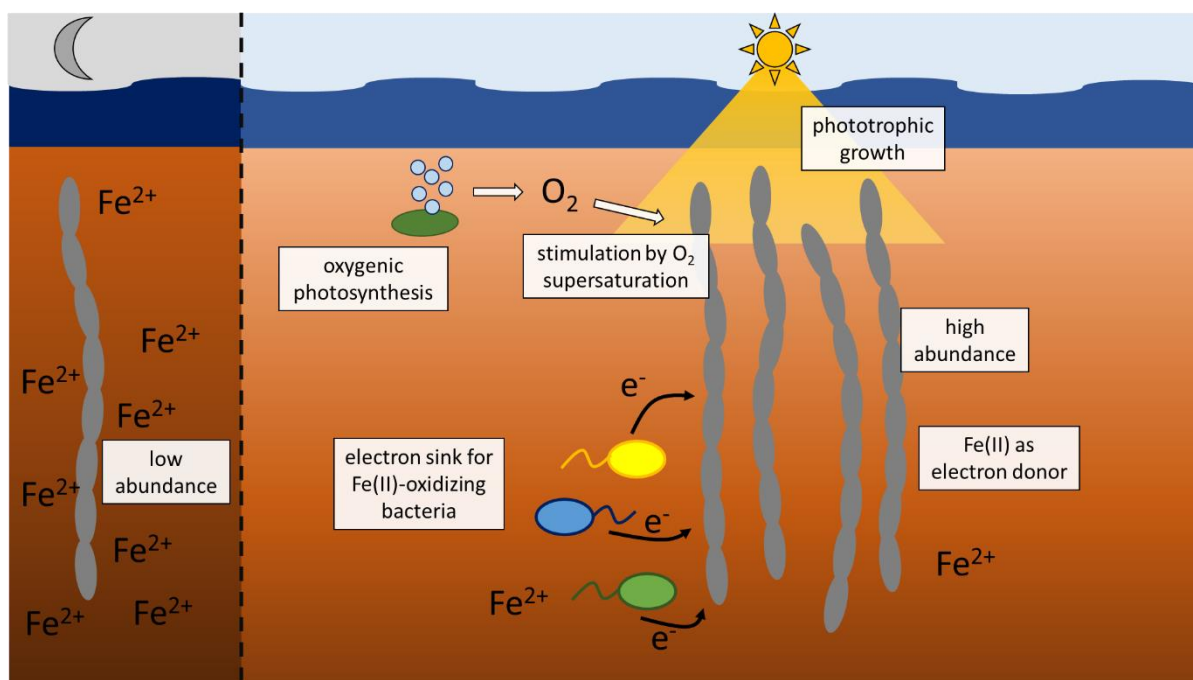
**Figure 6.2** Overview of observations and potential explanations for the observed differences in abundance of cable bacteria and $Fe^{2+}$ concentrations in light and dark illuminated sediments. In dark incubated sediment, high $Fe^{2+}$ concentrations and low abundance of cable bacteria were observed. In light incubated sediment, abundance of cable bacteria was high and $Fe^{2+}$ concentrations low. High abundance of cable bacteria in light illuminated sediment might be explainable by phototrophic growth or favorable growth conditions by oxygen ($O_2$) supersaturation produced by oxygenic photosynthesis. Low $Fe^{2+}$ concentrations might be explainable by direct Fe(II) oxidation of cable bacteria or the transfer of electrons from Fe(II)-oxidizing bacteria to cable bacteria using them as electron sink.

## 6.2 Importance of hidden Fe sources and sinks for the sedimentary Fe cycle

Besides the known control parameters of sedimentary Fe cycling, we were able to decipher so far hidden Fe(II) sources and sinks. Fe(II) was thought to originate from the Fe(III) reduction zone in deeper sediment layers (Canfield & Thamdrup, 2009). By diffusion or advection, it reaches upper sediment layers and gets oxidized by abiotic or microbial processes. However, sedimentary Fe(III) photoreduction (Chapter **3**) disturbs this view by adding an additional Fe(II) source to the upper sediment layers. This has consequences not only for Fe(II) fluxes but also for the substrate availability of Fe(II)-oxidizing bacteria. Similarly, the discovery of mobilization of $Fe^{2+}$ after physical perturbation of marine sediment, e.g. after storm events (Chapter **4**), adds another feature to the sedimentary Fe cycle. By the partial oxidation or dissolution of metastable iron-sulphur ($FeS_x$) mineral phases, $Fe^{2+}$ is released into the sedimentary pore water. Those metastable $FeS_x$ potentially are highly reactive towards

dissolution, e.g. by acidification due to cable bacteria activity (Risgaard-Petersen et al., 2012) or oxidation reactions. During physical perturbation, also solid Fe phases in the sediment are shifted towards less crystallinity (Chapter **4**) with tremendous consequences for not only Fe-metabolizing bacteria but also for sorption processes including potentially sorbed Fe(II), nutrients like phosphate (Khare et al., 2005) or contaminants like heavy metals (Giammar & Hering, 2001; Dixit & Hering, 2003). It was shown that less crystalline Fe minerals can more easily be reduced by Fe(III)-reducing bacteria compared to higher crystalline Fe minerals (Hansel et al., 2004; Cutting et al., 2009). Therefore, storm events would potentially not only stimulate microbial Fe(II) oxidation by providing more $Fe^{2+}$ but also microbial Fe(III) reduction by providing less crystalline Fe minerals. By the decrease of $FeS_x$ mineral phases, sulphide is potentially released that might either get oxidized, reduce Fe(III) to form Fe(II) or react with Fe(II) to re-precipitate as $FeS_x$, Fe monosulphide (FeS) or pyrite ($FeS_2$) (Howarth, 1979; Pyzik & Sommer, 1981; Berner, 1984), thereby tremendously influencing the Fe(II) and Fe(III) availability in sediments. Considering the potential contribution of cable bacteria to microbial Fe(II) oxidation in sediments, either by directly being able to use $Fe^{2+}$ as electron donor or by serving as electron sink for other Fe(II)-oxidizing bacteria, adds another microbial process to the sedimentary Fe redox cycle that was not considered so far. A visual concept of a revised Fe cycle is shown in Figure 6.3.
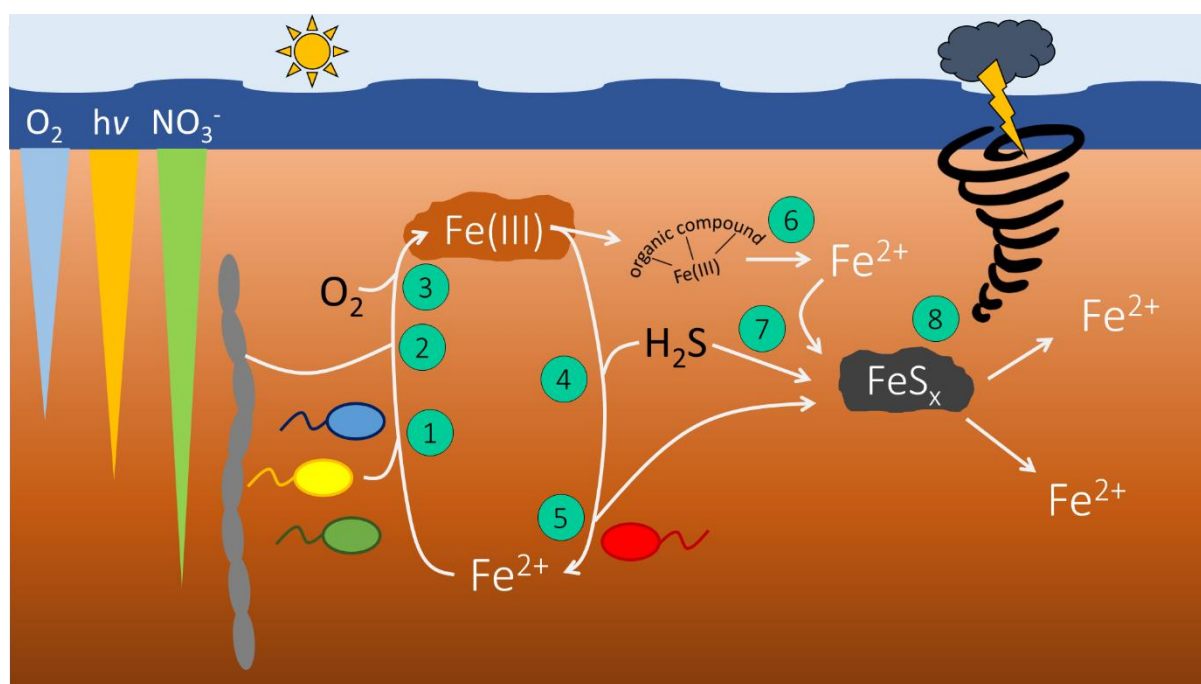
**Figure 6.3** Concept for a revised sedimentary Fe cycle with implemented novel Fe(II) sources. Fe(III) is shown as Fe(III) minerals, Fe(II) is shown as dissolved Fe(II) ($Fe^{2+}$). Concentration gradients of oxygen ($O_2$), light ($h\nu$) and nitrate ($NO_3^-$) are shown. 1) Microbial Fe(II) oxidation by microaerophilic, phototrophic or nitrate-reducing Fe(II)-oxidizing bacteria. 2) Hypothetical contribution of cable bacteria to microbial Fe(II) oxidation. 3) Abiotic Fe(II) oxidation, exemplary with $O_2$. 4) Abiotic Fe(III) reduction, exemplary with sulphide ($H_2S$). 5) microbial Fe(III) reduction by Fe(III)-reducing bacteria. 6) Fe(III) photoreduction of organically complexed Fe(III). 7) Precipitation of metastable Fe sulphide minerals ($FeS_x$).8) $Fe^{2+}$ mobilization from metastable $FeS_x$ into different sediment depths induced by physical perturbation.

Both, Fe(III) photoreduction and physical perturbation do not continuously deliver the same amount of $Fe^{2+}$ to sediments. Light conditions change depending on the time of the day, season and cloudiness. How much light and what wavelengths actually reach sediment surfaces also depends on the height of the overlying water column as well as the amount of light attenuating substances present in the water (Piazena et al., 2002). During night, $Fe^{2+}$ cannot photochemically be produced at all and is only oxidized in the upper oxic sediment layers by abiotic or microbial Fe(II) oxidation. Storms take place irregularly and the magnitude and hence the consequences of waves on sediments varies depending on the wind force. The geochemistry as well as the inhabiting microbial community of the sediment also determines the actual extent of Fe(II) oxidation or Fe(III) reduction reactions. If sulphide is not present at a sufficient high concentration, $FeS_x$ would not form and $Fe^{2+}$ release after physical perturbation would potentially be negligible. Also, in sediments with low sulphide concentrations, cable bacteria would most probably not be present or only in small abundance. In sediments with low cyanobacterial activity, oxygenic photosynthesis would not lead to $O_2$ supersaturation and

consequently to slower abiotic Fe(II) oxidation by $O_2$. The organic carbon content of sediments might differ depending on rainfall, seasonal surface runoff or deposition of plankton detritus from the water column. In low organic sediments, less ROS would be photochemically be formed including their subsequent reactions with Fe(II) or Fe(III) and Fe(III) photoreduction cannot produce sufficient $Fe^{2+}$ in upper sediment layers so that it can be quantified.

Therefore, the actual extent of several Fe(II) oxidizing or Fe(III) reducing processes and their exact contribution to the sedimentary Fe redox cycle cannot be generalized. Finally, if different sediment layers are shifted more towards Fe(II) oxidation or towards Fe(III) reduction and what kind of biogeochemical processes dominate, is determined by inhabiting microorganisms, different geochemical conditions and light availability. Therefore, $Fe^{2+}$ fluxes in the sediment are variable and it was shown that the sedimentary Fe cycle is very dynamic and variable towards changing conditions, which is in contrast to the rigid and fixed opinion of opposing gradients of Fe(II) and Fe(III). By adding those so far hidden sources, we need to think about a revised sedimentary Fe cycle including consequences for other element cycles and sorption processes.

## 6.3 Outlook on further experiments

Several additional sources and sinks of Fe(II) in sediments could successfully be deciphered during this PhD research that have been overlooked so far. For that, high-resolution measurements using microelectrodes in combination with targeted additional experiments were conducted. Traditional methods such as pore water analysis via e.g. the spectrophotometric ferrozine assay (Stookey, 1970) or acid extractions (Heron et al., 1994; Poulton & Canfield, 2005) were partly not sensitive enough to capture small scale variations of $Fe^{2+}$ concentration gradients in sediments.

However, after the discovery of those additions to the sedimentary Fe cycle, more experiments are necessary to completely resolve their mechanisms and dependences on geochemical or biological parameters. Experiments with natural sediment generally are quite complex and due to matrix effects such as reactions with other species present in natural sediments, it is difficult to figure out single processes. In order to decipher how the extent of photochemically produced $Fe^{2+}$ depends on the DOC concentration, it would probably not be sufficient to only add different amounts of DOC to the sediment and incubate it in light. The addition of organic carbon presumably also stimulates the activity of heterotrophic bacteria. By this, respiratory

processes would be enhanced, the spatial extent of the different redox zones potentially would shrink and therefore, change the geochemical conditions of the different sediment layers. Thus, the experimental setup needs to be simplified by exchanging the sediment and the pore water with well-defined solids and solutions. Instead of using natural sediment, a set of "artificial" sediment cores filled with sterile quartz sand particles coated with Fe(III) minerals such as ferrihydrite, amended with different amounts of DOC could be incubated in light and $Fe^{2+}$ concentration profiles could be recorded and compared. By using sterile sand particles surrounded by sterile medium solution, microbial processes as well as chemical reactions of $Fe^{2+}$ with other species present in sediments are prevented and the relationship between DOC and $Fe^{2+}$ produced by Fe(III) photoreduction could be quantified.

In order to better resolve the observed DOC dependence in the sediment cores with natural sediment, the pore water could be extracted and analyzed by FT-ICR-MS to characterize the kind of organic molecules naturally present in the sediment pore water (Marshall et al., 1998; Koch et al., 2008). By identifying their structure and functional groups, the percentage of potentially light susceptible Fe(III)-organic complexes to the overall organic molecules could be determined. The concentration and composition of organic molecules influences the amount of ROS that is presumably produced by photolysis in sediment pore water. So far, the contribution of ROS to the sedimentary Fe cycle, either by Fe(II) oxidation or by Fe(III) reduction, is not determined. ROS are generally not trivial to quantify due to their high reactivity with other species and their short half-life times (Burns et al., 2012). By analyte-specific chemiluminesence methods, $H_2O_2$ and superoxide can be quantified (King et al., 2007; Rose et al., 2008), however, those methods are based on flow injection analysis with relatively large sample volumes. Thus, another method needs to be developed to measure different ROS in-situ in sediment at a high spatial and temporal resolution. Voltammetric Au/Hg microsensors are able to detect $H_2O_2$ (Glazer et al., 2004; Moore et al., 2007), as it gets reduced to $H_2O$ at the Au/Hg surface at a potential of -1.2 V. However, during a voltammetric scan, $O_2$ gets reduced to $H_2O_2$ at -0.3 V, which then also is detected. Another possibility to quantify $H_2O_2$ on a small spatial resolution is a quasi-reversible luminescence-based optical $H_2O_2$ sensor that relies on the redox conversion of Prussian blue (Koren et al., 2016). However, reducing agents strongly affect the signal of the sensor. Burns et al. (2012) summarized different methods for the determination of ROS in aquatic environments, however, these methods need to be modified to be suitable for sedimentary systems.

The hypothesis that cable bacteria might be able to use light as energy source and/or that they can use $Fe^{2+}$ as alternative electron donor could not ultimately be proved. For that, additional control experiments are necessary. In order to quantitatively relate the abundance of cable bacteria to light intensities, sediment cores need to be illuminated with different light intensities and cable bacteria cell numbers need to be quantified e.g. using FISH analysis (Schauer et al., 2014; Sulu-Gambari et al., 2016). However, geochemical parameters such as $O_2$ concentration need to be kept as similar as possible in the different setups. Higher light intensities usually lead to higher photosynthesis rates and concomitant higher $O_2$ concentrations in the sediment pore water (Lassen et al., 1992). As $O_2$ can be used as electron acceptor by cable bacteria, higher $O_2$ concentrations and not higher light intensities could favor the growth of cable bacteria. No cable bacteria could visually be found in incubated sediment cores, when oxygenic photosynthesis was suppressed by adding 3-(3,4-dichlorophenyl)-1,1-dimethylurea (DCMU). Therefore, other approaches need to be found. The potential use of $Fe^{2+}$ as electron donor by cable bacteria could further be tested by regularly cutting cable bacteria with a wire as performed by Pfeffer et al. (2012). They could show that cable bacteria activity and concomitant $O_2$ consumption immediately dropped as a direct result of the interrupted electron conduction by cable bacteria. If $Fe^{2+}$ concentrations would not further decrease when cable bacteria activity is disturbed by cutting, it would be an evidence for Fe(II) oxidation by cable bacteria. However, the possibility that swarming Fe(II)-oxidizing bacteria use the cable bacteria as electron sink (Otte et al., 2018) cannot be excluded by this experiment. For testing the hypothesis of Fe(II) oxidation by cable bacteria, a sediment with less sulphide than the sediment incubated during this PhD research might be more suitable. So far, it is assumed that cable bacteria can only use sulphide as electron donor. From a thermodynamic perspective, more energy can be gained by coupling sulphide than coupling Fe(II) oxidation to $O_2$ reduction and cable bacteria presumably would perform the redox reaction with more energy gain for their metabolisms. Therefore, if the sediment was depleted in sulphide, cable bacteria might be forced to use an alternative electron donor instead, e.g. Fe(II).

## 6.4 Expect the unexpected

For centuries, people believed that the Earth was the center of the universe around which the planets, stars and the sun orbited until the 16<sup>th</sup> century when Nikolaus Kopernikus proved them wrong. The history of science is full of such incorrect hypotheses, about which we today shake our heads uncomprehendingly. Even these days, we regularly read or hear about new findings and discoveries that make us aware that humans are still only scratching the surface and there is much to be explored in order to understand the interconnections on Earth and the universe. Coming back to the sedimentary Fe cycle, the discovery of relevant, but so far hidden Fe sources and sinks during this PhD research makes clear that also other, still undiscovered processes might influence the Fe availability in sediments – only that they are not yet found. Before cable bacteria were discovered, nobody would have believed, or even suspected, that these uniquely structured filamentous bacteria with their metabolism of conducting electrons over centimeter distances could exist. The unraveling of cryptic element cycles in the recent years was only possible by applying novel and more sensitive measurement techniques as well as developing smart experimental approaches. Just because certain compounds do not show up at measurable concentrations in environmental systems does not mean that they cannot drive whole element cycles. Small scale processes need to be unraveled to see the bigger picture and get a more holistic view on environmental processes. Experimental results should first be critically examined but if they appear repeatedly and errors can be excluded, the currently accepted explanation should be questioned. Had scientists discarded all unexpected experimental data that did not fit within the long-held scientific beliefs and that, at first glance, appeared to be bizarre, they would never have discovered new findings.

In conclusion of this PhD research, I want to encourage people to be open minded, to expect the unexpected - it is worth thinking outside the box.

## 6.5 References

Barbeau, K. (2006). Photochemistry of organic iron(III) complexing ligands in oceanic systems. *Photochemistry and Photobiology*, **82**(6), 1505-1516.

Barbeau, K., Rue, E. L., Bruland, K. W. and Butler, A. (2001). Photochemical cycling of iron in the surface ocean mediated by microbial iron(III)-binding ligands. *Nature*, **413**, 409.

Berner, R. A. (1984). Sedimentary pyrite formation: An update. *Geochimica et Cosmochimica Acta*, **48**(4), 605-615.

Borer, P., Sulzberger, B., Hug, S. J., Kraemer, S. M. and Kretzschmar, R. (2009). Photoreductive dissolution of iron(III) (hydr)oxides in the absence and presence of organic ligands: experimental studies and kinetic modeling. *Environmental Science & Technology*, **43**(6), 1864-1870.

Bryce, C., Blackwell, N., Schmidt, C., Otte, J., Huang, Y.-M., Kleindienst, S., Tomaszewski, E., Schad, M., Warter, V., Peng, C., Byrne, J. M. and Kappler, A. (2018). Microbial anaerobic Fe(II) oxidation – Ecology, mechanisms and environmental implications. *Environmental Microbiology*, **20**(10), 3462-3483.

Burns, J. M., Cooper, W. J., Ferry, J. L., King, D. W., DiMento, B. P., McNeill, K., Miller, C. J., Miller, W. L., Peake, B. M., Rusak, S. A., Rose, A. L. and Waite, T. D. (2012). Methods for reactive oxygen species (ROS) detection in aqueous environments. *Aquatic Sciences*, **74**(4), 683-734.

Canfield, D. E., Rosing, M. T. and Bjerrum, C. (2006). Early anaerobic metabolisms. *Philosophical Transactions of the Royal Society B: Biological Sciences*, **361**(1474), 1819-1836.

Canfield, D. E. and Thamdrup, B. (2009). Towards a consistent classification scheme for geochemical environments, or, why we wish the term 'suboxic' would go away. *Geobiology*, **7**(4), 385-392.

Cutting, R. S., Coker, V. S., Fellowes, J. W., Lloyd, J. R. and Vaughan, D. J. (2009). Mineralogical and morphological constraints on the reduction of Fe(III) minerals by Geobacter sulfurreducens. *Geochimica et Cosmochimica Acta*, **73**(14), 4004-4022.

Dixit, S. and Hering, J. G. (2003). Comparison of arsenic(V) and arsenic(III) sorption onto iron oxide minerals: Implications for arsenic mobility. *Environmental Science & Technology*, **37**(18), 4182-4189.

Farjalla, V. F., Amado, A. M., Suhett, A. L. and Meirelles-Pereira, F. (2009). DOC removal paradigms in highly humic aquatic ecosystems. *Environmental Science and Pollution Research*, **16**(5), 531-538.

Garg, S., Rose, A. L. and Waite, T. D. (2011). Photochemical production of superoxide and hydrogen peroxide from natural organic matter. *Geochimica et Cosmochimica Acta*, **75**(15), 4310-4320.

Giammar, D. E. and Hering, J. G. (2001). Time scales for sorption−desorption and surface precipitation of uranyl on goethite. *Environmental Science & Technology*, **35**(16), 3332-3337.

Glazer, B. T., Marsh, A. G., Stierhoff, K. and Luther Iii, G. W. (2004). The dynamic response of optical oxygen sensors and voltammetric electrodes to temporal changes in dissolved oxygen concentrations. *Analytica Chimica Acta*, **518**(1–2), 93-100.

Hansel, C. M., Benner, S. G., Nico, P. and Fendorf, S. (2004). Structural constraints of ferric (hydr)oxides on dissimilatory iron reduction and the fate of Fe(II). *Geochimica et Cosmochimica Acta*, **68**(15), 3217-3229.

Hansel, C. M., Ferdelman, T. G. and Tebo, B. M. (2015). Cryptic cross-linkages among biogeochemical cycles: novel insights from reactive intermediates. *Elements*, **11**(6), 409-414.

Heron, G., Crouzet, C., Bourg, A. C. M. and Christensen, T. H. (1994). Speciation of Fe(II) and Fe(III) in contaminated aquifer sediments using chemical extraction techniques. *Environmental Science and Technology*, **28**(9), 1698-1705.

Horvath, H. (1993). Atmospheric light absorption—A review. *Atmospheric Environment. Part A. General Topics*, **27**(3), 293-317.

Howarth, R. W. (1979). Pyrite: Its rapid formation in a salt marsh and its importance in ecosystem metabolism. *Science*, **203**(4375), 49-51.

Jørgensen, B. B., Revsbech, N. P., Blackburn, T. H. and Cohen, Y. (1979). Diurnal cycle of oxygen and sulfide microgradients and microbial photosynthesis in a cyanobacterial mat sediment. *Applied and Environmental Microbiology*, **38**(1), 46-58.

Khare, N., Hesterberg, D. and Martin, J. D. (2005). XANES investigation of phosphate sorption in single and binary systems of iron and aluminum oxide minerals. *Environmental Science & Technology*, **39**(7), 2152-2160.

King, D. W., Cooper, W. J., Rusak, S. A., Peake, B. M., Kiddle, J. J., O'Sullivan, D. W., Melamed, M. L., Morgan, C. R. and Theberge, S. M. (2007). Flow injection analysis of $H_2O_2$ in natural waters using acridinium ester chemiluminescence: Method development and optimization using a kinetic model. *Analytical Chemistry*, **79**(11), 4169-4176.

Koch, B. P., Ludwichowski, K.-U., Kattner, G., Dittmar, T. and Witt, M. (2008). Advanced characterization of marine dissolved organic matter by combining reversed-phase liquid chromatography and FT-ICR-MS. *Marine Chemistry*, **111**(3), 233-241.

Koren, K., Jensen, P. Ø. and Kühl, M. (2016). Development of a rechargeable optical hydrogen peroxide sensor – sensor design and biological application. *Analyst*, **141**(14), 4332-4339.

Kühl, M., Cohen, Y., Dalsgaard, T., Jørgensen, B. B. and Revsbech, N. P. (1995). Microenvironment and photosynthesis of zooxanthellae in scleractinian corals studied with microsensors for $O_2$, pH and light. *Marine Ecology Progress Series*, **117**(1/3), 159-172.

Larsen, H. (1952). On the culture and general physiology of the green sulfur bacteria. *Journal of Bacteriology*, **64**(2), 187-196.

Lassen, C., Ploug, H. and Jorgensen, B. B. (1992). Microalgal photosynthesis and spectral scalar irradiance in coastal marine sediments of Limfjorden, Denmark. *Limnology and Oceanography*, **37**(4), 760-772.

Laufer, K., Nordhoff, M., Røy, H., Schmidt, C., Behrens, S., Jørgensen, B. B. and Kappler, A. (2016). Coexistence of microaerophilic, nitrate-reducing, and phototrophic Fe(II)-oxidizers and Fe(III)-reducers in coastal marine sediment. *Applied and Environmental Microbiology*, **82**(5), 1433-1447.

Marshall, A. G., Hendrickson, C. L. and Jackson, G. S. (1998). Fourier transform ion cyclotron resonance mass

spectrometry: A primer. *Mass Spectrometry Reviews*, **17**(1), 1-35.

Mayer, L. M., Schick, L. L., Skorko, K. and Boss, E. (2006). Photodissolution of particulate organic matter from sediments. *Limnology and Oceanography*, **51**(2), 1064-1071.

Moore, T. S., Nuzzio, D. B., Deering, T. W., Taillefert, M. and Luther III, G. W. (2007). Use of voltammetry to monitor $O_2$ using Au/Hg electrodes and to control physical sensors on an unattended observatory in the Delaware Bay. *Electroanalysis*, **19**(19-20), 2110-2116.

Otte, J. M., Harter, J., Laufer, K., Blackwell, N., Straub, D., Kappler, A. and Kleindienst, S. (2018). The distribution of active iron-cycling bacteria in marine and freshwater sediments is decoupled from geochemical gradients. *Environmental Microbiology*, **20**(7), 2483-2499.

Page, S. E., Logan, J. R., Cory, R. M. and McNeill, K. (2014). Evidence for dissolved organic matter as the primary source and sink of photochemically produced hydroxyl radical in arctic surface waters. *Environmental Science: Processes & Impacts*, **16**(4), 807-822.

Pfeffer, C., Larsen, S., Song, J., Dong, M., Besenbacher, F., Meyer, R. L., Kjeldsen, K. U., Schreiber, L., Gorby, Y. A., El-Naggar, M. Y., Leung, K. M., Schramm, A., Risgaard-Petersen, N. and Nielsen, L. P. (2012). Filamentous bacteria transport electrons over centimetre distances. *Nature*, **491**, 218.

Piazena, H., Perez-Rodrigues, E., Häder, D. P. and Lopez-Figueroa, F. (2002). Penetration of solar radiation into the water column of the central subtropical Atlantic Ocean — optical properties and possible biological consequences. *Deep Sea Research Part II: Topical Studies in Oceanography*, **49**(17), 3513-3528.

Poulton, S. W. and Canfield, D. E. (2005). Development of a sequential extraction procedure for iron: implications for iron partitioning in continentally derived particulates. *Chemical Geology*, **214**(3), 209-221.

Pyzik, A. J. and Sommer, S. E. (1981). Sedimentary iron monosulfides: Kinetics and mechanism of formation. *Geochimica et Cosmochimica Acta*, **45**(5), 687-698.

Reguera, G. (2018). Biological electron transport goes the extra mile. *Proceedings of the National Academy of Sciences*, **115**(22), 5632-5634.

Riggsbee, J. A., Orr, C. H., Leech, D. M., Doyle, M. W. and Wetzel, R. G. (2008). Suspended sediments in river ecosystems: Photochemical sources of dissolved organic carbon, dissolved organic nitrogen, and adsorptive removal of dissolved iron. *Journal of Geophysical Research: Biogeosciences*, **113**(G3).

Risgaard-Petersen, N., Revil, A., Meister, P. and Nielsen, L. P. (2012). Sulfur, iron-, and calcium cycling associated with natural electric currents running through marine sediment. *Geochimica et Cosmochimica Acta*, **92**, 1-13.

Rose, A. (2012). The influence of extracellular superoxide on iron redox chemistry and bioavailability to aquatic microorganisms. *Frontiers in Microbiology*, **3**(124).

Rose, A. L., Moffett, J. W. and Waite, T. D. (2008). Determination of superoxide in seawater using 2-methyl-6-(4-methoxyphenyl)-3,7-dihydroimidazo[1,2-a]pyrazin-3(7H)-one chemiluminescence. *Analytical Chemistry*, **80**(4), 1215-1227.

Santana-Casiano, J. M., González-Dávila, M. and Millero, F. J. (2006). The role of

Fe(II) species on the oxidation of Fe(II) in natural waters in the presence of $O_2$ and $H_2O_2$. *Marine Chemistry*, **99**(1), 70-82.

Schauer, R., Risgaard-Petersen, N., Kjeldsen, K. U., Tataru Bjerg, J. J., B Jørgensen, B., Schramm, A. and Nielsen, L. P. (2014). Succession of cable bacteria and electric currents in marine sediment. *The Isme Journal*, **8**, 1314.

Schmidt, C., Behrens, S. and Kappler, A. (2010). Ecosystem functioning from a geomicrobiological perspective a conceptual framework for biogeochemical iron cycling. *Environmental Chemistry*, **7**(5), 399-405.

Scully, N. M., Cooper, W. J. and Tranvik, L. J. (2003). Photochemical effects on microbial activity in natural waters: the interaction of reactive oxygen species and dissolved organic matter. *FEMS Microbiology Ecology*, **46**(3), 353-357.

Southwell, M. W., Mead, R. N., Luquire, C. M., Barbera, A., Avery, G. B., Kieber, R. J. and Skrabal, S. A. (2011). Influence of organic matter source and diagenetic state on photochemical release of dissolved organic matter and nutrients from resuspendable estuarine sediments. *Marine Chemistry*, **126**(1), 114-119.

Stookey, L. L. (1970). Ferrozine - a new spectrophotometric reagent for iron. *Analytical Chemistry*, **42**(7), 779-781.

Sulu-Gambari, F., Seitaj, D., Meysman, F. J. R., Schauer, R., Polerecky, L. and Slomp, C. P. (2016). Cable bacteria control iron–phosphorus dynamics in sediments of a coastal hypoxic basin. *Environmental Science & Technology*, **50**(3), 1227-1233.

van Grondelle, R., Dekker, J. P., Gillbro, T. and Sundstrom, V. (1994). Energy transfer and trapping in photosynthesis. *Biochimica et Biophysica Acta (BBA) - Bioenergetics*, **1187**(1), 1-65.

Voelker, B. M., Sedlak, D. L. and Zafiriou, O. C. (2000). Chemistry of superoxide radical in seawater: reactions with organic Cu complexes. *Environmental Science & Technology*, **34**(6), 1036-1042.

Waite, T. D., Szymczak, R., Espey, Q. I. and Furnas, M. J. (1995). Diel variations in iron speciation in northern Australian shelf waters. *Marine Chemistry*, **50**(1), 79-91.

Widdel, F., Schnell, S., Heising, S., Ehrenreich, A., Assmus, B. and Schink, B. (1993). Ferrous iron oxidation by anoxygenic phototrophic bacteria. *Nature*, **362**(6423), 834-836.

Yurkov, V. V. and Beatty, J. T. (1998). Aerobic anoxygenic phototrophic bacteria. *Microbiology and Molecular Biology Reviews*, **62**(3), 695-724.

# Statement of personal contribution

The work described in this PhD Thesis was funded by grants from the Deutsche Forschungsgesellschaft (DFG) to Dr. Caroline Schmidt (SCHM2808/2-1, SCHM2808/4-1).

The conceptual background to this project was designed by Dr. C. Schmidt. Prof. Andreas Kappler was the main supervisor throughout the project and Prof. Bo Barker Jørgensen was the second supervisor. Unless otherwise stated, the experiments were either conceptualized by myself or together with Dr. C. Schmidt and/or Prof. A. Kappler and Prof. B.B. Jørgensen. The experiments were carried out by me. The discussion and analysis of the obtained results, as well as writing of all manuscripts were completed in cooperation with Dr. C. Schmidt; for chapters 2, 3 and 4 also in cooperation with Prof. A. Kappler and Prof. B.B. Jørgensen; for chapter 4 additionally in cooperation with Markus Maisch and Dr. Katja Laufer. In detail, the contributions of the named people including myself, as well as other people are as stated below:

**Field Work:** Several people were involved in the field work during sampling campaigns at Lake Constance and Norsminde Fjord. During sampling at Lake Constance in May 2016, Dr. Cindy Lockwood and Franziska Schädler helped me with the field work. In September 2017, Dr. C. Schmidt and M. Maisch supported me with collecting samples from Lake Constance. Dr. C. Schmidt and M. Maisch also collected sediment from Lake Constance for me in November 2017. The sampling campaign to Norsminde Fjord in August 2016 was joined by Dr. Nia Blackwell and Dr. Casey Bryce. In March 2017, I got help with the field work and collecting samples from Norsminde Fjord by Dr. N. Blackwell, Dr. C. Bryce, Dr. Julia Otte and Dr. K. Laufer.

**Chapter 2:** Dr. C. Schmidt, Prof. A. Kappler and Prof. B.B. Jørgensen revised the manuscript.

**Chapter 3:** Dr. C. Schmidt helped with the experimental design and, together with Prof. A. Kappler and Prof. B.B. Jørgensen, helped with data analysis and revising the manuscript. Analysis of dissolved and total organic carbon content of the sediment was performed by Ellen Röhm.

**Chapter 4:** Dr. C. Schmidt and M. Maisch helped with the experimental design. M. Maisch performed Mössbauer spectroscopy and XRD analysis and evaluated the data. He also wrote the material and methods part as well as parts of the results section concerning the Mössbauer and XRD data. Dr. K. Laufer provided data that she recorded after a real storm at the field site. Dr. C. Schmidt, Prof. A. Kappler, Prof. B.B. Jørgensen, M. Maisch and Dr. K. Laufer helped with data analysis and revising the manuscript.

**Chapter 5:** Dr. C. Schmidt and M. Maisch helped with the experimental design. M. Maisch helped me with sampling during the experiment. Dr. C. Schmidt, Prof. A. Kappler and Prof. B.B. Jørgensen helped with data analysis. Dr. C. Schmidt revised the manuscript.

I state hereby that I have not plagiarized or copied any of the text. Chapters 2-5 have been or will be submitted to different scientific journals, so that they might be published in a slightly modified version elsewhere in the future.

# Curriculum Vitae

## Personal information

| | |
|---|---|
| Name: | Ulf Lüder |
| Current address: | Brucknerweg 2 |
| | 72076 Tübingen |
| | Germany |
| Email: | ulf.lueder@uni-tuebingen.de |
| Date of birth: | February 23$^{th}$, 1990 |
| Place of birth: | Heidenheim an der Brenz, Germany |
| Citizenship: | German |

## Academic education

**Ph.D. in Umweltnaturwissenschaften,** Eberhard Karls Universität Tübingen, Germany

**since 05/2016**

Ph.D. thesis title: *Hidden sources and sinks of Fe(II) in the sedimentary biogeochemical iron cycle – the role of light*

Supervisors: Prof. Dr. Andreas Kappler, Prof. Dr. Bo Barker Jørgensen
Workgroup Geomicrobiology, Center for Applied Geoscience, Eberhard Karls Universität Tübingen, Germany

**M.Sc. in Applied and Environmental Geoscience,** Eberhard Karls Universität Tübingen, Germany

**2013 – 2016**

Master thesis title: *Monitoring $O_2$- and Fe(II)-concentrations in opposed gradient tubes: Application of amperometric and voltammetric methods*

Supervisors: Prof. Dr. Andreas Kappler, Dr. Caroline Schmidt
Workgroup Geomicrobiology, Center for Applied Geoscience, Eberhard Karls Universität Tübingen, Germany

**B.Sc. in Umweltnaturwissenschaften**, Eberhard Karls Universität Tübingen, Germany

**2010 – 2013**

Bachelor thesis title:  *Optimierung der Probenvorbereitung für das Target Screening von Wasserproben*

Supervisors: Prof. Dr. Christian Zwiener, Dr. Marco Zedda
Workgroup Environmental Analytical Chemistry, Center for Applied Geoscience, Eberhard Karls University of Tübingen, Germany

## Training Experience

Training course "Microsensor Analysis in the Environmental Sciences" (June 2016), Rønbjerg, Denmark

Assistance in lab course "Geomicrobiology and Environmental Microbiology" (October 2016 and October 2017), Tübingen, Germany

Assistance in practical session of the lecture "Aquatic & Environmental Chemistry – Hydrogeochemical modelling" held by Dr. Caroline Schmidt (May 2018 – July 2018), Tübingen, Germany

Assistance in workshop "Tools in Biogeochemistry – Practical Part Microelectrodes" held by Prof. Gregory Druschel, Ph.D. (August 2019), Tübingen, Germany

# Appendix

Publications

**Published**

Maisch, M., **Lueder, U.**, Laufer, K., Scholze, C., Kappler, A., Schmidt, C. (2019) Contribution of microaerophilic iron(II)-oxidizers to iron(III) mineral formation. *Environmental Science and Technology* 53, 8197-8204.

> Contribution: Gradient tube preparation, microsensor measurements, assistance with kinetic calculations

**Lueder, U.**, Druschel, G., Emerson, D., Kappler, A., Schmidt, C. (2018) Quantitative analysis of $O_2$ and $Fe^{2+}$ profiles in gradient tubes for cultivation of microaerophilic Iron(II)-oxidizing bacteria. *FEMS Microbiology Ecology*, Volume 94, Issue 2, 1 February 2018, fix177, doi.org/10.1093/femsec/fix177

> The publication is printed below. As part of the data collection for the publication was not performed during this PhD and as the publication did not focus on sedimentary Fe cycling, it was not included as separate chapter of the PhD thesis.

Schaedler, F., Lockwood, C., **Lueder, U.**, Glombitza, C., Kappler, A., Schmidt, C. (2018) Microbially mediated coupling of Fe and N cycles by nitrate-reducing Fe(II)-oxidizing bacteria in littoral freshwater sediments. *Applied and Environmental Microbiology*, 84:e02013-17.

> Contribution: Sample collection and microsensor measurements

**Accepted for publication**

Maisch, M., **Lueder, U.**, Kappler, A., Schmidt, C. (2019) Iron Lung – How rice roots induce iron redox changes in the rhizosphere and create niches for microaerophilic Fe(II)-oxidizing bacteria. *Environmental Science & Technology Letters* (accepted).

> Contribution: Voltammetric microsensor measurements

**Submitted**

**Lueder, U.**, Jørgensen, B.B., Kappler, A., Schmidt, C. (2019) Photochemistry of iron in aquatic environments. Submitted to *Environmental Science: Processes and Impacts*.

**Lueder, U.**, Maisch, M., Laufer, K., Jørgensen, B.B., Kappler, A., Schmidt, C. (2019) Influence of physical perturbation on Fe(II) supply in coastal marine sediments. Submitted to *Environmental Science and Technology*.

**Lueder, U.**, Jørgensen, B.B., Kappler, A., Schmidt, C. (2019) Fe(III) photoreduction producing $Fe^{2+}_{aq}$ in oxic freshwater sediment. Submitted to *Environmental Science and Technology*.

Schmidt, C., Nikeleit, V., Schaedler, F., Leider, A., **Lueder, U.**, Bryce, C., Hallmann, C., Kappler, A., (2019) Metabolic flexibility in a phototrophic co-culture enriched from a freshwater sediment and its relevance for biogeochemical iron cycling. Submitted to *FEMS Microbiology Ecology*.

Contribution: Assistance with record of absorbance spectra and light measurements

## Conference contributions

08/2017 Goldschmidt Conference, Paris, France,
Oral presentation: "Implications of Fe(III) photoreduction for sedimentary biogeochemical iron cycling". **Lueder, U.**, Kappler, A., Jørgensen, B.B., Schmidt, C.

08/2018 Goldschmidt Conference, Boston, USA,
Oral presentation: "The impact of light on iron biogeochemistry in sediments". **Lueder, U.**, Jørgensen, B.B., Maisch, M., Kappler, A., Schmidt, C.

08/2019 Goldschmidt Conference, Barcelona, Spain,
Oral presentation: "Metastable iron sulphur mineral phases drive highly dynamic biogeochemical cycles in marine sediments". **Lueder, U.**, Maisch, M., Jørgensen, B.B., Kappler, A., Schmidt, C.

Printed Publication

RESEARCH ARTICLE

# Quantitative analysis of O₂ and Fe²⁺ profiles in gradient tubes for cultivation of microaerophilic Iron(II)-oxidizing bacteria

U. Lueder[1], G. Druschel[2], D. Emerson[3], A. Kappler[1,4] and C. Schmidt[1,*]

[1]Geomicrobiology Group, Center for Applied Geoscience (ZAG), University of Tuebingen, Sigwartstrasse 10, D-72076 Tuebingen, Germany, [2]Department of Earth Sciences, Indiana University-Purdue University, 723 W Michigan Street, SL118, Indianapolis, IN 46202, USA, [3]Bigelow Laboratory for Ocean Sciences, 60 Bigelow Drive, East Boothbay, ME 04544, USA and [4]Center for Geomicrobiology, Department of Bioscience, Aarhus University, Ny Munkegade 114, Building 1540, 8000 Aarhus, Denmark

*Corresponding authors:* Geomicrobiology, Center for Applied Geosciences, University of Tuebingen, Sigwartstrasse 10, D-72076 Tuebingen, Germany. Tel: +49-7071-2975496; Fax: +49-7071-29-295059; E-mail: caroline.schmidt@uni-tuebingen.de

**One sentence summary:** The work provides insights on optimal growth conditions of microaerophilic iron(II)-oxidizing bacteria under which they can compete with fast chemical iron(II) oxidation by oxygen.

**Editor:** Tillmann Lueders

## ABSTRACT

The classical approach for the cultivation of neutrophilic microaerophilic Fe(II)-oxidizing bacteria is agar-based gradient tubes where these bacteria find optimal growth conditions in opposing gradients of oxygen (O₂) and dissolved Fe(II) (Fe²⁺). The goals of this study were to quantify the temporal development of O₂ and Fe²⁺ concentrations over time, to compare abiotic and microbially inoculated tubes and to test the suitability of different Fe(II)-sources for the cultivation of freshwater and marine microaerophilic Fe(II)-oxidizers. O₂ and Fe²⁺ gradients were monitored on a high spatial resolution as a function of time applying amperometric and voltammetric microsensors. Fe(II)-oxidizers could be cultivated well with FeS and zero-valent iron powder as Fe(II)-source, but FeCO₃ and FeCl₂ are extremely sensitive for this application. Fe(III) minerals accumulated in inoculated tubes within the first days in regions with an O₂ concentration of 20–40 $\mu$M and were confirmed to be related to bacterial growth. Microbial Fe(II) oxidation could compete only for the first days with the abiotic reaction after which heterogeneous Fe(II) oxidation, catalyzed by Fe(III) minerals, dominated. Our results imply that transfer of cultures to fresh tubes within 48–72 h is crucial to provide optimal growth conditions for microaerophilic Fe(II)-oxidizers, particularly for the isolation of new strains.

**Keywords:** microaerophilic iron(II) oxidation; iron(II)-oxidizing bacteria; iron cycling; gradient tubes

## INTRODUCTION

Iron is one of the most dominant chemical elements in the continental crust (Taylor 1964), and it is an important component of several geological, mineralogical, environmental and microbial processes. As an essential micronutrient, iron is integrated in many cellular compounds and has high relevance in modern and ancient, as well as in extraterrestrial environments. In the environment, iron is often involved in biotic and abiotic redox processes (Melton *et al.* 2014) and mainly occurs in two redox states: as oxidized ferric iron (Fe(III)) or as reduced ferrous iron (Fe(II)). At circumneutral pH, Fe(III) is poorly soluble (Cornell and Schwertmann 2003) and normally occurs as solid Fe(III)

minerals; soluble Fe(III) ($Fe^{3+}$), either, freely dissolved, or more often complexed with organic molecules, is only present at very low concentration in the range of $10^{-6}$–$10^{-9}$ M (Taillefert Bono and Luther 2000; Kappler and Straub 2005). In contrast, Fe(II) is more soluble and therefore more bioavailable for organisms (Melton *et al.* 2014); however, at neutral pH, it is rapidly chemically oxidized in the presence of oxygen ($O_2$) (Davison and Seed 1983; Stumm and Morgan 1996). During homogenous abiotic Fe(II) oxidation, dissolved Fe(II) ($Fe^{2+}$) is oxidized by dissolved $O_2$ and other intermediate oxygen species that are formed during the stepwise reduction of $O_2$ (Melton *et al.* 2014). The formed $Fe^{3+}$ will instantaneously react with water and precipitate as the Fe(III) oxyhydroxide mineral with a rusty-orange color (Emerson and Weiss 2004). These mineral precipitates serve as catalyst for further chemical Fe(II) oxidation, an autocatalysis reaction also called heterogeneous Fe(II) oxidation (Tamura Goto and Nagayama 1976; Rentz *et al.* 2007). Both, heterogeneous and homogeneous Fe(II) oxidation run in parallel; however, heterogeneous Fe(II) oxidation is faster so that homogeneous Fe(II) oxidation becomes of minor importance (Stumm and Sulzberger 1992; Park and Dempsey 2005) once sufficient iron oxyhydroxides are formed. Besides the chemical redox transformations, microbes contribute to a large extent to the cycling between the redox states of iron (Weber Achenbach and Coates 2006; Konhauser Kappler and Roden 2011). Fe(III)-reducing bacteria can reduce Fe(III) to Fe(II) under anoxic conditions using electron donors such as hydrogen ($H_2$), acetate or lactate (Kashefi and Lovley 2000; Lovley *et al.* 2011). On the other hand, Fe(II) can be oxidized enzymatically by photoautotrophic Fe(II)-oxidizers using light energy with bicarbonate as electron acceptor and carbon source (Widdel *et al.* 1993; Hegler *et al.* 2008). Other microorganisms couple Fe(II) oxidation to nitrate ($NO_3^-$) reduction under anoxic conditions (Straub *et al.* 1996). However, most nitrate-reducing Fe(II)-oxidizers need an additional organic cosubstrate to continually oxidize Fe(II) to Fe(III) (Straub *et al.* 1996; Klueglein *et al.* 2014). Microaerophilic Fe(II)-oxidizers can oxidize Fe(II) as a sole electron donor using $O_2$ as electron acceptor for lithotrophic growth (Emerson and Moyer 1997). Bacteria that are capable of aerobic neutrophilic Fe(II) oxidation have to compete with the abiotic reaction due to the short half-life of $Fe^{2+}$ in oxygenated water (Singer and Stumm 1970; Stumm and Morgan 1996; Hegler *et al.* 2012). Under microoxic conditions, the half-life of Fe(II) can be more than 300 times longer (Roden *et al.* 2004). It was shown that abiotic Fe(II) oxidation dominated at $O_2$ concentrations of 275 $\mu$M, while at 50 $\mu$M and below, microbial Fe(II) oxidation was faster than the abiotic reaction (Druschel *et al.* 2008). As a result neutrophilic Fe(II)-oxidizers are often restricted to live in areas with a constant source of Fe(II) and low $O_2$ concentrations where the biotic oxidation rates can outcompete the abiotic rates (Emerson and Weiss 2004).

The demands of microaerophilic Fe(II)-oxidizers in combination with the kinetics of abiotic Fe(II) oxidation make cultivation in laboratory setups difficult. The traditional technique used is the cultivation of microaerophilic Fe(II)-oxidizers in agar-stabilized gradient tubes with opposing gradients of $Fe^{2+}$ and $O_2$ (Emerson and Moyer 1997; Sobolev and Roden 2001; Emerson and Moyer 2002; Neubauer Emerson and Megonigal 2002; Edwards *et al.* 2003; Weiss *et al.* 2003; Emerson and Floyd 2005; Weiss *et al.* 2007; Druschel *et al.* 2008; Swanner Nell and Templeton 2011; Lin *et al.* 2012; MacDonald *et al.* 2014; Laufer *et al.* 2016). By analyzing $Fe^{2+}$ and $O_2$ concentrations at high spatial resolution as well as the development of the competitive pressure between biotic and abiotic Fe(II) oxidation, conclusions about optimal substrate demands and habitat limitations by kinetic constraints can be drawn. So far, the geochemical conditions in

gradient tubes were examined only in a few studies (Druschel *et al.* 2008; Swanner Nell and Templeton 2011). However, spatially highly resolved measurements as a function of time are missing. These measurements are important to determine the optimal time point for transfer of cultures, which is a critical parameter for isolation and continuous cultivation. Also, different Fe(II)-sources (Emerson and Moyer 1997; Druschel *et al.* 2008; Swanner Nell and Templeton 2011; Emerson *et al.* 2013; MacDonald *et al.* 2014) for gradient tubes are mentioned in the literature, but they have not been compared systematically in terms of suitability for growth of microaerophilic Fe(II)-oxidizers.

Therefore, the goals of this study were (i) to test and compare iron sulfide (FeS), iron carbonate ($FeCO_3$), zero-valent iron powder (ZVI) and iron chloride ($FeCl_2$) as Fe(II)-sources for the suitability of growth of selected freshwater and marine neutrophilic microaerophilic Fe(II)-oxidizing bacteria, (ii) to quantify $O_2$ and $Fe^{2+}$ profiles as a function of time at high spatial resolution using amperometric and voltammetric microsensors and (iii) to identify exact physico-chemical conditions for optimal growth to give recommendations and improve isolation and cultivation of new microaerophilic Fe(II)-oxidizers.

## MATERIAL AND METHODS

### Cultivation of bacteria

Gradient tube preparation was based on Emerson and Floyd (2005). Opposing gradients of $Fe^{2+}$ and $O_2$ in screw-cap vials (8 ml, 61 × 16.6 mm) were established by adding 750 $\mu$l of a 1% (wt/vol) high-melt agarose containing a plug (height approx. 5 mm) of FeS, $FeCO_3$, $FeCl_2$ or by spreading ZVI (200 mesh; metal basis; Alfa Aesar, Ward Hill, MA) at the bottom of the glass vial, in this latter case, no high melt agarose was used. FeS was synthesized in a modified way as described by Kucera and Wolfe (1957) by reacting equimolar amounts of sulfide with Fe(II) using $Na_2S \times 9H_2O$ and $FeSO_4 \times 7 H_2O$. After being separately dissolved in 80°C anoxic deionized water (Milli-Q Integral System, Merck Millipore), the $FeSO_4$ solution was quickly added to the $Na_2S$ solution resulting in instantaneous precipitation of FeS. This precipitate was allowed to settle overnight. The supernatant of the settled FeS was washed two to three times with each time 2 L warm anoxic distilled water (∼80–90°C) until the water above the FeS looked clear and had a pH around neutrality.

$FeCO_3$ was synthesized by reacting equimolar amounts of Fe(II) chloride with sodium bicarbonate. The Fe(II)-source was overlaid by 3.75 ml of a 0.15% (wt/vol) low-melt agarose containing semisolid mineral salt medium of either modified Wolfe's mineral medium (MWMM) or artificial seawater medium (ASW), including 1 ml $L^{-1}$ of 7-vitamin- (Pfennig 1978), SL10- (Tschech and Pfennig 1984) and selenite-tungstate (Tschech and Pfennig 1984) solutions. The media were buffered with 10 mM bicarbonate and the pH was adjusted to 6.5 by stepwise addition of 1 M HCl and constantly checking the pH with a pH electrode. MWMM contained of the following salts per liter: 0.1 g $NH_4Cl$, 0.2g $MgSO_4 \times 7 H_2O$, 0.1 g $CaCl_2 \times 2 H_2O$ and 0.05 g $K_2HPO_4$. Per liter, ASW was composed of 17.3 g NaCl, 8.6 g $MgCl_2 \times 6 H_2O$, 0.025 g $MgO_4 \times 7 H_2O$, 0.996 g $CaCl_2 \times 2 H_2O$, 0394 g KCl, 0.059 g KBr, 0.25 g $NH_4Cl$ and 0.05 g $K_2HPO_4$. For comparison, a batch of $FeCO_3$ was prepared following the protocol of Hallbeck, Ståhl and Pedersen (1993) using $Fe(NH_4)SO_4$ and $Na_2CO_3$ instead of $FeCl_2$ and $NaHCO_3$ for synthesis. The tubes were prepared anoxically and opened the first time during inoculation with bacteria one day after preparation, leading to an air-filled headspace.

154

The tubes were inoculated under sterile conditions with 50 $\mu$l, which was a tenfold diluted sample from another gradient tube and incubated at 20°C in the dark. An Fe(II)-oxidizing culture dominated by BETAPROTEOBACTERIA (belonging to GALLIONELLA sp.) and with minor traces of ALPHAPROTEOBACTERIA (belonging to *Azorhizobium* sp.) enriched from a freshwater sediment (Lake Constance, N 47° 41ᴶ42.63ᴶᴶ; E 9° 11ᴶ 40.29ᴶᴶ, Germany) was selected and a culture of a marine Fe(II)-oxidizer, belonging to the ZETAPROTEOBACTERIA (98% homolog to MARIPRofundus sp. M34), isolated from sediment from Aarhus Bay (N 56° 16.811ᴶ; E 010° 28.056ᴶ; Baltic Sea, Denmark) was used as marine Fe(II)-oxidizer representative (Laufer *et al.* 2016). The negative control was treated in a similar way without inoculation. Growth of bacteria was defined as positive if brownish accumulations that spread out from the inoculum could visually be observed and clear differentiation from the negative control could be done (Emerson and Floyd 2005). This will henceforth be called Fe(III) mineral accumulations.

## Cell counts

Bacterial cells in the top layers of freshly prepared MWMM with FeS gradient tubes were counted by fluorescent microscopy in triplicates at each time point to demonstrate bacterial growth. For cell counts, the top layer of the gradient tubes was centrifuged and the cell-mineral pellet was resuspended in 1.5 ml of 10 mM bicarbonate buffer. Paraformaldehyde at a final concentration of 2% was added and the samples were stored at 4°C until analysis. One ml of this suspension was added to 9 ml of oxalate solution (28 g L$^{-1}$ ammonium oxalate and 15 g L$^{-1}$ oxalic acid) to dissolve the Fe(III) minerals and further tenfold diluted in oxalate solution. Ten ml were then filtered onto a white GVWP filter (Millipore, 0.22 $\mu$m) and 1 $\mu$g ml$^{-1}$ DAPI stain was used to stain the cells. Cells were counted using a Leica DM5500B fluorescent microscope using the A4 filter.

## Geochemical measurements

Geochemical measurements were always performed in the same gradient tubes using microsensors at 20°C. For each setup, two gradient tubes were inoculated and two additional gradi- ent tubes were prepared as negative control. Concentration pro- files were performed only once in every gradient tube at each time point to disturb the system as little as possible. O₂ con- centration depth profiles were measured with a 100 $\mu$m tip di- ameter amperometric Clark-type O₂ microelectrode (Unisense, Aarhus, Denmark) as described by Revsbech (1989). A two-point calibration was done in air-saturated and in anoxic water. Ver- tical O₂ profiles in gradient tubes were recorded in triplicates in depth intervals of 0.5 mm using a motorized micromanipula- tor (Unisense) and used for the calculation of O₂ consumption rates using the program PROFILE 1.0 (Berg Risgaard-Petersen and Rysgaard 1998). The O₂ concentration measured at the top of the top layer (depth 0 mm) was chosen as first boundary condition,

an O₂ flux at the bottom of the tube (21 mm) of 0 $\mu$mol dm$^{-2}$ s$^{-1}$ was set as second boundary condition and an O₂ diffusion coef-

ficient of 2.4·10$^{-9}$ m² s$^{-1}$ (McMillan and Wang 1990) was used.

All microsensor data for measurements in gradient tubes were plotted as follows: depth 0 mm refers to the atmo- sphere/top layer (agar) interface, and the surface of the Fe(II)- source is located at approx. 21 mm. The time between the single measurement time points are 1 ($t_0 - t_3$) and 3 days ($t_3 - t_6$).

Fe²⁺ concentration depth profiles were determined by

voltammetry using a DLK-100A potentiostat (Analytical Instrument Systems, Flemington, NJ) with a standard three-

electrode system. The working electrode, a glass-encased 100 $\mu$m gold amalgam (Au/Hg) electrode, was constructed as described by Brendel and Luther (1995). The reference electrode was a solid-state Ag wire coated in Ag/AgCl; a Pt wire was used as counter electrode. Working and reference electrode were re- plated before every daily measurement. Fe²⁺ calibrations were done using Mn²⁺ standards with subsequent conversions to Fe²⁺ concentrations using the pilot ion method (Brendel and Luther 1995; Slowey and Marvin-DiPasquale 2012). A con- version factor from Mn²⁺ to Fe²⁺, called pilot ion factor was determined to be 1.3. For this, a proper calibration for Fe²⁺ and Mn²⁺ was performed in an anoxic glovebag to prevent any Fe²⁺ oxidation. The slopes of the calibrations were then divided by each other (Mn²⁺ /Fe²⁺ ). The determined conversion factor was later used for any calibrations that have been performed with Mn²⁺ prior to measurements. Cyclic voltammetry was performed for the detection of Mn²⁺ and Fe²⁺ at 1000 mV s$^{-1}$between −0.1 and −2.0 V (freshwater) or −1.8 V (seawater) vs Ag/AgCl. An initial conditioning step of applying −0.05 V for 5 s followed by holding −0.9 V for 10 s were set to remove previously deposited species (Brendel and Luther 1995). Af- ter the conditioning steps, the electrode equilibrated for 5 s before scan potentials were applied. 10 scans were run at each measurement point, the final 3 voltammograms were integrated using VOLTINT program for Matlab $\mathcal{S}$ (Bristow and Taillefert 2008). Data were recorded in 4 mm depth intervals using a manual micromanipulator (Unisense, Aarhus, Den- mark). Fe²⁺ consumption rates were not calculated because the low amount of data points led to statistically invalid results.

## Energetic and kinetic calculations

The overall reaction of homogeneous oxidation of Fe²⁺ by dis- solved O₂ to Fe³⁺ and further precipitation as Fe(III) hydroxide can be summarized as (Roden *et al.* 2004)

$$Fe^{2+} + 0.25\,O_2 + 2.5\,H_2O \rightarrow Fe(OH)_3 + 2\,H^+ \qquad (1)$$
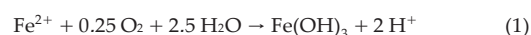
Values of Gibbs free energy $\mathit{O}G$ of this reaction in different depths and time points were calculated according to

$$\mathit{O}G = \mathit{O}G_0 + R \cdot T \cdot In\mathrm{Q} \qquad (2)$$

with $\mathit{O}G_0$ as the standard Gibbs free energy of the reaction (−109 kJ mol$^{-1}$ (Roden *et al.* 2004)), $R$ as the ideal gas constant, $T$ as the temperature in Kelvin and $Q$ as the activity product of the reaction.

Considering homogeneous Fe²⁺ oxidation only, the kinetic rate law for neutral solutions then is

$$-\frac{d[Fe^{2+}]_{hom}}{dt} = k \cdot [Fe^{2+}] \qquad (3)$$

with $k = k_0 \cdot [O_2] \cdot [OH^-]^2$ and the universal rate constant for homogeneous Fe²⁺ oxidation by O₂ $k_0$ being 2.3 · 10$^{-14}$ mol³ L$^{-3}$s$^{-1}$ at 25° C (Tamura Goto and Nagayama 1976). The total general rate equation of Fe²⁺ oxidation considering both, homogenous and heterogeneous oxidation, was found to be (Tamura Goto and Nagayama 1976)

$$-\frac{d[Fe^{2+}]}{dt} = (k + k' \cdot [Fe(III)]) \cdot [Fe^{2+}] \qquad (4)$$
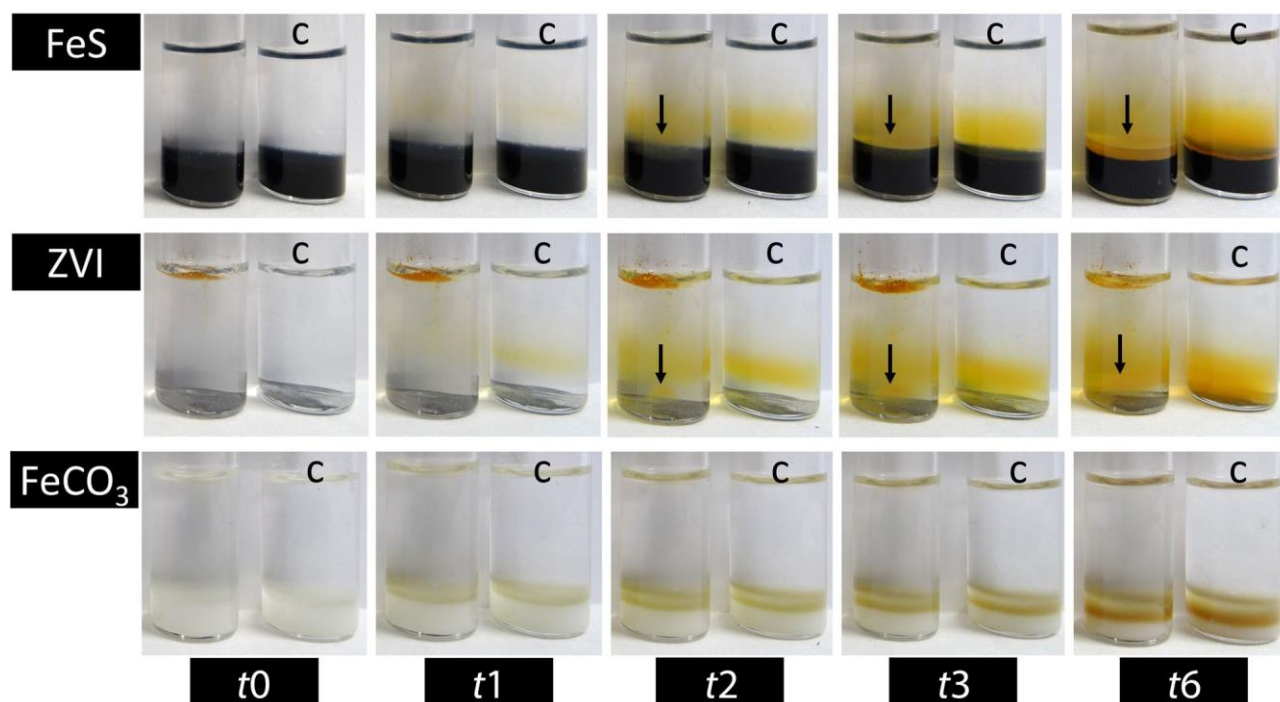
**Figure 1.** Images of the temporal development of negative control (c) and inoculated MWMM gradient tubes with an enrichment of freshwater microaerophilic Fe(II)-oxidizers from Lake Constance, Germany, with the Fe(II)-sources FeS, ZVI and FeCO₃ starting at the day of inoculation ($t_0$). Growth in FeS and ZVI gradient tubes is indicated by formation of sharp orange Fe(III) mineral accumulations within or below the orange colored top layer of the gradient tubes highlighted in the image with an arrow. Neither growth nor abiotic Fe(II) oxidation could be observed in FeCO₃ tubes within the top layer, only directly on the FeCO₃ plug at the bottom, indicated by a color change to brown. ($t_1$ = day 1, $t_2$ = day 2, $t_3$ = day 3 and $t_6$ = day 6 after inoculation)

Heterogeneous $Fe^{2+}$ oxidation is accelerated by Fe(III) minerals (Tamura Kawamura and Hagayama 1980). The amount of Fe(III) hydroxide precipitated is equal to the amount of oxidized $Fe^{2+}$ (Tamura Goto and Nagayama 1976); therefore, [Fe(III)] in the gradient tube top layer at any time can be calculated by

$$[Fe\,(III)] = [Fe^{2+}]_{t0} - [Fe^{2+}] \tag{5}$$

The rate law of heterogeneous $Fe^{2+}$ oxidation can be described as

$$-\frac{d[Fe^{2+}]_{het}}{dt} = k' \cdot [Fe(III)] \cdot [Fe^{2+}] \tag{6}$$

with $k' = \frac{k_{s,0} \cdot [O_2] \cdot K}{[H^+]}$ and the specific rate constant for the heterogeneous reaction $k_{s,0}$ being 73 mol $L^{-1} s^{-1}$ (Tamura Goto and Nagayama 1976) and the dimensionless adsorption constant of ferrous iron on ferric hydroxide $K$ being $10^{-4.85}$ (Sung and Morgan 1980). Additionally, half-life for $Fe^{2+}$ oxidation in the gradient tubes was calculated by equations (7) and (8) for homogenous or heterogeneous $Fe^{2+}$ oxidation, respectively

$$t_{\frac{1}{2},hom} = \frac{\ln(2)}{k} \tag{7}$$

$$t_{\frac{1}{2},het} = \frac{\ln(2)}{k' \cdot [Fe(III)]} \tag{8}$$

The energetic and kinetic calculations were exemplarily done for gradient tubes containing MWMM and FeS as Fe(II)-source.

## RESULTS

### Comparison of different Fe(II)-sources for suitability of growth of microaerophilic Fe(II)-oxidizers

We found that both FeS and ZVI are suitable Fe(II)-sources for the cultivation of freshwater and marine microaerophilic Fe(II)-oxidizers in opposed $Fe^{2+}$ -$O_2$ gradient tubes using agar as a stabilizing agent. In these gradient tubes, a diffuse orange-brownish smear was observed 1 day after inoculation in the center of the top layer in inoculated as well as in negative control tubes (for both MWMM and ASW medium) (Fig. 1). First distinct Fe(III) mineral accumulations appeared 2–3 days (freshwater Fe(II)-oxidizers) and 5–6 days after inoculation (marine

Fe(II)-oxidizers), respectively. Cell counts in freshly prepared gradient tubes containing MWMM and FeS clearly demonstrated an increasing cell number and thus microbial growth in the area of

the distinct Fe(III) mineral accumulations (Fig. 2). Depending on the identity of Fe(II)-source and the identity of the inoculated bacteria, the shape and the height of the formed distinct Fe(III) mineral accumulation (often described in the literature as band formations) can be different (Fig. 3), including flat plane (Fig. 3A and D), funnel-like (Fig. 3C and E), curved plane (Fig. 3B) and cloud structures (Fig. 3F).

In addition to these setups, ZVI was stabilized in a 1% high melt agarose bottom layer so the ZVI was not in direct contact with the low melt agarose where the bacteria grew. In this case, accumulations of Fe(III) minerals were observed only in minor amounts at the surface of the bottom layer (image not shown). Similar to the gradient tubes that contained FeCO₃ (mineral prepared following two different protocols) and FeCl₂ as Fe(II)-source, this setup did not reveal significant growth of Fe(II)-oxidizing bacteria (data not shown). The Fe(II)-sources in
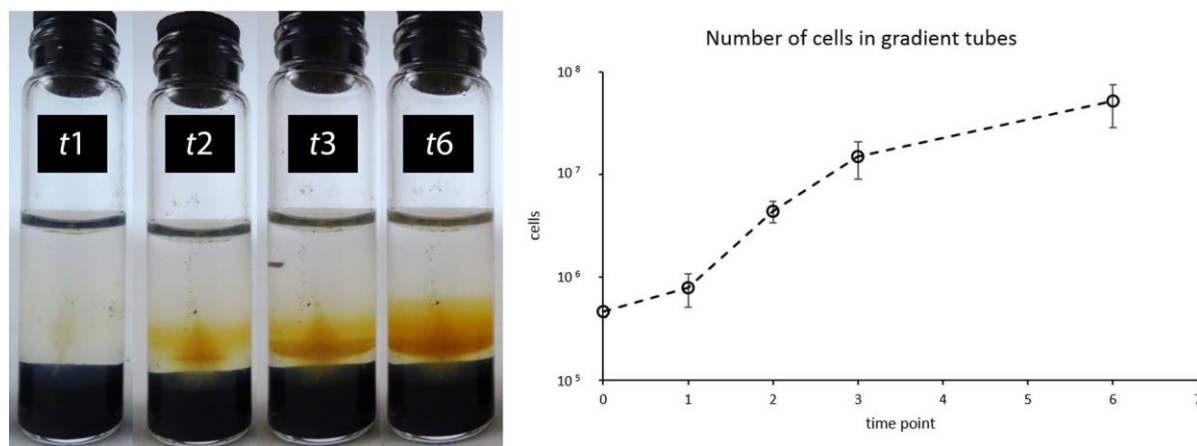
**Figure 2.** Cell numbers in gradient tubes containing MWMM and a FeS bottom layer at different time points (($t_1$ = day 1, $t_2$ = day 2, $t_3$ = day 3 and $t_6$ = day 6 after inoculation). An image showing the development of the Fe(III) mineral accumulations in the top layer is shown on the left side. The gradient tubes for cell counts were freshly prepared and are comparable to the tubes, in which the geochemical $O_2$ and $Fe^{2+}$ measurements were performed in. Error bars show the standard deviation of the counted triplicates.

gradient tubes that contained $FeCO_3$ as bottom layer got oxidized within a day after inoculation (Fig. 1) and therefore did not show any $Fe^{2+}$ gradients across the top layer. A similar absence of $Fe^{2+}$ gradients was obtained for tubes that had been kept anoxically for 2 days in order to provide optimal conditions for the establishment of a pronounced $Fe^{2+}$ gradient across the top layer. Spectrophotometric quantification of dissolved Fe(II) (ferrozine assay) revealed only low concentrations of $Fe^{2+}$ compared to water saturation (approximately 50 $\mu$M, data not shown). The mineralogical identity of $FeCO_3$ was verified by Mössbauer spectroscopy analysis (data not shown). $FeCl_2$ gradient tubes were set up with different concentrations in the bottom layer (1 mM, 500 $\mu$M, 200 $\mu$M). In none of these tubes were Fe(III) mineral accumulations observed. A summary of the observations is listed in Table 1.

## Geochemical depth profiles

Exemplary $O_2$ concentration depth profiles from gradient tubes inoculated with an enrichment of freshwater Fe(II)-oxidizers from Lake Constance (Fig. 3A and B) or with a marine isolate from Aarhus Bay (Fig. 3C) are shown in Fig. 4. The $O_2$ concentration decreased in all tubes towards the bottom of the tube. No $O_2$ reached the bottom of tubes during the day of inoculation ($t_0$) (Fig. 4). $O_2$ concentrations increased over time over the whole depth until stabilization beginning at $t_2$ (day 2; ZVI tubes) or $t_3$ (day 3; FeS tubes). At $t_2$, the first distinct Fe(III) mineral accumulations were formed in the inoculated FeS freshwater tubes at a depth of around 16 mm, corresponding to an $O_2$ concentration of approx. 20 $\mu$M. No $O_2$ was detected at $t_2$ below these accumulations, which were close to the Fe(II)-source at the bottom of the tube (Fig. 4A). In the ZVI freshwater tubes, Fe(III) minerals also accumulated at $t_2$ at a depth of approximately 18 mm. The temporal shifts of the $O_2$ distribution throughout the tubes containing ASW (Fig. 4C and D) mirror the trend that was observed in tubes containing MWMM (Fig. 4A and B). In all tubes the spatial $O_2$ distribution profiles shift from a concave to a linear shape over time, which reflects the shift of dominant $O_2$ consumption zones from top to bottom of the tubes (Fig. 5). $O_2$ concentrations were slightly lower in ASW setups. During the entire experiment, significant differences in $O_2$ concentrations between negative control tubes and inoculated tubes were

observed only during short time frames, e.g. at $t_2$ in freshwater FeS tubes (Fig. 4A).

Emerson and Moyer (1997) noted a depletion of $O_2$ in the headspace of inoculated gradient tubes. Renewing the headspace by opening the tube again led to the formation of a second growth band consisting of Fe(III) mineral accumulations below the already grown first band. In the present study, the tubes were opened daily to measure the $O_2$ concentrations, which led to a frequent regeneration of the headspace in the tubes. To ensure that the renewed headspace had no influence on the $O_2$ concentrations in the top layer, additional tubes were prepared that were all inoculated at the same time and just opened once again when they were measured. They did not have significantly lower $O_2$ concentrations than the tubes that were opened daily for measurements (data not shown). This also shows that no significant additional $O_2$ entered the top layer by the microelectrode insertion or removal.

$O_2$ consumption rates for gradient tubes containing MWMM and FeS are shown in Fig. 5. Consumption rates in the other gradient tubes that have been used for measurements were in a similar order of magnitude (0–12 nmol $L^{-1}\,s^{-1}$). Over time, the $O_2$ consumption shifted in all gradient tubes down towards the bottom of the tube. After 3–4 days, $O_2$ was only consumed below 15 mm in the top layer with $O_2$ consumption rates of below 10 nmol $L^{-1}\,s^{-1}$. No significant differences in $O_2$ consumption were observed between negative control tubes and inoculated tubes.

Exemplary $Fe^{2+}$ concentration depth profiles are shown in Fig. 6. The highest $Fe^{2+}$ concentrations were measured at the bottom of all tubes with decreasing concentrations upwards. At $t_0$, $Fe^{2+}$ concentrations of about 2.5 $\mu$M were measured directly above the bottom layer in freshwater FeS tubes (Fig. 6A). Fe(III) mineral accumulations were visually observed starting at $t_2$. First mineral accumulation appeared in the center of the tube (right at the inoculation funnel) and spread in all directions with $Fe^{2+}$ concentrations of approximately 300–400 $\mu$M. From $t_0$ to $t_2$, an additional peak in the voltammograms at $E_{1/2}$ = −1.1 V vs. Ag/AgCl in depths below 12 mm depth was detected in the cathodic wave that was identified as $FeS_{(aq)}$ signal. These data could not be quantified due to a lack of standards for $FeS_{(aq)}$ (Davison Buffle and DeVitre 1998; Luther *et al.* 2003; Ciglenecki
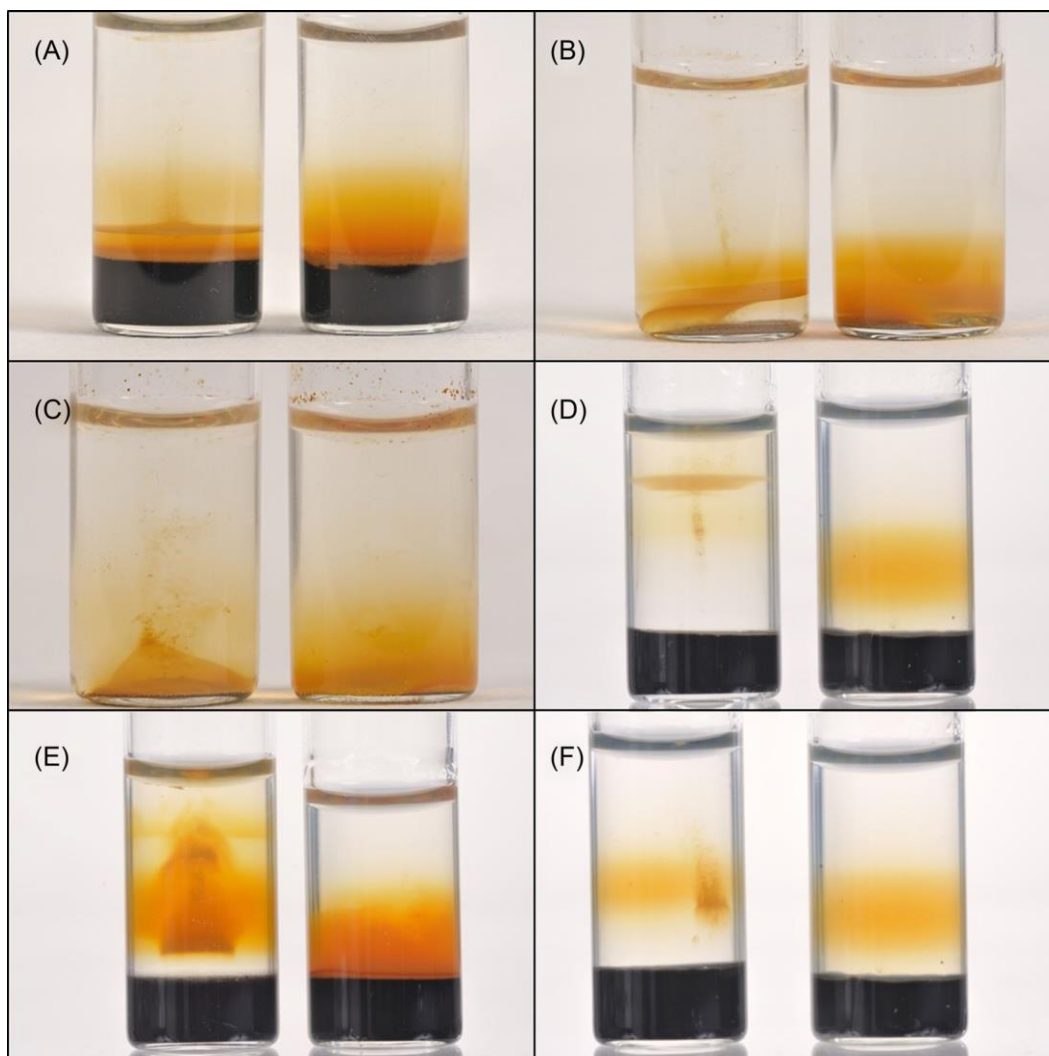
**Figure 3.** Images of inoculated (left tube) and negative control gradient tubes (right tube) with microaerophilic Fe(II)-oxidizers from different field sites, media and Fe(II)-sources at different time points. (**A**) freshwater lake sediment enrichment (Lake Constance), MWMM, FeS, 8 days after inoculation; (**B**) freshwater lake sediment enrichment (Lake Constance), MWMM, ZVI, 8 days after inoculation; (**C**) marine sediment isolate (Aarhus Bay, Denmark), ASW, ZVI, 31 days after inoculation; (**D**) freshwater ditch, MWMM, FeS, 3 days after inoculation; (**E**) sample from peat canal, MWMM, FeS, 17 days after inoculation; (**F**) isolate from microbial mat in a mine (Black Forest, Germany), MWMM, FeS, 3 days after inoculation. The dimensions of the tube are: height 6.1 cm, diameter 1.7 cm.

*et AL.* 2014). This leads to some underestimation of total dissolved $Fe^{2+}$ concentrations in these tubes. Similar to the FeS tubes, Fe(III) mineral accumulations in freshwater ZVI tubes were observed from $t_2$ in regions with about 300–400 $\mu$M $Fe^{2+}$. In gradient tubes containing ASW and a FeS bottom layer, a small extent of Fe(III) mineral accumulations was observed at $t_6$ directly at the bottom of the tubes, where $Fe^{2+}$ concentrations of approximately 100–200 $\mu$M were measured. No significant differences in measured $Fe^{2+}$ concentrations between negative control tubes and inoculated tubes were measured. In gradient tubes with ASW and ZVI as Fe(II)-source, first Fe(III) mineral accumulations appeared at $t_1$ in regions with about 500–700 $\mu$M $Fe^{2+}$. In general, $Fe^{2+}$ concentrations decreased over the time of the experiment. Higher $Fe^{2+}$ concentrations were generally measured in gradient tubes using FeS as Fe(II)-source. The gradients in negative control tubes and inoculated tubes were with some exceptions very similar (Fig. 6).

Calculations using Gibbs free energy show potentially higher energy for the metabolism of Fe(II)-oxidizing bacteria during Fe(II) oxidation at greater depths within the top layers of

the gradient tubes (Fig. 7A). However, the amount of energy that can be obtained decreases with time. Kinetic calculations reveal higher rates of homogeneous Fe(II) oxidation near the top layer headspace interface (depth 0 mm) due to higher $O_2$ concentrations and consequently a shorter half-life of $Fe^{2+}$ in solution (Fig. 7B and C). A comparison between homogeneous and heterogeneous Fe(II) oxidation rates in 16 mm depth of the top layer exhibit a rapid overtaking of the heterogeneous oxidation leading to a dramatic decrease of $Fe^{2+}$ half-life times from $t_1$ in this depth (Fig. 7D).

## DISCUSSION

### Suitability of different Fe(II)-sources for cultivation in gradient tubes

In this study, we have compared the suitability of the different Fe(II)-sources FeS, $FeCO_3$, ZVI and $FeCl_2$ for the cultivation of freshwater and marine microaerophilic Fe(II)-oxidizers in agar-stabilized gradient tubes. Although successful growth has been

**Table 1.** Summary of observations in opposed gradient tubes with different Fe(II)-sources.

| Fe(II)-source | Diffuse orange smear in the top layer | Characteristic appearance of the Fe(III) mineral accumulations |
|---|---|---|
| FeS | - Started 1 day after inoculation in all tubes<br>- Started in the center of the top layer<br>- Extent increased towards top and bottom | MWMM: observed 2 days after inoculation as sharp flat band a few mm above the bottom layer<br><br>ASW: observed 5 days after inoculation as cloudy, colony-like accumulations close to or directly on the bottom layer |
| ZVI without additional agarose plug | - Started 1 day after inoculation in all tubes<br>- Started in the center of the top layer<br>- Extend increased to top and bottom | MWMM: observed 2 days after inoculation as sloping bands a few mm above the ZVI powder<br><br>ASW: observed 5–6 days after inoculation as sloping bands almost directly on ZVI powder |
| ZVI inserted in bottom layer | - Started 3 days after inoculation in all tubes<br>- Only in regions close to the bottom layer | MWMM: observed 3 days after inoculation as darker orange color compared to the negative control directly on the surface of the bottom layer<br><br>ASW: observed 5 days after inoculation starting as small colonies directly on the surface of the bottom layer |
| FeCO$_3$ | Not observed | No mineral accumulations were formed |
| FeCl$_2$ | Not observed | No mineral accumulations were formed |

reported in the literature for all Fe(II)-sources (Emerson and Moyer 1997; Sobolev and Roden 2001; Neubauer Emerson and Megonigal 2002; Edwards *et al.* 2003; Weiss *et al.* 2007; Druschel *et al.* 2008; McBeth *et al.* 2011; Swanner Nell and Templeton 2011; Kato *et al.* 2012; Kato *et al.* 2013; MacDonald *et al.* 2014; Laufer *et al.* 2016), in the present study we have only observed the formation of orange Fe(III) (oxyhydr)oxide minerals using FeS and ZVI. In FeCl$_2$ and FeCO$_3$ tubes, no diffusion of Fe$^{2+}$ was observed into the top layer, leading to the lack of the orange band and no growth of microaerophilic Fe(II)-oxidizers. We could show that FeCO$_3$ and FeCl$_2$ are highly sensitive in handling with respect to stability and oxygen sensitivity. Minor variations in handling and preparation cause failure of the method. Rapid oxidation directly at the Fe(II) plug confirmed that chemical oxidation by O$_2$ prevents the establishment of an Fe$^{2+}$ gradient throughout these FeCl$_2$ and FeCO$_3$ tubes. These observations are in agreement with geochemical properties of these Fe(II) phases. The FeCO$_3$ solubility at room temperature and low ionic strength has been shown to be in the range of $3.72 \times 10^{-11}$ to $9.33 \times 10^{-12}$ mol$^2$ L$^{-2}$ (Sun Nešić and Woollam 2009). The fast rate of chemical Fe$^{2+}$ oxidation, combined with the low solubility of FeCO$_3$ and low diffusion of Fe$^{2+}$ ($0.719 \times 10^{-9}$ m$^2$ s$^{-1}$ (Lide 2008)) leads to rapid depletion of Fe$^{2+}$ in the top layer of gradient tubes. The solubility product of FeS has been determined to be significantly higher, in the range of $10^{-2.95}$ (amorphous FeS) (Davison 1991) to $10^{-3.5}$ (Rickard and Luther 2007). Increasing solubility of the Fe(II) minerals enhances the diffusion of Fe$^{2+}$ into the top layer. However, an accurate estimation of released Fe$^{2+}$ to the top layer from the FeS bottom plug is impossible, as the mineral ageing of FeS (including Ostwald ripening and mineral transformation) significantly affects FeS solubility.

Few studies reported on the successful growth of microaerophilic Fe(II)-oxidizers in gradient tubes using FeCO$_3$ as Fe(II)-source (Emerson and Moyer 1997; Swanner Nell and Templeton 2011; Emerson *et al.* 2013; MacDonald *et al.* 2014; Field *et al.* 2016; Chiu *et al.* 2017). In these studies, FeCO$_3$ was synthesized following the protocol of Hallbeck, Ståhl and Pederse (1993). Following this procedure, we revealed similar results compared

to the use of FeCO$_3$ that was prepared after our lab protocol. This confirms the high sensitivity of this mineral for the application as Fe(II)-source for gradient tubes, using Fe(NH$_4$)SO$_4$ and Na$_2$CO$_3$ instead of FeCl$_2$ and NaHCO$_3$ for synthesis. In these studies, it was also noted that only fresh FeCO$_3$ could be used, since the FeCO$_3$ lost potency to release Fe$^{2+}$ within one week.

FeCl$_2$ concentrations used in this study (1 mM, 500 $\mu$M and 200 $\mu$M) were low compared to those used by Sobolev and Roden (2001). They used concentrations that were much too high (50 mM) compared to concentrations observed in natural systems in a 250 ml beaker overlaid by a 125 ml top layer to sustain an environmentally relevant Fe$^{2+}$ flux over the course of the experiment. As the glass vials used in this study only have a small volume of 8 ml, lower Fe(II) concentrations were chosen. Higher FeCl$_2$ concentrations (up to 10 mM) as iron source in the bottom layer were tested for the growth of microaerophilic Fe(II)-oxidizers (data not shown); however, no distinct Fe(III) mineral accumulations (that are linked to biotic Fe(II) oxidation) were observed in any of them. Only a fast color change to orange could be seen in the top layer, which is related to fast chemical oxidation.

A comparison between FeS and ZVI tubes showed that both Fe(II)-sources worked equally well for cultivation of both freshwater and marine microaerophilic Fe(II)-oxidizers. The method to use ZVI as Fe(II)-source in gradient tubes was used for marine strains as the corrosion rates are expected to be higher due to higher ionic strength. However, few studies using ZVI had success with freshwater strains ((Kato *et al.* 2012), this study). In ZVI gradient tubes, distinct Fe(III) mineral accumulations indicating growth of Fe(II)-oxidizers occurred sometimes slightly earlier than in FeS tubes. Finally, the differences in the gradient tubes are dependent on the physico-chemical parameters of the Fe(II)-source and the gradient tube medium. A higher solubility of the Fe(II)-source generally leads to steeper diffusion gradients and consequently to faster diffusion of Fe$^{2+}$ into the top layer.

The position and the shape of the Fe(III) mineral accumulations in FeS tubes inoculated with different bacterial strains varied. Emerson and Floyd (2005) pointed out that every batch of
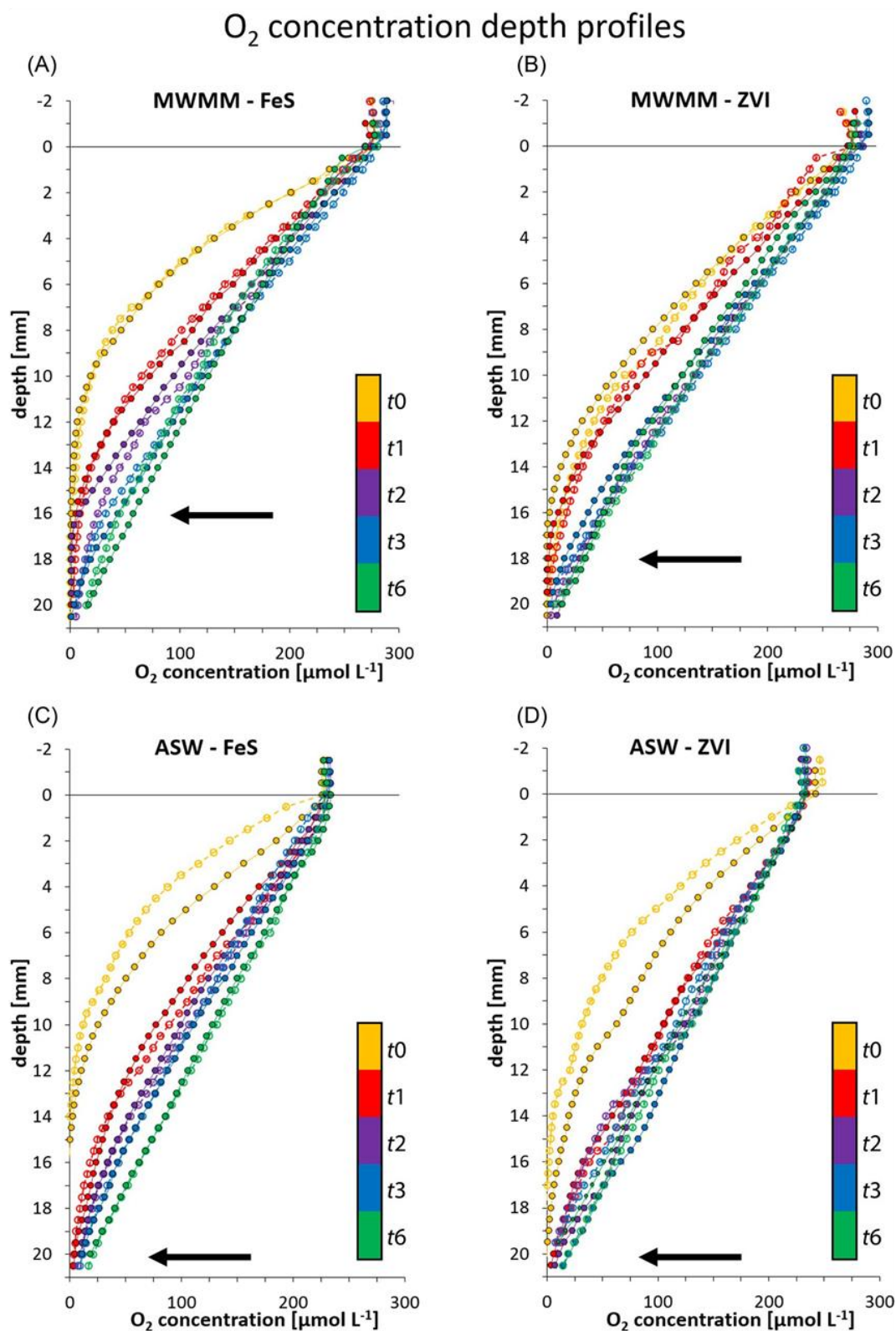
# O₂ concentration depth profiles



**Figure 4.** Selected $O_2$ concentration depth profiles in gradient tubes inoculated with an enrichment of freshwater microaerophilic Fe(II)-oxidizers from Lake Constance, Germany (A,B) or with an isolate of a marine Fe(II)-oxidizer from Aarhus Bay, Denmark (C,D). Open symbols and dashed lines represent negative control tubes, closed symbols and solid lines inoculated tubes. Error bars are not shown as the mean coefficient of variation of all profiles is below 3%. The colors display the different times of measurements starting the day of inoculation ($t_0$). Depth 0 mm shows the headspace-top layer interface; the Fe(II)-source starts in a depth of about 21 mm. The arrow indicates the approximate level where the growth band formed in inoculated tubes. (A) Gradient tubes with MWMM and FeS bottom layer; (B) Gradient tubes with MWMM and ZVI powder at the bottom; (C) Gradient tubes with ASW and FeS bottom layer; (D) Gradient tubes with ASW and ZVI powder at the bottom. ($t_1$ = day 1, $t_2$ = day 2, $t_3$ = day 3 and $t_6$ = day 6 after inoculation)|
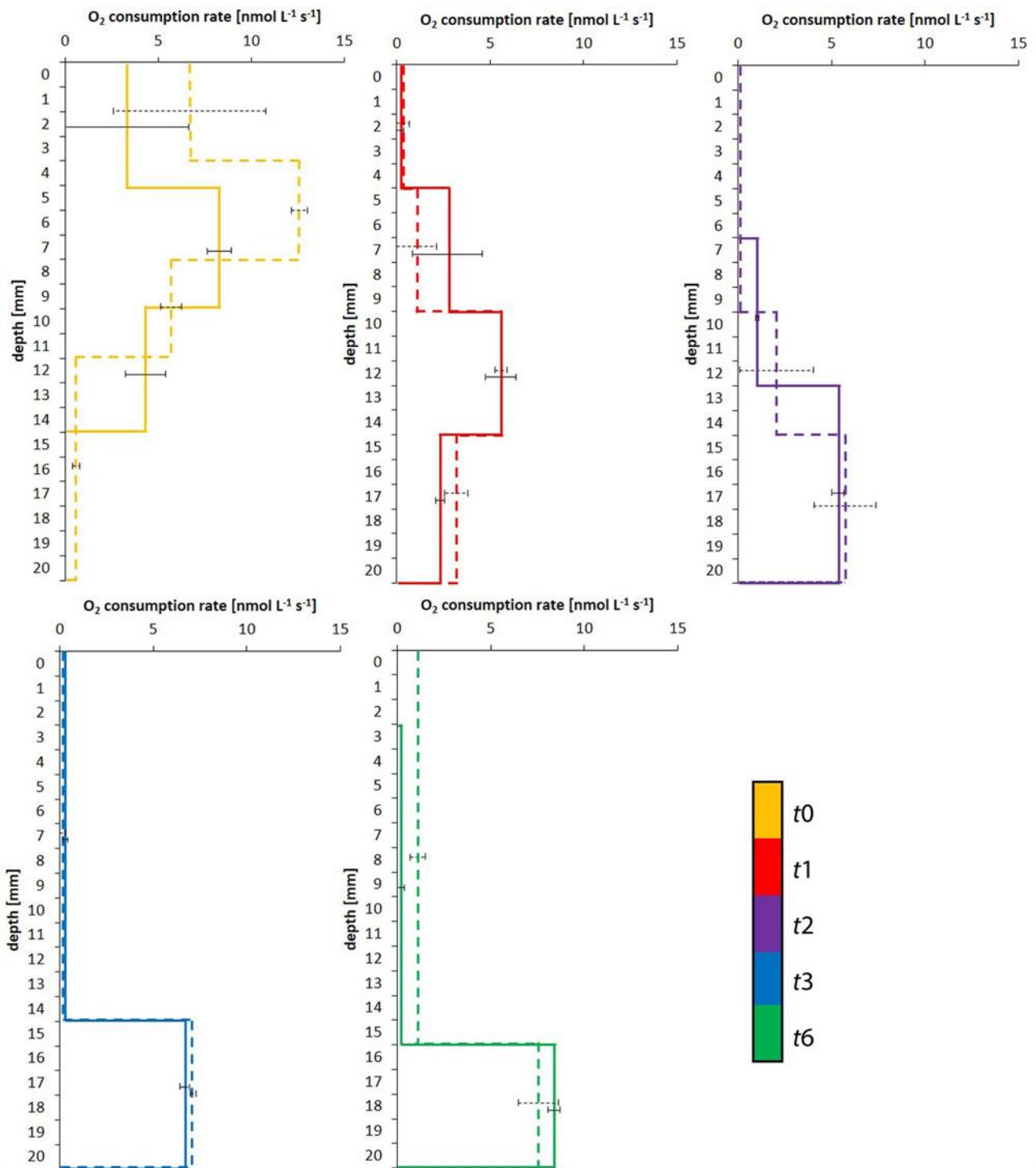
160

# O$_2$ consumption depth profiles – MWMM – FeS



**Figure 5.** O$_2$ consumption profiles for gradient tubes for negative control tubes (dashed lines) and inoculated tubes (solid lines) for different measurement time points ($t_0$ = day of inoculation, $t_1$ = day 1, $t_2$ = day 2, $t_3$ = day 3 and $t_6$ = day 6 after inoculation) in gradient tubes containing MWMM and a FeS bottom layer that starts at a depth of approx. 21 mm. Error bars show the minimum and maximum of the duplicate O$_2$ concentration measurements. Data were obtained using PROFILE 1.0. Oxygen consumption rates in inoculated tubes in the first 3 mm at $t_6$ are not shown due to falsified data resulting from irregularly measured O$_2$ concentrations at this depth. The differences in O$_2$ consumption between negative control and inoculated tubes at $t_0$ occurred through the temporal distance and between the measurements and the influence of the fast diffusion.

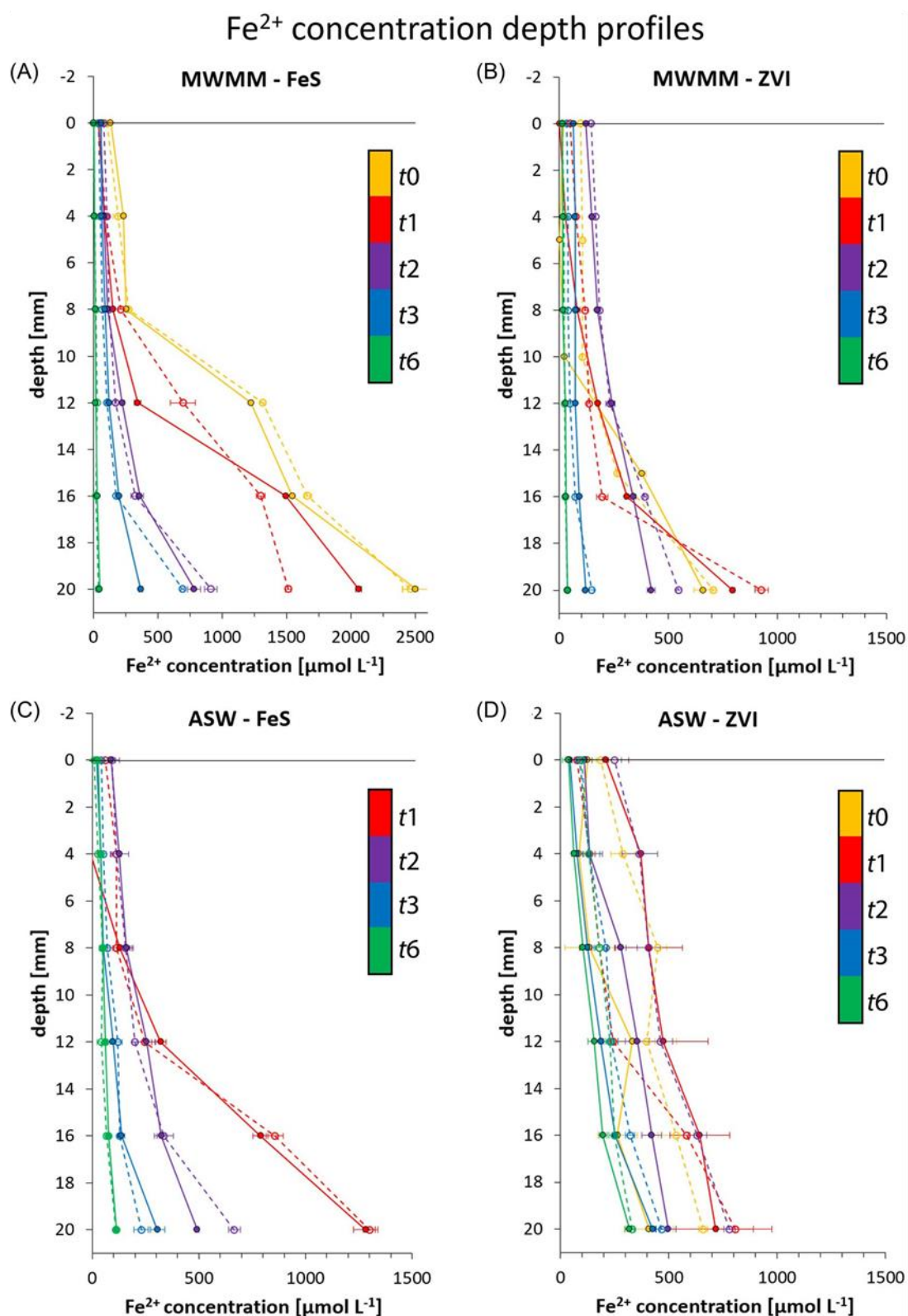# Fe²⁺ concentration depth profiles



Figure 6. Selected Fe²⁺ concentration depth profiles for gradient tubes inoculated with an enrichment of freshwater microaerophilic Fe(II)-oxidizers from Lake Constance, Germany (A) and (B) or with an isolate of a marine Fe(II)-oxidizer from Aarhus Bay, Denmark (C) and (D). Open symbols and dashed lines represent negative control tubes, closed symbols and solid lines inoculated tubes. Error bars show the standard deviation of the triplicate measurements. The colors display the different times of measurements starting at the day of inoculation ($t_0$). (A) Gradient tubes with MWMM and FeS bottom layer; (B) Gradient tubes with MWMM and ZVI powder at the bottom; (C) Gradient tubes with ASW and FeS bottom layer; (D) Gradient tubes with ASW and ZVI powder at the bottom. ($t_1$ = day 1, $t_2$ = day 2, $t_3$ = day 3 and $t_6$ = day 6 after inoculation)
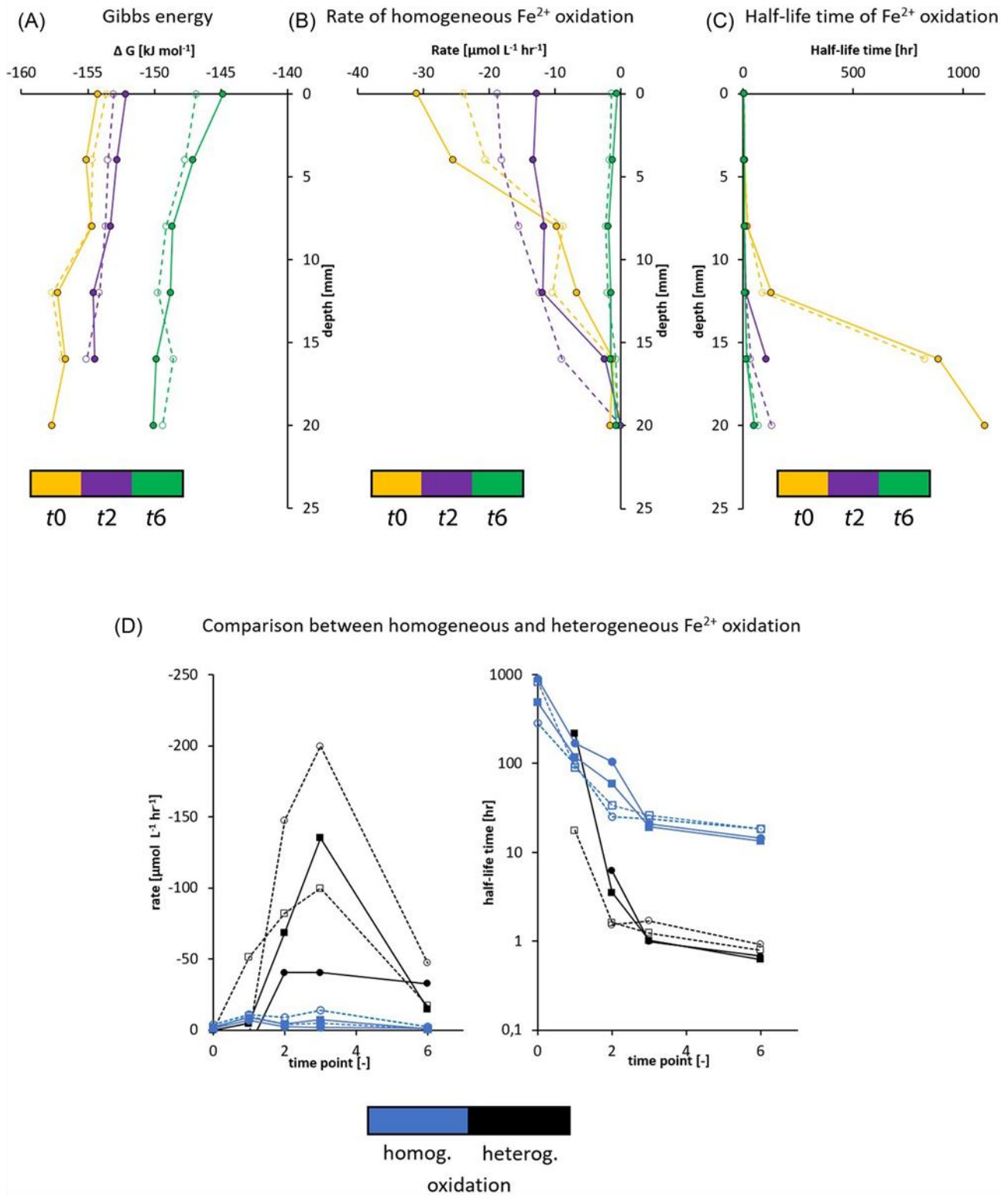
162

**Figure 7.** Representative energy, rate and half-life time profiles for gradient tubes containing MWMM and an FeS bottom layer at different time points. Open symbols and dashed lines represent negative control tubes, closed symbols and solid lines inoculated tubes. (A) Profiles of Gibbs free energy, (B) rate of homogeneous $Fe^{2+}$ oxidation, (C) half-life of homogeneous $Fe^{2+}$ oxidation, (D) comparison between homogeneous and heterogeneous $Fe^{2+}$ concentration in 16 mm depth over time. The depth was chosen according to the approximate level where the growth band formed in inoculated tubes. ($t_0$ = day of inoculation; $t_2$ = day 2, $t_6$ = day 6 after inoculation)

FeS is slightly different and FeS loses its ability to release $Fe^{2+}$ by aging. The quality of the FeS influences the solubility and diffusion of $Fe^{2+}$ leading to shifts of the optimum growth zone for microaerophilic Fe(II)-oxidizers. We have observed in the past that the rate of mixing Fe(II) and sulfide, the washing procedure (frequency and length of washing steps) and the storage of the FeS determines its suitability as Fe(II)-source in gradient tubes (unpublished data). Besides that, the medium composition and the cell number and activity of the inoculated strains determine the position of the Fe(III) mineral accumulations and lead to other forms of Fe(III) mineral accumulations than the shape of the classical growth bands as shown by e.g. Emerson (Emerson and Moyer 1997; Emerson and Floyd 2005) or in Fig. 3A and D. Due to these uncertainties, a quantitative visual evaluation between different Fe(II)-sources, strains or media cannot be done. However, gradient tubes are very suitable for bacterial cultivation and geochemical determination of optimum $O_2$ and $Fe^{2+}$ requirements of Fe(II)-oxidizing bacteria. The Fe(II)-sources FeS and ZVI showed the best results regarding growth of freshwater and marine microaerophilic Fe(II)-oxidizing bacteria in gradient tubes and worked reliably.

### Detection of optimal geochemical conditions for the growth of microaerophilic Fe(II)-oxidizers

Microaerophilic Fe(II)-oxidizing bacteria are in direct competition to chemical Fe(II) oxidation. Druschel *et al.* (2008) pointed out that chemical Fe(II) oxidation dominates at a $O_2$ concentrations of 275 $\mu$M and at 50 $\mu$M the biotic Fe(II) oxidation rate was faster than the abiotic rate. This fits well to our observation that Fe(III) mineral accumulations, which are produced by Fe(II)-oxidizing bacteria, occurred first in regions of $O_2$ concentrations of approximately 20–40 $\mu$M (Fig. 4). As most of the Fe(III) minerals accumulated very close to the Fe(II)-source at the bottom of the gradient tubes, a characteristic bend of the $O_2$ profiles in inoculated gradient tubes could not be observed as seen in the literature (Emerson and Moyer 1997; Edwards *et al.* 2003; Roden *et al.* 2004) where no $O_2$ was detected below cell growth bands. However, the tested freshwater culture was not completely pure. This might lead to slightly different conditions. The position of the Fe(III) mineral accumulations can be explained by the solubility of the Fe(II)-source, the faster $O_2$ diffusion (2.4 × $10^{-9}$ $m^2$ $s^{-1}$ (McMillan and Wang 1990)) compared to $Fe^{2+}$ diffusion (0.719 × $10^{-9}$ $m^2$ $s^{-1}$ (Lide 2008)), but also by the specific inoculated bacteria. The bacteria might also be responsible for the varying shapes of the Fe(III) mineral accumulations that were often not occurring as typical flat band by potential formation of different geochemical niches with optimal growth conditions.

The results indicate that most Fe(II) gets oxidized chemically. Differences in the $O_2$ concentrations between inoculated and negative control tubes could be observed only in the beginning of the incubation and within a short timeframe when first Fe(III) mineral accumulations occurred (Fig. 8). This illustrates the competitive pressure of microaerophilic Fe(II)-oxidizers towards chemical Fe(II) oxidation. The main $O_2$ consumption zone in the gradient tubes shifts downwards relatively fast. Starting at $t_2$, $O_2$ solely is consumed in the lower part of the gradient tube and there are no significant differences in $O_2$ consumption between inoculated and negative control tubes, which reinforce the assumption that the microorganisms are most of the time in strong competition with the chemical $O_2$ consumption.

When Fe(III) minerals precipitated as a result of micro- bial or homogeneous chemical Fe(II) oxidation, they serve as a catalyst for further chemical Fe(II) oxidation (autocatalysis)

and increase the rate of chemical Fe(II) oxidation (Stumm and Sulzberger 1992; Park and Dempsey 2005; Melton *et al.* 2014). This heterogeneous Fe(II) oxidation thus increases the contribution of chemical Fe(II) oxidation to the overall Fe(II) oxidation. Energetic and kinetic constraints support the hypothesis that best growth conditions for Fe(II)-oxidizing bacteria are found to be in the proximity of the Fe(II)-source in the first days after inoculation where not only the $Fe^{2+}$ concentration still is sufficient for bacterial growth but also more energy can be obtained from the oxidation of $Fe^{2+}$ for the bacterial metabolisms. Additionally, the bacteria at this location have the ability to compete with the half-life of the chemical $Fe^{2+}$ oxidation that decreases dramatically over time, especially due to heterogeneous $Fe^{2+}$ oxidation. The agreement between the Gibbs free energy and homogeneous $Fe^{2+}$ oxidation rate profiles (Fig. 7A and B) in abiotic and inoculated gradient tubes also indicate that most $Fe^{2+}$ in the gradient tube top layer is abiotically depleted.

Based on differences of the shape of the $O_2$ profiles in the inoculated tubes and the comparison of these $O_2$ profiles to the control tubes, it can be concluded that significant biotic Fe(II) oxidation is only dominating in the first hours to days, when distinct Fe(III) mineral accumulations occurred, which were shown to be related to bacterial growth as demonstrated by microscopic cell counts. The number of Fe(II)-oxidizing bacteria indeed increased most (Fig. 2), when spreading of the Fe(III) mineral accumulations could visually be observed. Based on these observations, bacterial cultures should therefore be transferred shortly after occurrence of distinct Fe(III) mineral accumulations to a new gradient tube before chemical Fe(II) oxidation becomes too dominant, in order to enhance the chance for isolation of microaerophilic Fe(II)-oxidizers.

### Suggestions for cultivation and isolation of microaerophilic Fe(II)-oxidizing bacteria from environmental samples

In the present study, the most suitable Fe(II)-sources for cultivation of freshwater and marine microaerophilic Fe(II)-oxidizers have been FeS and ZVI. Fe(III) mineral accumulations regularly occurred in inoculated gradient tubes using these Fe(II)-sources. Visual observations also showed that FeS and ZVI were less sensitive to chemical oxidation by $O_2$ than $FeCO_3$ and $FeCl_2$. The Fe(II)-sources $FeCO_3$ and $FeCl_2$ immediately began to oxidize based on the appearance of rust-colored oxides upon contact with air. However, it should be noted that using FeS or ZVI as Fe(II)-sources might stimulate the growth of other abundant microorganisms. Besides being a $Fe^{2+}$ source, FeS might also serve as sulfide source for microaerophilic sulfide-oxidizing bacteria (Nelson and Jannasch 1983; Gevertz *et al.* 2000). If sulfate gets produced biotically in these tubes, optimal conditions for heterotrophic sulfate reducers are prevalent as well if they can use carbon from organic compounds present in the agar. Due to hydrogen gas production during Fe(0) corrosion, gradient tubes using ZVI as bottom source might enrich bacteria that are capable of using hydrogen as electron donor (Jannasch and Mottl 1985; Dannenberg *et al.* 1992; Coleman *et al.* 1993). Additionally, it should be kept in mind that agar, which is used for the stabilization of the top layer of gradient tubes, is an organic substance that could be used for growth by heterotrophic bacteria. This is especially true for marine samples, as agar is prepared from algae that naturally serve as organic carbon source for marine microorganisms. Therefore, we suggest both, short-term transfers to fresh gradient tubes, and the use of different Fe(II)-sources for isolation of microaerophilic Fe(II)-oxidizing bacteria, namely
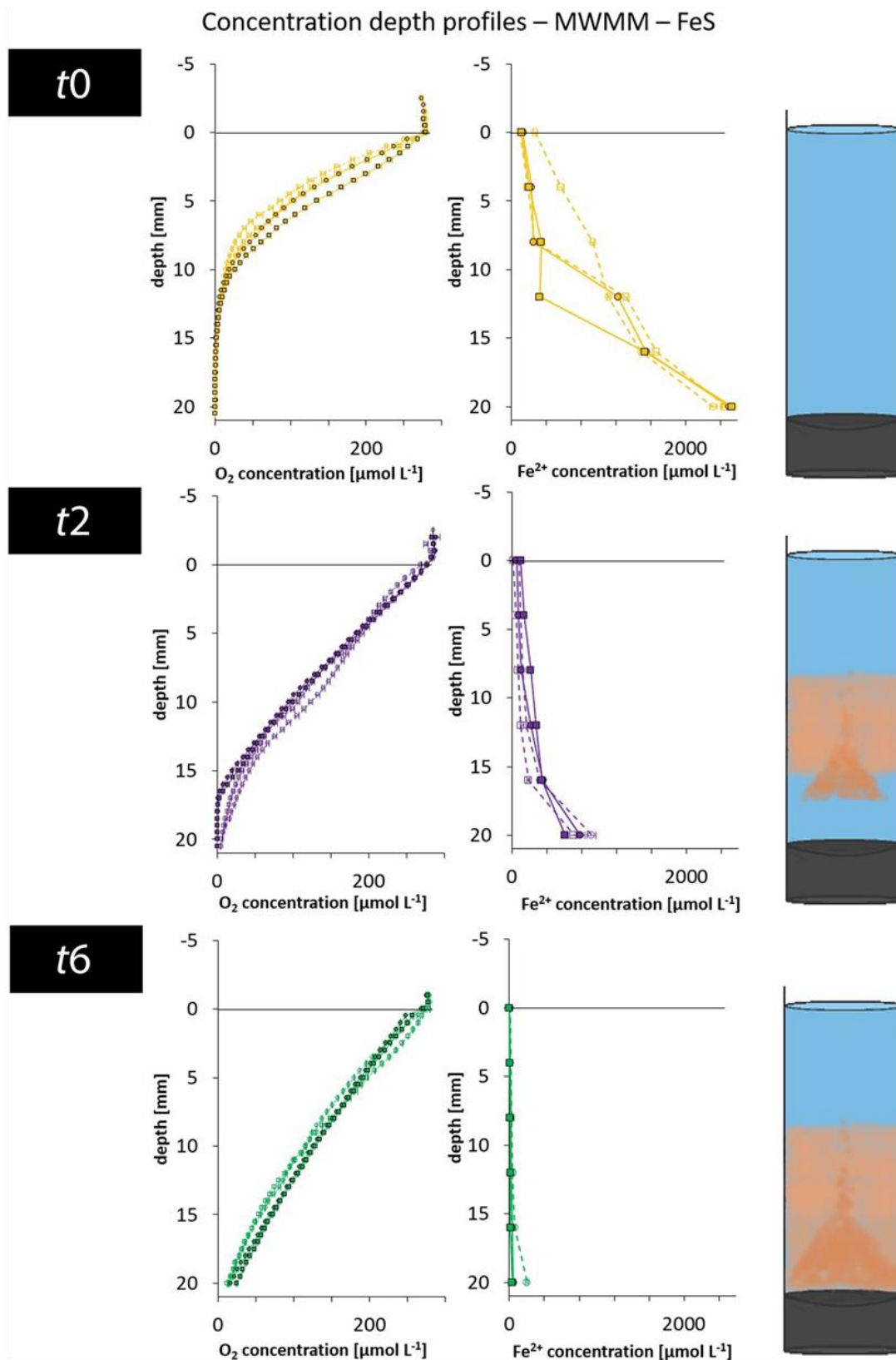
**Figure 8.** $O_2$ and $Fe^{2+}$ concentration depth profiles for gradient tubes containing MWMM and an FeS bottom layer at $t_0$, $t_2$ and $t_6$ ($t_0$ = day of inoculation; $t_2$ = day 2, $t_6$ = day 6 after inoculation). Open symbols and dashed lines represent negative control tubes, closed symbols and solid lines inoculated tubes. Error bars show the standard deviation of the triplicate measurements. The sketches next to the profiles show the look of the gradient tubes at the respective measurement time points.

using alternating FeS and ZVI as Fe(II)-source. For enhancing the chance to remove heterotrophic bacteria from the sample, the bacterial cultures could be transferred to petri dishes containing only medium and ZVI powder (McBeth *et al.* 2011). Enrichment in the so-called gradient plates was successfully applied in the literature (Emerson and Weiss 2004; McBeth *et al.* 2011; Laufer *et al.* 2016). Freshly synthesized $FeCO_3$ according to Hallbeck, Ståhl and Pederse (1993) could also be used to suppress the growth of bacteria that are additionally feeding on substrates that are released from the Fe(II)-source, e.g. S-species. However, we recommend doing transfers between FeS and ZVI in gradient tubes and gradient plates as $FeCO_3$ is quite sensitive towards oxidation by $O_2$ and only poorly releases $Fe^{2+}$, especially if it is not freshly synthesized.

## REFERENCES

Berg P, Risgaard-Petersen N, Rysgaard S. Interpretation of measured concentration profiles in sediment pore water. *Limnol Oceanogr* 1998;**43**:1500–10.

Brendel PJ, Luther GW. Development of a gold amalgam voltammetric microelectrode for the determination of dissolved Fe, Mn, $O_2$, and S(-II) in porewaters of marine and freshwater sediments. *Environ Sci Technol* 1995;**29**:751–61.

Bristow G, Taillefert M. VOLTINT: a Matlab®-based program for semi-automated processing of geochemical data acquired by voltammetry. *Comput Geosci* 2008;**34**:153–62.

Chiu BK, Kato S, McAllister SM *et al.* Novel pelagic iron-oxidizing zetaproteobacteria from the Chesapeake Bay oxic–anoxic transition zone. *Front Microbiol* 2017;**8**:1280.

Ciglenecki I, Margus M, Bura-Nakic E *et al.* Electroanalytical methods in characterization of sulfur species in aqueous environment. *J Electrochem Sci Eng* 2014;**4**:155–63.

Coleman ML, Hedrick DB, Lovley DR *et al.* Reduction of Fe(III) in sediments by sulphate-reducing bacteria. *Nature* 1993;**361**:436–8.

Cornell RM, Schwertmann U. *The Iron Oxides: Structure, Properties, Reactions, Occurrences, and Uses*. Weinheim: Wiley-VCH, 2003.

Dannenberg S, Kroder M, Dilling W *et al.* Oxidation of $H_2$, organic compounds and inorganic sulfur compounds coupled to reduction of $O_2$ or nitrate by sulfate-reducing bacteria. *Arch Microbiol* 1992;**158**:93–99.

Davison W. The solubility of iron sulphides in synthetic and natural waters at ambient temperature. *Aquat Sci* 1991;**53**:309–29.

Davison W, Seed G. The kinetics of the oxidation of ferrous iron in synthetic and natural waters. *Geochim Cosmochim Acta* 1983;**47**:67–79.

Davison W, Buffle J, DeVitre R. Voltammetric characterization of a dissolved iron sulphide species by laboratory and field studies. *Anal Chim Acta* 1998;**377**:193–203.

Druschel GK, Emerson D, Sutka R *et al.* Low-oxygen and chemical kinetic constraints on the geochemical niche of neutrophilic iron(II) oxidizing microorganisms. *Geochim Cosmochim Acta* 2008;**72**:3358–70.

Edwards KJ, Rogers DR, Wirsen CO *et al.* Isolation and characterization of novel psychrophilic, neutrophilic, Fe-oxidizing, chemolithoautotrophic $α$- and $γ$-proteobacteria from the deep sea. *Appl Environ Microbiol* 2003;**69**:2906–13.

Emerson D, Moyer C. Isolation and characterization of novel iron-oxidizing bacteria that grow at circumneutral pH. *Appl Environ Microbiol* 1997;**63**:4784–92.

Emerson D, Moyer CL. Neutrophilic Fe-oxidizing bacteria are abundant at the Loihi seamount hydrothermal vents and play a major role in Fe oxide deposition. *Appl Environ Microbiol* 2002;**68**:3085–93.

Emerson D, Weiss JV. Bacterial iron oxidation in circumneutral freshwater habitats: findings from the field and the laboratory. *Geomicrobiol J* 2004;**21**:405–14.

Emerson D, Floyd MM. Enrichment and isolation of iron-oxidizing bacteria at neutral pH. *Methods Enzymol*, 2005;**397**:112–23.

Emerson D, Field EK, Chertkov O *et al.* Comparative genomics of freshwater Fe-oxidizing bacteria: implications for physiology, ecology, and systematics. *Front Microbiol* 2013;**4**:254.

Field EK, Kato S, Findlay AJ *et al.* Planktonic marine iron oxidizers drive iron mineralization under low-oxygen conditions. *Geobiology* 2016;**14**:499–508.

Gevertz D, Telang AJ, Voordouw G *et al.* Isolation and characterization of strains CVO and FWKO B, two novel nitrate-reducing, sulfide-oxidizing bacteria isolated from oil field brine. *Appl Environ Microbiol* 2000;**66**:2491–501.

Hallbeck L, Ståhl F, Pedersen K. Phytogeny and phenotypic characterization of the stalk-forming and iron-oxidizing bacterium *Gallionella ferruginea*. *Microbiology* 1993;**139**:1531–5.

Hegler F, Posth NR, Jiang J *et al.* Physiology of phototrophic iron(II)-oxidizing bacteria: implications for modern and ancient environments. *FEMS Microbiol Ecol* 2008;**66**:250–60.

Hegler F, Lösekann-Behrens T, Hanselmann K *et al.* Influence of seasonal and geochemical changes on the geomicrobiology of an iron carbonate mineral water spring. *Appl Environ Microbiol* 2012;**78**:7185–96.

Jannasch HW, Mottl MJ. Geomicrobiology of deep-sea hydrothermal vents. *Science* 1985;**229**:717–25.

Kappler A, Straub KL. Geomicrobiological cycling of iron. *Rev Mineral Geochem* 2005;**59**:85–108.

Kashefi K, Lovley DR. Reduction of Fe(III), Mn(IV), and toxic metals at 100°C by *Pyrobaculum islandicum*. *Appl Environ Microbiol* 2000;**66**:1050–6.

Kato S, Chan C, Itoh T *et al.* Functional gene analysis of freshwater iron-rich flocs at circumneutral pH and isolation of a stalk-forming microaerophilic iron-oxidizing bacterium. *Appl Environ Microbiol* 2013;**79**:5283–90.

Kato S, Kikuchi S, Kashiwabara T *et al.* Prokaryotic abundance and community composition in a freshwater iron-rich microbial mat at circumneutral pH. *Geomicrobiol J* 2012;**29**:896–905.

Klueglein N, Zeitvogel F, Stierhof Y-D *et al.* Potential role of nitrite for abiotic Fe(II) oxidation and cell encrustation during

nitrate reduction by denitrifying bacteria. *Appl Environ Microbiol* 2014;**80**:1051–61.

Konhauser KO, Kappler A, Roden EE. Iron in microbial metabolisms. *Elements* 2011;**7**:89–93.

Kucera S, Wolfe RS. A selective enrichment method for *Gallionella ferruginea*. *J Bacteriol* 1957;**74**:344–9.

Laufer K, Nordhoff M, Røy H *et al.* Coexistence of microaerophilic, nitrate-reducing, and phototrophic Fe(II)-oxidizers and Fe(III)-reducers in coastal marine sediment. *Appl Environ Microbiol* 2016;**82**:1433–47.

Lide DR. *CRC Handbook of Chemistry and Phyics*, 88th edn. Boca Raton: CRC Press, 2008.

Lin C, Larsen EI, Nothdurft LD *et al.* Neutrophilic, microaerophilic Fe(II)-oxidizing bacteria are ubiquitous in aquatic habitats of a subtropical australian coastal catchment (ubiquitous FeOB in catchment aquatic habitats). *Geomicrobiol J* 2012;**29**:76–87.

Lovley DR, Ueki T, Zhang T *et al.* Geobacter: the microbe electric's physiology, ecology, and practical applications. *Adv Microb Physiol* 2011;**59**:1–100.

Luther GW, Glazer B, Ma S *et al.* Iron and sulfur chemistry in a stratified lake: evidence for iron-rich sulfide complexes. *Aquat Geochem* 2003;**9**:87–110.

MacDonald DJ, Findlay AJ, McAllister SM *et al.* Using in situ voltammetry as a tool to identify and characterize habitats of iron-oxidizing bacteria: from fresh water wetlands to hydrothermal vent sites. *Environ Sci Process Impacts* 2014;**16**:2117–26.

McBeth JM, Little BJ, Ray RI *et al.* Neutrophilic iron-oxidizing "zetaproteobacteria" and mild steel corrosion in nearshore marine environments. *Appl Environ Microbiol* 2011;**77**:1405–12.

McMillan JD, Wang DIC. Mechanisms of oxygen transfer enhancement during submerged cultivation in perfluorochemical-in-water dispersionsa. *Ann NY Acad Sci* 1990;**589**:283–300.

Melton ED, Swanner ED, Behrens S *et al.* The interplay of microbially mediated and abiotic reactions in the biogeochemical Fe cycle. *Nat Rev Micro* 2014;**12**:797–808.

Nelson D, Jannasch H. Chemoautotrophic growth of a marine Beggiatoa in sulfide-gradient cultures. *Arch Microbiol* 1983;**136**:262–9.

Neubauer SC, Emerson D, Megonigal JP. Life at the energetic edge: kinetics of circumneutral iron oxidation by lithotrophic iron-oxidizing bacteria isolated from the wetland-plant rhizosphere. *Appl Environ Microbiol* 2002;**68**:3988–95.

Park B, Dempsey BA. Heterogeneous oxidation of Fe(II) on ferric oxide at neutral pH and a low partial pressure of $O_2$. *Environ Sci Technol* 2005;**39**:6494–500.

Pfennig N. *Rhodocyclus purpureus* gen. nov. and sp. nov., a ring-shaped, vitamin B12-requiring member of the family Rhodospirillaceae. *Int J Syst Evol Microbiol* 1978;**28**:283–8.

Rentz JA, Kraiya C, Luther GW *et al.* Control of ferrous iron oxidation within circumneutral microbial iron mats by cellular activity and autocatalysis. *Environ Sci Technol* 2007;**41**:6084–9.

Revsbech NP. An oxygen microsensor with a guard cathode. *Limnol Oceanogr* 1989;**34**:474–8.

Rickard D, Luther GW. Chemistry of iron sulfides. *Chem Rev* 2007;**107**:514–62.

Roden E, Sobolev D, Glazer B *et al.* Potential for microscale bacterial Fe redox cycling at the aerobic-anaerobic interface. *Geomicrobiol J* 2004;**21**:379–91.

Singer PC, Stumm W. Acidic mine drainage: the rate-determining step. *Science* 1970;**167**:1121–3.

Slowey A, Marvin-DiPasquale M. How to overcome inter-electrode variability and instability to quantify dissolved oxygen, Fe(II), mn(II), and S(II) in undistured soils and sediments using voltammetry. *Geochem Trans* 2012;**13**:6.

Sobolev D, Roden EE. Suboxic deposition of ferric iron by bacteria in opposing gradients of Fe(II) and oxygen at circumneutral pH. *Appl Environ Microbiol* 2001;**67**:1328–34.

Straub KL, Benz M, Schink B *et al.* Anaerobic, nitrate-dependent microbial oxidation of ferrous iron. *Appl Environ Microbiol* 1996;**62**:1458–60.

Stumm W, Sulzberger B. The cycling of iron in natural environments: considerations based on laboratory studies of heterogeneous redox processes. *Geochim Cosmochim Acta* 1992;**56**:3233–57.

Stumm W, Morgan JJ. *Aquatic Chemistry: Chemical Equilibria and Rates in Natural Waters*. New York: Wiley, 1996.

Sun W, Nešić S, Woollam RC. The effect of temperature and ionic strength on iron carbonate ($FeCO_3$) solubility limit. *Corros Sci* 2009;**51**:1273–6.

Sung W, Morgan JJ. Kinetics and product of ferrous iron oxygenation in aqueous systems. *Environ Sci Technol* 1980;**14**:561–8.

Swanner ED, Nell RM, Templeton AS. Ralstonia species mediate Fe-oxidation in circumneutral, metal-rich subsurface fluids of Henderson mine, CO. *Chem Geol* 2011;**284**:339–50.

Taillefert M, Bono AB, Luther GW. Reactivity of freshly formed Fe(III) in synthetic solutions and (pore)waters: voltammetric evidence of an aging process. *Environ Sci Technol* 2000;**34**:2169–77.

Tamura H, Goto K, Nagayama M. The effect of ferric hydroxide on the oxygenation of ferrous ions in neutral solutions. *Corros Sci* 1976;**16**:197–207.

Tamura H, Kawamura S, Hagayama M. Acceleration of the oxidation of $Fe^{2+}$ ions by Fe(III)-oxyhydroxides. *Corros Sci* 1980;**20**:963–71.

Taylor SR. Abundance of chemical elements in the continental crust: a new table. *Geochim Cosmochim Acta* 1964;**28**:1273–85.

Tschech A, Pfennig N. Growth yield increase linked to caffeate reduction in *Acetobacterium woodii*. *Arch Microbiol* 1984;**137**:163–7.

Weber KA, Achenbach LA, Coates JD. Microorganisms pumping iron: anaerobic microbial iron oxidation and reduction. *Nat Rev Micro* 2006;**4**:752–64.

Weiss J, Emerson D, Backer S *et al.* Enumeration of Fe(II)-oxidizing and Fe(III)-reducing bacteria in the root zone of wetland plants: implications for a rhizosphere iron cycle. *Biogeochemistry* 2003;**64**:77–96.

Weiss JV, Rentz JA, Plaia T *et al.* Characterization of neutrophilic Fe(II)-oxidizing bacteria isolated from the rhizosphere of wetland plants and description of *Ferritrophicum radicicola* gen. nov. sp. nov., and *Sideroxydans paludicola* sp. nov. *Geomicrobiol J* 2007;**24**:559–70.

Widdel F, Schnell S, Heising S *et al.* Ferrous iron oxidation by anoxygenic phototrophic bacteria. *Nature* 1993;**362**:834–6.
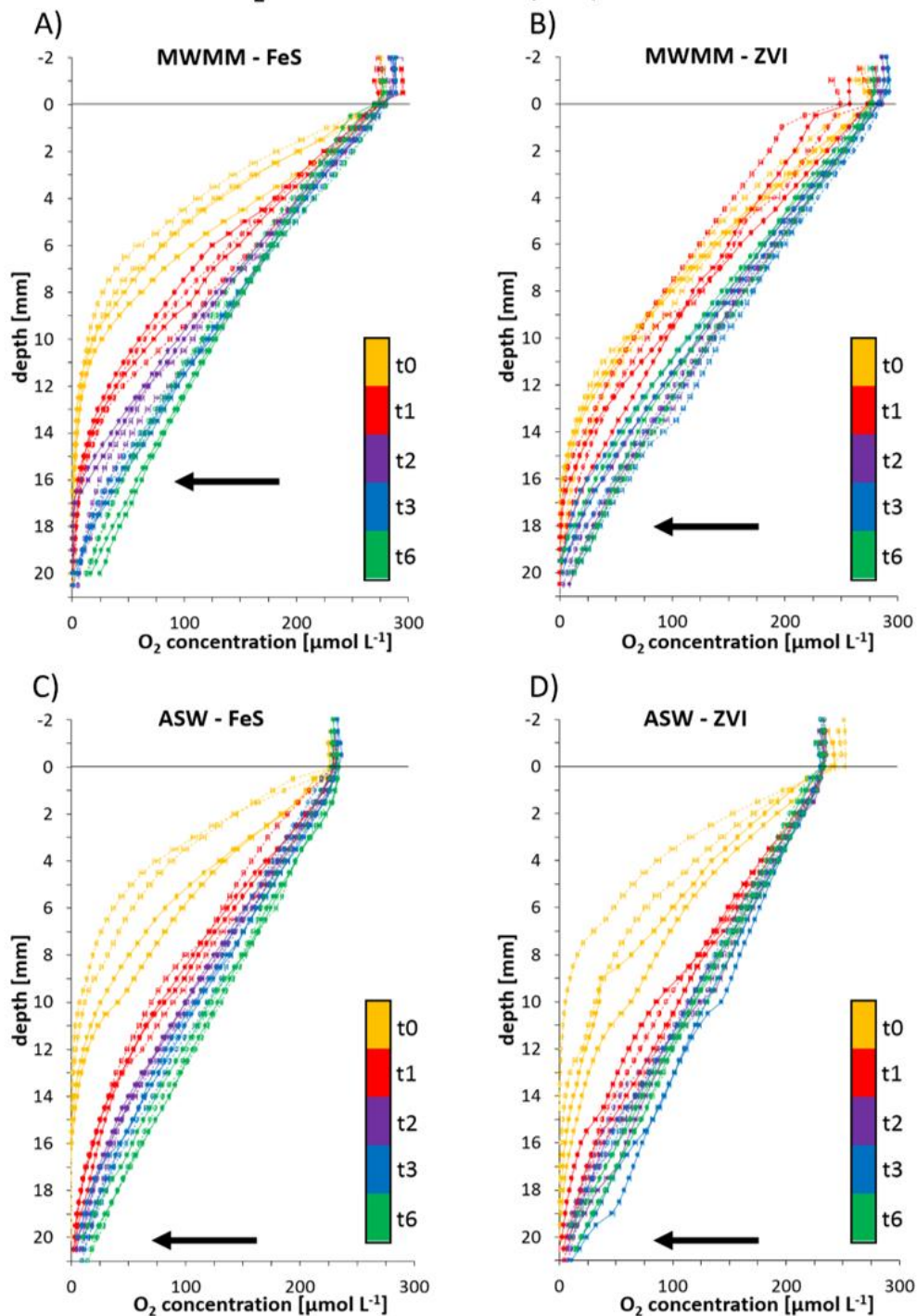
Figure S1: Duplicate $O_2$ concentration depth profiles in gradient tubes inoculated with an enrichment of freshwater microaerophilic Fe(II)-oxidizers from Lake Constance, Germany (A,B) or with an isolate of a marine Fe(II)-oxidizer from Aarhus Bay, Denmark (C,D). Open symbols and dashed lines represent negative control tubes, closed symbols and solid lines inoculated tubes. Error bars are not shown as the mean coefficient of variation of all profiles is below 3%. The colors display the different times of measurements starting the day of inoculation (t0). Depth 0 mm shows the headspace-top layer interface; the Fe(II)-source starts in a depth of about 21 mm. The arrow indicates the approximate level where the growth band formed in inoculated tubes. A) Gradient tubes with MWMM and FeS bottom layer; B) Gradient tubes with MWMM and ZVI powder at the bottom; C) Gradient tubes with ASW and FeS bottom layer; D) Gradient tubes with ASW and ZVI powder at the bottom. ($t_1$ = day 1, $t_2$ = day 2, $t_3$ = day 3 and $t_6$ = day 6 after inoculation)
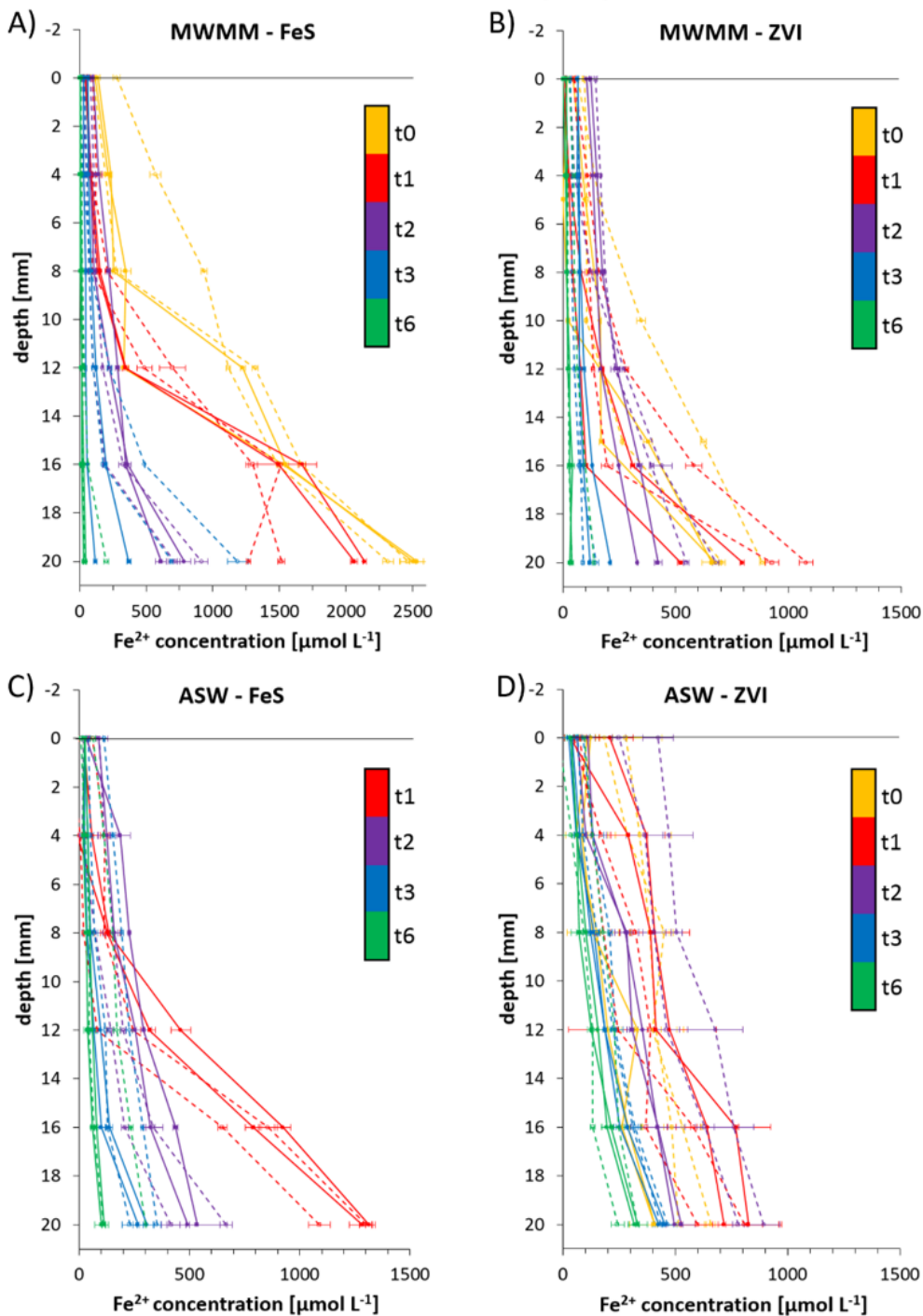
Figure S2: Duplicate Fe²⁺ concentration depth profiles for gradient tubes inoculated with an enrichment of freshwater microaerophilic Fe(II)-oxidizers from Lake Constance, Germany (A,B) or with an isolate of a marine Fe(II)-oxidizer from Aarhus Bay, Denmark (C,D). Open symbols and dashed lines represent negative control tubes, closed symbols and solid lines inoculated tubes. Error bars show the standard deviation of the triplicate measurements. The colors display the different times of measurements starting at the day of inoculation (t0). A) Gradient tubes with MWMM and FeS bottom layer; B) Gradient tubes with MWMM and ZVI powder at the bottom; C) Gradient tubes with ASW and FeS bottom layer; D) Gradient tubes with ASW and ZVI powder at the bottom. ($t_1$ = day 1, $t_2$ = day 2, $t_3$ = day 3 and $t_6$ = day 6 after inoculation)

# Acknowledgements

In the first place, I would like to thank Caroline Schmidt for her endless support during my PhD. I stayed in this workgroup because she offered me this PhD position. She has spent hours and hours with discussing experimental designs, data analysis, revisions of manuscripts or replying to my emails. Her creativity improved many of my presentations. She was always patient with me, even when I came up with stupid or stubborn ideas. Her attitude to set aside her own needs is unprecedented and if I ever needed help, I knew, I could come to her. Thank you for your friendship.

I am grateful to Andreas Kappler for enabling me doing my PhD in his lab. He always had an open door to listen to my wishes and problems. He is available 24/7 for any concerns and manuscripts I have sent to him got revised within a day. By organizing a lab retreat, a summer event and a Christmas party every year, he makes us feeling part of a big family and by that, spending time in the lab is not only work but also a lot of fun.

My thanks also go to Bo Barker Jørgensen for being my 2$^{nd}$ supervisor. We regularly stayed in contact during my PhD by sending and discussing experimental data and when I did not send him emails for a longer period of time, I got a polite request for an update – thank you for caring so much about the progress of my work. His ability to improve and clarify written manuscripts by only changing some expressions is amazing. Thank you also for your time and hospitality during our fieldtrips to Aarhus.

During the last years, I never felt alone thanks to wonderful friends I found during my PhD. Markus Maisch is probably the most positive person I know. With his characteristic good mood and his helpfulness, he makes the lab to a place, where it is nice to spend time. If someone is in a jam, he is ready to help, even if he has only little time. He is excellent in finding solutions; both, when experiments did not work out the expected way, but also in personal life. Together with Caroline, we were an amazing team during my PhD. Thank you for being such a good friend. I could always rely on Ellen Röhm. Thanks for the hundreds of cakes you baked for breakfast. If any analysis needed to be done or if any material for experiments could be found – she knows the lab inside out and her effective way of working keeps the lab running. Preparing gradient tubes together with Lars Grimm is one of my favorite works I do in the lab, while talking about everything. Due to his calm nature, I always felt welcome to discuss any problems I had and if I needed support in the lab, he was ready to help. Julian Sorwat got my best 20-degree room office mate. His creative ideas significantly improved different figures I needed to prepare for manuscripts or presentations. I also want to thank Monique Patzner. She is a very considerate and attentive person and always cared how I felt when situations got very stressful.

I especially want to mention Elif Köksoy, who supervised me during master thesis. Because of her positive and lively attitude and her way to treat new people, I felt welcome from day one in this workgroup. Before she unfortunately left our lab, we got good friends and I am happy that she was still around at the beginning of my PhD and during conferences for any questions or conversations.

There are more helpful people, who supported me during my PhD. In the first months, Cindy Lockwood helped me with the setup of my first experiments. If I had any questions concerning geochemistry, she was able to answer them. I hope, her lab space was cherished by me. Katja Laufer was an incredible help during our last field trip to Aarhus when she sampled sediment for us in freezing water in her diving suit. It is always great to see her around during conferences. Thanks also to Franziska Schädler, who showed me the Lake Constance field site and did molecular biology analysis for me. The time during sampling in Aarhus was always amazing due to "Team Aarhus" Casey Bryce and Nia Blackwell. We had a terrific time there and I really enjoyed our conversations, also in the lab. Thanks to Nia also for proof reading part of this thesis. Finally, I want to thank all current and former members of the geomicrobiology group that I did not mention by name.

One of the nicest professors I met during my PhD is Greg Druschel. He is so down-to-earth and he never consider himself too good to share his knowledge or help with any voltammetry question I had. It was a privilege helping him during the tools in biochemistry workshop – he is just a great guy.

I also want to express my gratitude to Stefan Haderlein and Peter Grathwohl, who agreed to be examiners for my thesis defense.

Many more thanks also go to people that spend time and distract me outside the lab. Klaus Röhler is the main reason for my considerably improved tennis skills – I will win our next match ☺. I am very happy, that I am friends with my "Umwis" since my bachelor's degree. Although living at different places in the meanwhile, we still manage to see each other several timers per year. I also want to thank my friends from where I grew up and that I know since school or even kindergarten. It's always great to spend time with you or to play table tennis or tennis matches against you.

Finally, I of course want to thank my family, who always supported and spend time with me whatever happens, not only during the last years; to Nils & Janin, to Lars (special thanks for the help with the graphical design of numerous figures), to my mum and to my dad, who unfortunately could not live to see the end of my PhD. Thank you.